REFERENCE ONLY

UNIVERSITY OF LONDON THESIS

Degree PhD Year 2005 Name of Author FRANCIS, R.J.

Antibody Directed Enzyme Prodrug Therapy -

A Mechanistic Approach

Dr Roslyn Jane Francis

University College London

Ph.d. Oncology

ProQuest LLC
789 East Eisenhower Parkway
P.O. Box 1346
Ann Arbor, MI 48106-1346

DEDICATION

This thesis could not have been written without the support of my family, who provided encouragement, motivation and unfaltering belief in my ability to complete this work. I would also like to thank the many people who helped along the way, particularly with the ADEPT clinical trials, which could not have been conducted without the good will and commitment of a great many people. My special thanks goes to Professor Begent who gave me this opportunity to be involved in ADEPT, and under whose guidance I have gained so much. Under his nurturing I have developed as a doctor, a scientist and as a person. For this I am enormously grateful.

I offer my enduring thanks to the research nurses, in particular Laura Hope-Stone, who gave so much support and friendship, and who made working as a team so rewarding. The staff from the CRUK Drug Development Office (Luiza Sena, Adele Robbins, Clare Cruickshank) were at all times such a pleasure to work with and I thank them for making my role so much easier. The physicists, including Dr Alan Green, Kathryn Adamson and Sandra Baig, also deserve special recognition for the time and support they gave to me, and their patience with my many 'demands'.

Last of all, and most importantly, I would like to thank each and every patient who participated in the clinical trials I have reported in this thesis. Your bravery, strength and hopes have been inspiring to me, and without your participation, this research would never have been performed. I will remember all of you; your contributions, your sacrifices, and above all your faith that a therapy will be developed to help not you, but others who come after you, so that their lives would not be cut short, as yours have been, by cancer.

ABSTRACT

Antibody directed enzyme prodrug therapy (ADEPT) is a two-step targeting system, which utilises pretargeting of antibody-enzyme to tumour followed by administration of a prodrug, which is converted to an active cytotoxic by the enzyme at tumour sites. This system aims to overcome cancer resistance mechanisms by the tumour specific generation of large quantities of a cytotoxic agent.

ADEPT is a complex therapeutic strategy as it involves multiple components, each of which has their own unique requirements for the system as a whole to be successful. It is hypothesised that by measuring mechanism in a clinical trial setting, a greater understanding of ADEPT can be achieved. Additionally, rational modifications can be determined and implemented, thereby accelerating the development process.

This thesis demonstrates how mechanistic data attained from one phase I/II ADEPT clinical trial lead to the development of a novel genetically engineered antibody-enzyme fusion protein for ADEPT, which was shown in a second clinical trial to have enhanced features for tumour targeting in ADEPT. The metabolic assessment of tumours using [F-18] FDG PET was assessed during both ADEPT trials and shown to provide additional information when compared with conventional response assessment, particularly in the assessment of patients with radiological stable disease. As the data generated on ADEPT from both preclinical and clinical development is large, and the possibilities for modification to the system are numerous, an Ontology and Conceptual Model have been developed to organise the data attained on ADEPT.

This thesis demonstrates that although ADEPT is a complex therapeutic strategy it can be successfully studied in a clinical setting using mechanistic clinical trial design, rational modifications can be made and data can be organised to facilitate development for the future.

DECLARATION

All of the work in this thesis has been performed by me, personally, except where due acknowledgement has been made.

Roslyn Jane Francis

January 2005

Table of contents

List of Tables

List of Figures

List of abbreviations

5FU	5fluorouracil
A5CP	A5B7 F(ab′)$_2$ chemically conjugated to CPG2
ADCC	antibody directed cellular cytotoxicity
ADEPT	Antibody directed enzyme prodrug therapy
AE	adverse event
ARSAC	Administration of Radioactive Substances Committee
AUC	area under the curve
BSA	bovine serum albumin
C_0	concentration extrapolated back to time 0 minutes
C-14	carbon-14
cDNA	copy deoxyribonucleic acid
CEA	carcinoembryonic antigen
C_H	constant heavy chain (immunoglobulin)
CIRB	CRUK Institutional Review Board
C_L	constant light chain (immunoglobulin)
CMDA	4-[2-chloroethyl)(2-mesyloxyethyl)amino]benzoyl-L-glutamic acid
Cmax	maximum concentration
CO	carbon monoxide
CPG2	carboxypeptidase G2
CR	complete response
CRUK	Cancer Research United Kingdom
Cs-137	caesium-137
CT	computerised tomography
CTC	common toxicity criteria
DLT	dose limiting toxicity
DNA	deoxyribonucleic acid
DPD	dihydropyrimidine dehygrogenase
ELISA	enzyme linked immunosorbance assay
[F-18]	fluorine-18
FDA	Food and Drug Administration
FDG PET	fluoro-2-deoxy-D-glucose positron emission tomography

FPLC	fast perfusion liquid chromatography
GDEPT	gene directed enzyme prodrug therapy
GluT	glucose transporters
HACPG2A	human anti-CPG2 antibody
HAMA	human anti-mouse antibody
H + E	haemotoxylin and eosin
his tag	Hexahistidine tag
HPLC	high performance iquid chromatography
HSA	human serum albumin
IC_{50}	concentration of drug to inhibit cell growth by 50%
IMAC	immobilised metal ion-affinity chromatography
ip	intraperitoneal
ITLC	instant thin layer chromatography
iv	intravenous
kD	dissociation constant
kDa	kilodalton
keV	kiloelecton volts
L	litre
LD10	lethal dose to 10% mice
LREC	Local Research Ethics Committee
m^2	metres squared
M	molar
MDEPT	MPEG-directed enzyme prodrug therapy
MFECP1	glycosylated MFE-23::CPG2 fusion protein
mg	milligrams
mins	minutes
mL	millilitres
MPEG	methoxypolyethylene glycol
MTD	maximum tolerated dose
NA	not applicable
NCI CTC	National Cancer Institute Common Toxicity Criteria
PBS	phosphate buffered saline
PCR	polymerase chain reaction

PDEPT	polymer-directed enzyme prodrug therapy
PD	progressive disease
PR	partial response
RECIST	Response Evaluation Criteria in Solid Tumours
RIGS	radioimmunoguided surgery
ROI	region of interest
RP-HPLC	reverse phase high performance liquid chromatography
RR	response rate
RSA	rat serum albumin
RTM	reduction in tail moment (comet assay)
scFv	single chain variable fragment
SD	stable disease
SPECT	single photon emission computerised tomography
SUV	standardised uptake value
$T_{½}$	half-life
Tc-99m	technetium-99m
TcCO	technetium carbonyl [99mTc(H2O)3(CO)3]+
TLC	thin layer chromatography
TP	thymidine phosphorylase
U	units
µg	micrograms
VDEPT	virus directed enzyme prodrug therapy
V_H	variable heavy chain (immunoglobulin)
V_L	variable light chain (immunoglobulin)
VOI	volume of interest
VOIsub	volume of interest subtraction
V_{SS}	volume of distribution at steady state
WBC	white blood cells
WHO	World Health Organisation
ZD2767D	bis-iodo phenol mustard drug
ZD2767P	bis-iodo phenol mustard prodrug

1 Introduction

1.1 Background

Cancer is the second largest cause of death in developed countries and its incidence is continuing to rise. Cancer currently causes 25% of all deaths in the United Kingdom (Cancer Research UK, 2002). Despite the recent vast increase in research into new chemotherapy agents including combination regimens, high dose therapies and novel strategies, few have made significant advances in the cure or long term survival of patients with advanced or metastatic solid tumours. Drug resistance remains a significant obstacle to therapy (Pastan and Gottesman, 1987; Juranka *et al*, 1989; Kaye, 1998; Gottesman *et al*, 2002). The maximum dose of chemotherapy is limited by the development of systemic toxicities due to treatments not being tumour specific. One strategy to overcome resistance mechanisms is to specifically target tumour cells, thereby limiting systemic effects and increasing therapeutic potential. This forms the basic principle of antibody directed enzyme therapy (ADEPT), which is the focus of this thesis. A successful treatment requires a detailed understanding of the condition it is directed against, and the *in vivo* effects of the treatment on both tumour and normal tissues. From this information therapeutic strategies may be modified and developed with the aim of constructing a cure for a complex and serious disease.

1.1.1 Colorectal cancer

Colorectal cancer is the main solid tumour discussed throughout this thesis. It is a leading cause of cancer death in the UK, being responsible for 11% of all cancer deaths (second only to lung cancer), and resulting in nearly 17 000 deaths per annum in England and Wales (Quinn *et al*, 2001). The incidence of colorectal cancer is 48 cases /100 000 people per year in the UK (Quinn *et al*, 2001). The current 5-year survival for patients with colorectal cancer (all stages) is 40%. Once metastases develop the median survival for a patient is 11 months (Advanced Colorectal Cancer Meta-analysis Project, 1992). Conventional chemotherapy is unable to cure patients with advanced or metastatic disease, so there is an urgent need to develop novel therapies.

5Fluorouracil (5FU) has historically been the mainstay of chemotherapy for colorectal cancer, with maximum response rates of approximately 20-30% in metastatic disease (Lokich *et al*, 1989; Advanced Colorectal Cancer Meta-analysis Project, 1992; Meta-analysis Group in Cancer, 1998). It is an anti-metabolite with predominantly S-phase activity. Infusional regimens have been compared to bolus administration and are associated with an increase in response rate and a different toxicity profile, with a slight increase in overall survival (Lokich *et al*, 1989; Meta-analysis Group in Cancer, 1998). Bolus 5FU is associated with more haematological toxicities (grade III or IV in 31% of patients) compared with infusional schedules (grade III or IV in 4% of patients), however the occurrence of plantar-palmer syndrome is higher in infusional schedules (34%) compared with bolus administration (13%) (Meta-analysis Group in Cancer, 1998). Diarrhoea, nausea and vomiting, or mouth ulcers occur in approximately 15% of patients for both schedules (Meta-analysis Group in Cancer, 1998). Many centres have undertaken trials using variations on infusional or bolus regimens, with or without the addition of biomodulating agents (e.g.: folinic acid), with little impact on overall survival (Advanced Colorectal Cancer Meta-analysis Project, 1992; Leichman *et al*, 1995; Rougier *et al*, 1997).

Recently two new chemotherapeutics have been shown to have efficacy in advanced colorectal cancer. These are irinotecan (CPT11), a topoisomerase I inhibitor, and oxaliplatin, a synthetically derived platinum. Single agent irinotecan has an objective response rate of 13% as second line treatment for metastatic disease, with another 40-50% of patients achieving stable disease (Rougier and Mitry, 2000). An increased median survival of approximately 2 months has been shown in two randomised controlled trials comparing single agent irinotecan administered after the failure of 5FU compared to best supportive care or an infusional 5FU regimen (Cunningham *et al*, 1998; Rougier *et al*, 1998). As a first line treatment for metastatic colorectal cancer, irinotecan in combination with 5FU has a response rate of 39-41% compared to 21-23% with 5FU alone, with a statistically significant improvement in time to progression and overall survival (Douillard *et al*, 2000; Saltz *et al*, 2000). The side-effects associated with irinotecan are diarrhoea, myelosuppression

(neutropaenia), acute cholinergic syndrome, nausea and vomiting. Grade 3 or 4 diarrhoea has been reported in 20-40% of patients with single agent irinotecan or irinotecan in combination with 5FU (Cunningham *et al*, 1998; Douillard *et al*, 2000; Saltz *et al*, 2000). Grade 3 or 4 neutropaenia has been reported in up to 54% of patients (Saltz *et al*, 2000).

Single agent oxaliplatin used as first line chemotherapy for metastatic colorectal carcinoma has a response rate of approximately 22%, which is comparable with single agent 5FU(Armand *et al*, 2000). Significant synergy has been shown in vitro between oxaliplatin and 5FU, so most clinical trials have utilised this combination. In first-line therapy for metastatic disease the combination of oxaliplatin with 5FU has resulted in a response rate of approximately 50% (de Gramont *et al*, 2000; Giacchetti *et al*, 2000). The toxicities seen include neutropaenia, diarrhoea, peripheral neuropathy, nausea and vomiting (de Gramont *et al*, 2000; Giacchetti *et al*, 2000). There were improvements seen in time to progression, but overall survival was not significantly improved by the addition of oxaliplatin to a 5FU regimen (de Gramont *et al*, 2000; Giacchetti *et al*, 2000).

Despite the introduction of both irinotecan and oxaliplatin into the management of advanced colorectal cancer and the increased response rates that have been seen, these treatments have remained essentially palliative and long-term cures have not been achieved. Improvements in survival have, in some trials, been attained, but these improvements have been in terms of months, rather than years. Also, these treatments are associated with significant toxicities for patients, which is not only undesirable but also limits the dose of chemotherapy that can be administered. The need therefore remains for a more effective and tumour specific treatment.

1.2 Antibody therapies for cancer

Antibody targeted therapy has the promise of the 'magic bullet' proposed by Paul Ehrlich almost a century ago. The aim is to develop a system that will target therapeutic agents to specific tissues such as tumours to maximise effect, while at the same time reducing systemic toxicity. Since the 1980's monoclonal antibody

therapy, either alone or conjugated to therapeutic agents such as radionuclides, drugs, toxins, enzymes or growth factors have been recognised as emerging agents for the diagnosis and treatment of cancer.

Antibody therapy for cancer was used as early as 1895 when Hericourt and Richet immunized animals with human tumour extracts and gave the serum to patients resulting in some tumour responses (Hericourt and Richet, 1895). Polyclonal antibodies were used from the 1940's and shown to react with tumour antigens (for review - Boschoff and Begent, 1996). However, the development of hybridoma technology in 1975 by Kohler and Milstein allowed for the first time the generation of monoclonal antibodies with defined specificities (Kohler and Milstein, 1975). More recently techniques such as the development of phage technology for generating large libraries of monoclonal antibodies with the ability to select for desirable characteristics have further expanded the possibilities of monoclonal antibody therapy (Huse *et al*, 1989).

A normal immune response to a foreign antigen involves the activation of B-lymphocytes to secrete antibodies that bind to various epitopes of the antigen. This polyclonal antibody response has heterogeneous specificities and affinities. Each 'batch' of polyclonal antiserum made to an antigen is also variable. Monoclonal antibodies, however, bind to the antigen (a defined epitope) with one specificity and one affinity, and can be manufactured in large amounts in the laboratory under standard conditions. This 'uniformity' makes them more suitable for therapeutic use.

Genetic engineering has lead to the design of various antibody-derived molecules (Hawkins and Chester, 1996). A whole IgG antibody is 150kDa and consists of 2 variable light chains (V_L), 2 variable heavy chains (V_H), 2 constant light chains (C_L) and 6 constant heavy chains ($2xC_H1$, $2xC_H2$, $2xC_H3$) (**figure 1**). The domains of V_L, V_H, C_L and C_H1 make up the antigen-binding end of the molecule (Fab). The C_H2 and C_H3 domains comprise the Fc portion, which is important in recruitment of the host immune response and persistence of the antibody in the circulation.

Figure 1: Schematic diagram of whole IgG

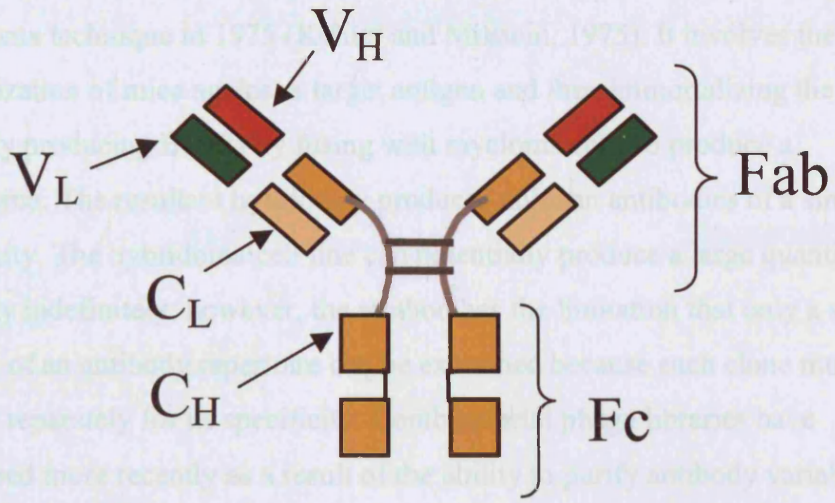

Diagrammatic representation of IgG, which consists of 2 variable light chains (V_L), 2 variable heavy chains (V_H), 2 constant light chains (C_L) and 6 constant heavy chains ($2xC_H1$, $2xC_H2$, $2xC_H3$). The Fab region of the molecule is associated with antigen interaction, and the Fc portion is involved in recruitment of effector cells.

Single chain Fv (scFv) are the smallest antibody fragments retaining full antibody specificity, but only remain stable if the V_H and V_L chains are joined by a flexible linker (Huston *et al*, 1988). A scFv has a molecular weight of 27kDa (**figure 2**).

Figure 2: Schematic diagrams of whole antibody and antibody fragments

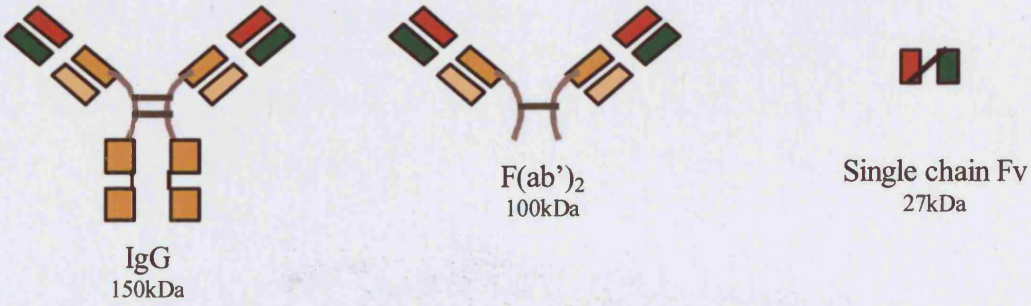

Diagrammatic representation of IgG, with the antibody fragments F(ab')$_2$, and scFv. The F(ab')$_2$, fragment consists of 2 variable light chains (V_L), 2 variable heavy chains (V_H), 2 constant light chains (C_L) and 2 constant heavy chains (C_H1). ScFv consists of 1 variable light chain (V_L), and 1 variable heavy chain (V_H) with a flexible linker.

The two main methods of generating monoclonal antibodies are hybridoma technology and combinatorial phage libraries. Kohler and Milstein developed the hybridoma technique in 1975 (Kohler and Milstein, 1975). It involves the immunization of mice against a target antigen and then immortalizing the antibody producing B cells by fusing with myeloma cells to produce a hybridoma. The resultant hybridoma produces uniform antibodies of a single specificity. The hybridoma cell line can potentially produce a large quantity of antibody indefinitely; however, the method has the limitation that only a small amount of an antibody repertoire can be examined because each clone must be studied separately for its specificity. Combinatorial phage libraries have developed more recently as a result of the ability to purify antibody variable region genes from populations of B cells by polymerase chin reaction (PCR) using specific primers. Copy deoxyribonucleic acid (cDNA) encoding Fab or V_H and V_L joined by a synthetic linker, is cloned into a bacteriophage genome where it encodes the antibody protein. If filamentous phage are used, the protein product can be displayed on the cell surface, therefore allowing the bacteriophage to be used directly to select for required specificity and binding characteristics (**figure 3**) (Huse *et al*, 1989; McCafferty *et al*, 1990; Chester *et al*, 1994; Verhaar *et al*, 1995).

Figure 3: Combinatorial phage library

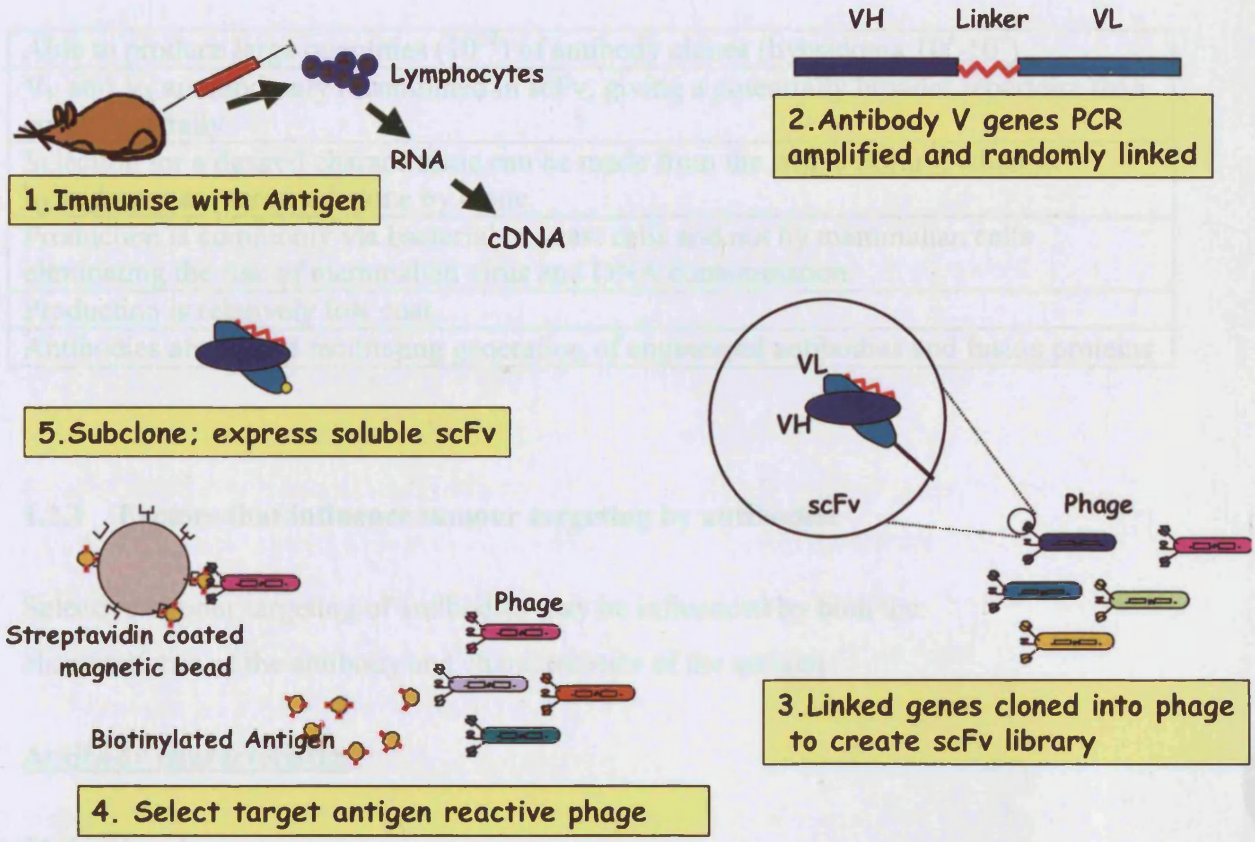

Schematic representation of generation of a combinatorial phage library Abbreviations: RNA- ribonucleic acid; cDNA-copy deoxyribonucleic acid; scFv-single chain variable fragment; V_H-variable heavy fragment; V_L-variable light fragment (reproduced with permission from K Chester).

The advantages of phage libraries over hybridoma technology are listed in **Table 1.**

Table 1: The advantages of phage libraries compared to hybridoma technology for the production of monoclonal antibodies

Able to produce large quantities (10^{12}) of antibody clones (hybridoma 10^3-10^4)
V_H and V_L are randomly recombined in scFv, giving a potentially broader repertoire than occurs naturally
Selection for a desired characteristic can be made from the whole library, whereas hybridomas are screened clone by clone
Production is commonly via bacterial or yeast cells and not by mammalian cells eliminating the risk of mammalian virus and DNA contamination.
Production is relatively low cost
Antibodies are cloned facilitating generation of engineered antibodies and fusion proteins

1.2.1 Factors that influence tumour targeting by antibodies

Selective tumour targeting of antibodies may be influenced by both the characteristics of the antibody and characteristics of the antigen.

Antibody characteristics

Molecular size

The molecular weight of an antibody influences both the penetration of the antibody into a tumour and the rate of clearance from the circulation. Large antibodies, such as IgG, escape from the vasculature into the tumour slowly and penetrate through the tumour slowly (Russell *et al*, 1992). They therefore tend to remain in peripheral areas of the tumour close to blood vessels (Buchegger *et al*, 1983; Pedley, 1996). Their larger molecular size reduces their renal clearance and they remain in the systemic circulation for longer. They have low tumour: blood ratios over the first 4-48 hours after administration, with peak tumour: blood ratios usually occurring at 72-96 hours post administration (Lane *et al*, 1994; Behr *et al*, 1995). Smaller fragments (scFv or Fab fragments) penetrate further into the tumour (Buchegger *et al*, 1983; Russell *et al*, 1992; Yokota *et al*, 1992; Begent *et al*, 1996). They also circulate systemically for shorter periods of

time due to rapid renal filtration (Colcher *et al*, 1990; Milencic *et al*, 1991; Verhaar *et al*, 1995; Begent *et al*, 1996). Positive tumour: blood ratios occur earlier than with whole antibodies, however, the rapid clearance from the circulation results in less total antibody available for tumour binding and lower absolute tumour antibody levels (Yokota *et al*, 1992, Pedley *et al*, 1993, Behr *et al*, 1995).

Affinity and avidity

Affinity is a measure of the strength of the bond between antigen and antibody. Measurements of affinity relate to equilibrium conditions, and can be expressed by a kinetic 'on-rate' and 'off rate'. The affinity of an antibody for its antigen is important for targeting especially when antigen concentration is low within a tumour. High affinity antibodies often have a slow 'off rate' (ie: once they bind antigen they remain bound to it) (Adams *et al*, 2001). These antibodies have been shown to deposit heavily in areas closely adjacent to tumour vasculature, with very little diffusion through the tumour (Adams *et al*, 2001). This phenomenon has been theorized to be due to a 'binding site barrier', which proposes that macromolecular ligands are prevented from penetrating tumours by their successful binding to their receptor (Fujimori *et al*, 1990; Weinstein and van Osdol, 1992). The barrier is greater with higher affinity antibodies. This may be overcome to some degree by increasing the administered dose of antibody or by prolonging the infusion time, but this may result in lower tumour to blood ratios as more antibody is present systemically (Fujimori *et al*, 1990). Low affinity antibodies, with a rapid off rate, diffuse further into the tumour, but are not retained for as long as higher affinity antibodies (Adams *et al*, 2001). They therefore do not achieve as selective targeting.

Affinity describes a univalent interaction, however natural antibodies are polyvalent (i.e.: have more than one binding site), which results in a much more stable interaction. Avidity is used to describe a monovalent or polyvalent interaction; the latter can result in a large improvement in functional affinity. For example, IgG, which is a bivalent molecule, has an approximately 1000-fold increase in functional affinity in comparison to a single Fab fragment (Hawkins and Chester, 1996). It has been demonstrated, using image registration

techniques to correlate radiolabelled antibody tumour distribution with tumour morphology, that bivalent and trivalent antibodies have longer retention in viable tumour areas compared to monovalent antibodies (Chester *et al*, 2000; Flynn *et al*, 2002).

Specificity and selectivity

The specificity of an antibody for its antigen will influence its biodistribution. Specific antibodies bind to the antigen within tumour areas and are retained for a period of time, whereas non-specific antibodies do not bind and are therefore not retained. The tumour to normal tissue ratio of specific antibody therefore steadily increases with time, whereas for a non-specific antibody the ratios will remain low. Microdistribution studies have shown that specific antibodies remain retained for longer in viable tumour areas, whereas non-specific antibodies pass quickly through to the necrotic centre of tumours, where there is little therapeutic potential (Flynn *et al*, 1999).

The selectivity of an antibody for its antigen will determine the likelihood of cross-reactivity with normal tissue. Cross-reactivity is undesirable as it results in unwanted toxicity and unfavourable targeting ratios.

Immunogenicity

Murine antibodies are immunogenic in humans and in the presence of an intact immune system lead to the production of human anti-mouse antibodies (HAMA). Repeated administration results in progressively shorter circulating half-life of the antibody, with poor tumour localisation and retention. It may also lead to immune reactions such as anaphylaxis and serum sickness. The development of chimeric antibodies with murine variable regions and human constant regions has greatly reduced problems of immunogenicity (Boulianne *et al*, 1984; Neuberger *et al*, 1985). 'Reshaped' or 'humanised' antibodies have also been developed, in which only the antigen binding site, rather than the whole variable domain, is transplanted from rodent antibodies onto human antibodies, with the advantage of potentially even further reduced immunogenicity (Riechmann *et al*, 1988). Chimeric or humanised antibodies can be given repeatedly usually with no

significant reduction in circulating half-life. The half-life of chimeric antibodies in humans is much longer than murine antibodies, with half-lives in serum of 10 days or longer being reported (Begent *et al*, 1990; Amlot *et al*, 1995). It also appears that having a human effector Fc arm of the antibody results in better recruitment of the host immune response in particular, cell mediated immunity. It is possible to develop human antibodies to chimeric antibodies – either to the murine variable region (anti-idiotypic antibodies) or to the human constant regions, although in clinical practice to date this has not frequently been a significant problem.

Other methods of reducing immunogenicity to murine antibodies include using smaller antibody fragments, adding polyethylene glycol or glycosylations to the antibody or suppressing the immune system with drugs such as cyclosporin.

Antigen characteristics

Tumours may express certain antigens that differentiate them from normal cells and therefore provide targets for therapy. Important characteristics of a target antigen include its tumour specificity, the presence of a soluble form, the antigen's normal function and the distribution of the antigen in the tumour (Chester and Hawkins, 1995; Hawkins and Chester, 1996).

Tumour specificity of target antigen

Tumour antigens may be unique to the tumour or they may be in relative abundance in tumours compared to normal tissues. Antigens that are unique to tumour cells are less common, and include immunoglobulin idiotypes in B cell lymphomas and mutated cellular proteins such as mutated epidermal growth factor in gliomas and non-small cell lung cancer (Garcia de Palazzo *et al*, 1993; Weiner, 1999).

B cell lymphoma/ leukaemia result from the abnormal proliferation of a single clone of transformed cells (Levy *et al*, 1977). These transformed cells all express a cell surface immunoglobulin that contains a unique epitope that may be used to differentiate the cancer cell from other normal cells (Levy *et al*, 1977). It is a

very specific target as there is no normal tissue expression, however therapies against this target must be tailor-made as the epitope is also unique to individual patients. Polyclonal anti-idiotype sheep antibodies were used in an attempt to treat chronic lymphocytic leukaemia as early as 1979 (Hamblin *et al*, 1980; Gordon *et al*, 1984). Although tumour shrinkage was not seen, there was a transient fall in peripheral lymphocyte count with therapy (Hamblin *et al*, 1980; Gordon *et al*, 1984). The first example of an anti-idiotype murine monoclonal antibody being used therapeutically in a patient with poorly differentiated lymphocytic lymphoma was reported in 1982 (Miller *et al*, 1982). After being treated with 400mg of anti-idiotype antibody the patient obtained a complete remission from their disease (Miller *et al*, 1982). This remission lasted for 6½ years (Brown *et al*, 1989). Many other patients have since received anti-idiotype therapy with reproducible anti-tumour effects (Brown *et al*, 1989).

Immunotherapy using anti-idiotype scFv fragments has also been used as a treatment strategy. V-region sequences encoding idiotypic antigen are isolated from tumours and then assembled as scFv (± Fc antibody fragment) and incorporated into an adenovirus vector (Armstrong *et al*, 2002). The recombinant vector is then administered and is used to produce host- generated anti-idiotypic antibody and T cell mediated tumour cytotoxicity (Armstrong *et al*, 2002).

Initially the generation of anti-idiotype antibodies took approximately 1 year for each patient, which limited their clinical applicability (Brown *et al*, 1989). Advancements in phage technology have greatly reduced the time for individual antibodies to be developed and this improves the likelihood of anti-idiotype therapy becoming more widely available (Miller *et al*, 1989).

Most tumour antigens are not tumour specific, but are present in much higher quantities in tumour than in normal tissues. Examples of these include oncofetal antigens (carcinoembryonic antigen, α fetoprotein), growth factor receptors (her-2 neu, epidermal growth factor receptor), differentiation antigens (CD20, CD25, CD33), stromal antigens (integrins, fibroblast activation markers) and antigens associated with hypoxia or neovascularisation (HIFα, vascular endothelial growth factor –VEGF). New targets are constantly being identified from the study of mutations, gene expression profiling and as a result of a proteomic

studies (Alizadeh *et al*, 2000; Martin *et al*, 2000; Vogelstein *et al*, 2000; Reidhaar-Olson and Hammer, 2001). Tumour targeting can occur with these antigens, if the normal tissue expression is minimal, in non-essential tissues or is inaccessible to antibodies. Several antibodies have shown efficacy and have now been licensed for therapy against these 'relatively' tumour-specific antigens. These include rituximab anti-CD20 antibody (Rituxan® Genentech Inc. and IDEC Pharmaceuticals Corporation) and trastuzumab anti-Her-2 neu antibody (Herceptin® Genentech Inc).

Circulating antigen

Some tumour antigens have a circulating form in addition to the tumour-bound component. This has proved useful in the clinical situation for monitoring conventional chemotherapy, or for screening for primary or recurrent cancer (Bidart *et al*, 1999). Tumour antigens which are commonly used for this purpose include carcinoembryonic antigen, α fetoprotein and human chorionic gonadotrophin. It can however pose problems in antibody targeting as circulating antibody binds the secreted antigen systemically, making less available for tumour localisation (Martin *et al*, 1984; Pedley *et al*, 1989; Boxer *et al*, 1992).

Cellular function of antigen

Antigens may be derived from molecules which have a cellular function, such as a growth factor receptor or a tyrosine kinase enzyme. The binding of antibody to antigen may therefore result in the 'switching-off' (blocking antibodies) or 'switching-on' (activating antibodies) of this function. Overexpressed growth factor receptors or constitutively expressed tyrosine kinase enzymes will lead to abnormal cellular regulation, and have been recognised as one of the steps of cancer development. Blocking growth factor receptors or enzymes may therefore control tumour growth. In addition the binding of an antibody to a receptor and activating it to cause down-stream signalling may be another method of attaining cytotoxic effect.

Antigen location and accessibility

Antigens are cell surface bound, or intracellular. Intracellular antigens require internalisation of the antibody for efficacy. Cell surface antigens are therefore more accessible for targeting. The distribution of the antigen within the tumour is also important as antigens expressed adjacent to tumour vasculature are more accessible from the systemic circulation than antigens in the deeper parenchymal region (Boxer *et al*, 1992; Russell *et al*, 1992).

Antigens are often heterogeneously expressed within a solid tumour (Hockey *et al*, 1984; Chung *et al*, 1994; Boxer *et al*, 1999; Flynn *et al*, 2001). A therapy or targeting system that relies upon each target cell expressing the antigen will therefore lead to selective therapy to antigen expressing cells, with a proportion of cells escaping. Antibody therapies that exert a bystander effect onto neighbouring cells are therefore theoretically more likely to be efficacious.

1.2.2 Therapeutic approaches using antibodies

Antibodies can be used as molecules that influence biological processes, or as targeting moieties, used to deliver radiation, toxins, cytotoxics or enzymes specifically to a tumour site.

Antibodies as biomodulators

The interaction of an antibody with its antigen may produce biological effects that can be exploited for therapeutic purposes. Antibodies may block access of growth factors, cytokines or other soluble factors by either binding directly to the soluble factor itself or by binding to its receptor (Glennie and Johnson, 2000). They thereby interrupt the growth stimulus to a cancer cell. Antibodies may also mark the antigen-expressing cell for activation of complement and recruitment of cellular effectors against the target cell (Glennie and Johnson, 2000). An example of this is the anti-CD20 antibody rituximab, which activates antibody-directed cellular cytotoxicity (ADCC) killing of the target lymphoma cells. A third mechanism of action may be through signalling pathways that occur when antibodies crosslink the target molecule and deliver transmembrane signals that

control cell division. Rituximab also appears to have a direct cell-signalling role in CD20 positive cells (Johnson and Glennie, 2001). These more complex interactions often rely on the Fc arm of the antibody for effector function and do not function as effectively when antibody fragments are used (Glennie and Johnson, 2000).

Antibodies as targeting agents

Antibodies also can be used as targeting vehicles to deliver radiation, toxins, cytotoxics or enzymes to tumours.

Radioimmunotherapy

Radioimmunotherapy utilises antibodies to deliver radioactivity, usually in the form of β emitting radioisotopes, to tumours. This has been an encouraging strategy in the treatment of radiosensitive tumours, such as lymphoma, where sustained tumour responses have been observed. High dose radioimmunotherapy with autologous bone marrow rescue using and an iodine-131 labelled anti-CD20 antibody produced a complete response rate of 84% and partial response rate of 10% in 19 patients with relapsed B cell lymphoma (Press *et al*, 1993). Many of these patients were heavily pre-treated, and the responses were often sustained, with a progression free survival of 62% after 2 years. These results suggest that some of the patients may have been cured by the high dose therapy, which illustrates the potential of radioimmunotherapy.

Zevalin® (Biogen Idec), Y-90-ibritumomab tiuxetan, is an yttrium labelled murine anti-CD20 antibody, which is the first agent used for radioimmunotherapy to receive Food and Drug Administration (FDA) approval in the USA. Ibritumomab is the murine parent of rituximab, and forms the antibody component of Zevalin®. Zevalin® is indicated in the treatment of patients with relapsed or refractory low-grade, follicular, or transformed CD20 positive B-cell non-Hodgkin's lymphoma, including patients with rituximab refractory follicular non-Hodgkin's lymphoma. The overall response rate in patients receiving Zevalin® was 80%, compared to those randomised to receive rituximab alone who had a response rate of 56% ([1]Witzig *et al*, 2002). Duration

of response was not significantly different between the two groups, and survival data has not yet matured. Non-haematological toxicity was similar between the two groups ([1]Witzig *et al*, 2002). In addition a study was performed in patients refractory to rituximab, which found that there was a 74% response rate to Zevalin® in this patient group ([2]Witzeg *et al*, 2002).

Radioimmunotherapy has been used in phase I/II clinical trials for the treatment of common solid tumours. It has, however, generally been associated with a much lower response rates than when haematological malignancies are treated (Lane *et al*, 1994). Responses appear more likely when smaller volumes of disease are treated (Behr *et al*, 2002).

Radioimmunotherapy has the advantage of a bystander effect, in that targeted radiation may cause DNA damage and cell death to antigen positive cells as well as adjacent antigen negative cells. However biodistribution and dosimetry studies reveal that it takes up to 24 hours until maximum antibody accumulation in tumour occurs and several days until background antibody clears and positive tumour to normal tissue antibody ratios are achieved. The absolute amounts of antibody retained in the tumour areas have been shown to be low when a radiolabelled antibody has been administered and tumour tissue radioactivity subsequently measured directly. One study showed that 0.001 of the total administered radioactivity was found in human tumours resected at an average of five post radiolabelled antibody administration (correction applied for radioactivity decay only) (Mach *et al*, 1980). A pre-clinical study showed that that the absolute amount of radioactivity in tumour after administration of tumour specific antibody was 0.015% of the injected dose per gram of tissue (Epenetos *et al*, 1986). The average tumour to normal tissue ratio obtained has been shown to be 5:1 - 10:1 (Mach *et al*, 1980; Lane *et al*, 1994; Wagner *et al*, 2002). Consequently a large amount of radiation may also be distributed elsewhere in the body resulting in haematological and other toxicities. Depending on the radioisotope chosen, radioimmunotherapy may also be associated with logistical problems such as the requirement for patients to be treated in specialist centres with appropriate radiation protection procedures in place.

Immunotoxins

Immunotoxins consist of an antibody linked to a cellular toxin, which is usually plant or animal derived. The antibody replaces the toxin's normal cell binding and internalisation domains in order to allow specific targeting of the toxin to an appropriate antigen on a cancer cell. The immunotoxin must usually be internalised into the cell for therapy as the toxin acts on intracellular targets such as ribosomes (Byers and Baldwin, 1988). These toxins have a very high potency and only a few molecules need to be internalised for effect. There is, however, no bystander effect, so theoretically each tumour cell must be targeted in order to produce 'cure'. A phase I study of an anti CD22 murine antibody linked to the immunotoxin, ricin A, was performed in 26 patients with refractory B cell lymphoma (Amlot *et al*, 1993). In 24 evaluable patients there was one complete response and five partial responses at 1 month (overall response rate 25%). The main side-effects were vascular leak syndrome and myalgia. The vascular leak syndrome was dose limiting. Responses were rapid (37.5% of patients had a > 50% reduction in size of tumours at 1 week) but generally not sustained (30-78 days for responders at 1 month). Vascular leak syndrome can be a serious problem, particularly when it involves the lungs and causes pulmonary oedema, which may be fatal.

More encouraging results were seen with BL22, which is an anti-CD22 Fv fused to a truncated pseudomonas exotoxin. When used in refractory hairy cell leukaemia eleven of sixteen patients attained a complete response, and a further two patients attained a partial response (Kreitman *et al*, 2001). The treatment was reasonably well tolerated, with only one patient developing a cytokine release syndrome (subsequent patients were pretreated with a cox-2 inhibitor and an anti-TNF antibody to prevent further episodes), and two patients developed haemolytic uremic syndrome (Kreitman *et al*, 2001).

Antibody-cytotoxic immunoconjugates

Antibodies may be used to target chemotherapeutics specifically to tumours. Initially it was hoped that this would improve the specificity of commonly used cytotoxics, however clinical trials to date with this approach have not been

encouraging (Tjandra *et al*, 1989; Elias *et al*, 1990; Tolcher *et al*, 1999). High potency cytotoxics, such as calicheamicin, conjugated to antibodies have, however, been more promising. CMA-676 (gemtuzumab ozogamicin; Mylotarg ® Wyeth Ayerst) is an immunoconjugate of a humanised anti-CD33 antibody with calicheamicin, which has be shown in clinical trials to produce responses in patients with refractory acute myeloid leukaemia (Sievers *et al*, 1999; Bernstein, 2000). It has recently been licensed for use in USA for the treatment of relapsed CD33 positive acute myeloid leukaemia in patients aged over 60.

Pretargeting strategies

Pretargeting strategies have been developed to improve therapeutic ratios between tumour and normal tissues. This is achieved in two or more steps. First, a targeting vehicle, which consists of an antibody with a tag attached, is administered. Once the tagged antibody has reached the tumour, a second conjugate is administered which will recognise the tag on the first antibody-complex (Stoldt *et al*, 1997). Ideally at this time the first antibody complex will be localised in the tumour, with minimal systemic retention. The second component is used to administer a cytotoxic effect, such as the delivery of radioactivity.

In a 2-step system the first antibody is allowed to clear by itself, and in a 3-step system a 'chaser' is given to accelerate systemic clearance of the first antibody. Without the use of a 'chaser' the antibody may take many days to clear to sufficient levels to administer the second molecule.

Pretargeting allows the generation or retention of high concentrations of the therapeutic molecule specifically in the tumour with reduced levels in normal tissues when compared with direct delivery systems such as radioimmunotherapy. Pretargeting systems have therefore the advantage of improved therapeutic ratios, with potentially less toxicity to normal organs. It has been predicted in mathematical models that the increase is up to 200% in tumour to background ratio (Zhu et al, 1998). The disadvantage is their added complexity and the requirement for careful timing and dosing in order to achieve high therapeutic targeting (Goodwin and Meares, 1997; Goldenberg, 2002).

Avidin-biotin systems, or streptavidin-biotin systems have been used for pretargeting and have feasibility for radioimmunotherapy and radioimmunoscintigraphy. Magnani *et al* demonstrated in patients undergoing enucleation for uveal melanoma using single photon emission computerised tomography (SPECT) imaging that the 3-step avidin-biotin system resulted in an increased tumour-to-nontumour ratio of 3.1 versus 1.5 for conventional radioimmunoscintigraphy (Magnani et al, 1996). Tumour responses have been demonstrated in patients treated with avidin-biotin or streptavidin-biotin pretargeting strategies (Stoldt et al, 1997; Paganelli et al, 1998; Grana et al, 2002). Avidin and streptavidin are, however, both immunogenic and opportunities for repeated therapy may be limited.

ADEPT is a pretargeted strategy, which utilises an antibody tagged with an enzyme as its first step, and a prodrug activation system as its effector function. Prodrug strategies are discussed in more detail below and ADEPT is further expanded in **section 1.4.**

1.3 Prodrug therapies for cancer

Anticancer prodrugs were being developed by Ross and Warwick as early as 1955 at Chester Beatty Research Institute (Bagshawe, 1987). The prodrugs were designed to be activated *in vivo* by enzymatic cleavage to release powerful alkylating agents. It was proposed that tumour specificity could be obtained by the cleavage of prodrugs by enzymes that were present in much higher concentrations in tumour than normal tissues (Connors, 1978; Carl *et al*, 1980).

One of their prodrugs, CB1954 (5-aziridinyl-2, 4-dinitrobenzamide), displayed impressive preclinical activity specifically in the Walker 256 rat carcinoma model (Cobb *et al*, 1969; Connors and Melzak, 1971). This tumour was found to express high levels of the enzyme, DT diaphorase, which activated the prodrug, CB1954 by a 2-electron reduction (Denny et al., 1996). Unfortunately CB1954 was subsequently found to be a much poorer substrate for human than rat DT diaphorase, which has limited its clinical applicability (Boland *et al*, 1991). CB1954 in the Walker rat carcinoma model however established the principle of tumour specific prodrug activation.

Aniline mustards were subsequently shown to produce 'cures' in established plasma cell tumours in mouse models (Whisson and Connors, 1965). Further investigation revealed that the therapeutic effect of aniline mustards were related to the enzyme, β glucuronidase, which was present at a 5 times greater concentration in the plasma cell tumours than in the normal mouse liver (Connors and Whisson, 1966). It was concluded that the therapeutic effect of the aniline mustards was as a consequence of glucuronide formation in the liver followed by the breakdown of the glucuronide-aniline mustard by β glucuronidase in the tumour to form a cytotoxic agent (Connors and Whisson, 1966). The high concentrations of β glucuronidase in the plasma cell tumours resulted in efficacy of the aniline mustard, whereas tumours with lower expression of β glucuronidase (sarcoma 180 and NK lymphoma) were more resistant to aniline mustard therapy (Connors and Whisson, 1966).

Bioreductive drugs are prodrugs that are selectively metabolised to cytotoxic agents in hypoxic areas (Connors, 1996; Denny *et al*, 1996). Tumours are known to have hypoxic regions, which are generally radioresistant and chemoresistant. It was initially proposed that bioreductive drugs would be activated in hypoxic conditions and kill hypoxic cells selectively. Subsequently it was suggested that if bioreductive drugs release a diffusible cytotoxic agent then a bystander effect could ensure a greater therapeutic potential by also having cytotoxic effects on surrounding normoxic tumour cells (Denny and Wilson, 1993). The activation of bioreductive prodrugs in hypoxic conditions may occur as a result of low pH, availability of oxygen for inactivation of chemical intermediates by chemical oxidation or by the presence of hypoxia specific enzymes, such as DT diaphorase (Denny *et al*, 1996). Mitomycin C is an example of a chemotherapeutic selectively activated by the enzyme DT diaphorase, which is present in hypoxia (Ross *et al*, 1993).

Capecitabine is a prodrug with tumour specific activation that has recently been developed and is in clinical use. Capecitabine is a fluoropyrimidine carbamate prodrug of 5FU. It is administered orally, is rapidly and almost completed absorbed in the upper gastrointestinal tract as an intact molecule, and is then converted by a 3 step enzymatic pathway to 5FU preferentially in tumour tissue

(Miwa *et al*, 1998; Judson *et al*, 1999; Twelves and Anthoney, 2000; Venturini *et al*, 2002). The first two enzymes involved in the conversion of capecitabine to 5FU, carboxylesterase and cytidine deaminase, are expressed mainly in the liver (Miwa *et al*, 1998). The final step depends on thymidine phosphorylase (TP), an enzyme that is present at higher concentrations in tumours than in normal tissues (Miwa *et al*, 1998). TP (also known as platelet-derived endothelial-cell growth factor; Pd-EGCF) expression in tumours is related to angiogenesis, enhanced tumour growth and invasion (Brown and Bicknell, 1998; Fox *et al*, 2001). It appears to be up-regulated by hypoxia and low pH, which are found in poorly perfused areas of tumours (Griffiths *et al*, 1997). It has been correlated with a poor prognosis in patients with colorectal cancer, non-Hodgkin's lymphoma, breast cancer, non small cell lung cancer and gastric cancer (Maeda *et al*, 1996; Takebayashi *et al*, 1996; Brown and Bicknell, 1998). TP activity measured in various types of human tumour tissues has been found to be 3-10 times higher in tumours than in normal tissue adjacent to the tumour (Miwa *et al*, 1998). The exception to this is the liver, where the enzyme activity was higher than in the other normal tissues. It has been demonstrated in mouse xenograft models of human breast and colorectal cancer that exposure to chemotherapeutic agents (paclitaxel, docetaxel, mitomycin C or cyclophosphamide) increases tumour TP activity 4-8 fold (Sawada *et al*, 1998; Endo *et al*, 1999). An increase in TP activity in tumours exposed to radiotherapy has also been shown (Sawada *et al*, 1999).

The tumour selectivity of capecitabine has been demonstrated in a study of 19 patients who had either primary tumours or liver metastasis resected after 5-7 days of oral capecitabine. In primary colorectal tumours the mean 5FU concentration was 3.2 times higher in tumour than in surrounding normal tissues ($p=0.002$), and tumour to plasma concentrations of 5FU exceeded 20 to 1 (Schuller *et al*, 2000). The ratio of 5FU concentration in colorectal tumours compared to other normal tissues was 8-10 to 1 (Schuller *et al*, 2000). The ratio of 5FU concentration in liver metastasis compared to adjacent normal liver was only 1.4 to 1 ($p=0.49$, not significant) (Schuller *et al*, 2000). This result confirms the colorectal tumour selective activation of capecitabine by TP. This effect is

much less pronounced in the liver where TP activity is approximately equal in tumour and normal liver.

Pharmacokinetic studies have shown that the maximum plasma concentration for both capecitabine and 5FU occurs at approximately 2 hours after oral administration (Reigner *et al*, 2001). The half-life of 5FU in plasma was approximately 0.75-1.15 hours (Reigner *et al*, 2001). This indicates that although 5FU may be preferentially formed in tumours it does circulate systemically. The area under the curve (AUC) for 5FU after administration of capecitabine is lower than after continuous 5FU infusion, however, it is likely that this circulating 5FU is resulting in toxicity to normal tissues which limits further dose escalation (Reigner *et al*, 2001).

Clinical studies have been performed with capecitabine and these have shown that the toxicities experienced were similar to those associated with infusional 5FU and included hand-foot syndrome, diarrhoea, nausea, vomiting, and stomatitis (Van Cutsem *et al*, 2000). Two large randomized phase III trials totalling 1207 patients have been undertaken to assess the efficacy of capecitabine compared to 5FU (Mayo regimen) for first line treatment of metastatic colorectal cancer (Hoff *et al*, 2001; Van Cutsem *et al*, 2001). Capecitabine showed a superior response rate (25.7% vs 16.7%, $p<0.0002$) with equivalent time to progression (4.6 months vs 4.5 months) and survival (12.9 months vs 12.8 months) when compared to 5FU (Twelves, 2002).

The efficacy of capecitabine is however limited by several factors. There is considerable variability in TP expression in colorectal tumours between patients. One study, in which TP expression by immunohistochemistry was measured in resected colorectal tumours (primary and liver metastasis) and adjacent normal tissue, showed that only 80% of patients had higher TP expression in the colorectal primary than in surrounding normal mucosa (Collie-Duguid *et al*, 2001). The range of tumour to normal tissue TP expression was 0.06-150.3 to 1 (Collie-Duguid *et al*, 2001). Normal liver has a higher level of TP activity than other tissues, resulting in lower ratios of TP for liver metastasis from colorectal cancer to background normal liver. The mean ratio of TP measured in liver

metastasis to background liver in the same study was 1.78:1 (range 0.35-17.23) (Collie-Duguid *et al*, 2001).

The rate limiting enzyme for the catabolism of 5FU is dihydropyrimidine dehygrogenase (DPD). DPD expression in colorectal tumours tends to be decreased compared to surrounding normal tissues, although, again, significant patient variability has been demonstrated (Collie-Duguid *et al*, 2001). Intratumoural gene expression of DPD has been shown to be inversely correlated with response to 5FU chemotherapy and to patient survival (Salonga *et al*, 2000). The efficacy of capecitabine has been shown in pre-clinical models to correlate very well with the ratio of TP:DPD levels (Ishikawa *et al*, 1998). This variability in both TP and DPD expression may therefore lead to a significant impact on efficacy of capecitabine in individual patients.

TP has been shown histologically to be concentrated in areas adjacent to necrotic tissue, where there is a low oxygen tension and low pH (Griffiths *et al*, 1997). This has implications for its effectiveness as a prodrug-activating enzyme. There may be problems with poor accessibility to systemically administered prodrug, and once the activated drug is formed the hypoxic and acidic environment may adversely affect its efficacy. Also the maximal drug concentrations will be formed in parts of the tumour where there are large numbers of cells that may already be dead, with less drug theoretically available to surrounding viable cancer cells.

5FU is an anti-metabolite with broad-ranging effects. It utilizes the same cellular transport and activation pathways as uracil, and once activated has effects on both deoxyribonucleic acid (DNA) and ribonucleic acid (RNA) (Sobrero *et al*, 2000). DNA synthesis is disrupted through inhibition of thymidine synthase (S phase specific effect). Incorporation of 5FU metabolites into both DNA and RNA results in alterations in its processing and function (non cell cycle dependent). Determinants of the factors important for sensitivity to 5FU are therefore complex, which leads to difficulties in the prediction of sensitivity and toxicity of 5FU in individual patients (Sobrero *et al*, 2000).

Drug resistance to 5FU has been identified. The resistance mechanisms that have been described include overexpression of thymidine synthase and reduced drug transport across the cell membrane, as well as increased DPD enzyme (Hughes and Calvert, 1999). The emergence of drug resistance to 5FU may reduce the effectiveness of capecitabine.

Capecitabine is therefore an example of a therapeutically useful prodrug, however its efficacy is limited by the low ratios of tumour to normal tissue enzyme levels. A strategy that can increase the tumour to normal tissue enzyme ratios may thereby result in improved efficacy for a prodrug system.

1.4 Antibody directed enzyme prodrug therapy (ADEPT)

1.4.1 Background

Antibody directed enzyme prodrug therapy (ADEPT) uniquely combines the advantages of antibody targeting therapies with those of tumour specific prodrug systems. It is a two-step pretargeting approach. The first step involves administration of an antibody-enzyme. The antibody is used to localise an enzyme specifically to a tumour. Once antibody-enzyme has cleared from the circulation an appropriate prodrug is administered. The prodrug is activated by enzyme at the tumour site, resulting in tumour specific therapy (Bagshawe, 1987; Bagshawe *et al*, 1988; Senter *et al*, 1988; Senter, 1990; [1]Bagshawe, 1994; [2]Bagshawe, 1994; [1]Blakey *et al*, 1995; Niculescu-Duvaz and Springer, 1995; Senter and Springer, 2001) (**figure 4**).

Figure 4: Schematic representation of ADEPT

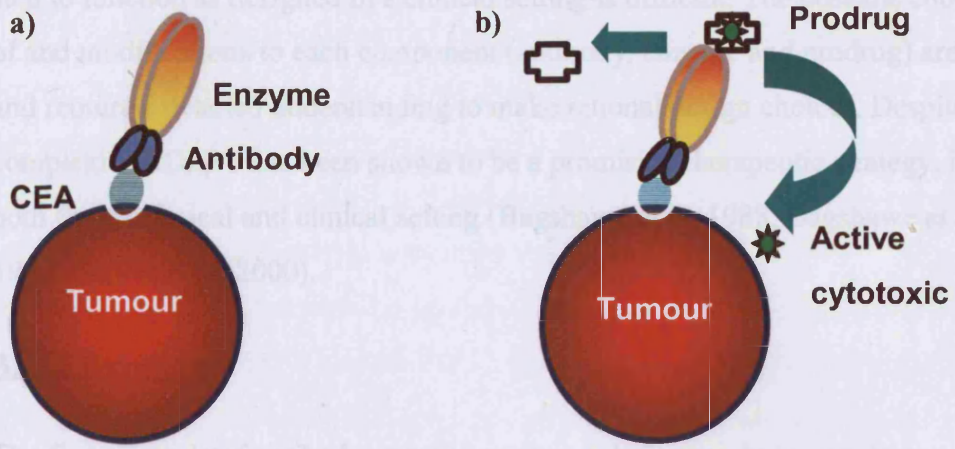

ADEPT is a pretargeting strategy, in which an antibody-enzyme complex is used to localise to tumour areas (a). This is followed by the administration of a prodrug, which becomes activated by enzyme at the tumour site (b).

ADEPT has several potential therapeutic advantages over conventional chemotherapy. It utilises antibody targeting to achieve tumour specificity. The two-step approach allows clearance of background enzyme to occur before the effector (prodrug/drug) is administered, further increasing tumour specificity and reducing the likelihood of systemic toxicity. One enzyme molecule can activate many molecules of prodrug thereby creating an amplification effect, which results in large amounts of drug being generated in the tumour. As active drug is generated extracellularly it can diffuse to neighbouring cells, resulting in cytotoxicity to both antigen positive and antigen negative cells (bystander effect). The amount of active cytotoxic generated at the tumour site should be much greater than could be administered systemically, consequently therapeutic efficacy should be improved and resistance mechanisms may potentially be overcome. The toxicity associated with conventional chemotherapy should be greatly reduced by targeting the treatment to tumours.

The disadvantage of ADEPT is that it is a complex multi-step treatment. The timing and dose of each component is crucial, and assessing the ability of each step to function as designed in a clinical setting is difficult. The possible choices of and modifications to each component (antibody, enzyme and prodrug) are vast and require a detailed understanding to make rational design choices. Despite this complexity ADEPT has been shown to be a promising therapeutic strategy, in both the preclinical and clinical setting (Bagshawe *et al*, 1988; Bagshawe *et al*, 1995; Napier *et al*, 2000).

ADEPT systems

The first example of antibody-enzyme conjugate being used to generate a cytotoxic agent was by Philpott in 1973 (Philpott *et al*, 1973). An antihapten antibody was conjugated to glucose oxidase and, in the presence of lactoperoxidase and iodide, was shown to result in selective iodination and cell killing of hapten substituted tumour cells. This effect was shown in a cell culture system only.

An ADEPT system was reported in a human xenograft model in1988 (Bagshawe *et al*, 1988). The $F(ab')_2$ fragment of an anti-human chorionic gonadotrophin antibody (W14) was chemically conjugated to the bacterial enzyme carboxypeptidase G2 (CPG2). This was administered to mice bearing human choriocarcinoma xenografts (Bagshawe *et al*, 1988). After sufficient time to allow accumulation in tumour and clearance from peripheral tissues, a benzoic acid mustard prodrug was administered. This prodrug was rapidly converted to drug by the CPG2 enzyme. Marked suppression of tumour growth was shown to occur after only one treatment, which was greater than achieved with commonly used cytotoxic agents (Bagshawe *et al*, 1988).

Senter also described an antibody directed prodrug system in 1988 (Senter *et al*, 1988). Anti-tumour monoclonal antibodies were covalently liked to alkaline phosphatase, and directed against antigen expressing tumour cells. Alkaline phosphatase was then used to convert relatively non toxic etoposide phosphate to the active cytotoxic, etoposide (Senter *et al*, 1988). In xenografts this system

showed delivery of the enzyme alkaline phosphatase to tumour, and, efficacy, with rejection of established tumours (Senter *et al*, 1988).

Many ADEPT systems have since been described utilizing different antibodies, enzymes and prodrugs (**table 2**). They may be classified according to the type of enzyme used, which may be non-mammalian or mammalian. Non-mammalian enzymes do not usually have human substrates, and so there are few problems with endogenous activation in non-target tissue. They are, however, immunogenic which may limit repeated exposure. Examples of non-mammalian enzymes used in ADEPT include CPG2, β-lactamase, penicillin G amidase and cytosine deaminase (Senter and Springer, 2001). Mammalian enzymes have problems with endogenous activation, which may reduce tumour specificity. However, they have fewer problems with immunogenicity than non-mammalian enzymes, and may be used in repeated therapies. Examples of mammalian enzymes used in ADEPT include alkaline phosphatase, carboxypeptidase A and β-glucoronidase (Senter and Springer, 2001).

Table 2: ADEPT systems

Enzyme	Drug formed	Reference:
Non-mammalian enzymes		
Carboxypeptidase G2	nitrogen mustards	(Bagshawe *et al*, 1988; Eccles *et al*, 1994; Bagshawe *et al*, 1995; Niculescu-Duvaz and Springer, 1995; Blakey *et al*, 1996; Napier *et al*, 2000)
β-lactamase	nitrogen mustard	([1]Vrudhula *et al*, 1993)
	doxorubicin	(Svensson *et al*, 1995)
	mitomycin	(Vrudhula *et al*, 1997)
	vinca alkaloids	(Meyer *et al*, 1993)
	paclitaxel	(Rodrigues *et al*, 1995)
	platinums	(Hanessian and Wang, 1993)
penicillin G amidase	doxorubicin, melphalan	([2]Vrudhula *et al*, 1993)
	palytoxin	(Bignami *et al*, 1992)
cytosine deaminase	5FU	(Wallace *et al*, 1994)
Mammalian enzymes		
alkaline phosphatase	doxorubicin	(Senter, 1990)
	etoposide	(Senter *et al*, 1988)
	mitomycin	(Senter *et al*, 1989)
	phenol mustard	(Wallace and Senter, 1991)
carboxypeptidase A	methotrexate	(Vitols *et al*, 1995; Perron and Page, 1996)
	antifolates	(Springer *et al*, 1996)
β-glucoronidase	doxorubicin	(Bosslet *et al*, 1992; Bosslet *et al*, 1994; Houba *et al*, 2001)
	phenol mustard	(Cheng *et al*, 1999)

Alternative enzyme-prodrug delivery systems

The use of an antibody to direct enzyme to tumour has some potential problems. The conjugation of the antibody to the enzyme may result in a large molecule, which will hamper penetration through tumour. Tumours are heterogeneous in their antigen expression and this may also reduce the likelihood of sufficient enzyme delivery. Also the conjugation process may either damage or result in conformal change in the antibody, which may affect subsequent antigen binding, and tumour specificity. Immunogenicity of non-human antibodies or enzymes will limit treatment repeatability.

The majority of these obstacles may conceivably be overcome with the development of genetic engineering techniques resulting in rationally designed genetic fusion proteins of antibody fragments with enzyme. Smaller, more stable and potentially less immunogenic molecules may be developed.

Several alternative strategies for delivering enzyme and prodrug selectively to tumours have also been developed, included the delivery of genetic code for enzymes to tumour cells, and the use of polymers as an alternative to antibody delivery systems.

VDEPT/ GDEPT

Virus-directed enzyme prodrug therapy (VDEPT) was first described in 1991 (Huber *et al*, 1991). It consists of a construct containing a tumour-specific transcriptional regulation sequence linked to the protein coding domain of a non-mammalian enzyme, which is delivered to tumour areas by a replication deficient retroviral vector (Huber *et al*, 1991). The transcriptional regulation sequence is used to allow selective expression the non-mammalian enzyme in tumour cells. A prodrug is then administered systemically and becomes activated in the tumour by the expressed enzyme. Huber described the system in hepatoma cells, with a varicella zoster virus tyrosine kinase being selectively expressed in α-fetoprotein positive cells (Huber *et al*, 1991). The prodrug used was araM, which was

converted by the varicella zoster virus tyrosine kinase to form araATP (Huber *et al*, 1991).

Gene directed enzyme prodrug therapy (GDEPT) similarly involves the tumour directed delivery of a gene encoding a foreign enzyme followed by administration of a suitable prodrug which is activated locally by the expressed enzyme. The delivery of the gene construct in GDEPT is usually via liposomal delivery systems (Xu and McLeod, 2001). Both VDEPT and GDEPT have inherent difficulties of vector delivery, and with expression of adequate amounts of DNA and consequently enzyme (Xu and McLeod, 2001). Most VDEPT/ GDEPT systems rely on the intracellular expression of enzyme and subsequent conversion of prodrug to drug. This may limit any bystander effect, unless the converted drug is able to diffuse out of the cell and act locally, or be transferred to adjacent cells through gap junctions or apoptotic vesicles (Greco and Dachs, 2001). The bystander is particular important in VDEPT/ GDEPT systems as it is unlikely that greater than 10% transfection rate of tumour cells will occur (Greco and Dachs, 2001).

Preclinical and clinical trials have been performed in GDEPT/VDEPT using the gene for herpes simplex virus thymidine kinase as the enzyme and with ganciclovir as the prodrug. Ganciclovir is converted 1000 fold more efficiently to its monophosphate form by herpes simplex virus thymidine kinase than by mammalian nucleoside monophosphate kinase (Greco and Dachs, 2001). Ganciclovir phosphate is then catalysed further by cellular enzymes to form toxic metabolites that interfere with DNA synthesis. Ganciclovir is S-phase specific so it is necessary that targeted cells are actively dividing for effect. The cytotoxic active metabolites of ganciclovir are highly charged and insoluble in lipid membranes – making cell-cell diffusion difficult (Greco and Dachs, 2001). This strategy has been promising in preclinical models, however in the clinical setting it has been less successful. This may be due to insufficient gene transfer throughout the tumour, the S phase specific effect of ganciclovir or to the dose limiting bone marrow effects of ganciclovir, preventing higher doses being administered (Greco and Dachs, 2001).

GDEPT has been studied in the preclinical setting using the bacterial enzyme CPG2 in combination with the mustard alkylating prodrug, 4-[2-chloroethyl)(2-mesyloxyethyl)amino]benzoyl-L-glutamic acid (CMDA) (Marias *et al*, 1996). This is the same combination that has been successfully used in ADEPT (**section 1.4.2**). It was shown that in cell culture of a variety of different cell lines, total cell kill could occur when only 4-12% of cells expressed CPG2 enzyme, indicating a substantial bystander effect (Marias *et al*, 1996). Three newer mustard prodrugs have recently been assessed in combination with CPG2 for GDEPT using preclinical human tumour xenografts in nude mice (Friedlos *et al*, 2002). These have shown improved potency over CMDA, and again demonstrated that if low cell transduction rates are attained, a large bystander effect is required for efficacy (Friedlos *et al*, 2002). One of the prodrugs used was a bisiodophenol mustard, ZD2767P, which is the prodrug used in the ADEPT clinical trials described in this thesis (**chapter 2 and 4**). ZD2767P was found to be the most potent of the three prodrugs used, however had less bystander effect. It was therefore most efficacious when there was a high proportion of cells expressing CPG2 (Friedlos *et al*, 2002).

PDEPT/ MDEPT

Polymer-directed enzyme prodrug therapy (PDEPT) utilizes polymer-enzyme complexes and polymer prodrugs. MPEG -directed enzyme prodrug therapy (MDEPT) utilises methoxypolyethylene glycol (MPEG) coated enzyme for tumour specific delivery. Polymer coated drugs and proteins may passively accumulate in tumours because of the leaky vasculature and poor lymphatic drainage of tumours (Satchi *et al*, 2001). This is referred to as the enhanced permeability and retention effect of tumours (Matsumura and Maeda, 1986). PDEPT/ MDEPT strategies do not require individualisation to tumours expressing different antigens and polymerized products tend to be non or minimally immunogenic. Early preclinical studies have shown minor therapeutic benefit, although further optimization is required (Satchi *et al*, 2001).

ADEPT, GDEPT/ VDEPT and PDEPT/ MDEPT are all based on the principle of delivery of enzyme to tumour, followed by administration and activation of prodrug. The mechanism of delivering enzyme differs for each system. Enzyme

may be delivered as a functioning protein (ADEPT, PDEPT), or its DNA may be delivered, and subsequently transcribed to functioning enzyme (GDEPT, VDEPT). The delivery of functioning enzyme obviates the complex process of transfection and subsequent transduction of DNA to protein in target cells, with all its associated problems. However there is the opportunity for greater tumour selectivity with GDEPT/ VDEPT as both selective gene delivery and selective promoter gene expression can be used to ensure tumour specificity. With ADEPT/ PDEPT if the targeting of functioning enzyme to tumour is poor, enzyme will be present in non-tumour sites and non-specific activation of prodrug will result in toxicity.

The advantages of using antibody to deliver enzyme to tumour over VDEPT/ GDEPT or PDEPT/ MDEPT strategies are summarised in **table 3**. The main advantages with antibodies are that there is the potential for good tumour targeting due to the specificity of antibody-antigen interaction. Intact enzyme is delivered, which obviates the need for complicated cellular DNA delivery and subsequent transfection and transcription. Enzyme is present extracellularly, rather than being generated intracellularly, which improves the availability to prodrug and increases the likelihood of a bystander effect. In addition, as will be outlined in **section 1.4.2**, significant progress has already been made towards the development of a successful ADEPT strategy in the clinical setting using a bacterial CPG2 enzyme, and mustard prodrug alkylating agents.

Table 3: Comparison of enzyme-prodrug systems

	ADEPT	VDEPT/ GDEPT	PDEPT/ MDEPT
Enzyme delivery system	Antibody	Viral vector or liposomal delivery system	Polymer or MPEG
Mechanism of attaining tumour specificity	Antibody-antigen interaction	Tumour specific transcriptional regulation sequences	Passive accumulation (leaky vasculature, poor lymphatics)
Enzyme functional status on delivery	Delivered intact and functional	Needs to be transcribed	Delivered intact and functional
Site of enzyme	Extracellular	Intracellular	Extracellular
Potential for bystander effect	High (enzyme accessible)	Low due to reduced accessibility of enzyme	High (enzyme accessible)
Potential for non-target tissue activation	Moderate due to potential for cross-reactivity or if poor systemic clearance	Low if both selective gene delivery and selective promoters used	High due to non-specific delivery system of active enzyme

1.4.2 ADEPT – A5CP in combination with CMDA

ADEPT with A5B7 F(ab′)$_2$ antibody chemically conjugated to the bacterial enzyme CPG2 (termed 'A5CP') in combination with benzoic acid prodrugs was first developed for colorectal tumours in 1989 (Bagshawe, 1989). This ADEPT system will be examined in some detail as it forms the basis for two subsequent ADEPT clinical trials that are the focus of this thesis.

The ADEPT system consists of four essential components: the target, the antibody, the enzyme and the prodrug/drug. Each of these components are expanded below for ADEPT with A5CP in combination with the benzoic acid prodrug, CMDA,

Target antigen - CEA

Carcinoembryonic antigen (CEA) is a cell surface glycoprotein expressed by most colorectal tumours, and a proportion of other common epithelial malignancies such as breast, pancreatic, gastric, lung and ovarian carcinomas (Hammarstrõm, 1999). It is an oncofetal antigen, which was first described and characterised by Gold and Freedman in 1965 (Gold and Freedman, 1965). It is a member of the immunoglobulin gene superfamily and is composed of a single polypeptide chain of approximately 688 amino acids and is highly glycosylated (Mitchell, 1998). It has one V-type and six C2-type immunoglobulin domains. The molecular weight of CEA is approximately 180kDa. The gene for CEA is on chromosome 19 (Hammarstrõm, 1999).

Attempts to crystallize CEA have been thwarted by its high carbohydrate content; however, its structure has been further elucidated by small angle Xray, neutron scattering and modelling (Boehm *et al*, 1996). Its length was found to be 27-33nm, and it was shown to be arranged with its seven domains (CEA 1-7) in an extended linear zig-zag pattern (Boehm *et al*, 1996; Boehm and Perkins, 2000).

CEA is expressed in normal adult tissue, with the main site being in the 'fuzzy coat' (glycocalyx) of the luminal surface on the top of the microvilli of the columnar epithelium of the colon (Benchimol *et al*, 1989; Hammarstrõm, 1999). It is also present to a small degree in the mucosa of the stomach, the squamous epithelial cells of the tongue, oesophagus and cervix, in sweat glands and in the epithelial cells of the prostate (Hammarstrõm, 1999). In a normal healthy adult approximately 50-70mg of CEA is released a day into the colon (Hammarstrõm, 1999). The normal function of CEA is not clear. Its strategic location and its structure suggest it may have a role in the maintenance of innate immunity. CEA may trap microorganisms in the glycocalyx and prevent them from invading the luminal gut cells (Hammarstrõm, 1999).

In colon cancer tumour cells lose their polarity and CEA is expressed on all surfaces (not just the luminal surface) (Benchimol *et al*, 1989; Hammarstrõm, 1999). CEA has been shown in tumour cell lines to act as an intercellular

adhesion molecule and may have a role in the metastatic potential of malignant cells (Benchimol *et al*, 1989). It has been proposed that overproduction of CEA leads to disruption of normal intercellular adhesion forces, which may contribute to tumourogenesis by creating abnormal tissue architecture or increasing metastatic potential (Benchimol *et al*, 1989; Ordoñez *et al*, 2000).

Systemically administered anti-CEA antibodies are not able to penetrate through to the luminal surface of the normal intestine due to the presence of tight junctions between cells. Consequently specific tumour targeting can be achieved.

CEA –related antigens occur in several tissues and cross-reactivity can be a problem with non-specific anti-CEA antibodies. The most common sites of cross reactivity are with granulocytes, monocytes, Kupffer cells, bile canaliculi, pancreatic acini and lymphocytes (Nap *et al*, 1992). This cross-reactivity has been shown to be as a result of shared epitopes between and CEA and these tissues (Nap *et al*, 1992). This cross-reactivity is independent of affinity (Nap *et al*, 1992). Most specific antibodies do not, however, have this cross-reactivity.

CEA also has a secreted form, which is released into the systemic circulation. Circulating serum CEA levels are used clinically to monitor response of patients to therapy, and for early detection of tumour relapses (Minton *et al*, 1985; Fletcher, 1986; Ward *et al*, 1993; Mitchell, 1998; Bidart *et al*, 1999). Raised circulating CEA levels at the time of surgical resection have also been shown to be an independent prognostic factor for survival (Lindmark *et al*, 1995; [1]Compton *et al*, 2000). The extent to which CEA is secreted into the systemic circulation varies for individual patients. A very high circulating CEA level may lead to reduced targeting efficiency of anti-CEA antibodies, as they bind to accessible CEA in the circulation, and are less available for binding to cell surface CEA in tumour areas (Boxer *et al*, 1992). In one study, serum CEA levels of > 2000μg/L was associated with the lowest amounts of tumour anti-CEA radiolabelled antibody localisation (Boxer *et al*, 1992).

CEA expression within tumours is heterogeneous, and antibody binding throughout tumours has been shown to be non-uniform (Boxer *et al*, 1992). This heterogeneity has proved to be a limiting factor for therapies that require

antibody internalisation, or utilise antibody-effector systems, as areas of the tumour may be unaffected. The bystander effect of ADEPT, provided by the diffusion of active drug locally in the tumour, has been designed to overcome this problem as it can result in cytotoxic effects to both antigen positive and antigen negative tumour cells.

In summary, CEA has the advantage of being a common target, present in the majority of patients with colorectal cancer, as well as some other solid tumour types (breast, pancreatic, gastric, lung and ovarian carcinomas). It is often abundantly expressed in tumour tissue. It is easily identifiable as a target on tumour tissue by immunohistochemistry on resected tumour specimens. It is expressed on some normal tissues, in particular on normal bowel epithelium, however this expression is on the luminal side of mucosal cells, which is inaccessible to systemically administered antibodies. The limitations of using CEA as a target includes its secreted form, which may lead to sequestration of antibody in the circulation with reduced tumour targeting, and its heterogeneous tumour expression, which may lead to inadequate tumour targeting. The first limitations may be minimised if patients with high serum CEA levels are excluded from treatment, and the second limitation may be overcome to some degree by the bystander effect of ADEPT, which will lead to cytotoxicity to both antigen negative and antigen positive cells.

Antibody-A5B7

A5B7 is an IgG1 murine antibody to CEA (Harwood *et al*, 1986; Pedley *et al*, 1987). The $F(ab')_2$ fragment of A5B7 has a molecular weight of 100kDa and is derived from whole A5B7 by enzymatic digestion with pepsin (Lamoyi and Nisonoff, 1983).

A5B7 whole IgG and $F(ab')_2$ fragment have been used extensively both preclinically and in clinical trials of radioimmunotherapy (RIT), radioimmunoscintigraphy and radioimmunoguided surgery (Blair *et al*, 1990; Dawson *et al*, 1991; Pedley *et al*, 1993; Lane *et al*, 1994). Preclinical studies of radioimmunotherapy demonstrated that twice the activity of I-131 radiolabelled antibody must be administered to produce the same therapeutic effect if the

$F(ab')_2$ fragment is used compared to whole antibody (Pedley *et al*, 1993). This is due to rapid circulatory clearance of the $F(ab')_2$ fragment which results in lower absolute amounts of radiolabelled antibody delivered to tumour. However, more favourable tumour to normal tissue ratios were attained with the $F(ab')_2$ fragment, in particular with less potential toxicity to bone marrow (Pedley *et al*, 1993).

Clinical trials have confirmed that A5B7 both as whole antibody and $F(ab')_2$ fragment localise effectively to CEA expressing tumours (Dawson *et al*, 1991; Lane *et al*, 1994). Gamma camera imaging was utilised to quantify biodistribution of radioimmunotherapy with I-131 radiolabelled A5B7 whole IgG and $F(ab')_2$ fragment (Lane *et al*, 1994). It was found that whole IgG A5B7 reached peak tumour concentrations of antibody at 27 hours, whereas the $F(ab')_2$ fragment reached peak tumour concentration approximately 4 hours after administration (Green *et al*, 1990; Lane *et al*, 1994). Tumour responses were seen in both patient groups (Lane *et al*, 1994).

As A5B7 is a murine antibody it is immunogenic in humans. Without the concurrent administration of immunosuppressive drugs only one administration is usually possible before HAMA form (Ledermann *et al*, 1991). The presence of HAMA may lead to rapid clearance of the administered murine antibody by the immune system, with inadequate tumour targeting, and may result in more serious complications including serum sickness or anaphylaxis.

The combination of the smaller molecular size of the $F(ab')_2$ fragment of A5B7 and its rapid tumour penetration made it suitable for combining with an enzyme to form an antibody-enzyme molecule for ADEPT.

Enzyme – CPG2

A number of bacterial and mammalian enzymes have been used experimentally in ADEPT systems (**see table 2**). As discussed previously, mammalian enzymes (alkaline phosphatase or β-glucuronidase) are usually non-immunogenic and therefore can be used repeatedly. They have the disadvantage, however, that, as they have human equivalents, endogenous enzyme may lead to non-specific

activation of prodrug and subsequent toxicity. Bacterial enzymes, such as β-lactamase and carboxypeptidase G2 (CPG2) have no human equivalent, so there should be very little chance of endogenous activation of prodrug. However bacterial enzymes are immunogenic, which limits the number of ADEPT treatments that can be administered.

CPG2 is a bacterial zinc metalloenzyme derived from *Pseudomonas* sp strain RS16 (Sherwood *et al*, 1985; Bagshawe, 1987). CPG2 catalyses the hydrolysis of folates to pteroates and L-glutamic acid (Sherwood *et al*, 1985). CPG2 is active *in vivo* as a dimer of 83 kDa (Sherwood *et al*, 1985; [2]Bagshawe, 1994). There is no known human equivalent. In addition to being a useful enzyme for therapeutic ADEPT systems, it also can be used to metabolise methotrexate to 4-(*N*(2,4-diamino-6-pteridinyl methyl)amino) benzoic acid. This has been used clinically in the treatment of methotrexate toxicity. The rate of formation of the metabolite from methotrexate can be used to estimate CPG2 enzyme activity in vivo (plasma or tissue samples), by correlating known CPG2 enzyme levels with the rate of metabolism of methotrexate (Blakey *et al*, 1996; Martin *et al*, 1997).

Antibody-enzyme conjugate – A5CP

A chemical conjugate was formed of the $F(ab')_2$ fragment of the murine anti-CEA antibody, A5B7, linked by a stable thio-ether bond to CPG2 (A5CP) (Melton *et al*, 1983). A5CP has a molecular weight of 180 kDa. The chemical conjugation process can result in some reduction in antibody binding or to enzyme activity and may lead to the formation of a heterogeneous product.

Preclinical studies were performed using A5CP in LS174T human CEA colorectal mouse xenograft models. This is a model with tumour CEA expression, with no circulating CEA. These preclinical studies indicated that clearance of A5CP from plasma was slow, and that a safe level of plasma CPG2 activity (<0.3U/mL) only occurred after 6-7 days, by which time tumour enzyme levels had also fallen (Bagshawe, 1989; Sharma *et al*, 1990; Sharma *et al*, 1991). The administration of prodrug before this time was fatal, due to high plasma CPG2 enzyme levels leading to systemic activation of prodrug.

A galactosylated murine IgG antibody directed to the active site of CPG2, SB43-gal, was therefore used to accelerate clearance of A5CP from the circulation (Sharma *et al*, 1990; Sharma *et al*, 1994). The mechanism by which SB43 inactivates CPG2 appears to involve binding at or near the active site of the enzyme, or at a distant site resulting in conformational change in CPG2 (Sharma *et al*, 1990). In order to prevent SB43 inactivating CPG2 in tumour sites, it was galactosylated, which allowed it to be cleared rapidly from the circulation by hepatic galactose-specific receptors (Thornburg *et al*, 1980; Bagshawe, 1989; Sharma *et al*, 1990; [2]Bagshawe, 1994; [1]Sharma, 1996). It was demonstrated that using SB43-gal, CPG2 enzyme could be cleared from the peripheral circulation, without significantly altering enzyme levels in the tumour or the amount of drug generated in the tumour (Rogers *et al*, 1995; [1]Sharma, 1996;). The administration of SB43 allowed prodrug to be given as early as 24 hours after A5CP without toxicity ([1]Sharma, 1996).

Prodrug

Ideally a prodrug for ADEPT should be a compound of low toxicity, which is converted, only by the action of one specific enzyme, to a highly cytotoxic active drug (Bagshawe, 1987). The active drug should be a small molecule, which is highly diffusible through a tumour (Bagshawe, 1987). Mustard alkylating agents have several properties that make them a rational choice as the drug/prodrug system for ADEPT. Their cytotoxicity is not cell-cycle specific so they have activity against both proliferating and quiescent cells. Solid tumours have large numbers of quiescent cells, which can be problematic for cell cycle specific drugs. Alkylating agents have activity against both well-oxygenated and hypoxic cells, which, due to the known poor perfusion of solid tumours, is again advantageous (Bagshawe, 1989). Low levels of resistance have been reported against alkylating agents by tumour cells, as they are not subject to multi-drug resistance (Frei *et al*, 1988; Ford and Hait, 1990). Alkylating agents exhibit dose dependent effects, which may be an advantage as ADEPT aims to selectively deliver much higher doses of drug to tumour sites than can be achieved with systemic chemotherapy (Frei *et al*, 1988). Chemical deactivation of mustard alkylating agents is feasible by using functional groups that are cleavable by

appropriate enzymes (Bagshawe, 1987; Bagshawe *et al*, 1988). These modifications can lead to > 100 fold differences in chemical reactivity between prodrug and drug ([1]Springer *et al*, 1991; Springer *et al*, 1995).

Benzoic acid mustard prodrugs that could be activated by CPG2 were developed for ADEPT. The chemical design required an aromatic ring to be linked to a glutamic acid moiety by an amide bond (Niculescu-Duvaz and Springer, 1995). This system minimises prodrug uptake into cells due to the two acidic functional groups, however, once the glutamate is cleaved and the drug is formed, it is much more lipophilic, and readily taken up into cells (Niculescu-Duvaz and Springer, 1995).

CMDA is a benzoic acid mustard prodrug which is activated by cleavage of a glutamate by CPG2. Its pharmacokinetic parameters are an IC_{50} of 100μM, K_m of 3μM and k_{cat} of $700s^{-1}$. (Niculescu-Duvaz and Springer, 1995; Senter and Springer, 2001). CMDA showed encouraging preclinical activity against both choriocarcinoma and colorectal human tumour xenografts (Bagshawe, 1989; [2]Springer *et al*, 1991; Blakey *et al*, 1993; [1]Blakey *et al*, 1995). It was therefore chosen as the first prodrug to be used in clinical trials of ADEPT.

1.4.3 ADEPT Clinical Trials with A5CP in combination with CMDA

Two clinical trials of ADEPT have been performed using A5CP in combination with CMDA for CEA expressing advanced colorectal tumours (Bagshawe *et al*, 1995; Napier *et al*, 2000). The galactosylated clearing enzyme, SB43, directed against the active site of CPG2 was used to accelerate clearance of A5CP from the peripheral circulation prior to prodrug administration.

The first clinical trial of this ADEPT system established that A5CP could be safely administered to patients at doses of 5000U-20 000U/ m^2 (Bagshawe *et al*, 1995). CMDA prodrug when administered alone to seven patients was inert and non-toxic, other than nausea and vomiting which may have been in part attributable to dimethylsulphoxide, in which CMDA had to be administered (Bagshawe *et al*, 1995). No active drug could be measured in serum when

CMDA was given alone, indicating that, as hypothesised, no endogenous activation was occurring.

An administration schedule was developed which involved infusing A5CP over 2 hours, followed 24 hours later by the clearing antibody, SB43-gal, as a continuous infusion. At 48 hours the CMDA prodrug was given as repeated bolus injections over 1-5 days (Bagshawe *et al*, 1995).

Myelosuppression was the main toxicity seen from ADEPT (Bagshawe *et al*, 1995). Active drug could be measured in plasma, which was thought to have been due either to leak-back of activated drug from tumour sites, or residual enzyme in the peripheral circulation, which may have activated CMDA peripherally (Springer *et al*, 1993). Plasma enzyme, at the time of prodrug administration, was below the detectable limit by spectrophotometric methotrexate reduction assay (0.02U/mL) (Bagshawe *et al*, 1995).

The bacterial enzyme CPG2, and the murine antibody, A5B7 were immunogenic, with all patients developing an immune response by day 10 unless immunosuppression with cyclosporin was given. The administration of cyclosporin allowed up to three cycles of ADEPT to be given over a 21day period (Bagshawe *et al*, 1995).

Tumour responses were seen – in seventeen patients who received ADEPT, there were four partial responses, one mixed response and three minor responses or disease stabilisations (Bagshawe *et al*, 1995). Response appeared to depend more on prodrug dose ratio than on plasma enzyme levels (Begent and Bagshawe, 1996)

The second clinical trial of ADEPT was a mechanistic study using fixed doses of A5CP, SB43-gal and CMDA (Napier *et al*, 2000). Ten patients with advanced or metastatic colorectal cancer who had previously received standard chemotherapy were treated with ADEPT. A5CP was administered at a dose of 10 000U/m^2. 24 hours later SB43-gal was administered as a constant infusion for 4 days, and CMDA was administered at a dose of 200mg/m^2 as a bolus injection at 48 hours, 72 hours and 96 hours after commencement of A5CP. The components of

ADEPT were measured in tumour and normal tissues in order to gain an understanding of whether effective conditions for therapy were met. Standard toxicity and response evaluations were also made.

The components of ADEPT measured were:

- Serum CPG2 enzyme levels measured by spectrophotometric and HPLC methotrexate reduction assay
- Tumour CPG2 enzyme levels from tumour biopsy specimens measured by methotrexate reduction assay on HPLC
- I-131 radiolabelled A5CP biodistribution in tumour and normal tissues assessed by quantitative SPECT analysis
- Prodrug and drug concentrations measured in plasma by high performance liquid chromatography (HPLC)
- HAMA and human anti-CPG2 antibody (HACPG2A) by enzyme linked immunosorbance assay (ELISA)

It was possible to demonstrate that at the time of prodrug administration the tumour: serum CPG2 enzyme levels exceeded 10 000:1 (Napier *et al*, 2000). Five patients had tumour biopsies performed with direct measurement of CPG2 enzyme levels, and these confirmed that tumour enzyme estimations by SPECT analysis of radiolabelled A5CP were valid. Median CPG2 enzyme concentration in tumour by HPLC (tumour biopsies) was 0.47U/g (range 0.32-0.62 U/g), and by SPECT it was 0.34U/g (range 0.19-0.63U/g). **Figure 5** shows the distribution of CPG2 enzyme in plasma and tumour after the administration of A5CP.

Figure 5: CPG2 enzyme levels in tumour and blood after administration of A5CP

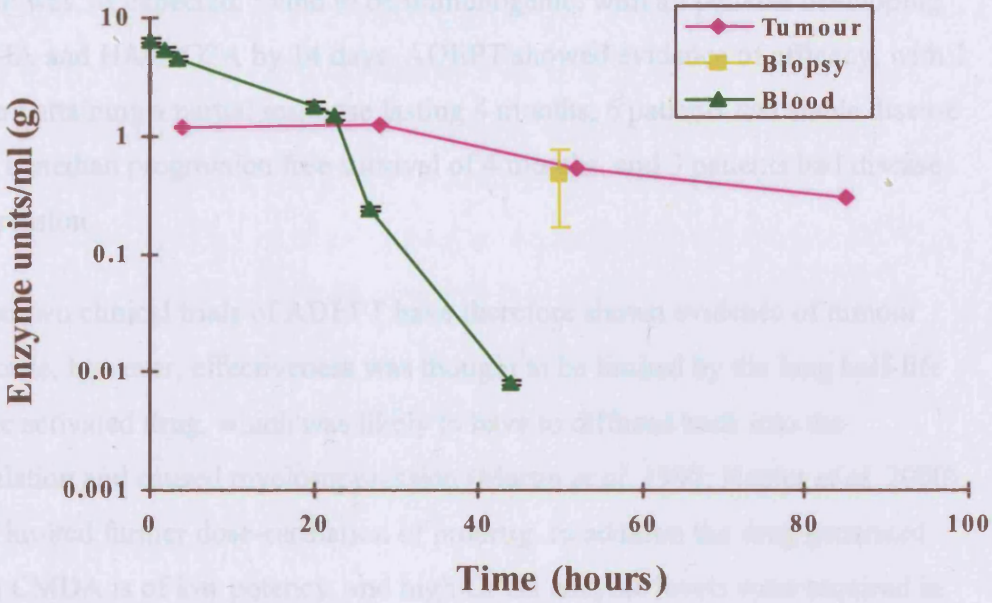

Biodistribution of A5CP after administration in ADEPT trial. SB43, a clearing antibody, was administered at 24 hours. CPG2 enzyme activity was measured in blood by spectrophotometric analysis (methotrexate reduction assay). Tumour A5CP localisation was measured by serial SPECT imaging of 1-131 radiolabelled A5CP and confirmed in a small number of patients with tumour biopsies, in which CPG2 enzyme activity was measured on HPLC (methotrexate reduction assay). (Napier *et al*, 2000)

The plasma elimination half-life of CMDA prodrug was 18 ± 8mins (Martin *et al*, 1997) The active drug was measurable in plasma and had a biological half-life of 36 ± 14 minutes (Martin *et al*, 1997).

ADEPT was well tolerated with dose-limiting toxicity consisting of myelosuppression. Four patients had common toxicity criteria (CTC) grade 3 or 4 neutropaenia or thrombocytopaenia. The median times to nadir were for 35 days for neutropaenia and 25 days for thrombocytopaenia (Napier *et al*, 2000). This was thought to be due to the presence of active drug in the circulation, which was likely to have occurred from leak-back after activation in tumour areas. It was unlikely to have been due to activation of CMDA by CPG2 enzyme in plasma, as at the time of prodrug administration plasma CPG2 enzyme levels

were undetectable (less than 0.001U/mL by HPLC) (Martin *et al*, 1997; Napier *et al*, 2000).

A5CP was, as expected, found to be immunogenic, with all patients developing HAMA and HACPG2A by 14 days. ADEPT showed evidence of efficacy, with 1 patient attaining a partial response lasting 4 months, 6 patients had stable disease with a median progression free survival of 4 months, and 3 patients had disease progression.

These two clinical trials of ADEPT have therefore shown evidence of tumour response, however, effectiveness was thought to be limited by the long half-life of the activated drug, which was likely to have to diffused back into the circulation and caused myelosuppression (Martin *et al*, 1997; Napier *et al*, 2000). This limited further dose-escalation of prodrug. In addition the drug generated from CMDA is of low potency, and high CPG2 enzyme levels were required in the tumour to create tumoricidal concentrations of drug. A prodrug that generated a more potent drug may not require such high levels of tumour CPG2 enzyme.

The targeting system used in these trials gave high tumour to blood ratios of antibody-enzyme conjugate (>10,000:1), and high tumour CPG2 enzyme levels at the time of prodrug administration (0.47U/g), however it required additional administration of a clearing antibody directed to the active site of CPG2. This adds a further level of complexity to the ADEPT system, and requires the addition of a potentially immunogenic antibody.

1.4.4 ADEPT – the next step

The experience gained in the clinical trials of ADEPT using A5CP in combination with CMDA indicated that in order to improve efficacy and reduce toxicity with ADEPT it was desirable to develop a new prodrug-drug system. In particular the drug formed from the activation of prodrug by CPG2 should have a short half-life to prevent 'leak-back' of activated drug into the systemic circulation. In addition it was hypothesised that if the drug formed from the activation of prodrug was of high potency that a tumoricidal effect may occur at lower tumour enzyme concentration than was required for CMDA. The clearing

antibody approach was a requirement when CMDA was used as a prodrug, as high tumour enzyme concentrations were required for efficacy. The clearing antibody allowed prodrug to be administered at 48 hours after antibody-enzyme, when high tumour enzyme levels were still present. Without a clearing antibody many days may be required for systemic CPG2 enzyme levels to fall to levels safe enough to allow administration of prodrug without systemic activation. Tumour enzyme concentrations will also fall during this time. A more potent drug should be tumoricidal at lower drug concentrations, and the tumour CPG2 enzyme levels attained at later timepoints without a clearance system, may be adequate to generate a sufficient concentration of drug for efficacy. This would obviate the need for the clearing antibody system, which is undesirable as it adds a further levels of complexity to an already complicated therapy, and introduces another immunogenic protein into ADEPT.

These were the working hypotheses that lead to the development of the ADEPT clinical trial outlined in **chapter 2.** The design of the clinical trial was carefully constructed in order to incorporate mechanistic measures to try and ascertain whether the components of ADEPT were functioning as designed on the clinical setting. The issues surrounding the design of mechanistic phase I/II clinical trials are discussed below.

1.5 Phase I/II clinical trial design

Phase I clinical trials of anti-cancer treatments conventionally aim to assess toxicity of a new treatment and to define the maximum tolerated dose (MTD) of the drug being tested. The standard pharmacokinetic profiles of the new drug are also assessed. A preliminary phase II component may also been included once a MTD has been defined. This will consist at looking at the efficacy of the agent in a small number of patients.

Patients who participate in phase I/II trials usually have incurable advanced cancer and have already pursued conventional treatment options. Some of these patients will have been very heavily pre-treated with chemotherapy and/ or radiotherapy, likely to make them more vulnerable to the side-effects of new therapies and less likely to respond to them. As the chance of a patient receiving

a therapeutic benefit during a phase I/II trial is minimal as few patients as possible should be treated.

1.5.1 Issues in the design of phase I/II clinical trials of anti-cancer therapies

Designing phase I/II clinical trials of anti-cancer drugs holds many challenges both practically and ethically. Basic issues which need consideration include the start dose, the dose escalation scheme, the number of patients required, the type of patient required (inclusion and exclusion considerations), and issues regarding patient information and informed consent.

Start dose and dose escalation scheme

In the majority of phase I clinical trials an agent being tested would not have previously been used in humans. Consequently, although the side-effect profile may be to some degree predicted from preclinical studies, the safety of the agent cannot be guaranteed and the dose that may cause toxicity is uncertain. Most phase I clinical trials conventionally will commence at a dose level which is thought to be very unlikely to cause toxicity. This is usually at a dose $1/10^{th}$ of the mouse dose required to be lethal to 10% (LD_{10}) from preclinical studies (Newell *et al*, 1999; Eisenhauer *et al*, 2000). At such a low dose there is a low chance of toxicity, however there is also a low likelihood of efficacy.

Until recently the standard method for escalation from the starting dose was by treating three patients at each dose level, and to use a 'Modified Fibonacci' dose escalation schema to direct further dose increments. An example of this schema is shown in **table 4**. Once any grade 3 or 4 toxicity is experienced, the cohort is expanded to 6 patients. Once 2 of 6 patients develop grade 3 or 4 toxicity dose escalation is stopped and dose limiting toxicity defined (DLT).

Table 4: Modified Fibonacci dose escalation schema

dose level	% increase in dose	actual dose (mg/m^2)
1 (start dose)		20 mg/m^2
2	100%	40 mg/m^2
3	50%	60 mg/m^2
4	33%	80 mg/m^2
5	25%	100 mg/m^2

This is an example of a modified Fibonacci dose escalation schema. A minimum of 3 patients are treated at each dose level – resulting in at least 15 patients being treated to take the dose from 20mg/m² to 100mg/m²

There has however, more recently, been criticism of this dose schema as it is likely that many patients will be treated at subtherapeutic doses with very little chance of benefit, and lengthy trials result which slow down the development process of novel agents (Ratain *et al*, 1993; Mani and Ratain, 1997; Eisenhauer *et al*, 2000). Although the response rates in phase I clinical trials are low, the majority of them occur within 80%-120% of the recommended phase II dose (Von Hoff and Turner, 1991).

An accelerated titration design has been proposed as an alternative to standard Modified Fibonacci escalation schemas. This involves an accelerated phase of dose escalation in which only one patient is treated in each cohort and dose escalations of 100% are made until grade 2 drug related toxicity is attained (Simon *et al*, 1997). After this the dose escalation is slowed and between three and six patients may be treated at each dose level. This was simulated and effectively shown to reduce the number of patients undertreated and to speed up the completion of phase I studies (Simon *et al*, 1997). Using dose doubling and one patient at each dose level commencing at 20mg/m² as in **table 4**, providing there was no dose limiting toxicity, four patients would be treated in order to reach a dose of 160mg/m². Using the Modified Fibonacci schema displayed, at least fifteen patients were required to be treated to reach a dose of 100mg/m². This highlights the advantages of accelerated titration schemas, as fewer patients are required to be treated at potentially subtherapeutic doses.

The disadvantage of this system is that little data is collected at the earlier timepoints, and therefore information on interpatient variability in toxicity or pharmacokinetics is not obtained (Eisenhauer *et al*, 2000). In addition, more

information than just toxicity may be useful, and will be unlikely to be collected in sufficient amounts by just treating one patient at each dose level. This may be important when an understanding of mechanism is part of the trial design. Accelerated dose escalation may also be problematic if the drug has a narrow therapeutic window. It is usually recommended that pharmacokinetic modelling is performed concurrently to try and minimise the likelihood of unexpected drug accumulation and subsequent toxicity (Cavalli and Sessa, 1999; Emilien *et al*, 2000).

The MTD is a dose below the DLT, at which toxicity is predictable and manageable. This is the dose that is usually recommended for phase II testing of efficacy. In reality an initial Phase II component is often incorporated into Phase I trials in order to obtain a preliminary idea of efficacy. Usually this will involve treating 14 patients at MTD. If no patient responds the investigator may conclude with 95% probability that the drug being tested has a response rate of less than 20% in the population tested (Ratain *et al*, 1993). If one or more patients respond the group is usually expanded to 25 patients in order further define efficacy.

Patient selection

The target group for a phase I/II clinical trial needs consideration. The trial should be performed in a tumour type for which the chance of therapeutic benefit is maximal. However, restricting the tumour type may reduce the rate of accrual and lengthen the development time (Mani and Ratain, 1997). As efficacy is not a primary endpoint of phase I clinical trials it may be argued that restricting the tumour type should be applied only to phase II trials, in which the assessment of efficacy is of primary importance.

For therapeutic strategies designed against a specific target or mutation, the presence of that target is an inclusion requirement. As ADEPT is a targeted strategy against CEA, it is required that patients have CEA expressing tumours. This may be assessed by immunohistochemistry of tumour resection or biopsy specimens, or by measuring serum CEA levels. Immunohistochemistry involves ascertaining the presence of CEA on tumour cells by using an anti-CEA antibody on fixed specimens. The amount of CEA present cannot be accurately quantified.

Measuring CEA in the blood is possible as CEA is a secreted protein. It is measured quantitatively by radioimmunoassay or ELISA, and expressed as micrograms per litre (μg/L). Low levels of CEA are found in the blood normally, however greater than 10 μg/L is considered abnormal. ADEPT is unlikely to be effective if there are very high levels of circulating CEA, as this will inhibit tumour targeting, and reduce antibody circulation time due to the formation of antigen-antibody complexes in the circulation (Boxer *et al*, 1992). Therefore the ADEPT trials are restricted to patients with a serum CEA level of less than 1000 μg/L.

Due to the uncertainty of both toxicity profiles and efficacy of agents in phase I trials, it is a usual requirement that patients who participate in them have locally advanced or metastatic cancer which is not curable by conventional treatments. In addition patients should have been offered standard chemotherapy or radiotherapy regimens. Some patients will prefer to try 'experimental' therapies in preference to conventional treatments and so may participate in phase I trials fairly early in their disease course, whereas other patients may only consider phase I/II clinical trials after they have exhausted all conventional treatment options.

Most phase I/II clinical trials will exclude patients with abnormal renal or hepatic function, as this may disrupt the metabolism of the agent being tested, leading to an increased likelihood of toxicity. In addition patients should have normal haematological parameters as they may otherwise be more vulnerable to myelosuppression. It is usually required that all toxicities from a previous chemotherapy regimen have resolved prior to commencing the phase I/II trial. Patients are excluded if they have a concurrent medical illness that could reduce their ability to tolerate the treatment or the trial protocol. It is usually stipulated that the life-expectancy of patients participating in phase I or II trials is at least 3-4 months, in order that they may be expected to complete the treatment and follow-up period. In addition patients are required to have a good performance status to be included in a phase I/II trial. Patients with a poor performance status are less likely to complete the trial and may be more at risk of serious toxicities.

Although efficacy is not a primary endpoint of phase I clinical trials, it is usually an inclusion requirement that patients have measurable disease according to standard criteria. Response assessments are included in the trial protocol and response data is collected. In addition the protocol will stipulate that patients should not be concurrently on any anti-cancer treatment and that a specified period of time should have elapsed between the completion of a previous therapy and the commencement of the clinical trial. This is to reduce the likelihood of additive toxicities and to ensure no confusion over the cause of a particular response.

Patient Information and Informed Consent

It is important that adequate patient information and informed consent are provided in Phase I clinical trials. It is therefore also a requirement that only patients who are able to understand the complexities of the trial and the information provided may enter the study. Information must be provided in a way that patients can comprehend. It is a difficult concept to have patients fully understand that phase I clinical trials are not focussed on efficacy, as it is this which is a patient's usual motivation for entering a trial. It is also difficult to obtain consent from a patient when the toxicities of a treatment are not yet known. It may be argued that part of informed consent should include updating patients with the progress of the trial to date, toxicities experienced and efficacy assessments (Ratain *et al*, 1993). This could be done verbally or with regularly updated patient information sheets or consent forms (Ratain *et al*, 1993). Another ethical concern is how to obtain consent from patients who are treated at the first few dose levels, when the therapeutic will almost certainly be ineffective. It must be recognised that the population in whom phase I/II cancer clinical trials are conducted are a vulnerable group as they have incurable cancer with a limited life expectancy, but a good performance status. Obtaining true informed consent may therefore be very difficult, as the agenda of the patient and the investigator may be quite different.

1.5.2 Mechanistic clinical trial design for ADEPT

The ADEPT system has been thought of as complex, as it involves the combination of antibody targeting, an enzyme activation system and a prodrug/cytotoxic drug system. Each of these components has their own unique requirements in order for the system as a whole to be successful, and understanding this system may only be possible when each component can be investigated individually. A mechanistic clinical trial design involves quantitatively measuring each component of ADEPT in order to ascertain if ADEPT is functioning as designed. It is hypothesised that by measuring mechanism, a greater understanding of ADEPT can be achieved. Additionally, rational modifications can be determined and implemented, thereby accelerating the development process. The collection of quantitative data is important, so that estimations of the amount of improvement required in order to attain efficacy can be expressed in numerical terms.

Designing phase I clinical trials to measure mechanism of a therapy may result in an increased number of interventions for each patient. This may be from an increase in number of blood tests to more invasive investigations such as complex radiological or isotope imaging studies or even tumour biopsies. However, the increased data obtained from each individual patient should ensure that overall fewer patients are required to be treated to ascertain if a new treatment is functioning as hypothesised.

In ADEPT the components of the mechanism that are essential for efficacy include the antibody mediated selective delivery of functional enzyme to tumour, the conversion of prodrug to drug, and the cytotoxic effect of activated drug. It would be desirable to be able to quantitatively measure each of these steps in a clinical setting. The ADEPT trials discussed within this thesis have utilised mechanistic studies in order to be able to make these quantitative measurements. The mechanistic studies are discussed in detail in the context of the clinical trials in this thesis.

A large amount of data may be acquired by undertaking mechanistic studies in a clinical trial. Interpreting the data may become difficult due to the volume of data

collected and the number of co-existing variables which may occur in each patient. A relational ontology is one means of organising this data in a logical way, to aid in interpretation of the data. An ontology for clinical trials of ADEPT has been developed using Protégé, which is a hierarchical Ontology tool. This subsequently may be used as a platform for developing a database to store the data or as a foundation for a model of ADEPT, which characterises the relationship between each of the components of the ADEPT treatment within a patient. The model may be defined mathematically, using either measured clinical data, predicted data based on experience acquired with ADEPT, or on preclinical data. The aim of collecting and organising all of this data is that it aids interpretation of ADEPT and should accelerate development of ADEPT by directing rational changes to the ADEPT system. These concepts are discussed in detail and applied in **Chapter 7**.

1.6 [F-18] FDG PET for response assessment

The ability to objectively measure response of a tumour to therapy is an essential element of clinical trials designed to assess efficacy of new cancer therapies, as well as being part of standard patient care. Assessments of response have been conventionally based on changes in dimensional measurements of tumours on standard radiological imaging modalities, such as CT scans. Although this is widely accepted and almost universally adopted, it is plagued by several limitations, which are discussed in detail below. Particularly problematic is the assessment of novel therapies, as the patient group in which they are tested are often heavily pre-treated and their biological mechanism may not be likely to attain more than disease stabilisation. A potentially promising agent may thereby be misleadingly discounted as 'non-efficacious'.

Previous trials of ADEPT have been associated with many patients with 'stable disease'. It is unclear whether this 'stable disease' represents 'some therapeutic effect' or 'no therapeutic effect'. As ADEPT is a treatment with very low systemic toxicity, the attainment of stable disease may be an acceptable endpoint, if the stable disease was actually as a result of some therapeutic effect. It is clear that a more sensitive method of assessment of therapeutic effect is required.

[F-18] fluorodeoxyglucose positron emission tomography ([F-18] FDG PET) has attracted considerable interest recently, particularly in the field of Oncology. It already has a role in the staging of patients prior to potentially curative surgical resections, and in the differentiation of benign from malignant lesions (Hustinx *et al*, 2002). However, it may also have an additional role, in the assessment of response to therapy.

1.6.1 'Conventional' response assessment

Phase II clinical trials of novel chemotherapeutics or other anti-cancer strategies rely upon objective evidence of response before they can proceed further in their development. Phase I clinical trials are now frequently adopting a phase II component in order to gain preliminary evidence of efficacy once safety had been established and the MTD has been defined. Additionally, in everyday Oncology practice in order to make an informed decision regarding a patient's response to chemotherapy, a formal response assessment is usually required.

The World Health Organization (WHO) in 1979, and Miller *et al* in 1981 published criteria for assessment of response based on radiological imaging or clinical findings in an attempt to standardise the reporting of response to cancer therapies (WHO, 1979; Miller *et al*, 1981). These criteria defined four terms which describe response to therapy; complete response (CR), partial response (PR), stable disease (SD) and progressive disease (PD). The method recommended use of bi-dimensional measurements of lesions, before and after treatment, to quantify change.

Over time it became clear that there were some areas of ambiguity in these criteria for response assessment and a new system, termed Response Evaluation Criteria in Solid Tumours (RECIST) was developed (Therasse *et al*,2000). The RECIST criteria are based on using the sum of maximal unidimensional measurements of tumours. These criteria more clearly define the 'measurability' of lesions, response criteria, recommended frequency of response assessments, response reporting and specifications for radiological imaging (Therasse *et al*, 2000).

Unfortunately there are limitations associated with these current methods of response assessment. The information displayed from conventional radiological imaging, such as CT scans, is anatomical. However, tumours are heterogeneous, and contain viable and necrotic regions (Flynn *et al*, 1999). These are not well accounted for on CT scans, Xray or MRI. An efficacious therapy should have an effect on the viable area of tumours, and it would be advantageous to be able to image and assess this. Current radiological techniques may lead to the misinterpretation of an area of necrosis as tumour, thereby under-representing an actual tumour response.

Problematic areas for accurate radiological measurements include skeletal metastasis, pleural or pericardial effusions or ascites, meningeal disease, inflammatory masses (eg: inflammatory breast tumours), interpretation of lesions which lie within previous radiotherapy fields, defining tumour from post-surgical or post-radiotherapy fibrosis, and diffuse tumours, such as pleural thickening or omental masses. Another problem area is the interpretation of lymphadenopathy, whether it is malignant or reactive, and defining 'complete response', as a residual lymph node mass usually remains post treatment. A method of assessing response that can identify tumour areas from non-tumour may overcome some of these problems.

Current radiological techniques, and the response criteria, assess tumours as two-dimensional objects, whereas in reality they have 3 dimensions (volumes). This may lead to misinterpretation of changes in size of lesions, due to a change in shape, or due to technical issues such as slice thickness for CT scans. A small lesion imaged on CT scan may be misinterpreted due to slice thickness, which may determine whether the lesion is imaged through its middle, or at its upper or lower edge.

It is also well recognised that in the treatment of solid tumours it may take many weeks for radiological imaging to show a reduction in size of a tumour. It is recommended that an assessment be undertaken at least 6-8 weeks after commencing a therapy (Therasse *et al*, 2000). Common practice is to assess for response after approximately 3 months of treatment. This may result in patients being exposed to potential toxicities from several cycles of treatment, before a

response evaluation can be made. An effective therapy, however, will be causing cytotoxicity and resultant tumour damage within hours of administration, and these effects should be assessable earlier than 6-8 weeks. Radiological imaging is insensitive to biological effects of treatment, and it is only when very significant changes have occurred in tumour size that they will be recognised.

Although the RECIST criteria have now much more clearly defined the procedure for radiological and clinical response assessment, the measurements do remain somewhat subjective, and inter-user variability can be problematic. It is recommended that for trials in which objective response rate is a primary objective, all responses be confirmed by an expert (Therasse *et al*, 2000).

In summary the limitations of conventional response assessment to therapy include not being able to define viable tumour from necrotic tissue or fibrosis, difficulty with measuring lesions that are poorly delineated, problems with representing three dimensional tumour volumes in two dimensions, insensitivity to the biological anti-tumour effect of treatments and measurement inconsistencies. These limitations are even more problematic when attempts are made to assess the effect of novel biological therapies, in which the aim may be for disease stabilisation, with minimal toxicity, rather than tumour shrinkage. In addition, patients who undertake phase I/II trials are often heavily pre-treated and the likelihood of them attaining a response to therapy maybe reduced. Therefore there is a need for a method of response assessment that reflects the biological change within tumours, rather than just tumour dimensions.

1.6.2 Positron Emission Tomography

Positron emission tomography (PET) utilises cyclotron produced proton rich radionuclides, which decay by positron emission. The nuclear conversion of a proton to a neutron releases a positron (a positively charged electron). This positron has kinetic energy and travels a small distance from the parent nucleus and then reacts with a neighbouring electron, resulting in an annihilation reaction. This releases energy according to $E=mc^2$, and thereby produces two photons each with an energy of 511keV at 180°to each other (Budinger, 1998) (**Figure 6**). Detectors placed around a patient will record 'co-incidences', which

are photon pairs that arrive simultaneously. The origin of the positron emitter must be along the line of the co-incidence. Computational reconstruction is then required to form a 3 dimensional image of the distribution of the emitter.

Figure 6: Diagrammatic representation of a positron emitting radionuclide

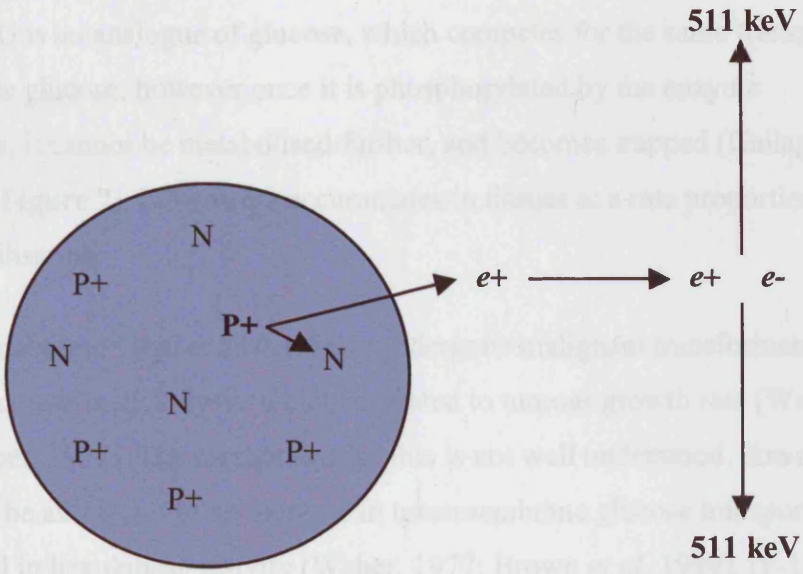

The nuclear conversion of a proton (P^+) to a neutron (N) is associated with the release of a positron (e^+), which leaves the nucleus and travels a short distance randomly in the surrounding tissue. It then collides with a neighbouring electron (e^-), and an annihilation reaction forms, which results in the release of 2 photons of energy of 511 keV at 180° to each other. This can be recorded as a 'coincidence' by surrounding detectors.

PET imaging has increased sensitivity over SPECT imaging, as there is no need for collimation to determine the line of source of the photon, this is instead determined by the path of the coincidence. Scattered and random events do occur, however they present less of a problem than with SPECT. Compton scatter may occur if a photon is deflected from its original path, with the resultant

effect of an inaccurate path of coincidence. This deflection results in loss of energy of the photon and consequently large deflections may be eliminated by energy windowing. Random events may result from coincident detection of two unrelated photons.

1.6.3 [F-18] Fluoro-2-deoxy-D-glucose ([F-18] FDG

Fluorine-18 is a positron-emitting radioisotope with a half-life of 110 minutes. [F-18] FDG is an analogue of glucose, which competes for the same transport into cells as glucose, however once it is phosphorylated by the enzyme hexokinase, it cannot be metabolised further, and becomes trapped (Gallagher *et al*, 1978) (**Figure 7**). It therefore accumulates in tissues at a rate proportional to glucose utilisation.

It has been observed that cells that have undergone malignant transformation have an increase in glycolysis, which is related to tumour growth rate (Warburg, 1956; Weber, 1977). The mechanism for this is not well understood, however, is thought to be as a result of an increase in transmembrane glucose transporters (GluT) and in hexokinase activity (Weber, 1977; Brown *et al*, 1999). [F-18] FDG is therefore taken up into malignant cells and retained, resulting in metabolic images of tumour glucose metabolism. [F-18] FDG that is not phosphorylated by hexokinase is excreted via the kidneys, unlike glucose, which is actively reabsorbed by the renal proximal tubule (Gallagher *et al*, 1978). Consequently background levels of FDG are lower than would be expected, and excellent tumour signal to background noise ratios can be attained.

The use of [F-18] FDG is originally derived from the work of Sols and Crane who studied carbon-14 [C-14] 2-deoxyglucose, and showed that 2-deoxyglucose was transported into cells in a similar way to glucose, but then becomes metabolically trapped (Sols and Crane, 1954). Sokoloff developed a three compartment model of regional glucose metabolism in the brain using [C-14] 2-deoxyglucose and autoradiography (Sokoloff *et al*, 1977). The principles of this work continue to be used today with dynamic cerebral [F-18] FDG PET kinetic modelling.

Figure 7: Representation of the metabolism of glucose and [F-18] FDG

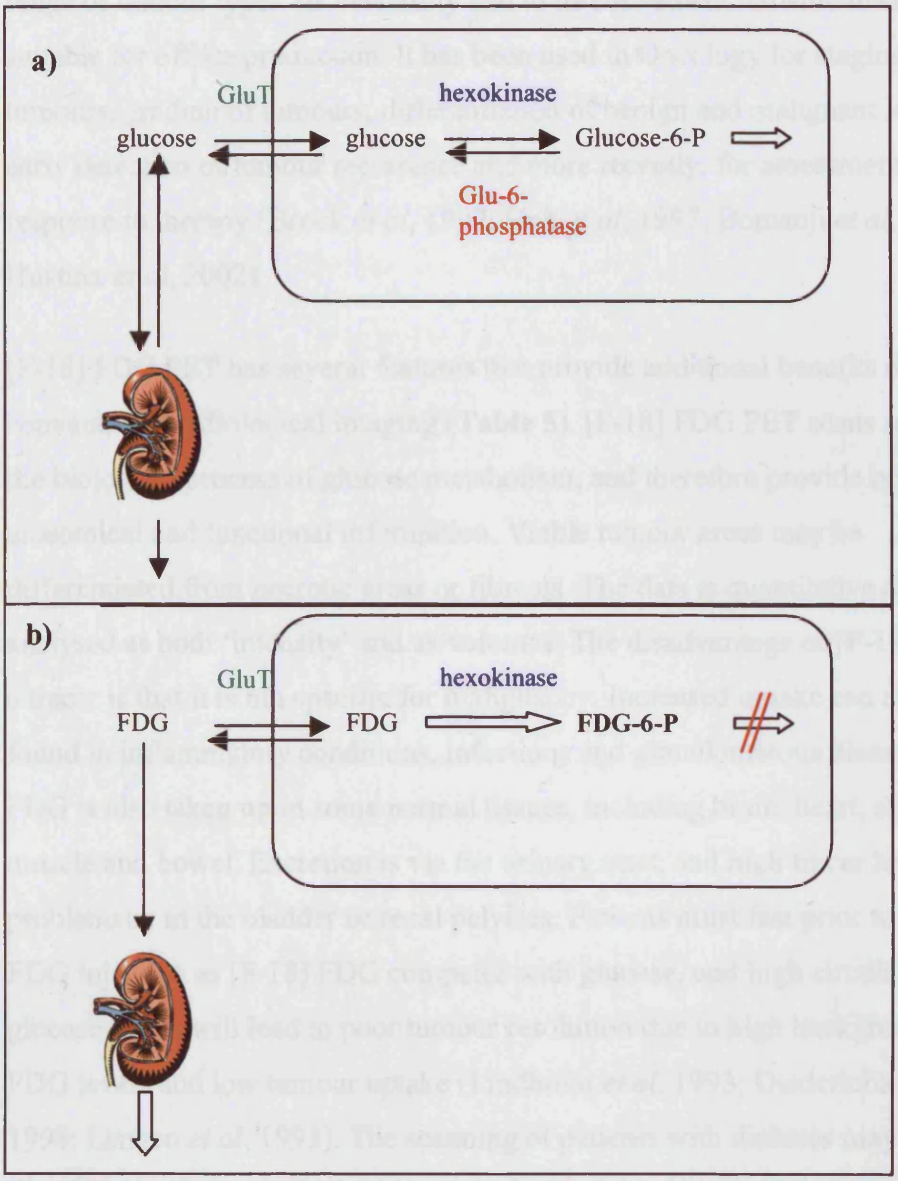

The differences in metabolism between (a) glucose and (b) [F-18] FDG are shown diagrammatically. [F-18] FDG is taken up into tumour cells by glucose transporters (gluT) in the same way as glucose, and is phosphorylated by hexokinase to form [F-18] FDG-6-phosphate. However, it is then trapped within the cell and cannot enter further metabolic pathways. There is very little dephosphorylation of [F-18] FDG-6-phosphate by the enzyme glucose-6-phosphatase, further increasing its intracellular accumulation. Glucose is actively reabsorbed by the proximal convoluting tubules of the kidney, however free [F-18] FDG is not, leading to rapid urinary clearance, and lack of accumulation in the systemic circulation and non-metabolising tissues.

[F-18] FDG has become the most widely used positron-emitting tracer in Oncology. This is due to its good imaging properties, its applicability to a wide range of tumour types, its versatility and to its convenient half-life making it suitable for offsite production. It has been used in Oncology for staging of tumours, grading of tumours, differentiation of benign and malignant lesions, early detection of tumour recurrence and more recently, for assessment of response to therapy (Brock *et al*, 1997; Hoh *et al*, 1997; Bomanji *et al*, 2001; Hustinx *et al*, 2002).

[F-18] FDG PET has several features that provide additional benefits over conventional radiological imaging (**Table 5**). [F-18] FDG PET scans represent the biological process of glucose metabolism, and therefore provide both anatomical and functional information. Viable tumour areas may be differentiated from necrotic areas or fibrosis. The data is quantitative and can be analysed as both 'intensity' and as volumes. The disadvantage of [F-18] FDG as a tracer is that it is not specific for malignancy. Increased uptake can also be found in inflammatory conditions, infections and granulomatous disease. [F-18] FDG is also taken up in some normal tissues, including brain, heart, skeletal muscle and bowel. Excretion is via the urinary tract, and high tracer levels can be problematic in the bladder or renal pelvises. Patients must fast prior to [F-18] FDG injection as [F-18] FDG competes with glucose, and high circulating glucose levels will lead to poor tumour resolution due to high background [F-18] FDG levels and low tumour uptake (Lindholm *et al*, 1993; Diederichs *et al*, 1998; Langen *et al*, 1993). The scanning of patients with diabetes may be problematic. Patients must also be rested after injection, as skeletal muscle uptake can make interpretation of scans difficult. An awareness of these limitations is therefore very important and careful patient preparation is required for optimal results.

Table 5: Comparison between CT scans and [F-18] FDG PET scans

	CT scan	[F-18] FDG PET scan
Image type	Anatomical	Anatomical and functional
Data set	2 dimensional data collected in representative slices	3 dimensional volume data (entire data set acquired)
Lesion Resolution	1-2 mm (depends on lesion size and location)	4-5 mm (depends on lesion size, location and metabolic activity)
Quantitation	Measurable by dimensions	Quantitative by intensity and volume
Patient preparation	Fast 2 hours Oral/iv contrast	Fast 4-6 hours Rest after injection (1 hour) Consider iv frusemide
Scan time	10-20 mins	45min-1 hour
False positives	Necrosis Post surgical fibrosis Post radiotherapy fibrosis	Infection Inflammation Granulomatous disease Normal tissues – heart, skeletal muscle, bowel, urinary tract

1.6.4 Gamma camera PET/ Coincidence PET

Full ring PET scanners are very expensive, and are not routinely accessible to most Cancer Centres. There are presently only nine PET centres in the United Kingdom. Also they can only be used for PET and not for any other form of imaging. Gamma cameras, however, are widely available and are commonly used in routine Nuclear Medicine Departments. Modification of gamma cameras in order that they may be used for PET imaging may allow greater accessibility and affordability to PET. This is especially relevant with [F-18] FDG as its 110 minute half-life makes it suitable for off-site production. In addition the high resolution of dedicated full ring PET scanners may not be required for all imaging indications. The serial assessment of response of tumour lesions that are detectable by CT scans may, it is proposed, be adequately assessed by a lower resolution PET scanner.

In 1994 ADAC Laboratories developed a system to detect 511 keV photons by a SPECT scanner without a lead collimator (Wagner, 1998). This was termed

'Molecular Co-Incidence Detection' (MCD). It utilises 2 detectors that rotate around the patient and detect 'coincidences' of 511keV photons that arrive simultaneously (within 15 nanoseconds). New high count rate digital electronics were required to transmit this information, and they allowed the use of thicker crystals (5/8 inch) without compromising the performance of the camera in SPECT mode (Patton and Turkington, 1998; Wagner 1998). Most radioisotopes used for SPECT imaging have low energy emissions (<200keV), compared to the high energy emissions of positron emitting radionuclides, and allowance for imaging of both high and low energy emissions had to be incorporated into the design.

Attenuation correction using Caesium-137 (Cs-137) point sources has been developed to allow attenuation correction to be applied to the emission scans. This greatly improves the image quality, especially in the thorax, where attenuation is non-uniform, due to the low density of lung tissue.

One of the limitations of gamma camera PET is reduced sensitivity compared to full ring PET. This is attributed to by the loss of coincidences that occur between the 2 detector heads, and the mechanics of the detector system used which is not as efficient as those used in full ring PET scanners. There is a problem with 'dead time' which is the recovery time required of the crystals before another co-incidence can be registered. Imaging of high levels of radioactivity will lead to flooding of the detectors and the relationship between activity and detected co-incidences becomes non-linear. This also results in poor image resolution.

The low count rate capability of gamma camera PET systems requires that less [F-18] FDG be administered compared to dedicated full ring systems. Usually 370-500MBq of [F-18] FDG is administered to patients who are having full ring PET, and, in comparison, 100-185MBq of [F-18] FDG is administered to patients having gamma camera PET. This is an advantage with respect to radiation protection for patients and staff, but a disadvantage for image quality.

Many studies have now been performed comparing gamma camera PET to dedicated PET systems for detection of malignant lesions (Shreve *et al*, 1998;Tatsumi *et al*, 1999; Landoni *et al*, 1999). A recent review concluded that

for tumours >15mm, the detection rate for gamma camera PET is fairly similar to dedicated PET (Ak *et al*, 2001). However, for lesions <15mm, the sensitivity of gamma camera PET is only approximately 80% compared to dedicated PET (Ak *et al*, 2001). This limits the usefulness of gamma PET for staging, as a number of small lesions may be missed. However, gamma camera PET is satisfactory and cost-effective in situations where the detection of small lesions is not required. This includes the differentiation of benign from malignant lesions, providing the lesion to be examined is >2cm, and for monitoring response to therapy, where a change in size or intensity of a lesion is important, rather than the detection of small lesions.

1.6.5 [F-18] FDG PET for response assessment

[F-18] FDG PET scans reflect the metabolic process of glucose metabolism occurring within cells, and therefore may provide a better indicator of tumour viability with treatment than conventional radiological imaging. There are an increasing number of papers being published in which [F-18] FDG PET scans have been used to assess response to cancer therapies (**Table 6**). Evidence is emerging that [F-18] FDG PET scans are a valid measure of tumour response. It is also apparent that [F-18] FDG PET scans are more sensitive predictors of response to therapy than radiological imaging. In particular, changes in tumour [F-18] FDG uptake with therapy precede, by weeks to months, any radiological changes. Studies have confirmed that response to chemotherapy may be predicted after 1 cycle of treatment (<3 weeks), as opposed to conventional response assessment with radiological imaging, which is usually performed after 2-3 months of treatment. Some studies are now suggesting that a reduction in [F-18] FDG uptake may commence in the first 24 hours after treatment (Demetri *et al*, 2002).

Response assessment by [F-18] FDG PET in a clinical trial setting is, however, currently limited by a lack of agreed standard assessment criteria or procedures. The timing of a [F-18] FDG PET assessment, the frequency of assessments, details of patient preparation parameters and scanning protocols have not been standardised. In addition, the method of quantitative analysis has not been agreed. Even less has been published with response assessment using gamma

camera PET than dedicated PET, with, to date, only one published trial utilising gamma camera PET for assessing response to therapy. This was a visual study, and was not quantitative (Kostakoglu *et al*, 2002). There is a need, therefore, for a standardised approach for response assessment with [F-18] FDG PET. In addition, a method of quantitative response assessment with [F-18] FDG PET using a gamma camera PET system is required, in order for it to become established as a possible means of assessing response to therapy in clinical trials.

In **chapter 5** a novel method for defining and quantifying change in tumour [F-18] FDG uptake using gamma camera [F-18] FDG PET is developed. This methodology is validated in 31 patients receiving standard first or second line chemotherapy for metastatic disease, and compared with conventional response assessment. **Chapter 6** outlines the application of quantitative gamma camera [F-18] FDG PET to the phase I/II ADEPT clinical trials and its role in the interpretation of radiological stable disease in this setting.

Table 6: [F-18] FDG PET studies of response of tumours to therapy.

Tumour type	No. of patients	Timing of PET	Method	Comment	Reference
Breast	30	Before the first, second and fifth courses of chemo, and at the end (neoadjuvant)	Kinetic analysis (Patlak) and SUV	PET after 1 course of chemo able to predict a complete pathological response (sensitivity of 90%, specificity 74%)	(Smith *et al*, 2000)
Breast	11	Pre, day 8, day 21, day 45 and day 63 after chemo/ hormone Rx (neoadjuvant)	Kinetic analysis and SUV	Reduction in tumour [F-18] FDG uptake in responders antedated any reduction in anatomical size of lesions	(Wahl *et al*, 1993a)
Breast	8	Pre, after 1st and 3rd /4th cycles of chemo	SUV	Reduction in tumour [F-18] FDG uptake occurs after first cycle of chemo	(Jansson *et al*, 1995)
Oesophageal	40	Pre chemo, and 14 days post chemo (neoadjuvant)	SUV	Reduction in tumour [F-18] FDG uptake at 14days correlated with histopathological response to chemotherapy, and survival	(Weber *et al*, 2001)
Oesophageal	36	Pre CRT and 1 month after CRT (neoadjuvant)	Visual Tumour to liver ratio (T:L ratio)	PET response correlated strongly with pathological response and survival	(Flamen *et al*, 2002)
Oesophageal	10	Pre CRT and 2 weeks after CRT (neoadjuvant)	SUV	Reduction in tumour [F-18] FDG uptake after therapy predicted responders	(Kato *et al*, 2002)
Colorectal	20	Pre chemo, 1-2 weeks and 4-5 weeks post chemo	SUV T:L ratio	Reduction in T:L ratio at 1-2 weeks and reduction in T:L ratio and SUV at 4-5 weeks correlated with response.	(Findlay *et al*, 1996)
Germ cell tumours	23	Pre and after 2-3 cycles of induction chemo (prior to HD)	SUV	Reduction in tumour [F-18] FDG uptake predicted response to HD therapy, and correlated with survival	(Bokemeyer *et al*, 2002)
Lymphoma	24	Pre, after 3 cycles induction chemo, before and after HDT	SUV	Reduction in tumour [F-18] FDG uptake during induction chemo correlated with survival	(Cremerius *et al*, 2002)

Lymphoma	30	Pre chemo After 1 cycle After completion of chemo	Visual analysis	Gamma camera coincidence PET Residual disease on PET after 1 cycle of chemotherapy strongly correlated with early relapse, and complete response on PET correlated with prolonged progression free interval	(Kostakoglu *et al*, 2002)
Lymphoma	11	Pre chemo, 1 week and 6 weeks after chemo	Kinetic analysis (Patlak) and SUV	Responders had reduction in [F-18] FDG uptake at 1 week and 6 weeks. 6week [F-18] FDG PET predicted long-term outcome	(Römer *et al*, 1998)
NSCLC	32 (16 had pre+post scans)	Pre chemo and 2 weeks after completion CRT (neoadjuvant)	Kinetic analysis	Model used to correlate residual tumour glucose metabolism with pathological complete response	(Choi *et al*, 2002)
NSCLC	15	Pre chemo and after 3 cycles of chemo (neoadjuvant)	SUV	[F-18] FDG PET accurately assessed mediastinal lymph node downstaging post chemo and correlated with survival	(Vansteenkiste *et al*, 1998)
Paediatric bone sarcoma	26	Pre chemo and after completion chemo (neoadjuvant)	SUV	Tumour [F-18] FDG uptake correlated with histological response to chemo	(Hawkins *et al*, 2002)
Mixed	26	1 week before 2 weeks after completion of treatment	Tumour to muscle ratio (static scans) TUR (dynamic scans 10-60mins)	Some correlation with CT response found	(Ichiya *et al*, 1991)

This table outlines fifteen studies that have been performed to assess the utility of [F-18] FDG PET in the assessment of response to chemotherapy. All trials demonstrated the ability of [F-18] FDG PET to detect response to chemotherapy, and many showed that [F-18] FDG PET can predict response after only one 1 cycle of treatment. Evidence is also emerging that response to chemotherapy on [F-18] FDG PET may predict survival. Unfortunately there is no standardised protocol for scan times, method of analysis and outcome measures. Also the number of patients in each trial is small, with the maximum number of patients being 40.
Abbreviations: SUV-standardised uptake value; TUR – tumour uptake ratio; T:L ratio- tumour to liver ratio

1.7 Thesis overview and hypotheses

Three major hypotheses will be tested in this thesis.

(a) That a mechanistic approach to clinical trial improves the understanding and development of ADEPT

This hypothesis will be examined in **chapters 2-4** with the presentation of two successive Phase I/II clinical trials of ADEPT. The clinical trials were hypothesis led, with a mechanistic design employed in order that the hypotheses proposed at the initiation of the clinical trials could be answered by the data collected during the trial. This represents a change from the traditional phase I/II dose escalation and toxicity assessment trial protocols, which do not primarily assess the mechanism of action of therapeutic agents. It is proposed that by measuring mechanism a greater understanding of ADEPT may be attained and that the development process may thereby be rationally modified.

(b) That a quantitative method of metabolic response assessment in ADEPT may augment the assessment of response in a phase I clinical trial setting, and in particular it may aid in the interpretation of radiological stable disease.

The assessment of response in Phase I/II clinical trials has conventionally been by anatomical imaging, such as CT scans. The emergence of [F-18] FDG PET as a means of assessing both anatomic and metabolic change in a tumour after therapy may lead to improvements in the assessment of efficacy in phase I clinical trials. This may ensure that a non-optimised treatment is not pre-emptively discarded from further development. **Chapter 5** discusses the development and validation of a method of quantitatively measuring change in tumour [F-18] FDG uptake after therapy using gamma camera [F-18] FDG PET. This method takes into account changes that occur in tumour size and intensity, and employs an automatic program to improve reproducibility and efficiency. **Chapter 6** outlines the application of this methodology to the phase I/II ADEPT clinical trials, and the interpretation of the results obtained.

(c) That the organisation of the data collected in the ADEPT clinical trials into an Ontology and Conceptual Model of ADEPT can direct mechanistic clinical trial design and identify areas for improvement in ADEPT

Chapter 7 discusses the development of an Ontology and Conceptual Model of ADEPT designed to provide a framework for the collection of data relating to ADEPT. It is argued that with a complex therapy combined with the large quantity of data generated from mechanistic clinical trials, that organisation of this data is required in order to enhance understanding of ADEPT. It is hypothesised that the organisation of the data may lead to the identification of areas in which a mechanistic trial design may be augmented and the proposal of rational strategies for improving ADEPT. The Ontology and Model will be discussed with particular focus on those areas examined in most detail in **chapters 2-6** of this thesis. In addition, those areas identified as potentially being important in order to improve ADEPT will be discussed and priorities for further work established.

This thesis will demonstrate that complexity should not be a hindrance to therapy, as long as the system can be successfully studied *in vivo*, in order that improvements to the system can be logically made. In fact, as the process that leads to the development of cancer is complex, it in increasingly likely that it will take a complex strategy to counteract it. The principle of trying to measure mechanism and from that deriving data that can be organised into an understanding of a therapy is the pervading theme of this thesis. ADEPT is used as the therapeutic example here, but many of the principles of mechanistic clinical trial design and data organisation are widely applicable to phase I/II clinical trial design and rational therapeutic development.

2 ADEPT clinical trial - A5CP and ZD2767P

2.1 Background

ADEPT is a two-step targeted therapy designed to generate large quantities of cytotoxic agent specifically in tumour sites, therefore potentially overcoming resistance mechanisms and reducing systemic toxicities associated with conventional chemotherapy. The principles of ADEPT and the evolution of its development are outlined in **chapter 1**.

As outlined in **chapter 1**, two clinical trials have been undertaken with ADEPT using CEA as the target, A5CP as the antibody-enzyme and CMDA benzoic acid mustard as the prodrug (Bagshawe *et al*, 1995; Napier *et al*, 2000). A5CP consists of the $F(ab')_2$ fragment of the murine anti-CEA antibody, A5B7, chemically conjugated to the bacterial enzyme, carboxypeptidase G2 (CPG2). These trials also utilised a galactosylated second antibody directed against CPG2 (SB43-gal) to clear active CPG2 enzyme from the peripheral circulation before prodrug could be administered.

Studies performed during these clinical trials confirmed adequate tumour targeting of A5CP with tumour to blood ratios of CPG2 enzyme of >10 0000:1, and tumour CPG2 enzyme levels of 0.47 U/g in tumour biopsies, which was sufficient for activation of CMDA prodrug. Evidence of activation of CMDA into its active drug was attained, as active drug was measured in the systemic circulation. The active drug formed from CMDA however, had a long biological half-life of 36 minutes (Martin *et al*, 1997). It was likely that this long half-life resulted in leak-back of the drug into the peripheral circulation from the tumour and caused the dose-limiting myelosuppression seen (Napier *et al*, 2000). In addition, the low potency of the drug formed from the activation of CMDA meant that high tumour enzyme levels were required for generation of tumouricidal concentrations of drug. This was achieved by using the second antibody clearance system, in order to allow administration of prodrug at 48 hours when tumour CPG2 enzyme levels were high. The second antibody system

was, however, undesirable as it was immunogenic and added further complexity to ADEPT.

The experience gained in these clinical trials lead to three new hypotheses designed to improve ADEPT:

1) The utilisation of a prodrug that forms an active drug with a short half-life may prevent 'leak-back' and subsequent toxicity seen with CMDA. This may improve tumour selectivity and consequently allow more drug to be administered with improved efficacy.
2) A high potency active drug may lead to tumouricidal effects at lower drug concentrations than were required for efficacy from CMDA. Less CPG2 may therefore be required in tumour at the time of prodrug administration for generation of tumouricidal concentrations of active drug. Thus, it may be possible to achieve adequate tumour enzyme targeting using A5CP without a clearing antibody system. This would reduce the complexity of ADEPT.
3) The design of a phase I/II clinical trial should be mechanistic, and therefore allow a maximum of understanding about ADEPT. This will rationally direct modifications of ADEPT for the future.

2.1.1 ZD2767P

A new candidate prodrug was required for ADEPT to attain the desired characteristics of short half-life and high potency of the active drug. Phenol and aniline-mustard prodrugs were considered as it was demonstrated that oxycarbonyl and carbamic linkages were also substrates for CPG2 (Niculescu-Duvaz and Springer, 1995). These prodrugs, when activated, produce potent phenol and aniline mustards.

ZD2767P (4[*N*,*N*-bis (2-iodoethyl) amino] phenoxycarbonyl L-glutamic acid) is a bis-iodo phenol mustard which is converted by the cleavage of glutamate by CPG2 to its active mustard drug, ZD2767D (4[*N*,*N*-bis(2-iodoethyl) amino] phenol) (**figure 8**). It was designed specifically for ADEPT by Dr CJ Springer (ICR) and Mr RI Dowell (AstraZeneca Ltd).

Figure 8: Chemical structure of ZD2767P and ZD2767D

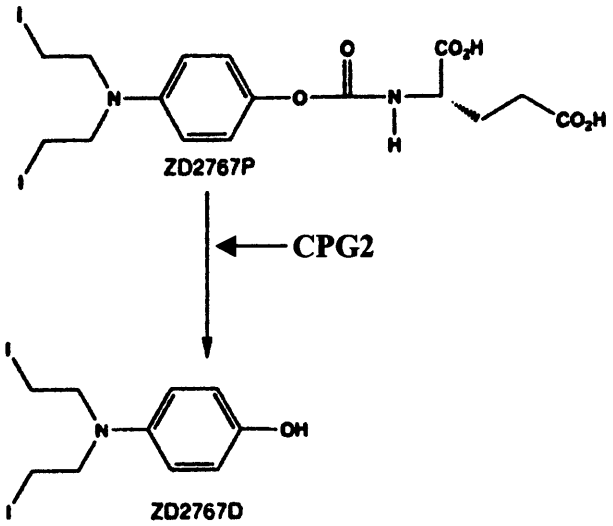

Chemical structure of ZD2767P and ZD2767D. The bacterial enzyme, CPG2, cleaves a glutamate to generate ZD2767D from ZD2767P.

Preclinical in vitro characteristics

In preclinical experiments the active drug formed from the cleavage of ZD2767P by CPG2, ZD2767D, has a chemical half-life of approximately two minutes in plasma ([1]Blakey *et al*, 1995). This short half-life has been designed to allow diffusion within the tumour, without significant escape into the peripheral circulation.

The potency of ZD2767P and its active drug, ZD2767D, were tested in vitro against LoVo, a CEA positive, colorectal tumour cell line. The concentration of drug required to inhibit cell growth by 50% is referred to as IC_{50}. The IC_{50} for ZD2767D exposed to proliferating LoVo cells for a one hour incubation in vitro is 0.34 μM (Blakey *et al*, 1996). The IC_{50} for the parent prodrug, ZD2767P, is over 100 fold more (**table 7**). The addition of CPG2 enzyme to ZD2767P results in an IC_{50} of the same level as ZD2767D. The drug released from ZD2767P by CPG2 enzyme is therefore over 300 fold more potent than the drug released from CMDA, which has an IC_{50} of 100μM (Bagshawe *et al*, 1988; Springer *et al*, 1991; Niculescu-Duvaz and Springer, 1995).

ZD2767D was also shown to have activity against quiescent LoVo cells, with an IC_{50} of 1.9μM (Blakey *et al*, 1996). Even after only 1-minute incubation with proliferating LoVo cells the active drug, ZD2767D, had an IC_{50} of 1.57μM (Blakey *et al*, 1996). This indicates that ZD2767D, which is very lipophilic, is rapidly taken up into cells.

Table 7: Potency of ZD2767P and its active drug, ZD2767D

Drug	IC_{50}
ZD2767D	0.34 ± 0.11 μM
ZD2767P	47 ± 31 μM
ZD2767P + CPG2	0.32 ± 0.28 μM
ZD2767D (quiescent cells)	1.9 ± 1.2μM
ZD2767D (1 minute exposure)	1.57 ± 0.41μM

The potency of ZD2767P and its active drug, ZD2767D were tested in vitro against LoVo colorectal tumour cell line. The IC_{50} is the concentration of drug required to inhibit cell growth by 50%. Drugs were incubated with proliferating LoVo cells for 1 hour (unless otherwise stated). (Blakey et al, 1996)

The K_m for ZD2767P as a substrate for CPG2 is <3μM (Springer *et al*, 1995; Senter and Springer, 2001). The k_{cat} is $30s^{-1}$ ([1]Blakey *et al*, 1995; Springer *et al*, 1995; Senter and Springer, 2001). The turnover of ZD2767P (k_{cat}/K_m) is therefore approximately 10 fold less than for CMDA. This lower rate of conversion to active drug is counteracted by the increased drug potency; consequently overall less CPG2 enzyme is required at the tumour site than CMDA to achieve anti-tumour activity.

The molecular weight of ZD2767P is 720 kDa as a hydroiodide salt, and 590 kDa as a free base.

Preclinical in vivo experiments

Preclinical toxicities studies were performed in mice and rats with ZD2767P alone. The maximum tolerated dose/lethal dose to 10% animals (MTD/LD10) occurred in mice at a dose of <315-405mg/m^2 x 3 administrations and in rats at 240-300mg/m^2 x 3 administrations. All of the toxicities observed were reversible by Day 28. Evidence of toxicity included myelosuppression, cardiac damage (myocardial necrosis, mineralisation and haemorrhage), hepatotoxicity (necrosis

with haemorrhage and inflammatory cell infiltrate), nephrotoxicity (cortical tubular necrosis and dilatation, elevations in plasma urea and/or creatinine and salivary gland acinar atrophy (D.Blakey, personal communication). In a venous irritation study in dogs, a 5mg/ml solution of ZD2767P did not damage the vascular wall at the site of injection. 25mg/ml and 50mg/ml led to local endothelial loss, thrombus formation, mural necrosis and extravasation (D.Blakey, personal communication). ZD2767P must therefore be administered via a central line (preferably a Hickman line) to avoid vascular damage.

Single bolus dosing of ZD2767P was compared with 3 doses of ZD2767P over 2hr (dose at 0, 1 and 2hr) in 6 separate studies. In all six studies, giving three split doses of ZD2767P following A5CP gave increased median growth delays, compared to the single bolus dose of ZD2767P (D.Blakey, personal communication). The data indicate that the split dosing regime is likely to be more effective than using a single bolus dose. Splitting the dose has the additional advantage that lower concentrations of ZD2767P can be administered, which may be important in view of the toxicity to blood vessels seen at ZD2767P concentrations> 10 mg/ml.

ZD2767P, in summary, is a bis-iodo phenol mustard prodrug, whose active drug is over 300 times more potent than CMDA and has a very short biological half-life of less than 2 minutes ([1]Blakey *et al*, 1995; Springer *et al*, 1995; Blakey *et al*, 1996). This short half-life should allow drug to diffuse locally in the tumour to cause cytotoxic effects, but should limit its ability to leak into the peripheral circulation. These characteristics are hypothesized to improve efficacy in ADEPT systems. ZD2767P requires characterisation in the clinical setting, in order to assess and define dose, toxicity, pharmacokinetics and efficacy.

2.1.2 A5CP without a clearing antibody

It is proposed that with the improved characteristics of ZD2767P, a clearing antibody system might not be required for ADEPT. This would be an advantage, as it would reduce the complexity of ADEPT. It would also obviate the need for a second immunogenic clearing antibody.

Preclinical in vivo experiments

Efficacy

The efficacy of ADEPT using A5CP in combination with ZD2767P, without a clearing antibody system, was assessed in a nude mouse model ([2]Blakey *et al*, 1995; Blakey *et al*, 1996). A5CP antibody/enzyme conjugate (3000U/m^2) was administered intravenously to nude mice bearing human xenografts of colorectal carcinoma (LoVo). Localisation to the tumour of approximately 1% of injected dose of A5CP occurred after 72 hours (Blakey *et al*, 1996). The ratio of tumour to normal tissue was 10-50:1 at 72 hours (Blakey *et al*, 1996). ZD2767P was then administered intraperitoneally (ip) as 3 bolus injections, 1 hour apart, and resulted in tumour regressions and tumour growth delays of over 30 days with very little toxicity as assessed by weight loss (Blakey *et al*, 1996). The ZD2767P dose used was 70mg/kg x 3 administrations (human equivalent 210mg/m^2) (Blakey *et al*, 1996). These preclinical experiments suggested that sufficient antibody-enzyme could be delivered to tumours without a clearing antibody system, and that efficacy could be achieved with the new prodrug, ZD2767P, without significant toxicity.

Toxicity

Preclinical studies toxicity studies were performed in mice, rats and marmosets using A5CP in combination with ZD2767P. The dose of A5CP used in these studies was 3000U/m^2. This A5CP dose produces plasma enzyme activity level of 0.5U/mL (mice), 0.4U/mL (rats) and 0.2U/ml (marmoset), at 72 hours. The MTD/LD10 for mice of ZD2767P occurred at 30mg/m^2 x 3 administrations, for rats it was 90-180mg/m^2 x 3 administrations and for marmosets it was 600mg/m^2

x 3 administrations. All of the toxicities observed were reversible by Day 32. Evidence of toxicity was the same as was found with for ZD2767P alone, however at lower doses of ZD2767P than with ZD2767P alone.

A5CP without a clearing antibody system, in combination with ZD2767P, has therefore shown efficacy in preclinical models, and has potential for clinical use (Blakey *et al*, 1996). This current study is therefore designed to study both the new prodrug, ZD2767P, and whether adequate targeting can be achieved using A5CP alone, without a second clearing antibody.

2.1.3 Mechanistic clinical trial design

ADEPT is a complex 2-step therapy, in which there are many components that could potentially be modified. Designing a clinical trial in which each component, where possible, can be quantified, should rationally direct pre-clinical development. Potentially this will accelerate development of ADEPT as the effect of modifications to the system can be measured and later predicted, based on mathematical models.

The basic design of this current ADEPT trial was to administer A5CP as a fixed dose, and to escalate ZD2767P to define dose limiting toxicity (DLT) and maximum tolerated dose (MTD). Once MTD was defined a phase II efficacy assessment phase was to be undertaken. The trial incorporates conventional phase I clinical trial measures, including toxicity and pharmacokinetics, with mechanistic studies in order to achieve a better understanding of ADEPT, and to direct modifications in ADEPT for the future.

Rationale for start dose of A5CP and ZD2767P and dose escalation of ZD2767P

The dose of A5CP chosen for the clinical trial is a fixed dose of 3000U/m^2. This is less than was used in previous ADEPT clinical trial (10 000U/m^2), as a second antibody clearance system would not be used to accelerate the clearance of CPG2 enzyme from the blood. Preclinical studies in a mouse xenograft model of human colorectal cancer, demonstrated that it was feasible to administer ZD2767P 72

hours after A5CP at this dose level, with a resultant mean growth delay 37 days in the tumour, and minimal toxicity as assessed by weight loss (Blakey *et al*, 1996).

In pre-clinical toxicity studies the LD_{10} in mice for ZD2767P, 72 hours after 3000U/m^2 of A5CP, was 24.9 mg/m^2 x 3. This was administered at a plasma CPG2 enzyme level of 0.5 U/ml. In this clinical study the enzyme level at the time of prodrug administration was planned to be $\leq$ 0.2 U/ml and therefore the starting dose was calculated to be double the 1/10th of the LD_{10} in mice, i.e. 4.9 mg/m^2 ZD2767P x 3.

The protocol determined three patients would be treated at the starting dose level and a minimum of one patient would be treated at each subsequent level. At each dose escalation the ZD2767P dose would be doubled, until drug-related toxicity was seen in any patient, when a further two patients would be treated at that same dose level. Escalations would then follow a "modified Fibonacci" scheme until the DLT was reached, with at least three patients treated at each dose level before further dose escalating. If any drug-related Grade 3 or Grade 4 haematological toxicity, or any drug-related Grade 2, Grade 3 or Grade 4 non-haematological toxicity (other than nausea, vomiting and alopecia) was seen in one or more patients at a given dose level, then a further three patients would be treated at that dose level.

Mechanistic studies

The aims of the mechanistic studies that have been incorporated into this ADEPT trial protocol were to quantitatively measure each possible component of ADEPT in the clinical setting. They should also provide the data to answer the hypotheses that lead to this trial.

The measurements used in this ADEPT trial are listed in **table 8**:

Table 8: Measurements in ADEPT trial

Toxicity of A5CP +ZD2767P	**Method of assessment**
Toxicity, MTD and DLT	NCI-CTC criteria

Characteristics of A5CP	**Method of assessment**
Serum CPG2 enzyme clearance	Methotrexate reduction assay
Tumour CPG2 enzyme levels	Methotrexate reduction assay (biopsy)
Blood I-131 radiolabelled A5CP clearance	Gamma counter
Localisation of I-131 radiolabelled A5CP	SPECT analysis of gamma camera data
Immunogenicity of A5CP	HAMA and HACPG2A by ELISA

Characteristics of ZD2767P	**Method of assessment**
ZD2767P pharmacokinetics	HPLC analysis
ZD2767D formation	Comet assay (for DNA cross-links)

Efficacy of A5CP + ZD2767P	**Method of assessment**
Anatomical	CT scans (WHO response criteria)
Functional	[F-18] FDG PET analysis
Serological	Serum CEA and CA19-9 levels
Survival	Kaplan-Meier survival analysis

Abbreviations: MTD – maximum tolerated dose; DLT – dose limiting toxicity; NCI-CTC – National Cancer Institute Common Toxicity Criteria; CPG2 – carboxypeptidase G2; SPECT – single photon emission computerised tomography; HAMA – human anti-mouse antibody; HACPG2A – human anti-CPG2 antibody; ELISA -enzyme linked immunosorbance assay; WHO – World Health Organisation; [F-18] FDG PET – [F-18] fluorodeoxyglucose positron emission tomography

The hypothesis that ZD2767P as the new prodrug for ADEPT may achieve less toxicity and greater efficacy than CMDA as a result of the short half-life and greater potency of its active drug, ZD2767D, should be addressed by the assessment of toxicity, by measuring the pharmacokinetic parameters of ZD2767P and by looking for evidence of ZD2767D formation, using comet assay, and the assessment of efficacy in combination with A5CP. The hypothesis that adequate tumour targeting for activation of ZD2767P, can be achieved using A5CP without a clearing antibody system should be addressed by the measurement of CPG2 enzyme levels in serum and tumour, in combination with the assessment of biodistribution of radiolabelled A5CP, and toxicity and efficacy assessments.

2.2 Trial outline

2.2.1 Patient Selection:

The trial had Local Research Ethics Committee (LREC), Department of Health United Kingdom, and Administration of Radioactive Substances Committee (ARSAC) approval. It was performed according to Good Clinical Practice, under the auspices of the Cancer Research Campaign Phase I/II Clinical Trials Group. The Cancer Research Campaign's Drug Development Office monitored the clinical data.

All patients gave written informed consent for the study. The eligibility criteria were unresectable, locally recurrent or metastatic colorectal carcinoma or other CEA expressing tumour; no anti-tumour treatment in the previous 4 weeks; bidimensionally measurable disease by plain X-ray, CT or ultrasound scan; age ≥ 18 years; life expectancy≥ 4 months; WHO performance status 0, 1 or 2; and normal haematological, biochemical, renal and hepatic function unless abnormal due to tumour. Pre-treatment serum CEA levels were required to be between 10μg/L and 1000μg/L: if the serum CEA was not raised, then CEA had to be demonstrated by immunohistochemistry on tumour biopsy (Boxer *et al*, 1994). Patients were excluded if they had pre-existing HAMA to A5B7 or HACPG2A;

the presence of active brain metastasis; if they were a poor medical risk; HIV, Hep B or C positive; or pregnant or lactating.

All patients had an intradermal skin test to the A5CP conjugate performed and would have been excluded if they formed a positive reaction to it. All patients had received previous conventional chemotherapy or radiotherapy, and had either relapsed or showed no response. Preclinical studies indicated the need for ZD2767P to be injected into a large bore vein, so all patients had a double lumen Hickman catheter inserted; in most cases this was into the subclavian vein. All patients who received I-131 radiolabelled conjugate also received thyroid blocking with potassium iodide 50mg qds for 10 days commencing one day prior to the administration of the radiolabelled product. Patients could receive metoclopramide 20 mg tds as an antiemetic if required after the administration of prodrug.

2.2.2 Materials

A5CP was manufactured by Lonza Biologics, and supplied by AstraZeneca Pharmaceuticals. A5CP was formulated as 50, 159 or 150 units/ml sterile aqueous solution packed in neutral (Type 1) glass vials with a nominal volume of 5 ml. A5CP was diluted in 0.9% sodium chloride and administered over two hours as a 500 ml intravenous (iv) infusion.

Radiolabelling of A5CP was performed using 370MBq of I-131 by the N-bromo-succinamide/L-tyrosine technique (Adam, 1989). Thin layer chromatography (TLC) was performed to assess iodine incorporation and antigen binding was assessed using a CEA column.

ZD2767P was manufactured and supplied by AstraZeneca as a non-sterile product containing 610 mg of crystalline ZD2767P Hydroiodide per vial (which was equivalent to 500 mg of ZD2767P free base). 10 ml of sodium bicarbonate solution was added to this and ZD2767P Hydroiodide salt was converted to ZD2767P di-sodium salt. The final solution contained 53.7 mg/ml of ZD2767P di-sodium salt, which was equivalent to 50 mg/ml of free base. ZD2767P was

administered as three doses an hour apart, via a fast running iv infusion of Dextrose 5%, through a central (Hickman) line.

2.2.3 Treatment Schedule

3000U per m^2 of A5CP in 500mL of 0.9% sodium chloride was given over 2 hours on day 0. 250U of A5CP was radiolabelled with 370MBq I-131 and administered as a slow iv bolus over 2 minutes at the end of the infusion. Daily serum CPG2 measurements were performed until the serum CPG2 enzyme levels fell below a pre-determined value. This level was initially 0.20U/mL (patients 1, 3- 9); however because of early toxicity it was lowered to 0.10U/mL (patients 2, 10-22) then 0.05U/mL for all subsequent patients. At this time ZD2767P was administered as 3 bolus injections, 1 hour apart, each over 5 minutes into a fast running 5% dextrose drip. Patients were then followed up for a period of at least 8 weeks from the time of conjugate administration.

2.3 Methods and Results:

2.3.1 Patient demographics

28 patients were recruited, of which, 27 patients (21 males and 6 females) were treated in between November 1997 and November 1999. One patient (patient # 8) became ineligible due to deterioration in liver function tests after recruitment and prior to treatment. This patient did not receive A5CP or ZD2767P and was excluded from further analysis.

The median age of patient's was 56 years (range 32-74 years). 15 patients (55%) had a WHO performance status of 0, 11 (41%) had a performance status of 1 and 1 patient (4%) had a performance status of 2 at the time of entry into the study (**table 9**).

Table 9: Patient demographics

	Male	Female	All Patients
Patients	21 (78%)	6 (22%)	27 (100%)
Age (years)			
Median	57	54.5	56
Minimum	32	32	32
Maximum	69	74	74
WHO Performance			
0	12	3	15 (55%)
1	8	3	11 (41%)
2	1	0	1 (4%)

25 patients had advanced colorectal cancer, 1 patient had a CEA expressing carcinoma of the pancreas, and one patient had CEA expressing non-small cell lung cancer. All patients had received prior chemotherapy or radiotherapy. The median number of prior chemotherapy regimens before entering the study was 2 (range 0-7) (**table 10**).

Table 10: Previous chemotherapy regimens in ADEPT patients

ZD2767P dose level (mg/m^2)	Number of patients	Time between last chemotherapy and ADEPT (days)		Number of chemotherapy regimens	
		Median	Range	Median	Range
4.9	5	105	48 – 710	2	1 - 3
6.0	1	95	95	1	1
6.37	4	111	41 – 299	3	2 - 4
8.28	3	72	39 – 105	2	1 - 3
12.42	2	88	46 – 130	2.5	2 - 3
15.50	7	87	84 - 91	1	0 - 1
18.63	5	137	130 - 143	3	2 - 7
All dose levels	**27**	**95**	**39 – 710**	**2**	**0 – 7**

2.3.2 Toxicity/MTD/DLT

The dose of A5CP remained fixed throughout the study, with the dose of ZD2767P being escalated until the MTD was established. The starting dose of ZD2767P was 4.9mg/m^2 x three doses. At 18.63mg/m^2 x three doses, drug-related dose limiting toxicity stopped further dose escalation. This consisted of Grade 4 thrombocytopaenia in 2 out of 5 patients. One patient at a dose of 18.63mg/m^2 also had a prolonged period of neutropaenia. The ZD2767P dose was subsequently reduced to 15.5mg/m^2 x three doses in order to establish the MTD (**table 11**).

Table 11: Dose escalation schedule of ZD2767P

Dose level (mg/m^2)	Percentage increase/decrease above preceding dose level
4.9	Starting dose
6.37	30%
8.28	30%
12.42	50%
18.63	50%
15.5	25% increase from 12.42 mg/m^2

From dose level 4.9 mg/m^2 to 15.5 mg/m^2 treatment was well tolerated with mainly Grade I-II haematological drug-related adverse events (AEs) (**table 12**).

Table 12: Highest NCI-CTC grade of haematological toxicity (ADEPT related) attained for each patient according to ZD2767P dose

	NCI-CTC toxicity grade (WBC)					NCI-CTC toxicity grade (Platelets)				
	0	**I**	**II**	**III**	**IV**	**0**	**I**	**II**	**III**	**IV**
4.9mg/m^2	4				1	4			1	
6.0mg/m^2		1						1		
6.37mg/m^2	4					3		1		
8.28mg/m^2	3					2	1			
12.42mg/m^2	2					1	1			
15.5mg/m^2	4	2		1		4	2	1		
18.63mg/m^2	2		2		1	1	1	1		2

Abbreviations: WBC – white blood cells; NCI-CTC – National Cancer Institute Common Toxicity Criteria

Overall 12 patients experienced Grade I-IV drug related thrombocytopaenia, with a median nadir of 4 weeks (27.5 days), and 8 patients experienced Grade I-IV drug related leucopaenia, with a median nadir of 6 weeks (41.5 days) (**table 13, 14**). **Figure 9** shows myelosuppression graphs for the MTD (15.5mg/m^2) and DLT (18.63mg/m^2) ZD2767P dose level.

Table 13: Platelet nadirs for patients with ADEPT related thrombocytopaenia

Pt No.	Prodrug dose level (mg/m^2)	Time to nadir (days)*	Platelet nadir ($x10^9/L$)	NCI-CTC Grade
#3	4.9	28	26	3
#6	6.0	27	66	2
#10	6.37	42	65	2
#11	8.28	31	97	1
#16	12.42	11	112	1
#17	18.63	27	21	4
#19	18.63	28	58	2
#20	18.63	27	120	1
#21	18.63	20	11	4
#24	15.5	24	68	2
#25	15.5	32	107	1
#28	15.5	35	128	1

*(*time to nadir calculated from day of A5CP (day 0))*

Table 14: WBC nadirs for patients with ADEPT related leucopaenia

Pt No.	Prodrug dose level (mg/m^2)	Time to nadir (days)*	WBC nadir ($x\ 10^9/L$)	NCI-CTCCTC Grade
#3	4.9	35	0.9	4
#6	6	49	3.8	1
#19	18.63	43	2.2	2
#20	18.63	35	2.8	2
#21	18.63	40	0.5	4
#24	15.5	50	1.4	3
#25	15.5	43	3.2	1
#27	15.5	38	3.3	1

*(*time to nadir calculated from day of A5CP (day 0))*

Figure 9: Myelosuppression graphs at MTD and DLT for patients receiving ADEPT

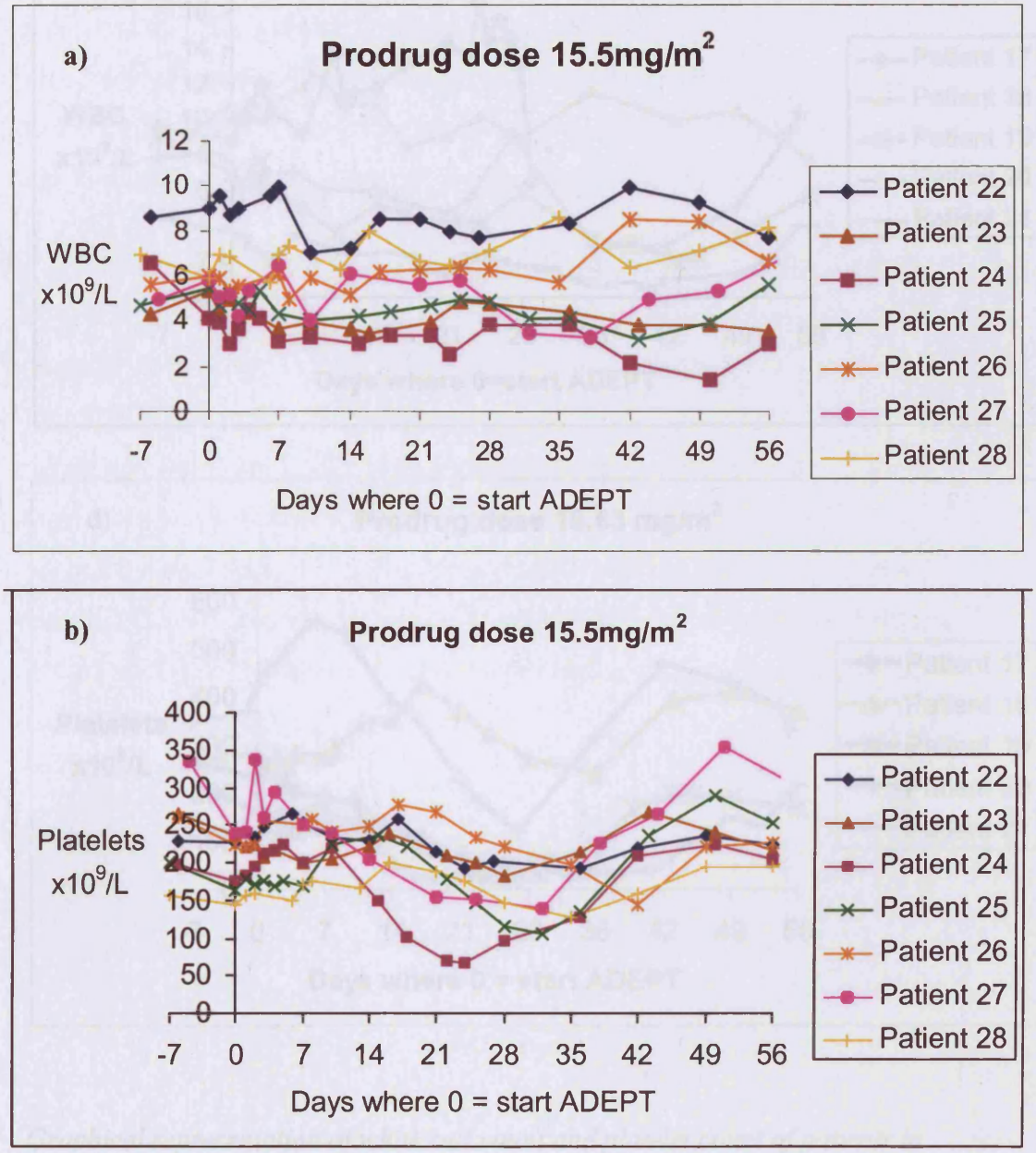

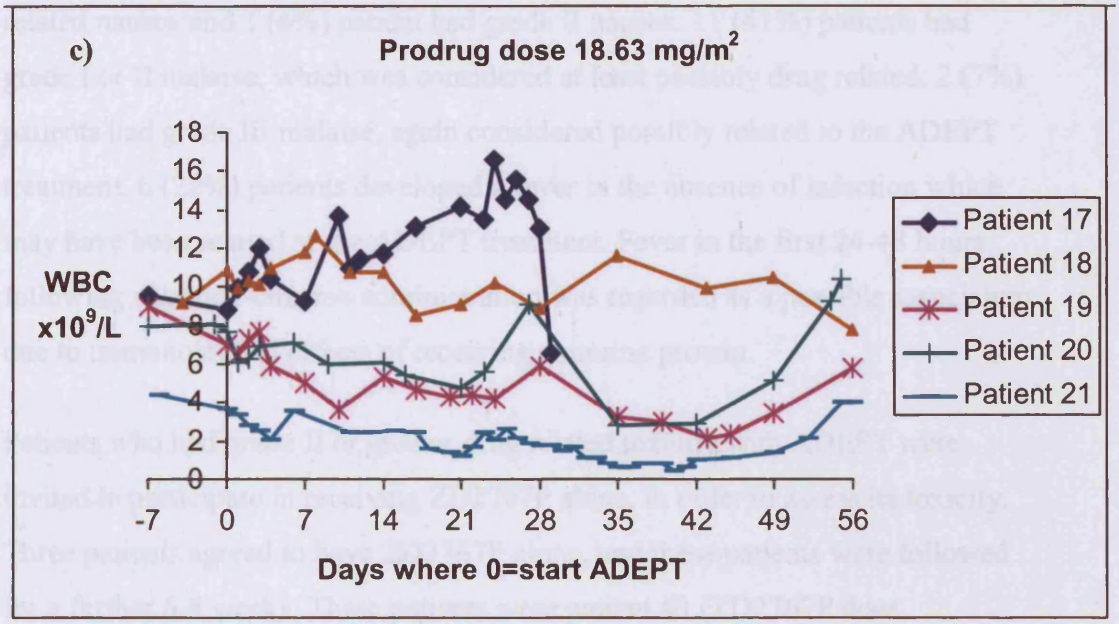

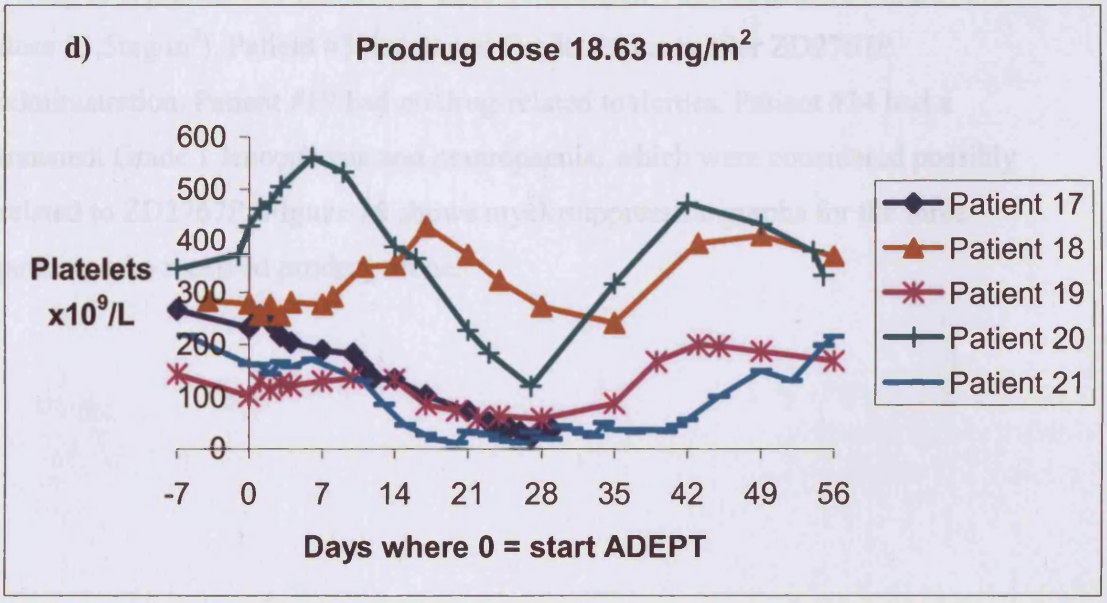

Graphical representation of white cell count and platelet count of patients in ADEPT trial. ***Figure 9a)*** *white blood cell count at MTD (ZD2767P dose 15.5mg/m^2)* ***b)*** *platelet count at MTD (ZD2767P dose 15.5mg/m^2)* ***c)*** *white blood cell count at DLT (ZD2767P dose 18.63mg/m^2)* ***d)*** *platelet count at DLT (ZD2767P dose 18.63mg/m^2). At the DLT dose of prodrug(18.63 mg/m^2) almost all patients had a fall in WBC and platelets with a nadir of WBC at day 42 and platelets at day 28.This was not so problematic at the MTD (prodrug dose 15.5mg/m^2).*

Abbreviations: MTD – maximum tolerated dose; DLT – dose limiting toxicity

Other side-effects from ADEPT were mild. 16 (59%) patients had grade I drug related nausea and 1 (4%) patient had grade II nausea. 11 (41%) patients had grade I or II malaise, which was considered at least possibly drug related. 2 (7%) patients had grade III malaise, again considered possibly related to the ADEPT treatment. 6 (22%) patients developed a fever in the absence of infection which may have been related to the ADEPT treatment. Fever in the first 24-48 hours following antibody-enzyme administration was regarded as a possible association due to immunological effects of receiving a murine protein.

Patients who had grade II or greater drug related toxicity with ADEPT were invited to participate in receiving ZD2767P alone, in order to assess its toxicity. Three patients agreed to have ZD2767P alone, and these patients were followed for a further 6-8 weeks. These patients were patient #3 (ZD2767P dose 4.9mg/m^2), patient #19 (ZD2767P dose 18.63mg/m^2) and patient #24 (ZD2767P dose 15.5mg/m^2). Patient #3 developed Grade 1 nausea after ZD2767P administration. Patient #19 had no drug-related toxicities. Patient #24 had a transient Grade 1 leucopaenia and neutropaenia, which were considered possibly related to ZD2767P. **Figure 10** shows myelosuppression graphs for the three patients who received prodrug alone.

Figure 10: Myelosuppression graphs for patients who received ZD2767P alone

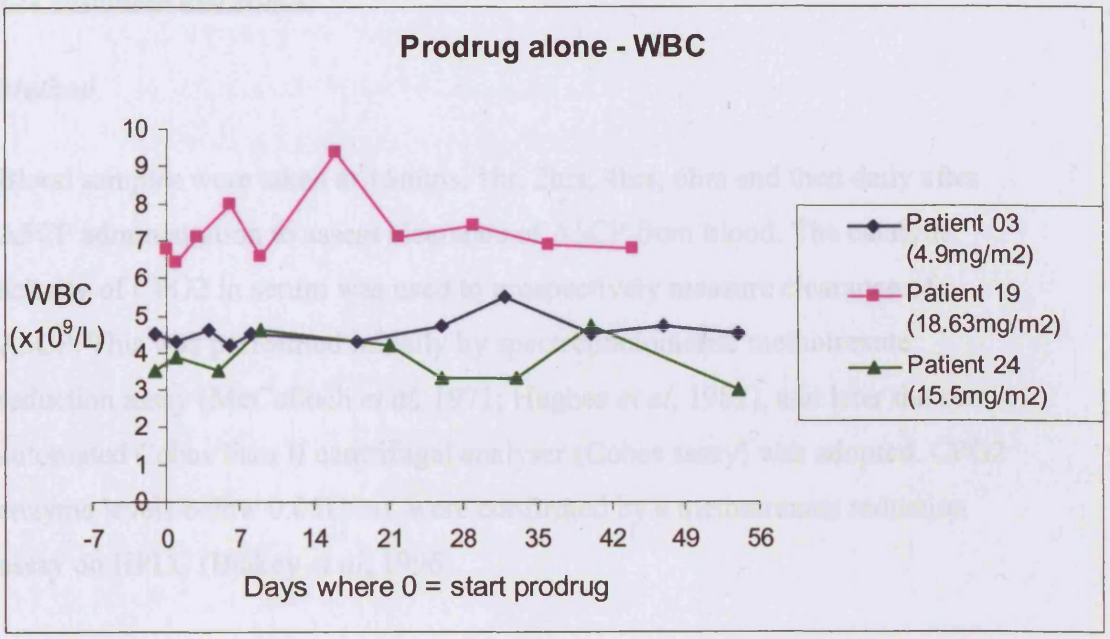

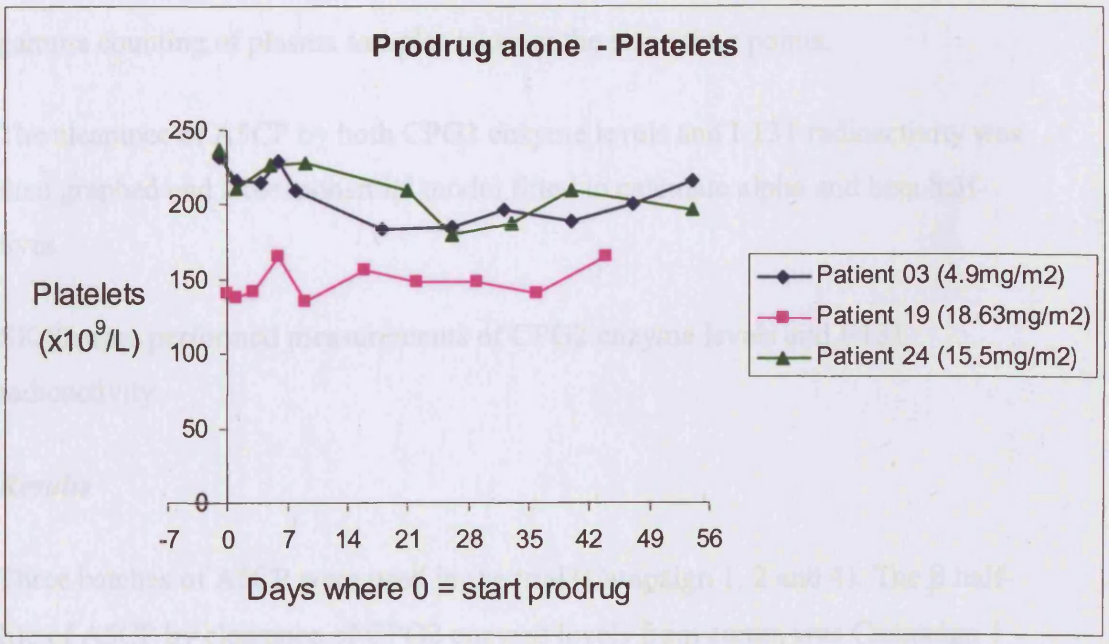

Graphical representation of white blood cells (WBC) and platelets in three patients who received the prodrug alone toxicity assessment part of ADEPT. There does not appear to be any drug related myelosuppression in these three patients.

2.3.3 Mechanistic studies

A5CP Pharmacokinetics – serum CPG2 enzyme levels and clearance of I-131 radiolabelled A5CP

Method

Blood samples were taken at 15mins, 1hr, 2hrs, 4hrs, 6hrs and then daily after A5CP administration to assess clearance of A5CP from blood. The catalytic activity of CPG2 in serum was used to prospectively measure clearance of A5CP. This was performed initially by spectrophotometric methotrexate reduction assay (McCulloch *et al*, 1971; Hughes *et al*, 1982), and later the semi-automated Cobas Fara II centrifugal analyser (Cobas assay) was adopted. CPG2 enzyme levels below 0.05U/mL were confirmed by a methotrexate reduction assay on HPLC (Blakey *et al*, 1996).

The clearance of I-131 radiolabelled A5CP was assessed retrospectively by gamma counting of plasma samples taken at the same time points.

The clearance of A5CP by both CPG2 enzyme levels and I-131 radioactivity was then graphed and a biexponential model fitted to calculate alpha and beta half-lives.

SK Sharma performed measurements of CPG2 enzyme levels and I-131 radioactivity.

Results

Three batches of A5CP were used in the trial (Campaign 1, 2 and 4). The β half-life of A5CP by clearance of CPG2 enzyme levels from serum was Campaign 1 = 8.95 hrs (spec assay), Campaign 2 =11.8 hrs (cobas) and Campaign 4 = 15.49 hrs (cobas).

The β half-life of A5CP by clearance of I-131 radiolabelled A5CP was Campaign 1 = 5.77 hrs, Campaign 2 = 5.08 hrs and Campaign 4 = 11.77 hrs.

Serum CPG2 enzyme levels on prodrug day

Method

A blood sample was taken immediately prior to prodrug administration and was analysed by methotrexate reduction assay on HPLC to confirm the CPG2 enzyme level in serum. Enzyme level measurements were performed by SK Sharma.

Results

The median serum CPG2 enzyme level on prodrug day was 0.033 U/ml (range 0.013-0.152 U/ml) by Spec/Cobas and 0.037 U/ml (range 0.011-0.18 U/ml) by HPLC. The number of days until prodrug administration was a median of 3 days (range 2-9 days). **Table 15** shows the serum CPG2 enzyme levels at the time of ZD2767P administration by both Spec/Cobas and by HPLC.

Table 15: Serum CPG2 enzyme levels immediately prior to ZD2767P administration

Pt No.	Conjugate Campaign	Days until prodrug administration	Prodrug dose (mg/m^2)	Enzyme level at time of prodrug (U/ml)	
				Spec/Cobas	HPLC
#1	1	2	4.9	0.045	0.0284
#2	1	2	6.37	0.033	0.041
#3	1	3	4.9	0.152	0.0964
#4	1	4	4.9	0.0285	0.037
#5	1	2	4.9	0.013	0.011
#6	1	2	6.0	0.023	0.0196
#7	1	2	4.9	0.035	0.0392
#9	1	2	6.37	0.093	0.063
#10	2	3	6.37	0.0175	0.0405
#11	2	3	8.28	0.03	0.0362
#12	2	3	6.37	<0.1	0.0365
#13	2	3	8.28	0.0265	0.0217
#14	2	3	8.28	0.036	0.0318
#15	2	3	12.42	0.036	0.025
#16	2	2	12.42	0.022	0.03
#17	2	3	18.63	0.018	0.012
#18	2	7	18.63	0.035	0.012
#19	2	3	18.63	0.0465	0.0775
#20	2	3	18.63	0.0145	0.0355
#21	2	3	18.63	0.046	0.104
#22	4	6	15.5	0.026	0.05
#23	4	4	15.5	0.028	0.0972
#24	4	4	15.5	0.037	0.0997
#25	4	4	15.5	0.038	0.18
#26	4	9	15.5	undetectable	0.041
#27	4	3	15.5	0.0321	0.033
#28	4	7	15.5	0.04	0.04275

Spec/ cobas enzyme measurements were from blood samples taken on the morning of prodrug administration.
HPLC enzyme measurements were from blood samples taken immediately prior to prodrug administration.
Note: Patients #1 to #14 - samples were frozen to -85°C and thawed twice prior to HPLC analysis; Patients #15 and #16 - samples were frozen to -85°C and thawed once prior to HPLC analysis. Patients #17 to #28 - samples were stored at 4°C prior to HPLC analysis.

CPG2 enzyme levels in tumour and normal tissue

Method

In patients who gave their consent, tumour or bone marrow biopsies were taken on prodrug day to assess A5CP conjugate localisation. These samples were assessed histologically to confirm whether tumour was present in the sample and then analysed for CPG2 enzyme levels by HPLC using a methotrexate reduction assay (Blakey *et al*, 1996). CPG2 enzyme measurement was performed by SK Sharma. Where appropriate samples were also placed on a phosphor plate and imaged overnight to assess for the presence of radioactivity in the biopsy specimen, which would indicate localisation of I-131 radiolabelled A5CP. Phosphor plate analysis was performed by G Boxer.

Results

The median CPG2 enzyme level in tumour biopsies was 0.010 U/g (range 0–0.208U/g) on prodrug day (n=7) (**table 16a**). The median CPG2 enzyme level in normal tissue was 0.005U/g (range 0–0.062 U/g) (n=5) (**table 16b**). The median ratio of CPG2 enzyme in tumour: blood on prodrug day was 0.4:1 (range 0-10.4:1) (**table 16c**).

Table 16: CPG2 enzyme levels in tumour and normal tissue

a)

Pt No.	Site	Histology	CPG2 Enzyme level (HPLC)		Tumour/ serum ratio	Phosphor Imager
			Tumour (U/g)	Serum (U/ml)		
#1	colon	tumour	0.014	0.028	0.5:1	negative
#2	colostomy	tumour/ necrosis	0.061	0.041	1.5:1	negative
#5	liver metastases	tumour	0.000	0.011	0	negative
#6	liver metastases	not done	0.208	0.020	10.4:1	negative
#15	liver metastases	tumour	0.010	0.025	0.4:1	positive
#23	liver metastases	tumour islands	0.000	0.097	0	negative
#25	liver metastases	normal liver/necrotic tumour debris	0.000	0.180	0	not performed

b)

Pt No.	Site	Histology	CPG2 Enzyme level (HPLC)		Normal tissue/ serum ratio	Phosphor Imager
			Normal tissue (U/g)	Serum (U/ml)		
#11	bone marrow	not available	0.005	0.036	0.1	not applicable
#13	subcutaneous node	subcutaneous tissue	0.062	0.022	2.8	negative
#18	bone marrow	not available	0.001	0.012	0.1	not applicable
#19	liver metastases	normal liver	0.049	0.077	0.6	negative
#22	bone marrow	not available	0.000	0.050	0	not applicable

c)

	Median CPG2 enzyme level	Range	Median ratio to serum	Range
serum (n=27)	0.037 U/mL	0.011-0.180 U/mL		
tumour biopsy (n=9)	0.010 U/g	0-0.208 U/g	0.4 : 1	0 -10.4 : 1
normal tissue (n=5)	0.005 U/g	0-0.062 U/g	0.1:1	0 - 2.8: 1

Results of CPG2 enzyme levels (by HPLC) in biopsies performed on day of administration of ZD2767P in patients in ADEPT study. Where performed, the phosphor imager data on I-131 labelled A5CP is also shown.
a) Tumour biopsies b) Normal tissue biopsies c) Summary of median CPG2 enzyme levels.

One patient (#12) had ascitic fluid analysed for CPG2 enzyme levels. The CPG2 enzyme level in the ascites was 0.00975 U/g (serum 0.0365 U/ml) with the enzyme level in ascites: serum ratio of 0.27:1.

Figure 11 shows the positive phosphor imager result obtained from a liver biopsy from ADEPT patient #15, showing heterogeneous distribution of radioactivity throughout the tumour core. Histology from the same liver biopsy is also shown.

Figure 11: Phosphor imager showing localisation of I-131 radiolabelled A5CP

a)

b)

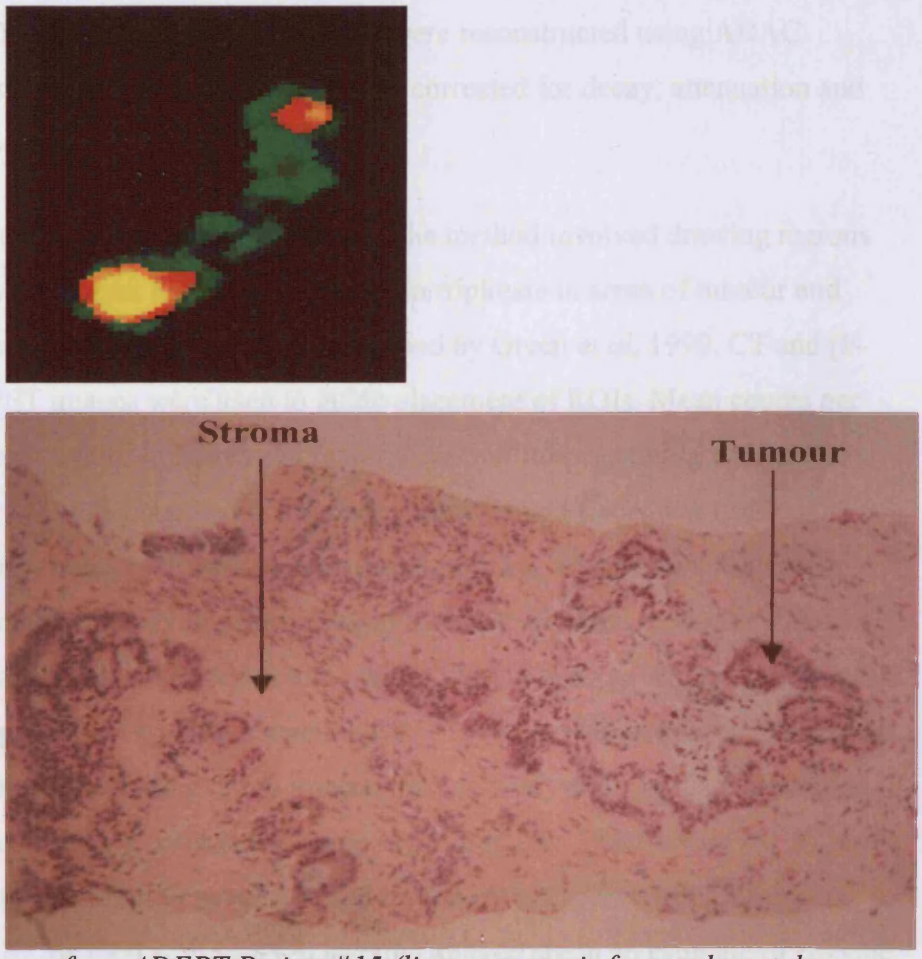

Tumour biopsy from ADEPT Patient #15 (liver metastasis from colorectal tumour) taken on prodrug day. a) phosphor imager, demonstrating heterogeneous radioactivity, indicating localisation and distribution of the I-131 radiolabelled conjugate b) is an haematoxylin and eosin section of the core of tissue. It shows areas of tumour heterogeneously distributed throughout normal liver stroma

Gamma camera imaging

Method

3 ml of A5CP radiolabelled with up to 370 MBq I-131 was administered to patients immediately after the A5CP infusion. The CEA binding and iodine incorporation of the radiolabelled A5CP were measured by a CEA column and TLC respectively. TLC and CEA binding were performed by SK Sharma.

Patients who received I-131 radiolabelled A5CP had gamma camera imaging performed at 4, 24, 48, 72 hours (and 96 hours if appropriate) on an ADAC Vertex Plus dual headed gamma camera. The imaging consisted of both planar and SPECT acquisitions. SPECT images were reconstructed using ADAC filtered-back projection software and were corrected for decay, attenuation and Compton scatter.

I performed the gamma camera analysis. The method involved drawing regions of interests, of at least nine voxels, placed in triplicate in areas of tumour and normal tissue (heart, lung, liver), as described by Green *et al*, 1990. CT and [F-18] FDG PET images were used to guide placement of ROIs. Mean counts per voxel were recorded. A calibration factor, obtained from scanning a phantom containing known amounts of I-131 under clinical conditions, was used to convert from counts per voxel to radioactivity per kg. This value was decay corrected and divided by the administered radioactivity dose to calculate the % injected radioactivity dose/ kg in tumour and normal tissues (**see Appendix 1 for example spreadsheets**). The enzyme level (U/g) was estimated in the tumour for prodrug day, by modelling the % injected radioactivity dose/ kg data as a mono-exponential clearance and extrapolating to prodrug day. The fraction of radioactivity estimated to have localised in tumour at the time of prodrug was multiplied by the total administered enzyme units to attain an estimate of enzyme level per gram of tumour.

Results

The results for the antigen binding (CEA column) and iodine incorporation (TLC) for I-131 radiolabelled A5CP are shown in **table 17.** The enzyme and protein concentration of each A5CP conjugate campaign was different, consequently the amount radiolabelled also differed. For Campaign 1, 150U (1.35mg) was radiolabelled and the protein concentration was 50U/mL (0.45mg/mL). For Campaign 2 477U (4.83mg) was radiolabelled and the protein concentration was 159U/mL (1.61mg/mL) and for Campaign 4 450U (*4.5mg) was radiolabelled and the protein concentration was 150U/mL (*1.5mg/mL).

Campaign 1 had a median CEA binding of I-131 conjugate of 6.56% (with a range of 2.2 – 24.83%) whilst Campaign 2 had a median CEA binding of 35.9% (with a range of 16.7- 68.3%) and Campaign 4 had a median CEA binding of 21.7% (with a range of 16.5 – 56%). The median iodine incorporation of I-131 conjugate was 60.75% for Campaign 1 (with a range of 13.37 – 90%), 88.36% for Campaign 2 (with a range of 59.7 – 95%) and for Campaign 4 it was 86.6% (with a range of 77 – 97%).

(Note: * - the protein concentration for Campaign 4 is an estimated value based on the specific gravity of the conjugate of approximately 100U/mg. The actual value could not be obtained at the time of printing the thesis)

Table 17: CEA binding and I-131 incorporation of I-131 radiolabelled A5CP

Pt No.	Conjugate Campaign	CEA binding of I-131 A5CP (%)	Iodine incorporation of I-131 A5CP (%)
#1	1	4.37	38.0
#2	1	2.2	13.37
#3	1	8.32	90
#4	1	4.8	40.0
#5	1	24.83	88.0
#6	1	11.0	81.5
#7	1	ND*	ND*
#9	1	ND*	ND*
#10	2	33.5	95
#11	2	68.3	93.6
#12	2	44.6	95.0
#13	2	38.3	95.0
#14	2	39	74.0
#15	2	21.3	86.6
#16	2	40.8	84.64
#17	2	16.7	85.4
#18	2	26.3	94.9
#19	2	39.5	90.12
#20	2	27.6	80.75
#21	2	18.39	59.7
#22	4	20	93.43
#23	4	23.4	79.8
#24	4	ND†	ND†
#25	4	ND†	ND†
#26	4	56	97.0
#27	4	ND†	ND†
#28	4	16.5	77.0

The % of CEA binding represents the % of the total label which bound to CEA on a CEA column. The % iodine incorporation is derived from the % of iodine that remains protein bound after being run on a TLC strip.

** There was no analysis performed on Patients #7 and #9 due to technical problems.*

† Patients #24, #25 and #27 did not receive I-131 A5CP

Abbreviations: ND = not done

Twenty-four patients had gamma camera scans performed. Three patients (#24, #25, #27) had no gamma camera scans performed due to technical problems with the camera (radiolabelled conjugate was not administered to these patients). In six patients (#1, #3, #4, #5, #6, #7) data was not collected using scatter windows, so scatter correction could not be applied to the scans and quantitative SPECT analysis could not be performed. Visual examination of the planar images from these six patients was not able to demonstrate clear evidence of localisation. Overall eighteen patients had SPECT scans performed that were suitable for quantitative analysis.

The overall median % injected dose/kg of radiolabelled conjugate in the tumour on prodrug day was 0.185 %/kg, range 0.0006 - 1.05 %/kg (**figure 12**). The median uptake of radiolabelled conjugate in heart (estimate for bloodpool) remained higher than in tumour for the 5hr, 24hrs and 46 hrs time-points, and for normal liver it remained higher than tumour at all measured time-points. These results are consistent with the low median tumour to blood ratio of enzyme activity of 0.4:1 attained by HPLC assay.

Figure 12: SPECT analysis of biodistribution of I-131 radiolabelled A5CP

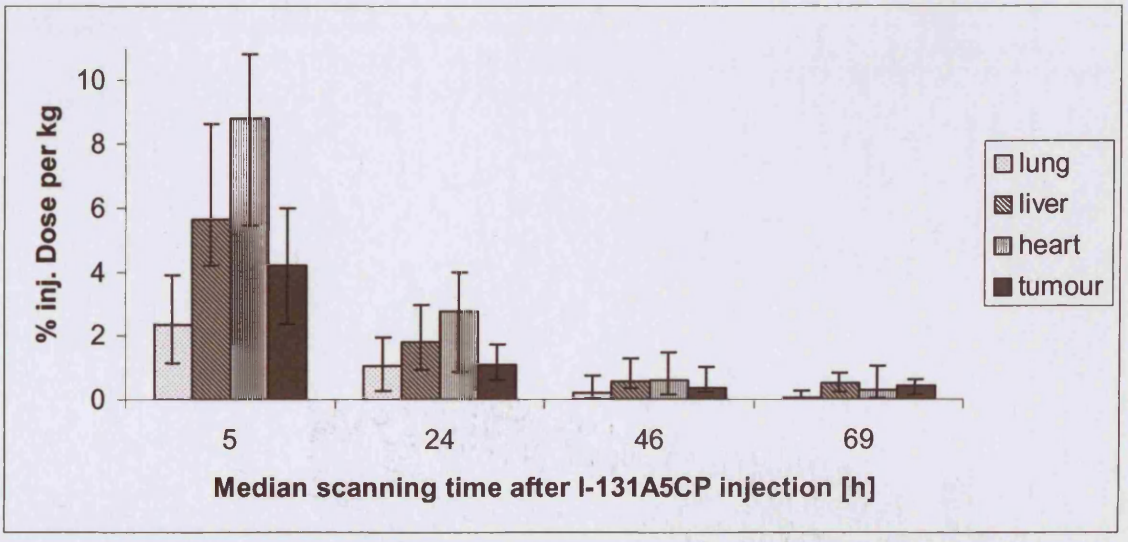

Distribution of I-131 radiolabelled A5CP in tumour and normal tissue over time by quantitative SPECT imaging. Each time-point is the median of 18 patients. The error bars include 70% of the data points.

Figure 13 demonstrates localisation of I-131 to a presacral tumour in patient #18.

Figure 13: SPECT scan at 96 hours showing localisation of I-131 to a presacral tumour

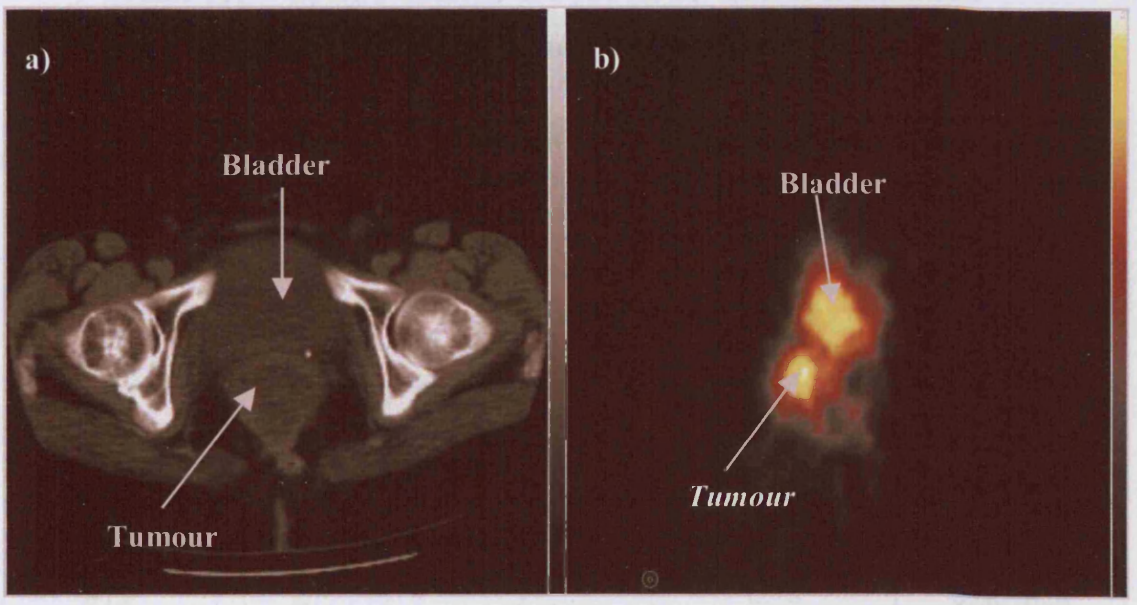

Pre-treatment CT scan of ADEPT Patient #18 (rectal carcinoma) demonstrating a presacral tumour mass behind the bladder. SPECT study in same patient at 96 hours after administration of I-131 radiolabelled conjugate. This study demonstrates uptake of radioactive tracer into the tumour area.

Table 18 displays the estimated enzyme units in tumour at the time of prodrug administration, based on extrapolation of a mono-exponential model. The median number of estimated enzyme units in the tumour at the time of prodrug administration was 0.010 U/g, range 0.000037 - 0.054 U/g.

Table 18: SPECT analysis of I-131 A5CP tumour localisation with extrapolated estimated tumour enzyme levels

Pt No.	Conjugate Campaign	Days until prodrug administration	% injected dose per kg	Enzyme Level extrapolation [U/g]
#2	1	2	0.13	0.006471
#9	1	2	0.24	0.013752
#10	2	3	0.12	0.00879
#11	2	3	0.19	0.011571
#12	2	3	0.65	0.035827
#13	2	3	0.6	0.027501
#14	2	3	0.04	0.002169
#15	2	3	0.02	0.001296
#16	2	2	0.19	0.010885
#17	2	3	0.18	0.009828
#18	2	7	1.05	0.054276
#19	2	3	0.06	0.004023
#20	2	3	0.47	0.022163
#21	2	3	0.49	0.028535
#26	4	9	0.0006	0.000037
#28	4	7	0.002	0.000108
		median	**0.185**	**0.010357**

Immunogenicity

Method

Blood was taken from patients pre-study and at weekly intervals post A5CP administration for 8 weeks. HAMA and HACPG2A response was measured by ELISA and compared with known positive and negative controls (Sharma *et al*, 1992). Data has been obtained from SK Sharma.

Results

26 out of 27 patients who received A5CP had sufficient blood samples taken for analysis of immunogenicity. All of these patients developed a positive HAMA response following the single administration of A5CP. The median number of days until developing a positive HAMA was 14 days (range 7-36 days). All patients except one (patient #13) developed a positive HACPG2A response. The overall median number of days until developing a positive HACPG2A was 15 days (range 7-50 days). **Table 19** shows the time to developing a positive HAMA or HACPG2A for each batch of A5CP conjugate.

Table 19: Immunogenicity of A5CP

Antibody	**Campaign**	**Time from A5CP administration to a positive result (days)**		**Number of patients**
		Median	**Range**	
HAMA	1	14	7 - 22	8
	2	14	7 - 36	11
	4	22	7 - 36	7
	All Campaigns	**14**	**7 - 36**	**26**
HACPG2A	1	14	7 - 22	8
	2	14.5	7 - 30	10
	4	28	21 - 50	7
	All Campaigns	**15**	**7 - 50**	**25**

ZD2767P (prodrug) pharmacokinetics

Method

ZD2767P concentrations in plasma were measured by HPLC. Plasma samples were taken for prodrug level estimations 2 minutes (mins) after the first and second prodrug injection, and at 2, 5, 10, 15, 30 and 60 mins after the third prodrug injection. A complete pharmacokinetic profile including concentration of ZD2767P extrapolated back to time 0 minutes (C0), volume of distribution in the body at steady state (Vss), area under the curve (AUC) and elimination half-life of prodrug ($T_{½}$) was determined for each evaluable patient using a non-compartmental model and *WinNonlin*® (Pharsight Corporation) software. Pharmacokinetic data has been obtained from C Springer and J Martin.

Results

All 27 patients had blood samples taken for pharmacokinetic analysis, however in some patients a full pharmacokinetic profile could not be obtained due to technical problems, in particular haemolysis of blood samples resulting in inaccurate and incomplete data.

Table 20 is a summary of the non-compartmental pharmacokinetic values calculated at each dose level for all patients in which reliable analysis could be performed. Average AUC values increased with increasing doses. The mean measured half-life of ZD2767P in plasma at the MTD was 14.5 minutes. The values for volume of distribution did not appear dose dependent.

Table 20: Pharmacokinetic parameters for ZD2767P by dose level

ZD2767P (mg/m^2)	Pt No.		$T_{½}$ (mins)	AUC (μg.ml.min)	Clearance (ml/min)	C_{max} (μg/ml)	V_{SS} (L)
4.9	#1, #3, #4	**Mean**	6.4	8.0	1253	1.1	9.4
		SD	1.3	2.1	495	0.4	5.2
		Range	3.6-6.2	5.7-9.8	915-1822	0.6-1.3	4.8-15
6.4	#2, #9, #10	**Mean**	5.4	10.6	1142	1.4	8.4
		SD	1.1	1.8	162	0.3	2.3
		Range	4.1-6.2	8.6-11.9	1026-1327	1.1-1.7	6.0-10.5
12.42	#16		4.7	33	734	3.7	5.0
15.5	#22-28	**Mean**	14.5	41	842	3.4	13.4
		SD	8.1	17	408	0.8	5.5
		Range	7.4-30.0	19-69	409-1547	2.5-4.8	6.2-22.6
18.63	#17-21	**Mean**	11.8	61	592	5.2	7.8
		SD	4.4	26	207	1.9	1.9
		Range	7.8-19	36-105	365-989	2.5-7.5	5.9-10.8

Summary of the non-compartmental pharmacokinetic parameters of ZD2767P calculated for all suitable patients. Patients #5, #6, # 7, #11, #12, #13, #14 and #15 are omitted due to technical problems preventing accurate analysis to be performed. Data for patient #21 (18.63 mg/m^2) were generated starting from 5 minutes, as the 2 minute time point was invalid.
Abbreviations: $T_{½}$ - half-life; AUC – area under curve; C_{max} – maximum concentration; V_{SS} – volume of distribution at steady state

The maximum concentration (C_{max}) of ZD2767P at an administered dose of 18.63mg/m^2 may be converted from 5.2 μg/ml to μM equivalent by using the molecular weight of ZD2767P (as a free base) of 590. This results in a molar concentration of 0.0085μM, which is significantly less than would be expected to result in cytotoxicity based on the cell cytotoxicity experiments from **table 7**.

Figure 14 shows the mean plasma prodrug elimination profiles following the third administration of prodrug, for each dose group of patients. This figure confirms that the prodrug is essentially cleared for all dose levels within 60 minutes of administration.

Figure 14: Mean plasma elimination profile for each dose level of ZD2767P

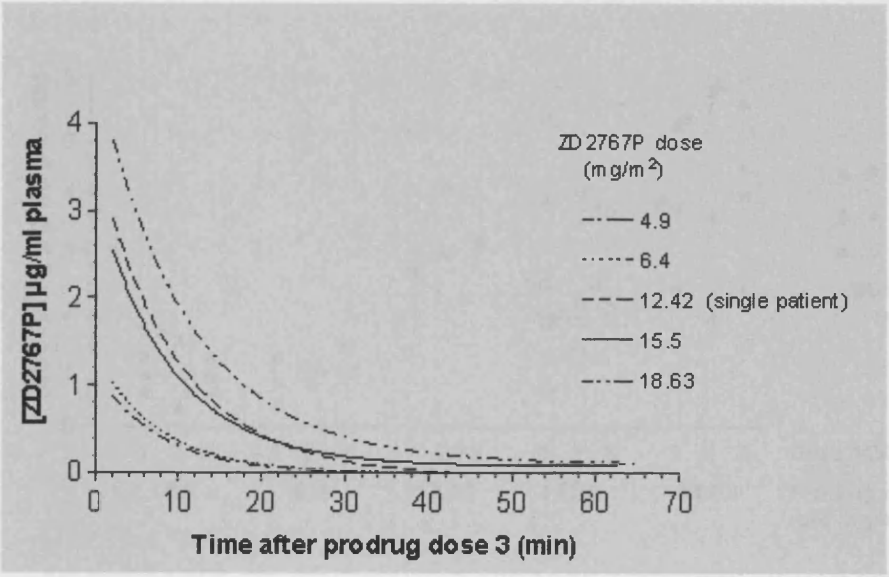

Mean plasma prodrug elimination profile following the third administration of ZD2767P for each dose group. Patients with incomplete pharmacokinetic analyses are excluded. The profile for the 12.42mg/m^2 group is that of a single patient.

Figure 15 shows the variation of ZD2767P levels after each of the three administrations of prodrug, at each different prodrug dose. There is no obvious accumulation of prodrug in the 1 hour interval between doses.

Figure 15: Plasma levels of ZD2767P measured 2 minutes after each ZD2767P administration

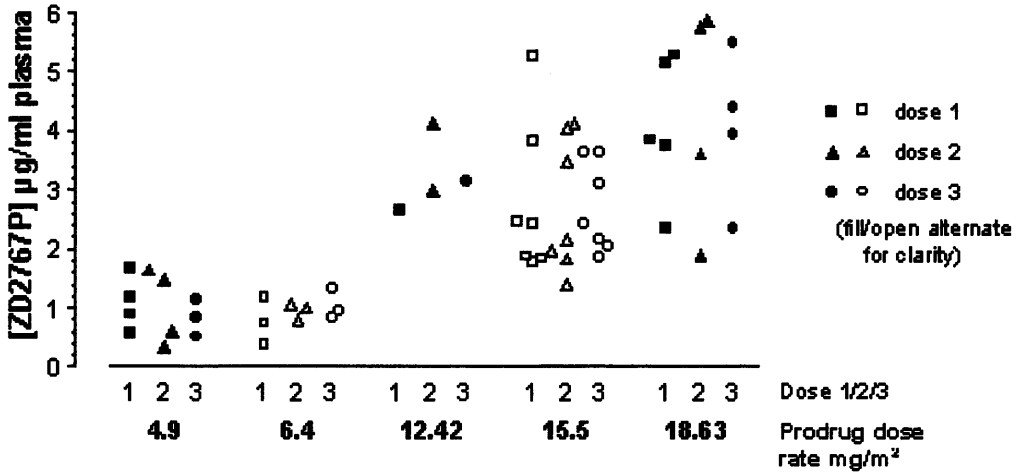

Plasma levels of ZD2767P measured 2 minutes after doses 1, 2 and 3. All valid values are included. Individual patients are not identified. Only 4 values are shown for the dose group 18.63 mg/m^2 after dose 3 as the pharmacokinetic calculations for one patient were made starting from the 5 minute time point.

Three patients who experienced toxicity with full ADEPT were given prodrug alone, and had pharmacokinetic studies performed. Patients #3 (4.9mg/m^2) and #19 (18.63mg/m^2) had pharmacokinetic parameters that were broadly similar to those when each was given ADEPT (although data for patient #3 were limited).

Comet assay

Method

The short half-life of the active drug of ZD2767P prevented it being directly measured in the clinical trial. However, as it is an alkylating agent, its lethality to cells is via the formation of DNA interstrand cross-links. The presence of DNA interstrand crosslinks was measured in the trial by a single cell comet assay. This was performed on tumour biopsy specimens and bone marrow aspirates. Peripheral blood lymphocytes taken at the same time as the biopsy were used as controls. All tumour or bone marrow biopsies were performed on the day of receiving prodrug, 1-2 hours after receiving the last prodrug injection (Webley *et al*, 2001). The results of the comet assay were expressed as a %reduction in tail moment (RTM). The comet assay was performed by S Webley.

Results

Nine patients had comet assays performed on tumour biopsy specimens (n=5) and normal tissue (n=4). 8 of the patients had no significant reduction in tail moment seen in the tissues or in the circulating blood lymphocytes measured as controls (**table 21**). However, the tumour biopsy of one patient (#15), had an 80% RTM in the comet assay thereby indicating the presence of significant DNA interstrand cross-links (**figure 16**). The circulating lymphocytes in the same patient did not have DNA interstrand cross-links.

Table 21: Comet assay

Pt No.	Site	Histology	Comet assay	
			Biopsy	Lymphocytes
#2	colostomy	tumour/necrosis	negative	no sample
#11	bone marrow	not available	negative (53% RTM)	negative (29% RTM)
#13	subcutaneous node	subcutaneous tissue	no analysis	negative (24% RTM)
#15	liver metastases	tumour	positive (80% RTM)	negative (24% RTM)
#18	bone marrow	not available	negative (10% RTM)	negative (0% RTM)
#19	liver metastases	normal liver	negative (0% RTM)	negative (0% RTM)
#20	liver metastases	not analysed	negative (0% RTM)	negative (0% RTM)
#23	liver metastasis	tumour islands	negative (8% RTM)	negative (8% RTM)
#25	liver metastasis	normal liver necrotic tumour debris	negative (17% RTM)	negative (6% RTM)

Comet assay results in all patients who had tumour or normal tissue biopsies performed. Patients #2, #15, #20, #23 and #25 were regarded as having tumour biopsies and patients #11, #13, #18 and #19 as having normal tissue biopsies. Comet assay of circulating peripheral blood lymphocytes was used as a control. Abbreviation: RTM-reduction in tail moment

Figure 16: Comet assay

a)

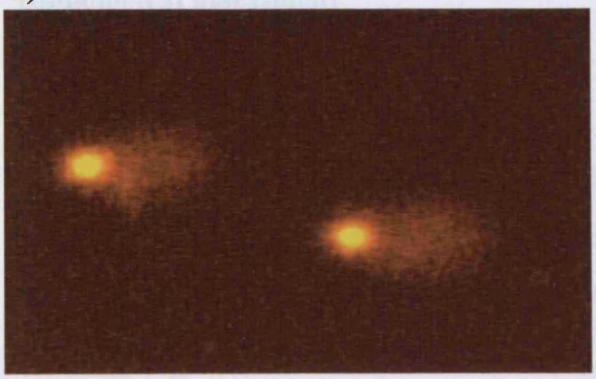

b)

c)

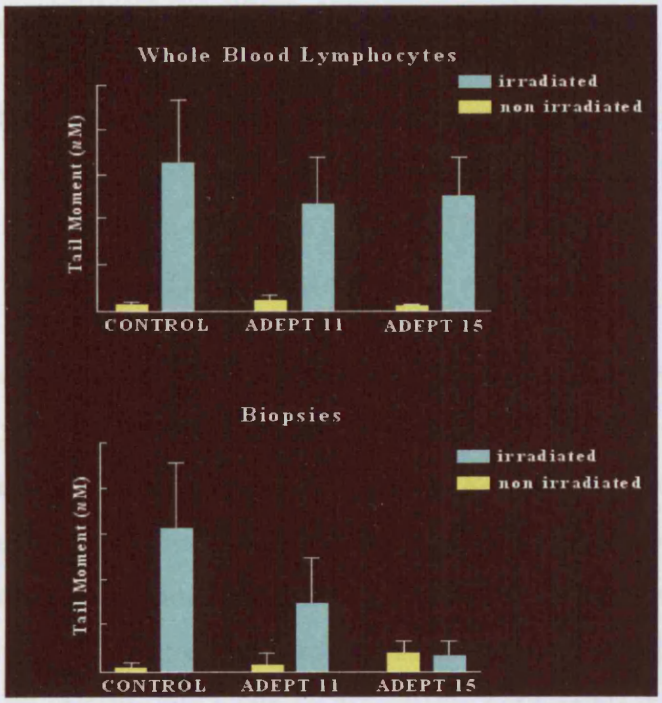

a) *Comet assay on peripheral blood lymphocytes from ADEPT Patient #15, showing a normal comet tail*
b) Comet assay on cells from a tumour biopsy (liver metastasis from colorectal ca) from ADEPT Patient #15, showing a loss of comet tail, indicating the presence of DNA interstrand cross-links.
c) Graphical representation of comet assay of lymphocytes and biopsies from ADEPT Patient #15 (biopsy of liver metastasis) and ADEPT patient #11 (bone marrow biopsy). The DNA from the tumour biopsy from patient #15 has a reduction in the comet tail, however the peripheral blood lymphocytes have not been affected. This indicates the selective formation of DNA crosslinks in the biopsied tumour cells. In patient #11 there has been a small, but not significant reduction in comet tail from bone marrow cell, and no reduction in comet tail in peripheral blood lymphocytes. Patient #11 did not have significant myelosuppression.

2.3.4 Efficacy

Radiological assessment

Method

Radiological assessment of response to ADEPT was performed within 3 weeks prior to commencing treatment, and then at 28 and 56 days after ADEPT. Response was assessed using standard WHO response criteria, based on change in bidimensional diameters of lesions (WHO, 1979). I performed the CT measurements under the guidance of a radiologist.

Results

Of the 27 patients, 26 were evaluated for response on day 28, and 22 were evaluated for response on day 56 (**table 22**). Two patients died on study, both due to progression of disease (patient #12 died on Day 15 of follow-up, patient #17 died on Day 31 of follow-up).

There were no objective responses in this study. Three patients (#15, #18 and #22) had stable disease at Day 56. Patients #15 and #18 were the only two patients with confirmed positive tumour localisation by either tumour biopsy or gamma camera imaging. In addition, patient #15 had a positive comet assay from a tumour biopsy indicating prodrug activation. A tumour biopsy could not be obtained from Patient #22, and no areas of tumour could be identified on gamma camera imaging and a tumour biopsy was not feasible due to the small size of the patient's metastasis.

Interestingly, the CT scans from Patient #24, showed that one of two mediastinal lesions had progressed by Day 28; however, by Day 56 the dimensions of this lesion had decreased in size and showed no change when compared to baseline. According to the response criteria used in this study, the response assigned was progressive disease because of the initial progression recorded. The [F-18] FDG PET results (see below) indicate at least stable disease on metabolic imaging.

Table 22: CT scan response and tumour marker levels for all ADEPT patients

Pt No.	CT response		CEA (µg/l)			CA19-9 (U/ml)		
	Day 28	Day 56	Pre-study	Day 28	Day 56	Pre-study	Day 28	Day 56
#1	PD	PD	325	376	523	169	270	443
#2	PD	PD	264	359	527	124	197	629
#3	PD	PD	140	234	512	67	119	505
#4	PD	PD	13	36	96	9	61	111
#5	PD	PD	846	1218	1496	2465	3008	4148
#6	PD	PD	901	1135	1446	43	50	41
#7	PD	PD	125	162	175	10839	12140	11754
#9	PD	PD	153	279	384	708	953	1336
#10	PD	PD	1067	1321	1266	41.8	65	88
#11	PD	PD	42	86	97	1108	1244	1244
#12	NE	NE	31	34	ND	96050	32570	ND
#13	PD	PD	3	4	10	18	20	62
#14	PD	NE	30	44	ND	10	14	ND
#15	SD	SD	874	1141	1180	7427	7637	9373
#16	PD	NE	826	ND	>500*	5140	3744	ND
#17	PD	NE	145	2156	ND	52	350	ND
#18	SD	SD	20	14	18	27	18	21
#19	SD	PD	236	298	348	223	305	391
#20	PD	PD	862	1700	1456	325	571	590
#21	PD	PD	541	513	513	18	19	26
#22	SD	SD	19	34	42	31	88	48
#23	PD	PD	22	26	29	89	120	145
#24	PD	PD	88	85	92	37	45	45
#25	PD	PD	347	436	1064	6	6	6
#26	PD	PD	3	3	3	10	14	18
#27	PD	NE	201	246	285	882	1017	ND
#28	PD	PD	3	3	3	6	11	8

* *analysis performed at a local hospital.*

Abbreviations: NE- not evaluable; ND- not done; SD – stable disease; PD – progressive disease

Serum tumour markers

Method

Serum tumour markers (CEA and CA19-9) were measured pre-study, at approximately day 28 and day 56.

Results

Table 22 shows the serum tumour marker levels in the patients on the ADEPT study. Almost all patients had an increase in serum tumour markers on study, which would be consistent with the lack of objective responses in this study. As A5CP is an anti-CEA antibody this may make interpretation of serum CEA levels difficult. Also the formation of HAMA may interfere with the serum marker laboratory assay.

[F-18] FDG PET scans

Chapter 6 contains comprehensive details on the analysis of the [F-18] FDG PET scans performed as part of this clinical trial. An overview of the methodology and results are presented here.

Method

[F-18] FDG PET scans were performed within 2 weeks prior to commencing ADEPT, at 4 weeks and then at 8 weeks after ADEPT. Scanning was performed on an ADAC Vertex Plus dual headed gamma camera. Patients received 150-185MBq of [F-18] FDG and scanning was performed at approximately 60 minutes post injection.

Reconstruction was performed using standard ADAC iterative reconstruction protocols. A correction for attenuation was performed using Chang attenuation correction of uniform ellipses (Chang, 1978). A rescaling factor was applied to the images prior to analysis, correcting for injected activity of [F-18] FDG and time to scanning. A formal correction for blood glucose levels was not made,

however data with blood glucose levels outside the range 4-7mmol/L were deemed unreliable.

Analysis was performed, where data was deemed reliable, using quantitative volume of interest (VOI) analysis as described in detail in **chapter 5**. This method uses a mathematically derived automated region growing program to objectively define tumour volumes. The total counts within these tumour volumes are then compared to assess response. I performed the quantitative analysis of all of the [F-18] FDG PET scans.

Results

Of the twenty seven patients who received ADEPT, fifteen patients completed three [F-18] FDG PET scans in accordance with the trial protocol. Six patients completed two of the three intended scans. Four patients had only their baseline [F-18] FDG PET scan performed. Two patients had no [F-18] FDG PET scans performed. The details of these scans are outlined in **chapter 6**.

Eleven patients (#2-#10, #12, #13) received 185MBq of [F-18] FDG and were scanned at 45-60 minutes. It was subsequently found that in these patients the count rate capability of the camera was exceeded and these scans were deemed non-quantitative.

Therefore there were nine patients in whom quantitative analysis would be valid. In two of these patients (patient #18 and #23) automated region drawing could not be performed. This was due to tumour being adjacent to bladder in one patient (patient #18), and poor resolution between tumour and surrounding normal tissue in another (Patient #23).

Table 23 outlines the change in total counts in the tumour VOI derived from the automated region growing program in the remaining seven patients.

Table 23: [F-18] FDG PET quantitative analysis

Pt No.	CT scan		[F-18] FDG PET (% change compared with baseline)	
	4 weeks	8 weeks	4 weeks	8 weeks
#15	SD	SD	539%	758%
#19	SD	PD	138%	161%
#11	PD	PD	146%	114%
#14	PD	NA	381%	NA
#20	PD	PD	111%	162%
#24	PD	PD	59%	102%
#26	PD	PD	184%	182%

Results of quantitative [F-18] FDG PET analysis using the percentage change in tumour [F-18] FDG uptake compared with baseline, Analysis was performed using VOI, with the total count statistic used to calculate the percentage change. Comparison is made with CT scan results, measured using WHO criteria. Abbreviations: SD – stable disease; PD – progressive disease; NA- not applicable

The total tumour [F-18] FDG uptake at 4 and 8 weeks increased in almost all patients compared to baseline. This was consistent with the CT scan findings, tumour marker measurements and clinical picture. The exception to this was patient #24, in whom the [F-18] FDG tumour uptake appeared to fall at 4 weeks, and remain stable at 8 weeks. This patient had a CEA expressing non small cell lung cancer with mediastinal lymphadenopathy, previously treated with radiotherapy. This patient remained well on follow-up after ADEPT for 10 months before relapsing with brain metastasis requiring radiotherapy. It appears that the metabolic activity of the tumour may have remained stable with ADEPT in this one patient.

Overall survival

Method

Survival times were calculated from the start of treatment. Overall survival was calculated at the time of the ADEPT Final Report (July 2000 is the date of last contact) and is plotted using Kaplan-Meier.

Results

At the time of issuing the Final Report on ADEPT, there were 22 confirmed deaths and 5 patients were known to still be alive. The median survival of the patients on the ADEPT study was 40 weeks (95% confidence interval 10 – 70 weeks) (**figure 17**). As survival was not an end-point in this study, no major conclusions can be drawn from this survival. A median survival of 40 weeks would, however, be not unexpected given the patient group's disease profile and demographics.

Figure 17: Kaplan-Meier Survival of patients on ADEPT study

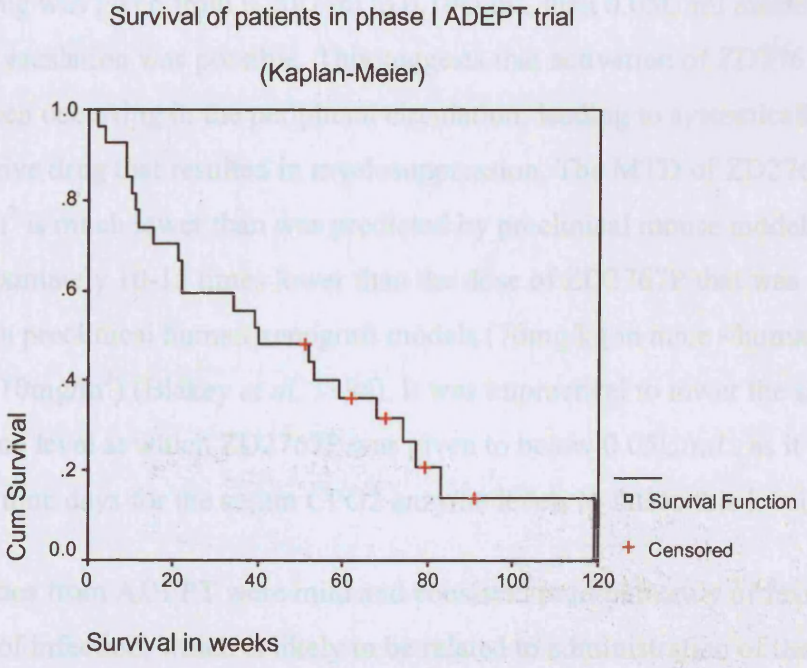

2.4 Discussion

The purpose of this ADEPT trial was to investigate a new prodrug (bis-iodo phenol mustard, ZD2767P) whose activated form is highly potent and has a short half-life, and to study tumour targeting of the antibody-enzyme conjugate, A5CP, without a clearance system. The trial was designed in a mechanistic fashion to allow the determination of whether conditions for effective therapy with ADEPT were met. This included the measurement of CPG2 enzyme levels in serum, tumour and normal tissues, I-131 labelled A5CP biodistribution studies, immunogenicity assessment, prodrug pharmacokinetic analysis and comet assay for DNA interstrand cross-links.

2.4.1 Toxicity

The toxicity of ADEPT consisted predominantly of myelosuppression, which proved dose limiting. DLT was established at a ZD2767P dose of 18.63mg/m^2 x 3 and MTD at 15.5mg/m^2 x 3. Myelosuppression occurred with a thrombocytopaenia nadir at 4 weeks and neutropaenia at 6 weeks. One patient developed Grade 3 thrombocytopaenia and Grade 4 neutropaenia at the first dose level (4.9 mg/m^2 - Patient #3), however reducing the serum enzyme level at which prodrug was given from 0.20U/ml to 0.10U/mL then 0.05U/ml meant further dose escalation was possible. This suggests that activation of ZD2767P may have been occurring in the peripheral circulation, leading to systemically available active drug that resulted in myelosuppression. The MTD of ZD2767P of 15.5mg/m^2 is much lower than was predicted by preclinical mouse models, and is approximately 10-15 times lower than the dose of ZD2767P that was efficacious in preclinical human xenograft models (70mg/kg in mice =human equivalent 210mg/m^2) (Blakey *et al*, 1996). It was impractical to lower the serum CPG2 enzyme level at which ZD2767P was given to below 0.05U/mL, as it was taking up to nine days for the serum CPG2 enzyme levels to fall to this level.

Other toxicities from ADEPT were mild and consisted predominantly of fever in the absence of infection, which is likely to be related to administration of the antibody-enzyme, grade I/II nausea, thought to be related to the prodrug and

grade I/II malaise. As ADEPT is designed to have very few systemic toxicities, this toxicity profile was as predicted.

Three patients with grade II or higher drug related toxicity from full ADEPT had ZD2767P alone administered. This was well tolerated with only a few transient Grade I 'possibly' drug related toxicities experienced. As the prodrug itself was shown *in vitro* to have cytotoxic activity at a level ten fold less than for the active drug (Blakey *et al*, 1996) it was important to demonstrate the safety of ZD2767P alone in the clinical setting. Patient #3 had grade 3 thrombocytopaenia and grade 4 leucopaenia with ADEPT, and had no myelotoxicity with ZD2767P alone. This patient did however have grade I nausea with the administration of ZD2767P alone. Patient #19 had grade 3 thrombocytopaenia and leucopaenia with ADEPT and again no myelotoxicity with ZD2767P alone. Patient #24 had grade 2 thrombocytopaenia and grade 3 leucopaenia with ADEPT, and a grade I transient 'possibly' leucopaenia with ZD2767P alone. ZD2767P alone therefore appears, as expected, to be less toxic than full ADEPT in the small number of patients in which it was studied.

2.4.2 Mechanistic studies

Studying the individual components in terms of their distribution and function facilitates developments of such a complex therapy system. It was also possible to monitor the different components of ADEPT through the course of therapy.

A5CP

Pharmacokinetics

The clearance of A5CP from the blood was calculated by two methods. An assay of CPG2 enzyme activity was performed using methotrexate reduction assay by spectrophotometry, Cobas or HPLC, and the clearance of I-131 radiolabelled A5CP was by measured by recording radioactivity in a sample of blood by gamma counter. There were three batches of A5CP produced for this clinical study. They varied significantly in enzyme activities (50U/mL – 159U/mL), and in their pharmacokinetic profiles. The β half-life of A5CP by clearance of CPG2

enzyme levels from serum was Campaign 1 = 8.95 hrs (spec assay), Campaign 2 =11.8 hrs (cobas) and Campaign 4 = 15.49 hrs (cobas). The β half-life of A5CP by clearance of I-131 radiolabelled A5CP was Campaign 1 = 5.77 hrs, Campaign 2 = 5.08 hrs and Campaign 4 = 11.77 hrs.

The CPG2 assays are functional measures of antibody-enzyme conjugate, which depend on the presence of intact CPG2. They are clinically relevant as they determine whether prodrug can be safely administered to avoid activation in the peripheral circulation. Measurement of radioactivity clearance may reflect not only intact antibody-enzyme, but also, fragments of antibody-enzyme with radioactivity attached. Radiolabelled material with low or absent enzyme activity may have been potentially metabolised in vivo, or damaged by the radiolabelling process, artificially shortening the circulating half-life. The shorter half-life of A5CP obtained by measuring clearance of radioactivity as opposed to functional CPG2 enzyme in this trial is therefore likely to be due to clearance of iodinated breakdown products of I-131 radiolabelled A5CP.

Localisation

The ability to selectively deliver antibody-enzyme to tumour is a critical component of ADEPT. It is therefore important to be able to measure both the amount of antibody-enzyme that reaches the tumour and its distribution in normal tissues. Localisation to tumours is required for efficacy, and uptake in non-tumour tissues may result in toxicity.

Radiolabelling antibodies with gamma emitting radioisotopes, followed by single photon computerised tomography (SPECT) scanning allows their biodistribution to be assessed non-invasively in the clinical situation. Gamma camera imaging provides both a visual representation of the distribution of radioactivity, and, if the camera is appropriately calibrated, a quantitative estimation of antibody localisation. The estimates of antibody localisation obtained using quantitative SPECT imaging can then be confirmed in a small number of patients in whom a tumour biopsy can be performed and CPG2 enzyme levels directly measured.

In order for the radiolabelled antibody to provide an adequate representation of the biodistribution of actual antibody-enzyme, it needs to remain with characteristics as similar as possible to the 'cold' unlabelled antibody-enzyme. In particular it must retain CEA binding, and have a comparable molecular size, conformity and charge. The radioisotope must have a suitable path length for quantitative gamma camera scanning, and a half-life that is compatible with the biological half-life of the antibody-enzyme. The radiolabel must also remain bound in a stable manner to the protein in order to represent its biodistribution. In addition, radioprotection issues for staff members should also be considered.

Two imaging methods on a gamma camera have been used to quantify localisation of radiolabelled antibodies. These are either planar scanning or SPECT scanning. Planar images provide anterior and posterior 2 dimensional data. Organs overlying tumour areas may lead to an over or underestimation of tumour uptake, due to either addition of radioactivity by overlying organs, or masking of the underlying tumour (Green *et al*, 1990). This is an inherent problem with the representation of three-dimensional data in two dimensions. Despite these limitations, quantitation has been used on planar imaging to estimate radiolabelled antibody localisation for clinical studies (Thomas *et al*, 1976; Press *et al*, 1993; Wiseman *et al*, 2003). Scanning times are much shorter with planar imaging, and data manipulation prior to analysis is minimal.

SPECT scans are acquired by rotating the gamma camera detectors around the body, thereby acquiring three-dimensional data. The accuracy of the estimation of radioactivity in tissues is reduced, however, by the presence of Compton scatter, which leads to blurring of the image. Region delineation without correction for this is problematic. Applying scatter correction has been demonstrated to overcome this problem and has lead to accurate quantitation in both phantom studies and in patients (Green *et al*, 1990). This method involves collecting two sets of data; one in the photopeak and one in the scatter window. A correction is then applied for Compton scatter, based on a method initially described for Tc-99m (Jaszczak *et al*, 1984). Attenuation correction using uniform ellipses can be applied to correct for attenuation of the photon through overlying tissues (Chang, 1978). More recently methods that measure actual

attenuation, rather than applying a linear correction, have been developed and are being applied.

Scanning times for SPECT acquisitions are usually longer than for planar imaging, in order to achieve adequate count rates for analysis. The detectors go through 32 frames around the patient, and usually separate acquisitions are required for the thorax and the abdomen (dependent on detector size). The time per frame can be altered dependent on the radioactivity levels in the patient, in order to achieve a suitable count rate for quantitation. Most SPECT scans are performed in 40-60 minutes (for 2 rotations).

SPECT analysis using a correction for both Compton scatter and for uniform attenuation, has been applied to estimate the localisation of radiolabelled antibody-enzyme in a previous ADEPT study (Napier *et al*, 2000). In this study the estimates of tumour enzyme activity by SPECT analysis of I-131 radiolabelled A5CP, were confirmed in 5 out of 10 patients by tumour biopsies. The CPG2 enzyme levels in tumour biopsies were measured by a methotrexate reduction assay on HPLC (Blakey *et al*, 1996; Martin *et al*, 1997). The median enzyme concentration in tumours by direct measurement from tumour biopsies was 0.47U/g (range 0.32-0.62 U/g) (Napier *et al*, 2000). The estimated enzyme units in the tumour based on the biodistribution of I-131 radiolabelled A5CP and SPECT analysis was 0.34 U/g (range 0.19-0.63 U/g) (Napier *et al*, 2000). It was therefore concluded that gamma camera estimates of enzyme concentrations in the tumour were valid. Gamma camera scanning has the advantage of being much less invasive than a tumour biopsy and should be suitable for a large number of patients, some of which may not have lesions suitable for biopsy.

The radioisotope chosen for radiolabelling of A5CP in this clinical trial was I-131. I-131 has a half-life of 8 days. This is appropriate use with for A5CP, which has a half-life of 8.95-15.49 hours (by clearance of CPG2 activity from blood). It was estimated that 370MBq of radiolabelled I-131 A5CP should be sufficient to allow quantitative scanning, with reasonable scan times.

Radiolabelling of A5CP with I-131 was performed using N-bromo-succinamide/L-tyrosine technique (Adam, 1989). Thin layer chromatography

was performed to assess iodine incorporation and antigen binding was assessed using a CEA column. There was variation in the CEA binding and iodine incorporation between the different batches of A5CP. Campaign 1 had a median CEA binding of 6.56%, Campaign 2 had a median CEA binding of 35.9%, and Campaign 4 had a median CEA binding of 21.7%. The median iodine incorporation of I-131 conjugate was 60.75% for Campaign 1, 88.36% for Campaign 2 and for Campaign 4 it was 86.6%. Campaign 1 had the lowest protein concentration, and this may have contributed to its particular poor labelling. All three campaigns had fairly low values for CEA binding post radiolabelling, indicating that the radiolabelling process may have damaged the antibody. Iodine radiolabelling is directed against tyrosine residues on a protein, and these may fall within the antigen binding site of an antibody, thereby disrupting antigen-antibody binding.

The radiolabelled antibody was administered as slow intravenous injections at the end of the cold antibody infusion. SPECT scans were performed at 4, 24, 48, and 72 hours (and 96 hours if appropriate) post administration of radiolabelled antibody.

By visual interpretation and quantitative analysis it was apparent that the I-131 radiolabelled A5CP did not successfully localise to tumour areas. The median uptake of radiolabelled A5CP in heart (estimate for bloodpool) remained higher than in tumour for the 5hr, 24hrs and 46 hrs time-points, and for normal liver it remained higher than tumour at all measured time-points. The overall median % injected dose/kg of radiolabelled conjugate in the tumour on prodrug day was 0.185 %/kg, range 0.0006 - 1.05 %/kg. This translates to an estimated enzyme concentration in the tumour at the time of prodrug administration of 0.01U/g. This is much lower than has been seen in mouse tumour model systems, and in previous clinical trials.

The tumour biopsy data from 7 patients also showed a median CPG2 enzyme level of 0.01 U/g in tumour at the time of prodrug administration, indicating a good correlation between SPECT analysis and direct measurement of enzyme activity by biopsy. An enzyme level of 0.01 U/g in tumour is, however, much lower than the value of 0.47U/g of enzyme activity, that was attained in the

previous clinical study in which a galactosylated clearing antibody was used to accelerate clearance of conjugate from the blood (Napier *et al*, 2000). This previous study did, however, use higher amounts of antibody-enzyme conjugate (10 000U/m^2) and the prodrug was given at an earlier time-point (48 hours), so the difference in enzyme levels must be at least partially attributable to these factors. However, the fact remains that the amount of enzyme measured in tumour in this study is very unlikely to be adequate for therapy. In addition the tumour to blood ratios of CPG2 enzyme activity based on methotrexate reduction assay were 0.4:1 at the time of prodrug administration, which is also in agreement with the lack of localisation seen with the SPECT scans. In the previous ADEPT trial tumour to blood ratios of > 10 000:1 were seen (Napier *et al*, 2000). The very low tumour to blood and tumour to normal tissue ratios in this trial greatly reduce the therapeutic window of ADEPT, and increase the likelihood of serious systemic toxicity due to activation of prodrug in non-tumour sites. It is likely that the myelosuppression seen at such an unexpectedly low ZD2767P dose is likely to have been due to activation of prodrug in the systemic circulation and non-tumour tissues. There was no gain to be achieved in waiting until further systemic clearance of active CPG2 enzyme had occurred, as tumour enzyme levels were already very low, and in some patients it was already taking up to 9 days for CPG2 serum enzyme levels of < 0.05 U/mL to be attained.

Immunogenicity

The formation of HAMA and HACPG2A occurred in all patients except one (Patient #13 - no HACPG2A formation). The median time to formation of antibodies was 14 days. CPG2 is of bacterial origin, and is used in ADEPT systems because it has no human equivalent that may lead to endogenous enzyme activation. The A5B7 $F(ab')_2$ antibody is murine. The immunogenicity of A5CP limits potential for repeated therapy although immunosuppressive therapy has been used to permit up to three therapies in the same patient in the past (Ledermann *et al*, 1991; Bagshawe *et al*, 1995; Bagshawe *et al*, 1996; Napier *et al*, 2000).

ZD2767P

ZD2767P pharmacokinetics

The pharmacokinetic profile of ZD2767P was measured in blood by HPLC. Average AUC values increased with increasing doses. The mean measured half-life of ZD2767P in plasma at the MTD (15.5mg/m^2) was 14.5 minutes. The prodrug was essentially cleared by 60 minutes in all dose levels, and there was no evidence of accumulation of prodrug with the 1 hour intervals between doses.

The maximum concentration of ZD2767P at an administered dose of 18.63mg/m^2 results in a molar concentration of 0.0085μM, which is significantly less than would be expected to result in cytotoxicity based on the cell cytotoxicity experiments from Blakey *et al*, 1996.

ZD2767P is very unstable and required administration within 20 minutes of reconstitution. Although this was possible within a clinical trial setting, this instability may limit the widespread use of ZD2767P outside a clinical trial environment

ZD2767P activation

The active drug formed from ZD2767P has such a short biological half-life that it could not be measured in this study. An indirect measurement instead used a comet assay on cells retrieved from tumour biopsies in order to ascertain the presence of DNA interstrand crosslinks. ZD2767D is an alkylating agent, and produces cell kill by DNA interstrand crosslink formation, so the presence of crosslinks in the tumour biopsy specimen would indicate that an alkylating agent had been active at the tumour site (Webley *et al*, 2001). Within 30 minutes of the tumour biopsy specimen being taken, peripheral blood was also taken to look for DNA crosslinks in circulating lymphocytes. Patient #15 had a biopsy of a liver metastasis of colorectal cancer. An 80% reduction in comet tail, indicating the presence of DNA interstrand crosslinks was demonstrated. The circulating peripheral lymphocytes were unaffected, showing no evidence of DNA crosslink formation. In this patient, the tumour biopsy specimen also showed evidence of

I-131 conjugate localisation on phosphor imager (**table 16a, figure 11**). This suggests that in this one patient effective antibody localisation and selective prodrug activation may have occurred. This patient had radiological stable disease at 56 days.

2.4.3 Efficacy

There were no convincing tumour responses seen in this study by CT scanning and only one patient's tumour appeared not to progress by quantitative metabolic imaging using [F-18] FDG PET. The mechanistic studies performed during this study indicated that there was inadequate targeting of enzyme to tumour and it was thought that even at the MTD responses would be unlikely. Consequently the phase II component of the trial was not undertaken.

2.5 Conclusion

This ADEPT trial was designed to study a new prodrug, ZD2767P, and to assess the targeting of A5CP without a clearing antibody. It was designed in a mechanistic fashion to allow an understanding of ADEPT and to direct changes to this system for the future.

With regard to the new candidate prodrug for ADEPT, ZD2767P, pharmacokinetic information was attained, and evidence of ZD2767P activation was obtained in the tumour of one patient by comet assay, and in the blood, indirectly, by the finding of myelosuppression when prodrug was given after antibody-enzyme and by lack of myelosuppression when prodrug was given alone. The dose achieved of ZD2767P was much less than predicted and this was almost certainly as a result of the slow clearance of A5CP from the circulation, with residual CPG2 in serum likely to have been causing systemic ZD2767P activation. The dose of ZD2767P administered is likely to have been too low to be efficacious.

Targeting of A5CP without a clearing antibody was found to be inadequate, with tumour to serum enzyme ratios of less than one, which is insufficient for selective prodrug activation in tumour. The slow blood clearance of A5CP made

it impractical to lower the level for serum CPG2 enzyme any lower than 0.05U/mL. Tumour biopsy and gamma camera data indicated that there would be insufficient enzyme in tumour at these late time points for adequate prodrug activation to occur. As was found previously the universal production of human antibody to A5CP prevented repeated therapy.

This trial demonstrates, however, that it was possible to measure serum CPG2 enzyme levels and to make a decision on the timing of administration of ZD2767P based on these. The toxicities experienced appeared dependent on the serum CPG2 enzyme level at the time of administration of ZD2767P. This suggests that if adequate tumour targeting of CPG2 can be attained, with corresponding low serum and normal tissue CPG2 enzyme levels, adequate dose escalation of ZD2767P may be achieved.

In conclusion this trial has demonstrated the potential of ZD2767P for use in further ADEPT studies, in which better tumour localisation of antibody-enzyme can be achieved. It has shown also that a clearance system should be used with the A5CP chemical conjugate, or a better antibody-enzyme targeting system needs to be developed. The mechanistic studies performed in this trial assisted with the interpretation of the trial outcomes and influenced decisions taken during the trial period, such as the lowering of serum CPG2 levels at the time of ZD2767P administration in order to allow further dose escalation. They also served to prevent the further treatment of up to 14 patients at MTD to assess response to ADEPT, as they indicated that the likelihood of response would be very low. Mechanistic studies should continue to be incorporated into the design of clinical trials of ADEPT for the future, as they have assisted in the understanding of ADEPT and the directing of preclinical development for the future.

2.6 Acknowledgements

This clinical trial involved the integration of many people, with specialist knowledge and expertise. The contributors to the clinical trial have been listed below, and their contribution is gratefully acknowledged (**table 24**). The data obtained from analysis performed from someone other than myself has been acknowledged in both the text and in the table below. As this data is so integral to the understanding of ADEPT it has been included in the main body of the text.

My contribution was as co-investigator in this trial and, as such, I was directly responsible for the clinical recruitment, treatment, follow-up and overall care for the patients who participated in the study. I performed the SPECT and [F-18] FDG PET analysis for all of the patients in the trial (**see chapters 5 and 6**). I was responsible for the collection and integration of all of the relevant data for this trial. I presented updates for quarterly Astra-Zeneca/ CRC meetings and wrote, with assistance from the Cancer Research Campaign, the interim and final reports for this trial, which were submitted to Astra-Zeneca. My contribution was also an intellectual one, to the interpretation of the data collected, and the amalgamation of it into a better understanding of ADEPT.

Table 24: Contributors to ADEPT A5CP and ZD2767P clinical trial

Contributor	Contribution
[1]Prof Richard Begent	Principal Investigator Recruitment, clinical care and management of patients
[1] Dr Surinder Sharma	CPG2 enzyme measurements (Spec/Cobas and HPLC) Immunogenicity -HAMA and HACPG2A by ELISA Radiolabelling of antibody (including TLC and CEA binding)
[2]Prof Caroline Springer [2]Jan Martin	ZD2767P pharmacokinetics
[1]Shareal Webley [1]Dr Daniel Hochhauser	Comet assay
[1]Geoff Boxer	Phosphor plate analysis
[1]Dr Alan Green [1]Kathryn Adamson [1]Sandra Baig	Gamma camera scanning of patients and reconstruction of data. Gamma counter calibration and analysis of samples
[1]Dr Daniel Hochhauser [1]Dr Eleni Tsiompanou [1]Laura Hope-Stone [1]Denise O'Malley	Contributed to the clinical care and management of patients
[3]Dr Luiza Sena [3]Adele Robbins [3]Lindsey Gumbrell	Data monitoring and data entry at CRC Drug Development Office. Assistance in writing of final and interim reports.

[1] *Cancer Research UK Targeting and Imaging Group, Department Oncology, Royal Free and University College Medical School, University College London, London NW3 2PF*
[2] *Cancer Research UK Centre for Cancer Therapeutics, Institute of Cancer Research, Sutton, Surrey, SM2 5NG*
[3] *Cancer Research Campaign (CRC) Drug Development Office (now 'Cancer Research UK' Drug Development Office)*

This trial was supported by Cancer Research Campaign, AstraZeneca, Ronald Raven Trust and The Wolfson Trust

2.7 Published papers

The data from this clinical trial have been published as:

Francis R, Sharma SK, Springer C, Green AJ, Hope-Stone LD, Sena L, Martin J, Adamson KL, A Robbins, L Gumbrell, O'Malley D, Tsiompanou E, Shahbakhti H, Webley S, Hochhauser D, Hilson AJ, D Blakey, Begent RHJ (2002) A Phase I Trial of Antibody Directed Enzyme Prodrug Therapy (ADEPT) in patients with advanced colorectal carcinoma or other CEA producing tumours *Br J Cancer* 87(6): 600-607

Webley SD, Francis RJ, Pedley RB, Sharma SK, Begent RH, Hartley JA, Hochhauser D (2001) Measurement of the critical DNA lesions produced by antibody-directed enzyme prodrug therapy (ADEPT) in vitro, in vivo and in clinical material. *Br J Cancer* 84(12): 1671-1676

3 Radiolabelling of glycosylated MFE-23::CPG2 fusion protein (MFECP1) with Technetium-99m, for quantitation of antibody-enzyme biodistribution in ADEPT

3.1 Background

The experience gained with ADEPT in the clinical setting using A5CP in combination with ZD2767P prodrug concluded that in the absence of a clearing antibody system, inadequate targeting of A5CP to tumour was attained (**chapter 2**). In addition, the chemical conjugation process required to form A5CP resulted in heterogeneous batches of A5CP, which all differed in enzyme activity, pharmacokinetic profile and radiolabelling profile. These findings directed the development of a novel genetically engineered fusion protein for ADEPT, consisting of a high affinity anti-CEA scFv, MFE-23, in combination with the bacterial enzyme CPG2 (Michael *et al*, 1996; Bhatia *et al*, 2000; [1]Chester *et al*, 2000). Genetic fusion proteins have the advantages of improved homogeneity and stability of their protein product, as they do not require further manipulation after expression. Also, as the genetic code is known, there are improved opportunities for modification of desired properties such as affinity, size, charge and immunogenicity ([2]Chester *et al*, 2000). The process leading to the development of this fusion protein is outlined in detail in **chapter 4**.

3.1.1 MFECP1 – preclinical characteristics

MFE-23 was selected using phage display technology for its affinity to CEA (Chester *et al*, 1994). MFE-23 has been studied in both pre-clinical models and in clinical trials of radioimmunoscintigraphy and radioimmunoguided surgery, and has been shown to effectively localise to CEA expressing tumours (Begent *et al*, 1996; Mayer *et al*, 2000). In addition, MFE-23 has been shown to be of low immunogenicity with none of fourteen patients developing HAMA after one administration (Begent *et al*, 1996).

The fusion protein of MFE-23 in combination with CPG2 was initially developed in an *Escherichia coli* expression system, and was shown to have many of the

properties desirable for use in ADEPT systems (Michael *et al*, 1996; Bhatia *et al*, 2000) (**see chapter 4**). The production of the fusion protein in *Escherichia coli* resulted, however, in yields that were too low to support a clinical trial. Production in *Pichia pastoris* was subsequently developed and resulted in a 100-fold increase in protein yields and a glycosylated product. In preclinical biodistribution experiments the glycosylated MFE-23::CPG2 fusion protein (termed MFECP1) resulted in excellent tumour targeting as early as 4-6 hours after administration. The tumour to plasma ratios of active CPG2 enzyme were 250:1 at 6 hours, with an enzyme activity in tumour of 1.3 U/g (±0.2U/g) (Sharma *et al*, 2000). This allowed ZD2767P to be administered at 4-6 hours after administration of MFECP1, resulting in tumour growth delays in xenograft models, with no resultant toxicity as assessed by weight loss in mice (Sharma *et al*, 2000). This product was therefore chosen as the antibody-enzyme component for the next ADEPT clinical trial.

3.1.2 Monitoring distribution of MFECP1 in clinical trials

The ability to quantify the biodistribution of antibody-enzyme in ADEPT in the setting of a clinical trial is important for the understanding and subsequent development of such a complex therapy. A non-invasive measure of the amount of antibody-enzyme in the tumour at the time of prodrug administration is desirable to be able to validate whether adequate tumour targeting of enzyme is occurring in order to activate prodrug. Secondly, it is important to ascertain whether any retention is occurring in non-tumour areas, which may lead to non-specific activation of prodrug, and consequent toxicity.

Radiolabelling a protein with a suitable γ emitting radionuclide and administering this to a patient allows gamma camera imaging to be performed, and a visual and quantitative assessment of biodistribution of that protein can be made. This technique has been shown to result in a valid assessment of tumour enzyme level in the last two ADEPT trials (Napier *et al*, 2000; Francis *et al*, 2002). The estimate of tumour enzyme activity attained by gamma camera imaging can be confirmed in a subset of consenting patients with a tumour biopsy.

As previously discussed, in order for the radiolabelled product to represent the biodistribution of the actual antibody-enzyme, it needs to remain as unaltered as possible by the radiolabelling process. In particular it must retain CEA binding, and have a comparable molecular size, conformity and charge. The radioisotope used must have a suitable path length for quantitative gamma camera imaging, and a half-life that is compatible with the biological half-life of the antibody-enzyme. The radiolabel should remain bound in a stable manner to the protein.

The rapid clearance of MFECP1 allows prodrug to be administered at 4-6 hours after fusion protein administration. Therefore imaging should be performed at this time. Technetium-99m (Tc-99m) is used extensively for both visual and quantitative gamma camera imaging due to its ready availability, ease and inexpensiveness of production, suitable imaging properties (140keV γray with 89% abundance) and a half-life of 6 hours (Mease and Lambert, 2001). It was therefore proposed to be a candidate radioisotope for radiolabelling MFECP1 for the new ADEPT clinical trial.

Several methods have been described for radiolabelling scFv with technetium. Since many scFv do not contain disulfide bridges, those methods which are dependent on free sulfhydryl groups could only be made available by either using a thiol containing chelator or by genetically engineering in a cysteine into the scFv. Chelation methods have been associated with instability of the labelled proteins, and attempts to genetically engineer in cysteine groups into proteins may lead to problems with protein expression, folding or stability (Verhaar *et al*, 1996). Transfer of technetium *in vivo* to other sulfur-containing ligands may also be a source of radiopharmaceutical instability (Stalteri *et al*, 1999).

Recently a new method has been developed for technetium radiolabelling of proteins in which a stable Tc-99m -carbonyl $[^{99m}Tc(H_2O)_3(CO)_3]^+$ (TcCO) intermediate is formed directly from pertechnetate $[^{99m}TcO_4]^-$ by reduction with sodium borohydride ($NaBH_4$), in a carbon monoxide (CO) atmosphere (Alberto *et al*, 1998). Formation of the TcCO intermediate can, using this method, be achieved using technetium in a sodium chloride solution (sodium pertechnetate), which is the commonest way technetium is eluted from a commercial molybdenum-99 (^{99}Mo)/^{99m}Tc generator. Once the TcCO intermediate is formed

it can readily exchange its three labile water ligands with a variety of donor ligands to form a stable complex. A possible donor ligand is histidine ([1]Waibel *et al*, 1999).

Hexahistidine tags (His tags) are commonly engineered onto recombinant proteins in order to facilitate purification using immobilised metal ion-affinity chromatography (IMAC) (Casey *et al*, 1995). IMAC purification was used in the production of MFECP1, so a His tag was readily available for site-specific labelling. The His tag of MFECP1 is located on the C terminal end of CPG2, away from the antigen binding site. This is an advantage as the label should not interfere with antigen binding and, as it is associated with the CPG2 end of the molecule, it should reflect the distribution of CPG2 enzyme, which is the component of MFECP1 ultimately responsible for prodrug activation in the ADEPT system. Technetium radiolabelling of MFE-23, has been successfully performed by this method, also using the His tag, and has been shown to be an effective and robust method in this setting ([2]Waibel *et al*, 1999).

The aims of these experiments therefore are to radiolabel MFECP1 with TcCO via site-specific radiolabelling to the His tag on the C terminus end of the protein. Once the conditions for radiolabelling have been defined, a preclinical biodistribution experiment will be performed to ascertain whether the localisation of TcCO radiolabelled MFECP1 accurately reflects distribution of active CPG2 enzyme in a human xenograft model. These results will be used to ascertain whether this method could be used to radiolabel MFECP1 in order to assess biodistribution of antibody-enzyme for the next ADEPT clinical trial.

3.2 Method

3.2.1 Formation of Tc-99m- carbonyl (TcCO)

Sodium carbonate (Na_2CO_3) 4mg, sodium potassium tartrate (NaK-Tartrate) 20mg, and sodium borohydride ($NaBH_4$) 5mg were added to an 8mL glass vial. This was then sealed and flushed with carbon monoxide for 10 minutes. To prepare the intermediate, 0.5mL of Tc-99m in saline solution was added to the vial, which was heated in a water bath at 75°C for 15 minutes. The mixture was

cooled to room temperature and neutralised with 0.1mL of 1M phosphate-buffered saline (PBS) and 0.12 mL of 1M hydrochloric acid (final pH=7.0).

Freeze dried kits

Freeze dried kits were prepared by dissolving sodium carbonate (Na_2CO_3) 4mg, sodium tartrate (Na_2Tartrate) 20mg, and sodium borohydride ($NaBH_4$) 5mg with 100μL of water added in 8mL glass vials and then lyophilised for 1 hour. The sealed vials were then purged with carbon monoxide for 10 minutes, before being stored for later use at -40°C. The TcCO complex was then made by adding 0.5mL of Tc-99m in saline solution to the vial, and heating in a water bath to 75°C for 15 minutes. The mixture was cooled to room temperature, neutralised with 0.1mL of 1M PBS and 0.12 mL of 1M hydrochloric acid (final pH=7.0).

The formation of TcCO was confirmed by reverse phase high performance liquid chromatography (RP-HPLC) using a Galaxy Jupiter column.

3.2.2 TcCO - MFECP1 complex

The TcCO - MFECP1 complex was made by simply mixing the MFECP1 solution and the TcCO solution together. The formation of TcCO - MFECP1 was monitored over time with size exclusion HPLC on a Biosep 3000 column eluted at 0.5ml/min with 0.1M phosphate buffer, pH 7, or by instant thin layer chromatography (ITLC) developed in 0.9% sodium chloride. The influence of temperature and protein concentration on the rate of formation of the TcCO MFECP1 complex was studied.

3.2.3 PD10 purification

A PD10 sepharose column (Amersham Life Sciences, Amersham, UK) was primed by washing through 20mL of PBS. The amount of activity of the radiolabelled antibody (1mL) was recorded and the radiolabelled antibody was then added to the column. 2mL PBS was added and collected into vial 1. 1mL PBS was then added and collected into vial 2. This process was repeated three times (vials 3, 4 and 5). The radioactivity was recorded for each vial and in the

column. Vial 2 contained the purified product. The purified product was confirmed by using size exclusion HPLC as outlined above.

3.2.4 CEA binding

CEA column

The CEA column was prepared by washing with 5mL of 3M ammonium thiocyanate. The column was regenerated by adding 20mL PBS. 5μL of radiolabelled antibody was diluted by adding 295μL of PBS. The activity was recorded with the gamma counter. The radiolabelled antibody in PBS (300μL) was added to the column. The non-bound fraction was washed out with 3mL PBS and collected for counting. The first 1mL was kept separate for reapplication to column. The bound antibody was eluted off the column using 3mL 50mM diethylamine (DEA). The bound fraction was collected for counting. The column was then regenerated with PBS. The first unbound fraction was reapplied (1mL) to column and the run repeated (in case of column saturation with the first run).

Cell binding assay

2 confluent flasks of MKN45 CEA expressing cells were trypsinased and resuspended in 5mL of cold 1% bovine serum albumin (BSA)/PBS in a universal. This was then centrifuged at 1000 rpm for 5mins. The supernatent was discarded and cells resuspended in 3mL cold 1% BSA/PBS. All cell clumps were broken by repeated syringing through a 23G (blue) needle.

2 rows of 5 eppendorf tubes were prepared. 0.5mL of cold 1% BSA/PBS was pipetted into tubes 2-5 of each row. 0.5mL of the cell suspension was pipetted into tubes 1 and 2 of each row. Tube 2 was briefly vortexed and 0.5mL of the contents were transferred to tube 3. Tube 3 was briefly vortexed and 0.5mL of the contents were transferred to tube 4. Tube 4 was briefly vortexed and 0.5mL of the contents were transferred to tube 5. Tube 5 was briefly vortexed and 0.5mL of the contents were discarded. The rows of tubes were labelled 1-5 and 6-10.

0.5mL of cell suspension was added to 2 further eppendorf tubes. These tubes were labelled NSB (non-specific binding). 50μL of unlabelled antibody was added to each of these tubes and they were vortexed briefly.

The radiolabelled antibody was diluted to a final concentration of 50ng/mL with cold 1% BSA/PBS and made to a final volume of 4mL. 250μL of the diluted radiolabelled antibody was pipetted into tubes 1-10, both NSB tubes and 2 further empty eppendorf tubes. The last 2 tubes were labelled T (total activity).

Tubes 1-10 and NSB were briefly vortexed and then inserted into sterilin universal containers. They were then incubated for 2 hours while rotating on the spiramix.

Tubes 1-10 and NSB were then placed in a microfuge for 2 mins at 1300rpm. The supernatant was discarded taking care not to disturb the pellet. 0.5mL of 1% BSA/PBS was then pipetted into each tube and vortexed to resuspend the pellet. Again the tubes were placed in the microfuge for 2 mins at 1300rpm and the supernatant was carefully removed and discarded the taking care not to disturb the pellet.

All eppendorf tubes were counted in the gamma counter (tubes 1-10, NSB and T).

The immunoreactive fraction was calculated by plotting the total/bound fraction against the dilution factor used, with the reciprocal of the y intercept giving the value for immunoreactive fraction.

3.2.5 Stability studies

Size exclusion fast perfusion liquid chromatography (FPLC) was performed to assess for stability of TcCO-MFECP1. TcCO labelled MFECP1 diluted in PBS was applied to a Superose-12 column (XK 16/60) run at a flow rate of 0.5mL/min (in PBS) using a Millipore-Waters 650E system. 2mL fractions were collected after they had passed through the column. Radiactivity in each fraction were counted in a Minaxi Auto-Gamma 5000 Series Gamma Counter (Packard

Instruments). Counts were plotted against fraction number to give a radioactivity profile.

Overnight incubation of TcCO radiolabelled MFECP1 in human serum (1:20) at 37°C was then performed, and the FPLC process repeated. A 1:9 dilution with PBS was made before applying the sample to the FPLC column.

3.2.6 Histidine challenge

A 10 000 fold excess of histidine was incubated with TcCO radiolabelled MFECP1.

The histidine solution was made by adding 70mg histidine to 0.5mL PBS (pH=4). The pH was normalised to 7 by adding 0.15mL sodium hydroxide (NaOH) and 0.35mL PBS.

TcCO radiolabelling of MFECP1 and PD10 purification was performed (size exclusion HPLC was used to confirm a pure product). 50µL of histidine solution was added to 500µL of radiolabelled MFECP1. 250µL of this solution was kept at 25°C and 250µL at 37°C. Of the remaining 500µL of TcCO-MFECP1, 250µL was kept as a control at 25°C, and 250µL as a control at 37°C.

Size exclusion HPLC, as described above, was performed on both histidine containing and control samples kept as 25°C and 37°C at 1 hour and 24 hours.

3.2.7 Biodistribution studies

The biodistribution of TcCO radiolabelled MFECP1 was assessed in LS174T nude mice xenografts. LS174T is a CEA expressing human colon adenocarcinoma cell line which, when implanted in nude mice, results in tumours that express CEA on their cell surface, but no measurable CEA in the circulation. Small tumour pieces ($1mm^3$) were implanted into the flanks of the mice and were allowed to grow until the tumours were 0.1-0.2cm^3 in size.

Radiolabelling was performed using freeze dried kits in which 300MBq of pertechnetate was labelled to 9.6mg/600U of MFECP1. The final labelled

volume was 2mL. 0.3mL was removed for analysis (TLC, CEA binding and FPLC), leaving a final volume of 1.7mL (170MBq, 8.16mg, 510U). This was then diluted with 0.9% sodium chloride to allow a volume of 0.2mL of to be administered via the tail vein of 3 groups of 5 mice as a single injection of 10MBq/ 0.48mg/30U TcCO MFECP1.

Tissues (blood, liver, kidney, lung, spleen, colon, muscle and tumour) were taken at 1 hour, 4 hours and 6 hours to assess distribution of radioactivity and for measurement of enzyme activity. The tissues taken for counting of radioactivity were weighed then dissolved overnight in 7M potassium hydroxide. The following day they were homogenised then counted in the Minaxi Auto-Gamma 5000 Series Gamma Counter (Packard Instruments). The tissues taken for assessment of enzyme activity were weighed then frozen at -70°C. Analysis of enzyme activity was performed by SK Sharma using a methotrexate reduction assay on HPLC as previously described (Blakey *et al*, 1996; Martin *et al*, 1997).

3.3 Results

3.3.1 Assessment of Formation of TcCO

The formation of the TcCO intermediate was assessed by reverse phase HPLC. >99% of activity was in the TcCO peak on the RP-HPLC trace, and <1% of activity was in the form of pertechnetate (**figure 18**).

Figure 18: Reverse phase HPLC trace of TcCO

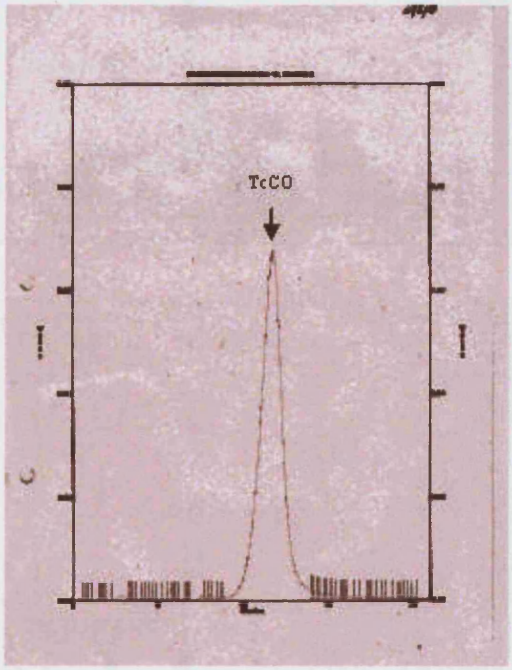

Freeze dried kits

Formation of TcCO was monitored by RP HPLC after storing the kits at -40°C. It was found that the kits remained viable for at least 6 months. Yield was >99%.

3.3.2 Assessment of Formation of TcCO-MFECP1 complex

The incorporation of TcCO onto MFECP1 was assessed by HPLC and ITLC. The TcCO-MFECP1 complex was found to be a heterogeneous product, consistent with known glycosylations causing variations in molecular weight of the product and produced several peaks on the HPLC trace (**figure 19**).

Figure 19: Size exclusion HPLC displaying formation of TcCO – MFECP1 complex

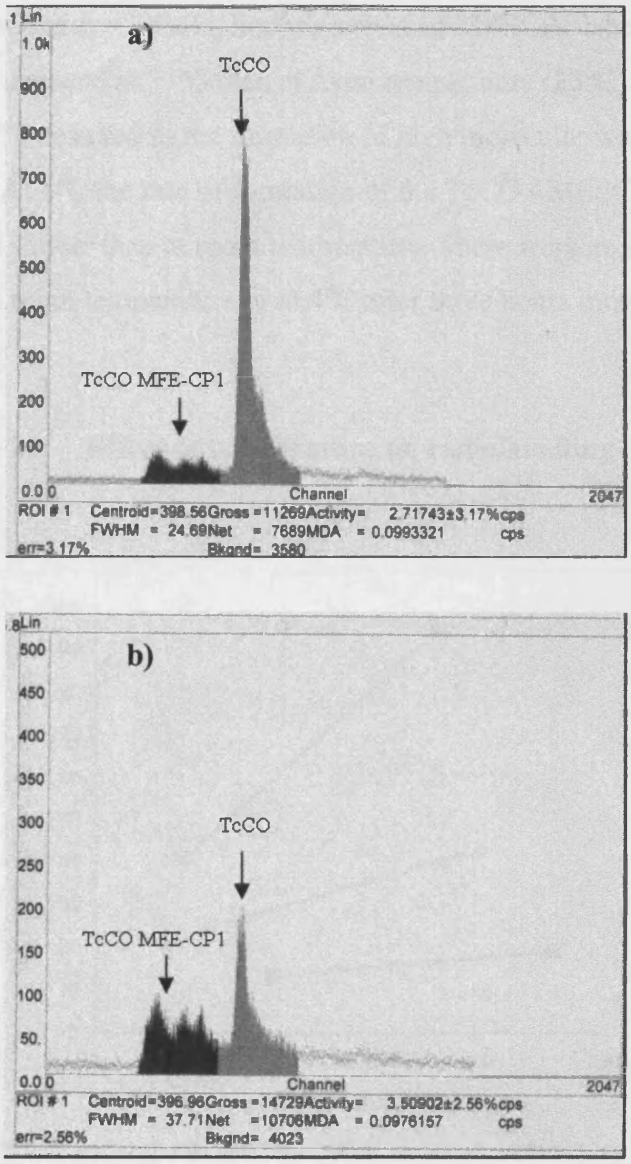

HPLC trace (size exclusion column) showing gradual incorporation of TcCO onto MFECP1 over time. Figure 19 a) is after 30 mins incubation of TcCO with MFECP1. Figure 19 b) is after 120mins incubation with TcCO and MFECP1. The TcCO MFECP1 peak increases with time and the TcCO peak decreases. The presence of several TcCO MFECP1 peaks is consistent with the heterogeneity of the protein due to its glycosylations.

Effect of Temperature on labelling:

The rate of formation of the TcCO - MFECP1 complex was found to be temperature dependent, with a higher proportion of MFECP1 labelled at 30 minutes when incubated at 37°C than at room temperature (25°C). However, incubating at 37°C resulted in the formation of high molecular weight aggregates, seen on HPLC. At 4°C the rate of formation of the TcCO - MFECP1 complex was found to be slower than at room temperature. There were no aggregates formed either at room temperature or at 4°C after three hours incubation (**figure 20).**

Figure 20: Effect of temperature on radiolabelling

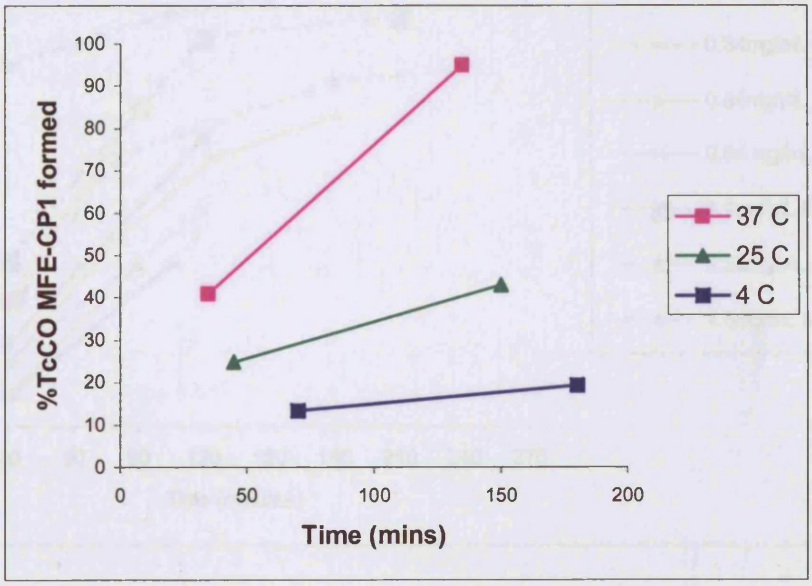

Effect of Concentration of MFECP1 on labelling

The %incorporation of TcCO to the MFECP1 varied with the concentration of MFECP1 used. At concentrations of protein >1mg/mL in the TcCO - MFECP1 solution, the rate of incorporation of TcCO to MFECP1 occurred slightly faster than at lower protein concentrations (**figure 21**).

Figure 21: The effect of varying protein concentrations on the rate of radiolabelling of MFECP1

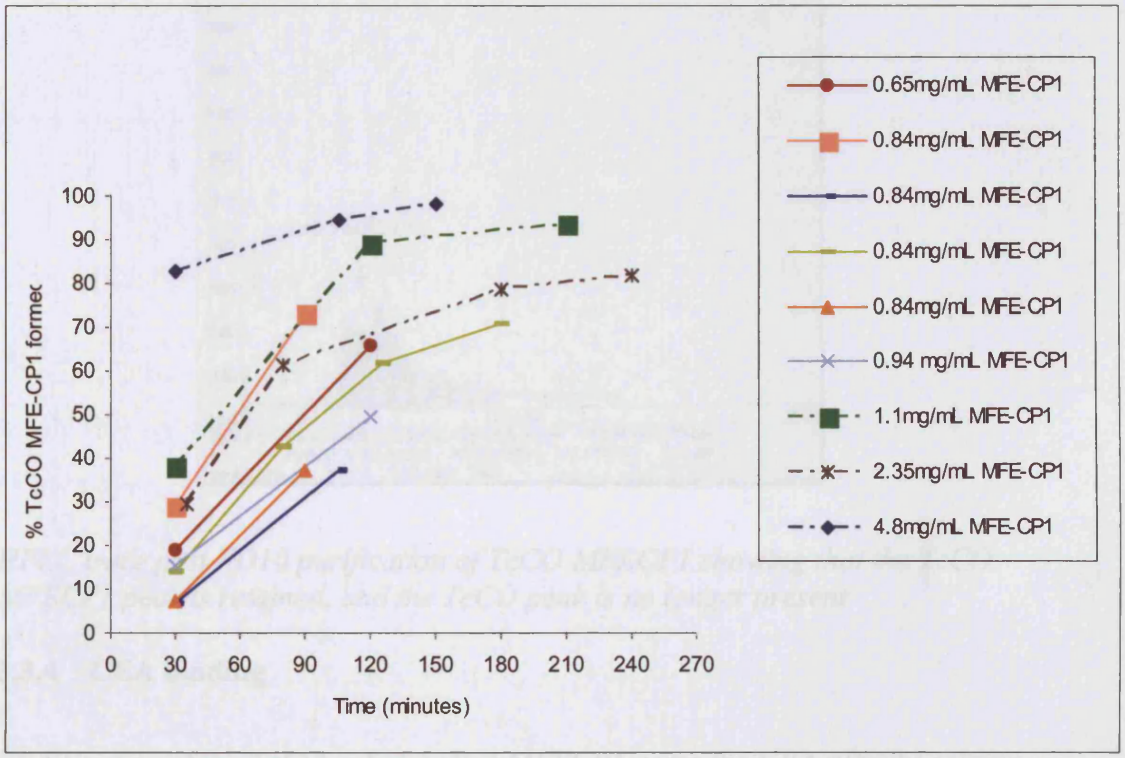

3.3.3 PD10 purification

PD10 purification was performed and shown by HPLC and ITLC to successfully be able to isolate the TcCO - MFECP1 complexes, with post purification traces showing efficient separation of the free TcCO and the TcCO MFECP1 complexes **(figure 22).**

Figure 22: PD10 purification

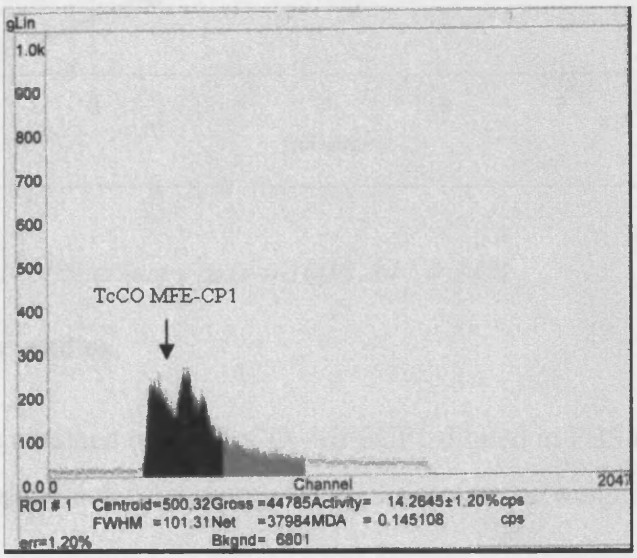

HPLC trace post PD10 purification of TcCO MFECP1 showing that the TcCO MFECP1 peak is retained, and the TcCO peak is no longer present

3.3.4 CEA binding

CEA binding of the TcCO radiolabelled MFECP1 using the CEA affinity column resulted in a median CEA binding of 75% (range 61-77%). As a control, binding to a sepharose column was used – this resulted in non-specific binding to the column of a median of 12% (range 6-16%).

The immunoreactive fraction of the tracer was also using a cell based assay. This resulted in CEA binding of 54% (4 dilutions) (**figure 23**).

Figure 23: Cell binding assay

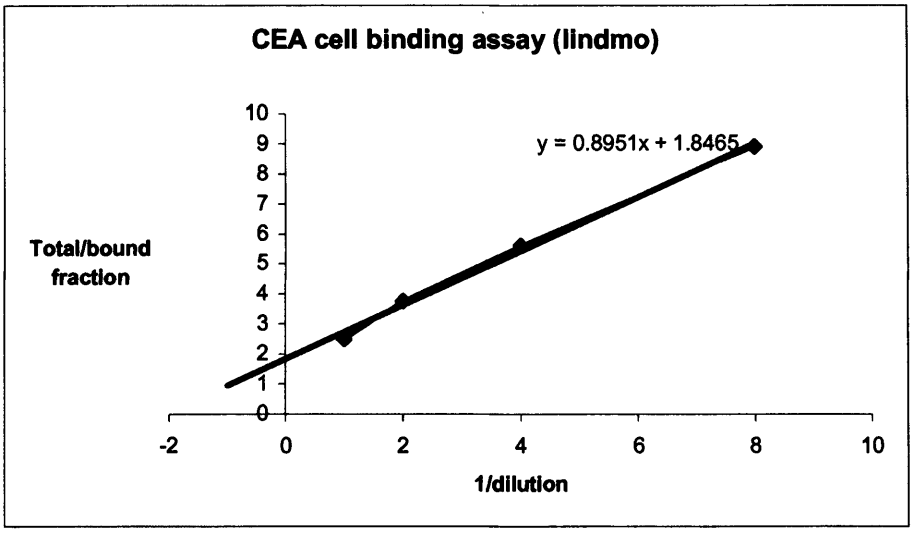

CEA binding =100/ intersect y axis = 100/1.84 = ***54%***

3.3.5 Stability studies

The FPLC trace obtained on the TcCO -MFECP1 diluted in PBS resulted in a single broad peak, which corresponded with the molecular weight of the protein (**figure 24**).

Figure 24: FPLC trace of TcCO-MFECP1 in PBS

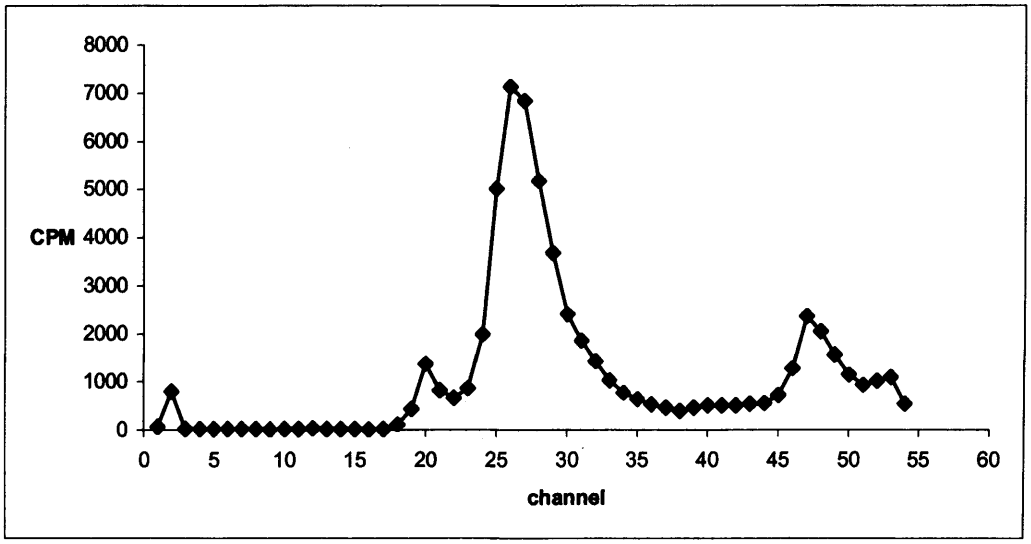

CPM – counts per minute

After overnight incubation in human serum at 37°C an addition high molecular weight appeared which would be consistent with some degree of aggregation of

the protein (**figure 25**). The majority of the activity stayed, however, within the peak corresponding to TcCO-MFECP1.

Figure 25: FPLC trace of TcCO-MFECP1 after overnight incubation in serum at 37°C

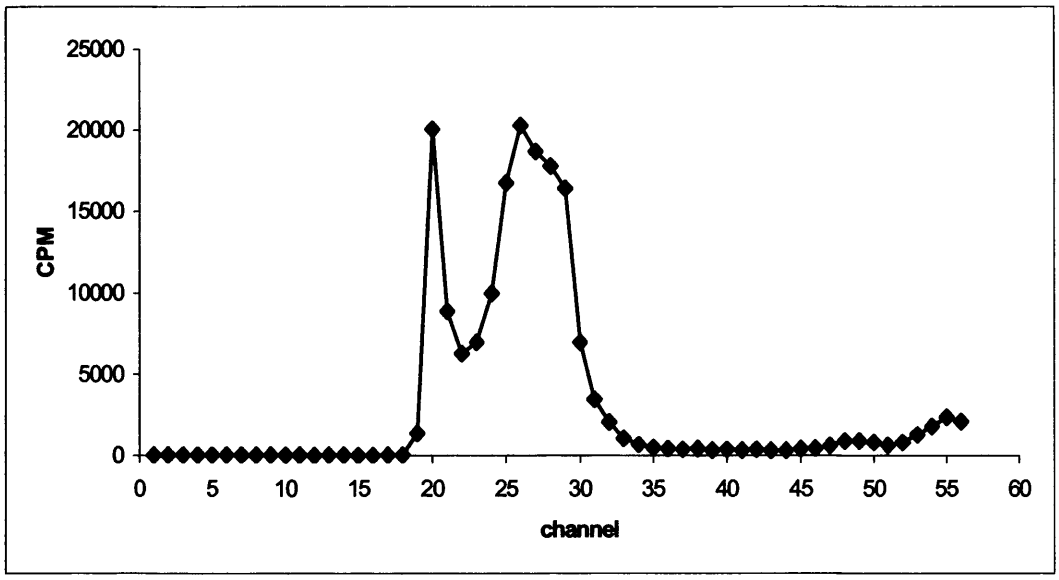

CPM – counts per minute

3.3.6 Histidine challenge

The retention time for a TcCO -histidine peak was identified by radiolabelling histidine with TcCO and running on size exclusion HPLC. Size exclusion HPLC analyses were then performed at approximately 1 hour and 24 hours on both histidine containing and control TcCO-MFECP1 samples and the % of total activity in the TcCO –histidine peak was measured. In the control samples after 1 and 24 hrs at both 25°C and 37°C, <4% of total radioactivity was in the TcCO-histidine peak while in the samples with 10 000 fold excess of histidine up to 25% of the total radioactivity occurred in the TcCO-histidine peak. This indicates that at high concentrations of histidine, displacement of technetium from the His tag onto free histidine can occur. A 10 000 fold excess of histidine is however not likely to arise in a physiological situation. These results are summarised in **table 25** and **figure 26**.

Table 25: Percentage activity in TcCO-histidine peak on HPLC

	25^{0}C		37^{0}C	
	1 hr	**24 hrs**	**1 hr**	**24 hrs**
control	1.1%	3.9%	2.5%	2.3%
His x 10 000	5.2%	15.9%	7.8%	24.6%

Figure 26: Histidine challenge

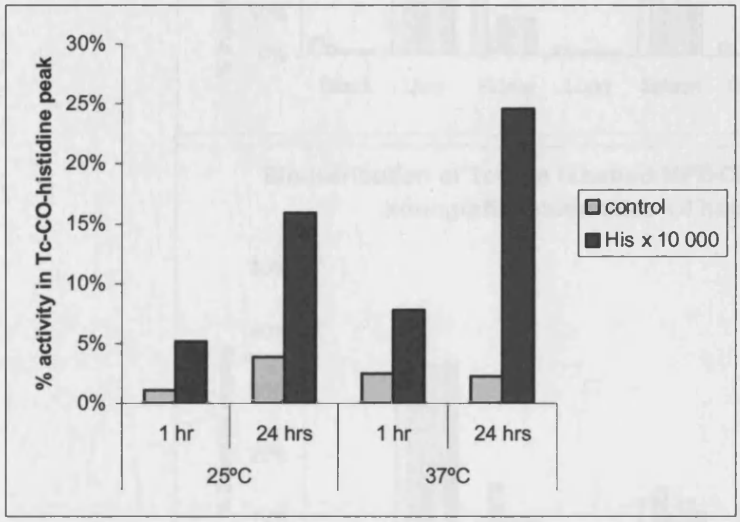

3.3.7 Biodistribution study

ITLC on radiolabelled TcCO-MFECP1 used for the biodistribution study confirmed >99% TcCO incorporation onto MFECP1. CEA binding was 75% on the CEA column.

The results of distribution of radioactivity in the tissues studied at 1 hour, 4 hours and 6 hours are shown in **figure 27**.

Figure 27: Biodistribution of TcCO-MFECP1 in mice bearing human colorectal cancer xenografts

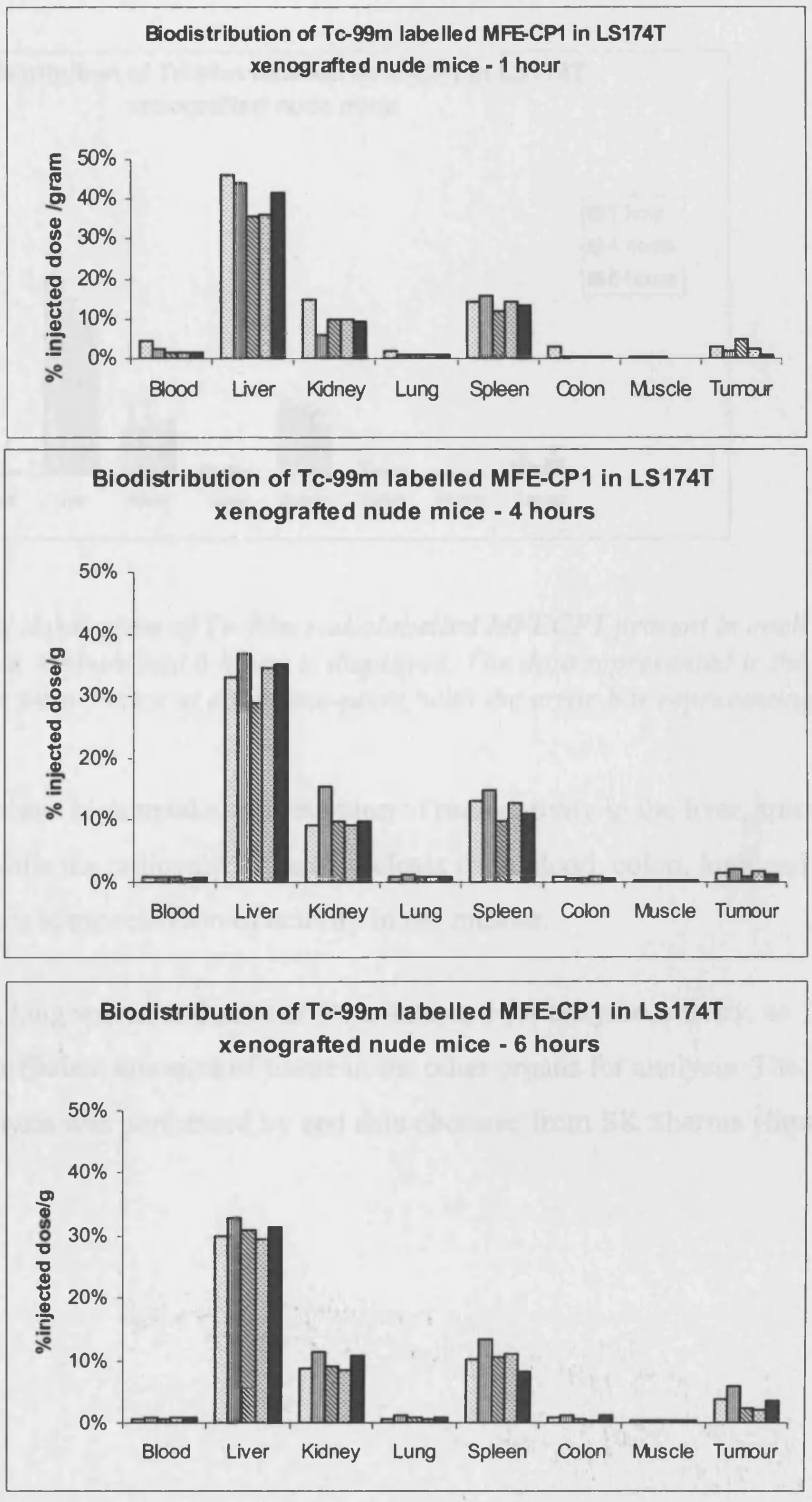

The median % injected radioactivity/ g for each tissue at each time point is shown in **figure 28**:

Figure 28: Median %injected dose/g tissue

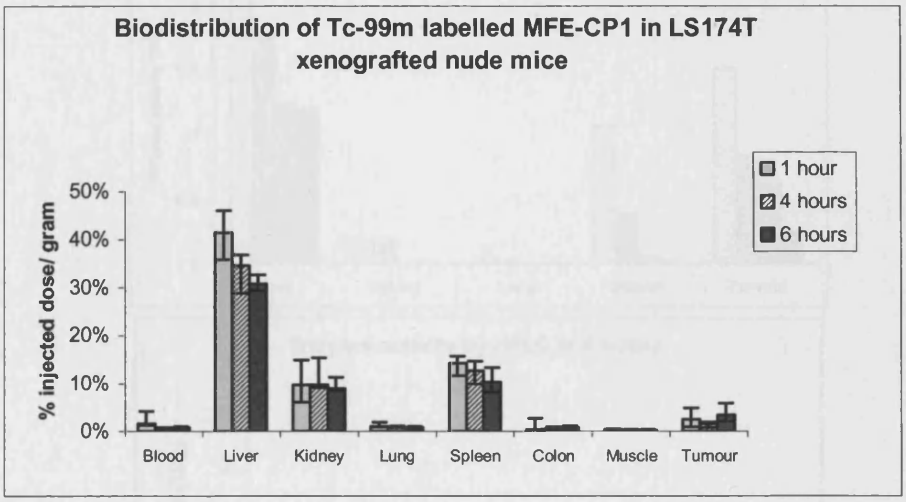

The % injected dose/ gram of Tc-99m radiolabelled MFECP1 present in each tissue at 1 hour, 4 hours and 6 hours is displayed. The data represented is the median results from 5 mice at each time-point, with the error bar representing the range.

These results show high uptake and retention of radioactivity in the liver, spleen and kidneys while the radioactivity rapidly clears from blood, colon, lung and muscle. There is some retention of activity in the tumour.

Liver, kidney, lung spleen and tumour were analysed for enzyme activity, as there were insufficient amounts of tissue in the other organs for analysis. The following analysis was performed by and data obtained from SK Sharma (**figure 29**).

Figure 29: CPG2 enzyme activity after administration of TcCO-MFECP1

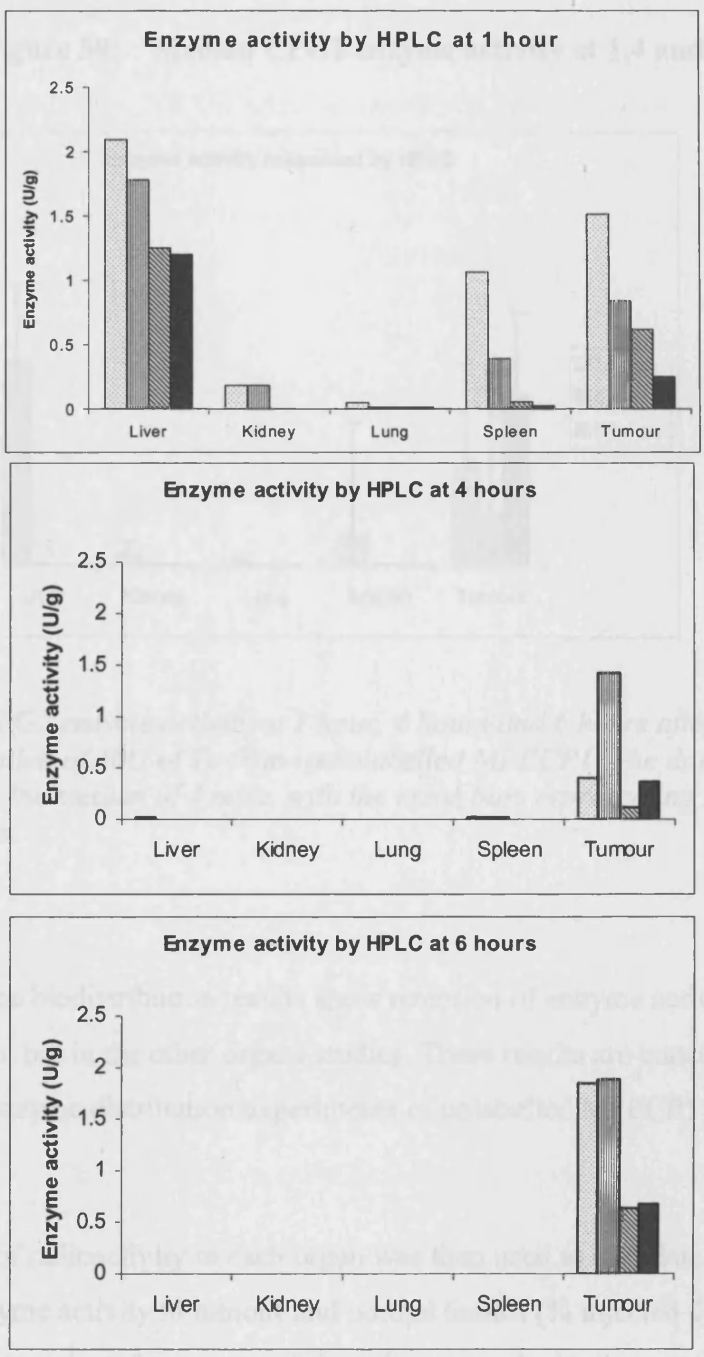

CPG2 enzyme activity as measured by a methotrexate reduction assay on HPLC at a) 1 hour, b) 4 hours and c) 6 hours after administration of 30U of TcCO radiolabelled MFECP1.

The median enzyme activity in each organ at 1, 4 and 6 hours is shown in **figure 30**.

Figure 30: Median CPG2 enzyme activity at 1,4 and 6 hours

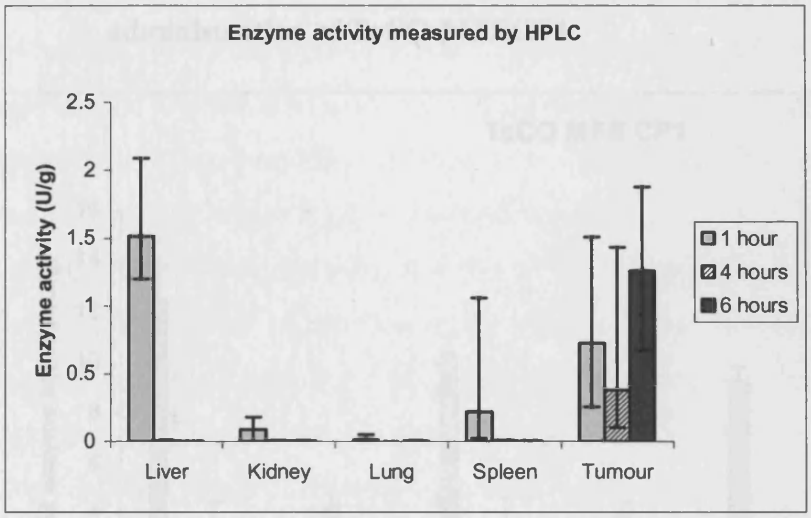

Median CPG2 enzyme activity at 1 hour, 4 hours and 6 hours after administration of 30U of Tc-99m radiolabelled MFECP1. The data set represents the median of 4 mice, with the error bars representing the range of data points.

The enzyme biodistribution results show retention of enzyme activity in the tumour, but not in the other organs studies. These results are consistent with previous enzyme distribution experiments of unlabelled MFECP1 (Sharma *et al*, 2000).

The level of radioactivity in each organ was then used to calculate an estimated CPG2 enzyme activity in tumour and normal tissues (% injected dose/g multiplied by injected enzyme units), and compared with the actual enzyme activity present as measured by methotrexate reduction assay by HPLC. **Figure 31** and **table 26** display the estimated enzyme units/g by radioactivity in each organ, compared with the actual measured enzyme units by HPLC at each timepoint.

In the tumour the TcCO radiolabelled MFECP1 provides an excellent estimate of actual enzyme activity, however it does not appear to provide a good estimate of enzyme distribution in most normal tissues.

Figure 31: CPG2 enzyme activity in various tissues after administration of TcCO-MFECP1

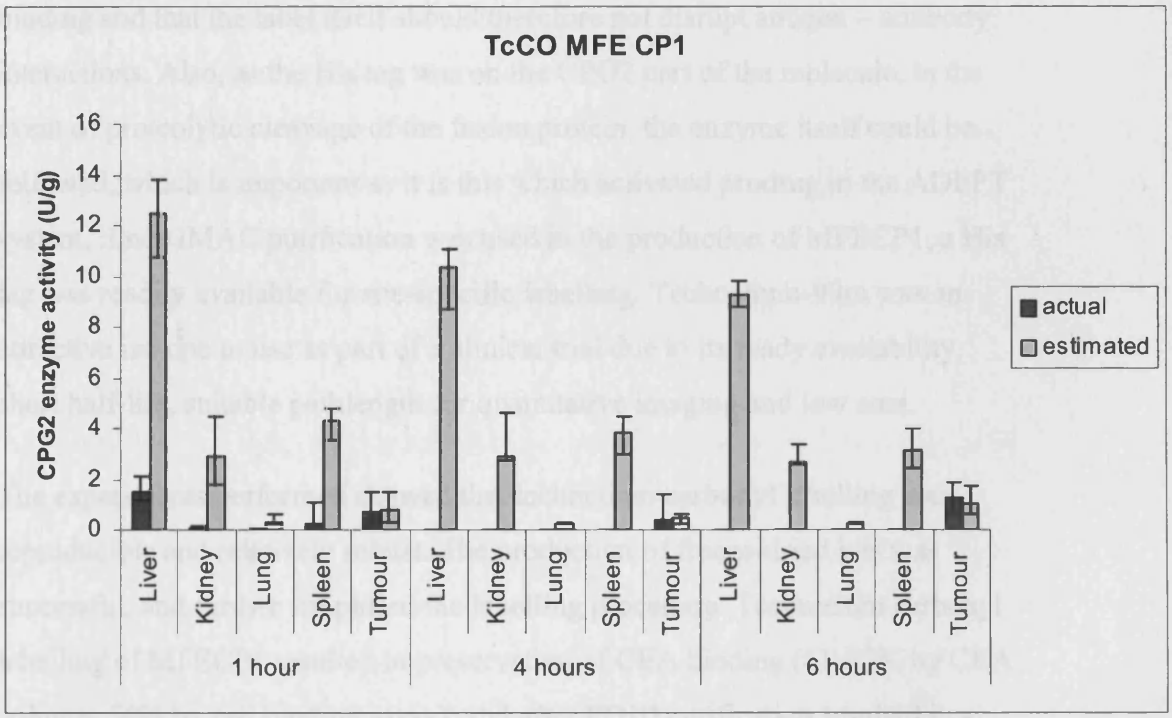

Graphical representation of the comparison between actual CPG2 enzyme activity (by HPLC) in various tissues at 1, 4 and 6 hours after administration of 30U of Tc-99m radiolabelled MFECP1, compared to estimated enzyme concentration in these tissues by the presence of radioactivity. The error bars represent the range of the data points.

Table 26: CPG2 enzyme activity in tumour and normal tissues

	1 hour (U/g)		4 hours (U/g)		6 hours (U/g)	
	actual	**estimate**	**actual**	**estimate**	**actual**	**estimate**
liver	1.52	11.20	0.00	8.66	0.00	7.16
kidney	0.09	2.71	0.00	2.42	0.00	2.08
lung	0.01	0.28	0.00	0.21	0.00	0.17
spleen	0.22	3.91	0.01	3.17	0.00	2.47
tumour	0.73	0.69	0.38	0.47	1.26	0.77

Table of the actual CPG2 enzyme activity in a variety of organs at 1, 4 and 6 hours, compared with the estimated CPG2 activity based on the localisation of TcCO MFECP1. The values shown are the median values of 4-5 mice at each timepoint.

3.4 Discussion

Technetium carbonyl site-specific radiolabelling to the hexahistidine tag of MFECP1 appeared a promising technique for use in the phase I ADEPT clinical trial, in order to non-invasively follow the biodistribution of MFECP1. Its advantages were that the label would be directed to a site not involved in antigen binding and that the label itself should therefore not disrupt antigen – antibody interactions. Also, as the His tag was on the CPG2 part of the molecule, in the event of proteolytic cleavage of the fusion protein, the enzyme itself could be followed, which is important as it is this which activated prodrug in the ADEPT system. Since IMAC purification was used in the production of MFECP1, a His tag was readily available for site-specific labelling. Technetium-99m was an attractive isotope to use as part of a clinical trial due to its ready availability, short half-life, suitable pathlength for quantitative imaging and low cost.

The experiments performed showed that technetium carbonyl labelling was reproducible and relatively robust. The production of freeze-dried kits was successful, and further simplified the labelling procedure. Technetium carbonyl labelling of MFECP1 resulted in preservation of CEA binding (61-77% by CEA column, 54% by cell binding assay), and after PD10 purification resulted in a sufficiently pure product (>99% by ITLC).). Stability studies indicated that the complex was quite stable in saline (3-4% loss in 24 hours) but that incubation with histidine in 10 000 fold excess could displace up to 25% of the technetium carbonyl. Incubation in serum indicated that the little or no proteolytic degradation occurs although some aggregation of the protein was seen.

The animal biodistribution experiments demonstrated that the amount of radioactivity reaching the tumour was a good estimate of actual measured enzyme activity. In addition, the measured enzyme activity by HPLC in tumour and other sites were comparable to previous biodistribution experiments using unlabelled MFECP1 (Sharma *et al*, 2000). This supports the idea that this form of radiolabelling did not appear to damage the antibody-antigen binding or the CPG2 enzyme activity of MFECP1. It may therefore provide a good estimate of antibody-enzyme localisation in the tumour for ADEPT therapy.

However, these experiments also revealed high uptake of technetium in the liver, spleen and kidneys, which did not correlate with enzyme activity. It seems likely that following non receptor-mediated uptake and cellular internalisation by these tissues (due in part to the glycosylations of MFECP1) the labelled fusion protein is rapidly catabolised resulting in loss of enzyme activity. However the technetium radiolabel, as a metal ion, is subsequently retained within the cells. In the tumour, internalisation of the labelled fusion protein is not expected to occur since CEA is not internalised to any great extent. Thus the enzyme activity remains intact and can be suitably estimated by the levels of radioactivity. This technique could therefore not be used to predict the levels of enzyme activity remaining in normal organs during ADEPT therapy and any uptake into tumour masses present in or adjacent to these organs may well be obscured by the high non-antigen mediated uptake.

Radiolabelling MFE-23 with technetium has been performed by Verhaar *et al* by genetically engineering in a cysteine in the C-terminal tail (MFE-23-cys) (Verhaar *et al*, 1996). This resulted in some dimerisation MFE-23-cys (12.5% of total protein was dimerised) due to the addition of the cysteine group (Verhaar *et al*, 1996). The labelling efficiency of technetium onto the MFE-23-cys protein was low (5-10%), however there was retention of CEA binding (55% bound to CEA by CEA column) (Verhaar *et al*, 1996). Biodistribution studies reported better tumour uptake of technetium radiolabelled MFE-23 than for iodine radiolabelled MFE-23 at 24 and 48 hours, however the tumour to blood ratios were not as high as with iodine, due to retention of technetium in normal organs for longer than iodine (Verhaar *et al*, 1996). The renal uptake of technetium was very high at both 24 and 48 hours.

Radiolabelling of MFE-23 with technetium has also been performed by genetically engineering MFE-23 with a metallothionein peptide attached to the C –terminal end for direct radiometal binding without the need for a chelator (Pietersz *et al*, 1998). Preclinical studies showed good tumour localisation from 4 hours post administration (5.37% injected dose/gram tumour) however, there was also high uptake in kidneys, spleen , liver and stomach (9.96%, 5.11%, 4.09% and3.61% injected dose/g respectively) resulting in poor ratios with these organs

at 4 hours (Pietersz *et al*, 1998). The ratios improved by 24 hours. The 24 hour time-point was not measured in the TcCO MFECP1 biodistribution experiments because the timepoint that was of interest was at 4-6 hours, when it was important to know what the biodistribution of MFECP1 was prior to administration of prodrug in ADEPT.

Radiolabelling with I-131 has been performed in previous ADEPT studies in order to quantify the biodistribution of the antibody-enzyme conjugate. I-131 has a half-life of 8 days, which is suitable for radiolabelling A5CP, which has a longer systemic circulating time of 9-16 hours, but is not ideal for MFECP1, which has a very short systemic half-life. I-123 may be used as an alternative, as it is a γ emitter with a half-life of 13.27 hours. It has a 159keV γ emission, which is suitable for imaging purposes, however I-123 is expensive and not readily available. Iodine radiolabels to the tyrosine residues of a molecule and can lead to iodination in multiple sites on the protein, including the antigen binding site. This has the disadvantage of potentially damaging the ability of the antibody to interact with its antigen.

Radiolabelling MFECP1 with I-123 using the chloramine T method was used as an alternative to TcCO ([1]Sharma *et al*, 2001). This resulted in CEA binding of 53.6%, measured on a CEA column. Iodine incorporation was 93.6%. The biodistribution of I-123 radiolabelled MFECP1 in the LS174T tumour model is shown in **figure 32**. (Experiments performed by and data obtained from SK Sharma).

Figure 32: Biodistribution of I-123 radiolabelled MFECP1 in LS174T xenograft model

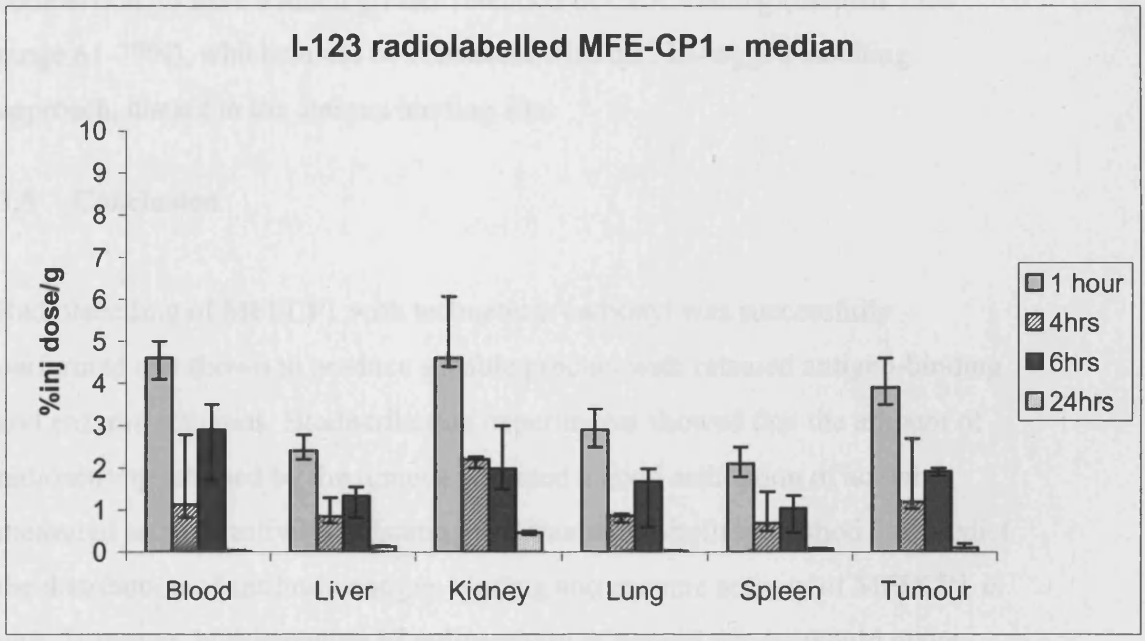

Biodistribution of I-123 radiolabelled MFECP1 in LS174T xenograft mouse model. The data shown are the median values with the error bars indicating the range. (Experiments performed by and data obtained with permission from SK Sharma).

The distribution of I-123 radioactivity is fairly similar in all measured organs. As I-123 may be present on multiple sites of MFECP1, catabolism of MFECP1 in non-target tissues may lead to the formation on non-functioning fragments, which retain some I-123 activity. This may account for background I-123 radioactivity in organs in which there would not be expected to be functional CPG2 enzyme at 4 and 6 hours. During catabolism of MFECP1 in non-target tissues it is also likely that dehalogenation of I-123 occurs leading to release of I-123 back into the blood and subsequent excretion through the kidneys.

At the 6 hour timepoint there is a median of 1.9% injected dose/g of radioactivity in the tumour. 25U of MFECP1 were administered in this experiment, so this equates to an estimated CPG2 enzyme level of approximately 0.5U/g (actual CPG2 enzyme levels were not measured in this experiment). This is less than is found in the tumour with unlabelled MFECP1 (median 1.3U/g at the 6 hour time-point) (Sharma *et al*, 2000). This would be in keeping with the reduced CEA

binding that occurs after radiolabelling with iodine, and suggests a reduction in antibody-antigen interaction. The TcCO method of radiolabelling appears in comparison, to have a much greater retention of CEA binding (median 75% range 61-77%), which would be consistent with the His-tagged labelling approach, distant to the antigen binding site.

3.5 Conclusion

Radiolabelling of MFECP1 with technetium carbonyl was successfully performed and shown to produce a stable product with retained antigen-binding and enzyme activities. Biodistribution experiments showed that the amount of radioactivity retained by the tumour provided a good estimation of actual measured enzyme activity, indicating that this radiolabelling method can predict the distribution of antibody-antigen binding and enzyme activity of MFECP1 *in vivo*. However, high retention of radioactivity in normal tissues would make imaging studies difficult, as surrounding high normal tissue uptake may impair tumour visualisation. The technetium carbonyl method remains, however, a promising technique for radiolabelling His tagged proteins for the future.

3.6 Acknowledgements

This work was carried out at St Bartholomews Hospital in the CRUK Nuclear Medicine laboratory under the supervision of Dr Steve Mather. The advice of Dr Kerry Chester and Dr Robert Waibel was also greatly appreciated.

4 ADEPT with MFECP1 and ZD2767P

4.1 Background

The clinical trial of ADEPT using A5CP, in combination with ZD2767P, reported in **chapter 2**, identified several areas where modifications could be directed in order to improve the likelihood of efficacy in ADEPT. In particular, the antibody-enzyme targeting system was found to be unsatisfactory, with tumour to normal tissue ratios of less than one attained and low quantities of CPG2 enzyme delivered to the tumour (0.01U/g). Tumour specificity was not achieved, and toxicity was thought to have arisen as a result of slow clearance of antibody-enzyme from normal tissues leading to systemic activation of prodrug. Reducing the CPG2 enzyme level at which a decision was made to proceed with prodrug administration from 0.2U/mL to 0.05U/mL allowed limited dose escalation of ZD2767P to occur. However, the maximum tolerated dose was defined at a lower dose of ZD2767P than was expected based on preclinical experience. Attempts to delay administration of prodrug until blood CPG2 levels fell further were futile, as in some patients up to nine days were required before prodrug could be administered, and by this time it was estimated that tumour CPG2 enzyme levels would be inadequate for efficacy.

As previously discussed, the slow clearance of A5CP was overcome in previous clinical trials of ADEPT by using a galactosylated second clearing antibody system directed against the active site of CPG2 (Bagshawe *et al*, 1995; Napier *et al*, 2000). This second antibody cleared residual A5CP from the peripheral circulation, and allowed prodrug to be administered at 48 hours after A5CP administration, at which time it was demonstrated that the tumour to blood ratio of CPG2 enzyme was >10 000:1 and the amount of CPG2 enzyme in tumour was 0.47 U/g (Napier *et al*, 2000). Tumour selectivity was thereby achieved. The drawbacks of re-introducing the second antibody clearance system for ADEPT however include the added immunogenicity of the second antibody and the further complexity of the system.

An additional limitation of A5CP is that a chemical conjugation process is required to link A5B7 F(ab′)$_2$ antibody to CPG2 (Melton *et al*, 1993) This process is not ideal as it may damage the protein, resulting in reduced enzymatic activity and potentially impairing its targeting ability. It is also a complex, expensive procedure, which is associated with difficulties in obtaining a homogeneous product. The three batches of A5CP used in the clinical trial reported in **chapter 2** varied significantly in their enzyme concentrations, pharmacokinetics and radiolabelling profiles.

In view of these limitations with A5CP new candidate antibody-enzyme complexes were explored. Genetic fusion proteins were investigated for ADEPT as they have several advantages over antibody-enzyme conjugates (Neuberger *et al*, 1984; Bosslet *et al*, 1992; Bosslet *et al*, 1994; Michael *et al*, 1996; Bhatia *et al*, 2000; Chester *et al*, 2000). They are much easier to manipulate and modify, as the genetic code is known. In addition it is possible to attain much greater product homogeneity as the entire antibody-enzyme is encoded from one construct. The production of large quantities of homogenous product is therefore much more feasible and there is a greater potential for modification to attain desired characteristics such as high affinity or low immunogenicity. They can also be produced in bacteria or yeast, which can be fairly rapid and reduces the risk of contamination with mammalian or viral DNA ([2]Chester *et al*, 2000).

4.1.1 Antibody-enzyme for ADEPT

The experience attained in the previous ADEPT clinical trials in combination with preclinical studies suggested that the following characteristics of antibody-enzyme are desirable to improve the efficacy of ADEPT:

- Ability to delivery high levels of enzyme to tumour
- Ability to attain a high tumour to normal tissue ratio (specificity)
- High viable to necrotic tissue ratio of enzyme
- Stability in production and in vivo
- Rapid localisation to allow same or next day therapy

- Low immunogenicity to allow repeated therapy without the need for immunosuppressive therapy

It is a core component of ADEPT that enough enzyme is delivered to the tumour to be able to activate prodrug. The intratumoural site of delivery is also important, as enzyme present in the viable tumour areas at the time of prodrug administration will ensure that active drug is being generated in these areas and not just in the necrotic centre of the tumour. In addition this may be of importance for accessibility of prodrug to enzyme. It has been shown by radioluminography on human colorectal tumour xenografts, that in the first 24 hours after administration, tumour specific antibodies are distributed predominantly in the viable areas of tumour, whereas non-specific antibodies pass into the necrotic centre of tumours, where they are unlikely to have any effect (Flynn *et al*, 1999; Flynn *et al*, 2002).

Tumour selectivity depends upon active enzyme being delivered to tumour and not being present in normal tissues at the time of prodrug administration. If enzyme is present in normal tissues when prodrug is administered activation will occur in non-tumour areas, and toxicity is likely to result. The timing of administration of prodrug is therefore very important, as if given too early, before systemic clearance has occurred, will result in toxicity, and if given too late there may be inadequate amounts of enzyme in the tumour, or the antibody-enzyme which is present may have passed through the viable tumour areas into the necrotic centre of the tumour, as is seen with antibodies alone (Flynn *et al*, 2001).

An antibody-enzyme that is stable in production is a practical requirement for a clinical product. It is also important that the antibody-enzyme complex remains intact *in vivo*, to allow tumour targeting of functional enzyme. This is dependent not only on the inherent stability of the product, but also on its susceptibility to proteolytic cleavage or metabolism. This may not be a problem in 'normal tissues', as functional enzyme is not required there, but it is a problem if it occurs in tumour, as it will result in inadequate amount of enzyme in the tumour to activate prodrug.

The immunogenicity of A5CP used in previous ADEPT clinical trials has limited the ability to administer repeated therapy. Although ADEPT is a tumour specific treatment with the potential for much larger amounts of cytotoxic agent to be generated in tumour than could be administered systemically, it is unlikely that a single treatment will result in cure. It would therefore be advantageous to be able to administered repeated treatments, without the need for immunosuppressive therapy. Currently the antibodies used for ADEPT are murine, although there is the potential to humanise the antibodies to reduce immunogenicity for the future. The enzyme currently used to activate prodrug, CPG2, is bacterial. It is now potentially possible with genetic engineering techniques to try and modify the immunogenicity of CPG2, whilst retaining its enzyme activity, and this is currently being explored (Spencer *et al*, 2002).

If ADEPT can be administered as a same or next day therapy it becomes not only more clinically feasible, but also it may allow several cycles of ADEPT to be administered before immunogenicity develops. This may be a further method if avoiding the use of immunosuppressive treatments.

4.1.2 MFECP1 (Glycosylated MFE-23::CPG2 fusion protein)

A genetically engineered fusion protein of the murine scFv, MFE-23, with the bacterial enzyme, CPG2 emerged as the lead candidate antibody-enzyme complex for ADEPT. ScFv antibodies consist of a V_H and V_L chain connected by a flexible peptide linker. They retain full antigen specificity, however are approximately one fifth the molecular weight of whole IgG. Their small molecular weight leads to rapid tumour penetration, however because they clear rapidly from the circulation overall less antibody may be delivered to tumour (Milenic *et al*, 1991; Flynn *et al*, 2002). Positive tumour to normal tissue ratios may be achieved as early as 4 hours after administration compared to 3-7 days for whole antibody (Colcher *et al*, 1990; Savage *et al*, 1993; Begent *et al*, 1996). ScFv derived from phage libraries are ideal for use as fusion proteins due to their small molecular size and because their genetic code is known, making the formation of genetic fusion proteins a relatively straightforward process. In addition, the removal of a large part of the antibody molecules appears to lead to reduced immunogenicity in scFv compared to whole IgG (Begent *et al*, 1996).

MFE-23

MFE-23 is a scFv of molecular weight 27kDa. It was derived from a filamentous phage display library and selected for its affinity for CEA from a library of 10^7 clones made from the spleen cells of a mouse immunized with CEA (Chester *et al*, 1994; Begent *et al*, 1996). MFE-23 has an affinity 10 times greater than A5B7 for CEA (Chester *et al*, 1994). The dissociation constant (kD) of MFE for CEA is 2.5nmol/L.

MFE-23 was produced in *E.coli* and purified using immobilised metal affinity chromatography (IMAC). IMAC purification exploits the binding of polyhistidines to metal chelates, such as copper, and allows purification for proteins that have a C-terminal hexahistidine tag engineered into their design (Casey *et al*, 1995). An imaging study was performed in 10 patients with CEA-expressing tumours using I-123 radiolabelled MFE-23 and a radioimmunoguided surgery (RIGS) study was performed in 35 patients using I-123 radiolabelled MFE-23 (Begent *et al*, 1996; Mayer *et al*, 2000). In both studies radiolabelled MFE-23 was shown to be safe and to localise effectively to CEA positive tumours (Begent *et al*, 1996; Mayer *et al*, 2000). Relatively high renal uptake of radiolabelled MFE-23 was found, which would be consistent with filtration of MFE-23 by the kidney, due to its small molecular weight (Begent *et al*, 1996). Intact MFE-23 was found in the urine, which would suggest very little proteolytic digestion was occurring *in vivo* (Begent *et al*, 1996). No unexpected areas of uptake were found. MFE-23 appeared to have low immunogenicity as no HAMA could be detected against MFE-23 after administration in all patients participating in the studies (Begent *et al*, 1996; Mayer *et al*, 2000).

The crystal structure of MFE-23 has been determined and a model for its interaction with CEA proposed (Boehm *et al*, 2000; Boehm and Perkins, 2000). This information suggests that a humanisation strategy may be feasible and provides some insight into the high affinity between CEA and MFE-23. All six antigen-binding loops of MFE-23 have been shown to be involved in the interaction with CEA in a proposed docking model (Boehm and Perkins, 2000). This detailed knowledge about MFE-23 may direct developments for the future.

MFE-23::CPG2 expressed in E.coli

A genetic fusion protein was developed consisting of MFE-23 and CPG2 (MFE-23::CPG2). This was initially expressed in *Escherichia coli* and purified using CEA affinity chromatography and size exclusion gel filtration (Michael *et al*, 1996). MFE-23::CPG2 delivery to tumours *in vivo* was assessed after intravenous injection of purified MFE-23::CPG2 into nude mice bearing CEA-expressing LS174T human colon adenocarcinoma xenografts. MFE-23::CPG2 cleared rapidly from circulation and CPG2 catalytic activity in extracted tissues showed tumour to plasma ratios of 1.5:1 (6 h), 10:1 (24 h), 19:1 (48 h) and 12:1 (72 h) (Bhatia *et al*, 2000). MFE-23::CPG2 catalytic activity was not retained in normal tissues resulting in excellent tumour to normal tissue enzyme ratios 48 h after injection. These were 371:1 (tumour to liver), 450:1 (tumour to lung), 562:1 (tumour to kidney), 1,477:1 (tumour to colon) and 1,618:1 (tumour to spleen) (Bhatia *et al*, 2000). The favourable tumour: normal tissue ratios occurred at early time points when there was still 21% (24 h) and 9.5% (48 h) of the injected activity present/g tumour tissue (Bhatia *et al*, 2000). These results showed that MFE-23::CPG2 delivered satisfactory quantities and high tumour to normal tissue ratios of CPG2 activity after a single injection without the need for a secondary clearance system.

The high tumour concentrations and selective tumour retention of active enzyme establish that MFE-23::CPG2 fusion protein expressed in *E.coli* had potential to give improved clinical efficiency for ADEPT. However, expression of the MFE-23::CPG2 fusion protein in *E.Coli* resulted in a relatively low yield (0.5-1.0 mg/L) which limited its suitability for clinical use. To obtain greater yields and improve the ease of purification, MFE-23::CPG2 with a hexahistidine tag (His tag) was expressed in yeast *Pichia pastoris.*

MFECP1 expressed in Pichia pastoris

Expressing MFE-23::CPG2 fusion protein in *Pichia pastoris* and purifying it with IMAC via the His tag resulted in a hundred-fold increase in yield and a glycosylated product ([1]Chester *et al*, 2000). This product is referred to as MFECP1 (**figure 33**).

Figure 33: Schematic diagram of MFECP1

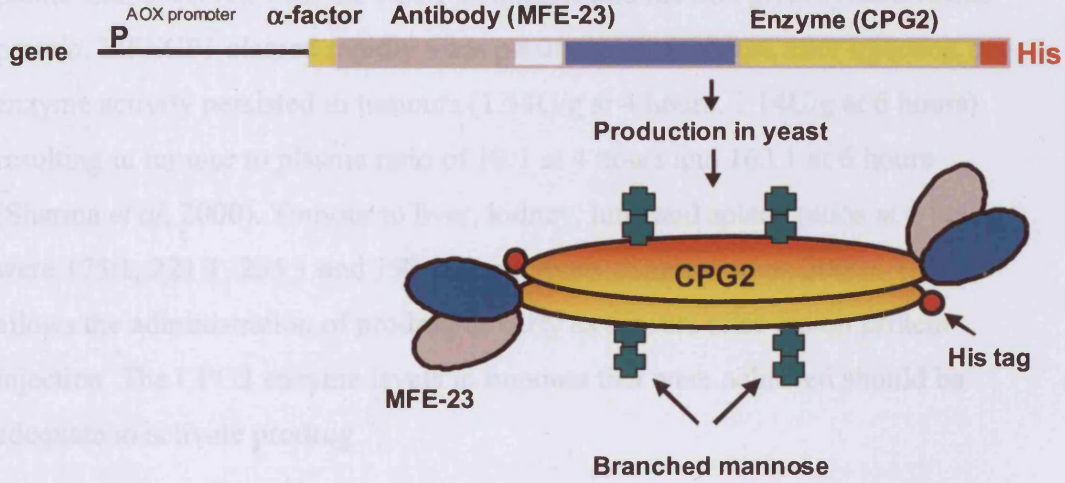

Schematic representation of the genetic construct of MFECP1 and the protein product. The genetic construct consists of MFE-23, CPG2 enzyme and a hexahistidine tag, with an AOX promoter, and a cleavage site. After production in Pichia pastoris, the protein is expressed as a dimer, with two MFE-23 scFv molecules, and 1 functional CPG2 moiety. MFECP1 is glycosylated by Pichia pastoris, with 2 short chain branch mannose chains. (Figure obtained with permission from K Chester).

CPG2 forms a dimer in its natural state, and it is required to be in this form for enzymatic function. Therefore for each moiety of MFECP1 there is one functionally active CPG2 molecule and two MFE-23 molecules. This should serve to improve the functional affinity of MFE-23. The glycosylations of MFECP1 have been characterised by Tandem Mass Spectroscopy, and have been found to be short-branched mannose, which are present on 2 of a possible 3 N-glycosylation sites on the molecule. The molecular weight of dimeric MFECP1 is

142.56 kDa -147.10 kDa (heterogeneity due to glycosylations from production in *Pichia pastoris*). There are 644 amino acids per monomer.

Preclinical biodistribution studies

Biodistribution studies of enzyme activity measurements in nude mice bearing human colon adenocarcinoma xenograft, LS174T, given intravenous injection of MFECP1 (1000U/kg = 3000U/m^2) showed localisation in tumours at earlier time points than observed with the A5CP conjugate and the non glycosylated fusion protein. MFECP1 cleared rapidly from plasma within 6 hours after injection but enzyme activity persisted in tumours (1.34U/g at 4 hours, 1.14U/g at 6 hours) resulting in tumour to plasma ratio of 19:1 at 4 hours and 163:1 at 6 hours (Sharma *et al*, 2000). Tumour to liver, kidney, lung and spleen ratios at 6 hours were 175:1, 221:1, 235:1 and 193:1 respectively (Sharma *et al*, 2000). This allows the administration of prodrug as early as 6 hours after fusion protein injection. The CPG2 enzyme levels in tumours that were achieved should be adequate to activate prodrug.

Studies using radiolabelled MFECP1 indicate that the mechanism of rapid systemic clearance of CPG2 enzyme is likely to be due to hepatic metabolism. Hepatic receptors for the glycosylations of MFECP1 clear the antibody-enzyme from the systemic circulation, and lead to protein degradation, resulting in loss of enzyme activity. Measurements of radioactivity demonstrate very high levels in the liver as early as 1 hour after administration, however this is without the presence of active enzyme (**chapter 3**). This would indicate that the radiolabel remains present on protein fragments, but there is no intact CPG2 present. Tumour radioactivity levels are, however, more consistent with measured CPG2 enzyme activity, suggesting that active enzyme is preserved in tumour sites. When the *in vivo* stability of MFECP1 was assessed in LS174T xenografts (using SDS polyacrylamide gel electrophoresis and autoradioluminography), I-125 radiolabelled fusion protein was shown to remain intact after 4 hours in the tumours (K. Chester personal communication).

Preclinical efficacy studies of MFECP1 in combination with ZD2767P

In LS174T xenograft models the average tumour growth delay achieved with a single cycle of ADEPT using MFECP1 (1000U/kg) and ZD2767P (70mg/kg x 3) was 9 days, and with the SW1222 xenograft model, which is a more sensitive tumour, average tumour growth delays of 15 days were achieved. Repeated cycle ADEPT, in which up to 3 cycles of ADEPT were administered 5-7 days apart, average tumour growth delays of 21 days were achieved in LS174T xenografts, with no increase in toxicity as assessed by weight loss (<10% weight loss). Repeated cycle ADEPT with MFECP1 in combination with ZD2767P therefore appears well tolerated and associated with improved efficacy as compared to single cycle treatment (SK Sharma, personal communication).

Advantages of MFECP1 compared to A5CP

MFECP1 was designed specifically for use in ADEPT systems. It is a robust, stable molecule that is produced in a homogeneous and pure form in a single process suitable for scaling up in an industrial setting. High tumour specificity and high affinity were obtained by selecting the antibody for affinity from an immunised phage library (Chester *et al*, 1994). Further functional affinity was obtained by designing the fusion protein to have two single chain Fv antibodies. High purity was achieved by engineering a hexahistidine tag onto the C-terminus of the molecule permitting purification by immobilised metal affinity.

Previous clinical trials of ADEPT demonstrated that rapid blood clearance was necessary to achieve low blood levels of enzyme at a time when there was still sufficient enzyme in the tumour for prodrug activation there. Rapid blood clearance is achieved by expressing the fusion protein in the yeast *Pichia pastoris,* which adds glycosylation with branched mannose to the fusion protein as a post-translational modification. Preclinical studies confirm rapid systemic clearance and high tumour to normal tissue ratios, which provides an advantage over A5CP (SK Sharma, personal communication). Same or next day therapy should be achievable. The rapid clearance should also result in lower circulating CPG2 levels and reduce the likelihood of systemic activation of prodrug, which may have contributed to the myelosuppression in the previous ADEPT study.

Repeated therapy has been demonstrated in preclinical models to be associated with improved efficacy and may be possible in the clinical setting before HAMA and HACPG2A responses develop.

These design features of MFECP1 required testing in a clinical setting.

4.1.3 Clinical Trial Design

The clinical trial of ADEPT with MFECP1 in combination with ZD2767P was designed to include conventional phase I/II endpoints of toxicity, pharmacokinetics and efficacy, in combination with mechanistic studies to examine whether the components of ADEPT were functioning as predicted in a clinical setting.

The hypotheses being tested in the clinical trial were

a) That MFECP1, a glycosylated fusion produced in *Pichia pastoris*, would be safe to administer to humans
b) That MFECP1 would provide superior tumour targeting when compared to A5CP
c) That the improved tumour targeting attained with MFECP1 would allow escalation of ZD2767P to doses comparable to those which produced efficacy in the preclinical setting
d) That repeated therapy with ADEPT may be possible without the requirement for immunosuppressive drugs
e) That the mechanistic studies included within the trial protocol would provide information on whether each component of ADEPT was functioning as designed in the clinical setting, and could be used to direct treatment decisions within the clinical trial, and aid identification of areas of ADEPT requiring refinement for the future.

MFECP1 safety

MFECP1 for the clinical trial was produced in a new Good Manufacturing Practice (GMP)-like production facility (Copley May Production Unit) in the CRUK Targeting and Imaging Group, Department of Oncology, Royal Free

Hospital. Non-glycosylated *Pichia* produced recombinant endostatin (Sim *et al*, 1999) has been used safely in humans (Herbst *et al*, 2002), however MFECP1 was, to our knowledge, the first glycosylated *Pichia* product to be administered to humans. Consequently its safety had to be established.

Administration was performed under controlled conditions, with full resuscitation facilities available. Toxicity was recorded according to The National Cancer Institute Common Toxicity Criteria (NCI CTC) Version 2.0. The starting dose of MFECP1 was 5000U/m^2. Preclinical studies had been performed with a dose equivalent to 3000U/m^2, however to try to ensure adequate enzyme delivery to tumours, the higher dose of 5000U/m^2 was proposed. Up to 20000U/m^2 of CPG2 enzyme had previously been safely administered as A5CP in a previous ADEPT clinical trial (Bagshawe *et al*, 1994), and the trial protocol was designed to allow the escalation of MFECP1 administered dose up to 20000U/m^2 if inadequate tumour enzyme levels were attained by tumour biopsy or quantitative SPECT imaging.

Tumour targeting of MFECP1

The features of MFECP1 that were designed to provide superior tumour targeting when compared with A5CP included rapid tumour localisation, good tumour to normal tissue ratios and the delivery of active CPG2 enzyme to tumour in quantities that should be sufficient for prodrug activation.

Measurements of CPG2 enzyme activity in serum by methotrexate reduction assay on HPLC was used to assess the half-life and systemic clearance of intact functional MFECP1 (Blakey *et al*, 1996). Where possible, tumour biopsies were performed, to measure tumour CPG2 levels by methotrexate reduction assay on HPLC (Blakey *et al*, 1996). A non-quantitative immunohistochemistry assay was also adopted using an anti-CEA antibody, and an anti-CPG2 antibody, to ascertain the presence of MFECP1 in tumour biopsies, and its microscopic distribution within the tumour areas.

MFECP1 was radiolabelled with I-123 in order to assess the biodistribution of radiolabelled MFECP1 by quantitative SPECT analysis, and clearance of I-123

radiolabelled MFECP1 from blood by gamma counting. Preclinical biodistribution experiments using iodine radiolabelled MFECP1 suggested that the distribution of radioactivity in sites other than tumour was not representative of intact MFECP1, due to the rapid hepatic metabolism of MFECP1, which was likely to have lead to iodinated breakdown products and dehalogenation ([1]Sharma *et al*, 2001) (**chapter 3**). Therefore the quantitative gamma camera analysis was used to estimate tumour CPG2 enzyme levels, which were confirmed in a small number of patients with tumour biopsies. In addition it was used to ascertain whether there was uptake of radiolabelled MFECP1 into unexpected areas, which may have lead to toxicity.

Dose escalation of ZD2767P

The previous clinical trial of A5CP in combination with ZD2767P established a MTD of ZD2767P of 15.5mg/m^2 x 3 administrations, with a serum CPG2 enzyme level of <0.05U/mL (Francis *et al*, 2002)(**chapter 2**). This dose of ZD2767P was much lower than was predicted by preclinical studies, and was proposed to be too low for efficacy. The dose of ZD2767P that resulted in growth delay of xenografts of human CEA expressing colorectal cancers in mice was 70mg/kg (scaled for surface area = 210mg/m^2). It was proposed therefore that the dose of ZD2767P would need to be escalated to 10-20x the MTD of the previous trial in order to attain efficacy.

The more rapid systemic clearance of MFECP1 compared to A5CP should result in much lower levels of CPG2 enzyme in normal tissues at the time of ZD2767P administration and therefore less systemic activation of ZD2767P should occur. It was likely therefore that further dose escalation may be achieved beyond the MTD in the previous ADEPT trial.

The proposed starting dose of ZD2767P was 12.42mg/m^2 (one dose level below MTD attained in the previous ADEPT study), with a serum CPG2 enzyme level of <0.05U/mL. Once safety was established at the first dose level, dose doubling was scheduled to be undertaken until grade II or higher drug related toxicity was experienced, at which time the cohort of patients was to be expanded to three, and dose increases to occur at 30% increments. At least 4 weeks was to elapse

before a new patient was treated at the next dose level, to ensure safety at the previous dose level. This scheme of dose escalation was designed to allow the attainment of potentially therapeutic dose of ZD2767P in 4-5 dose doublings, providing drug related toxicity did not ensue.

The toxicity of ZD2767P was assessed and recorded using the National Cancer Institute Common Toxicity Criteria (NCI CTC) Version 2.0.

Pharmacokinetic analysis of ZD2767P was performed, in the same manner as for the previous ADEPT trial. Comet assay was again used to indirectly assess for prodrug activation, by identifying the presence of DNA cross-links. There remains no suitable direct method of assessing drug formation, as the half-life of the active drug is too short for direct measurement. Blood samples were taken in all patients prior to and 60-120 minutes after administration of ADEPT to assess for DNA crosslinking in peripheral lymphocytes. In addition, comet assay were performed on cells obtained from tumour biopsies or bone-marrow biopsies.

Repeated therapy

The immunogenicity (HAMA and HACPG2A) of MFECP1 was assessed weekly by ELISA. This was used to help determine whether MFECP1 had reduced immunogenicity compared to A5CP, and whether repeat therapy in the second phase of the trial may be possible without immunosuppressive therapy,

Mechanistic studies

The mechanistic studies undertaken to ascertain whether the components of ADEPT were functioning as proposed, have been outlined above as they relate to each hypothesis being tested and are summarised in **table 27.**

Table 27: Mechanistic studies in ADEPT MFECP1 and ZD2767P clinical trial

Toxicity of MFECP1 +ZD2767P	**Method of assessment**
Toxicity, MTD and DLT	NCI-CTC criteria

Biodistribution of MFECP1	**Method of assessment**
Serum CPG2 enzyme clearance	Methotrexate reduction assay
Tumour CPG2 enzyme levels	Methotrexate reduction assay (tumour biopsy)
Tumour MFECP1 localisation	Immunohistochemistry (tumour biopsy)
Blood I-123 radiolabelled MFECP1 clearance	Gamma counter
Tumour localisation of I-123 radiolabelled MFECP1	SPECT analysis of gamma camera data

Immunogenicity	**Method of assessment**
Immunogenicity MFECP1	HAMA and HACPG2A by ELISA

Characteristics of ZD2767P	**Method of assessment**
ZD2767P pharmacokinetics	HPLC analysis
ZD2767D formation	Comet assay (for DNA cross-links)

Efficacy of MFECP1 + ZD2767P	**Method of assessment**
Anatomical	CT scans (RECIST)
Functional	[F-18] FDG PET analysis
Serological	Serum CEA and CA19-9 levels
Survival	Kaplan-Meier survival analysis

Efficacy of ADEPT with MFECP1 and ZD2767P was a secondary endpoint in this study and was assessed by conventional radiological assessment, with the newly adopted Response Evaluation Criteria in Solid Tumours (RECIST) criteria, which utilises the maximal unidimensional diameter of target lesions (Therasse *et al*, 2000). [F-18] FDG PET was used to assess functional changes in glucose metabolism in tumours with therapy.

Mechanistic studies were also incorporated into the protocol to guide decisions regarding timing of administration of prodrug, dose escalation decisions for MFECP1, and whether a repeated therapy component of the trial should be undertaken.

A new rapid (5 minute incubation) methotrexate reduction assay by HPLC was validated and adopted for this trial, in addition to the previously used 30 minute

incubation assay. The 5 minute assay was designed to be able to rapidly identify when serum CPG2 enzyme levels had fallen sufficiently to allow the safe administration of ZD2767P. Its limit of sensitivity for CPG2 enzyme activity was 0.005 U/mL. The 30 minute incubation assay was also modified, re-validated and streamlined, to allow a more rapid result to be made available. The 30 minute incubation assay was validated to a CPG2 enzyme activity of 0.002 U/mL. Decisions on whether to administer prodrug were made were based on the result of these assays.

The protocol had integrated in it the option to increase the administered dose of MFECP1 if inadequate tumour CPG2 enzyme levels were achieved, as measured on tumour biopsy and by quantitative SPECT analysis. In addition, prior to undertaking a repeated therapy part of the trial, the protocol was written to incorporate a 'data review', in which the mechanistic, toxicity and efficacy data were to be assessed and a decision to proceed based upon this data. This was designed to allow the transition between single dose and repeated dose ADEPT to occur without having to design an entirely new trial, as long as the mechanistic data collected suggested that the components of ADEPT were functioning as designed in the clinical setting.

The mechanistic studies incorporated within this clinical trial were therefore not only important for attaining a better understanding of ADEPT, and for directing its further development, they were also integral to the decisions made within the trial itself.

4.2 Trial outline

4.2.1 Patient Selection

The trial was conducted under a Doctors' and Dentists' Exemption (DDX) and had Cancer Research UK Institutional Review Board (CIRB), Local Research Ethics Committee (LREC) and Administration of Radioactive Substances Committee (ARSAC) approval. It was conducted according to the principles of the International Conference on Harmonisation of Good Clinical Practice (ICH

GCP). Cancer Research UK Drug Development Office monitored the clinical data.

All patients gave written informed consent for the study. The eligibility criteria were unresectable, locally recurrent or metastatic colorectal carcinoma; measurable disease according to the RECIST criteria; age ≥ 18 years; life expectancy≥ 4 months; WHO performance status 0, 1 or 2; and normal haematological, biochemical, renal and hepatic function unless abnormal due to tumour. Pre-treatment serum CEA levels were required to be between 10μg/L and 1000μg/L: if the serum CEA was not raised, then CEA had to be demonstrated by immunohistochemistry on tumour biopsy. Patients were excluded if they had pre-existing HAMA to A5B7, or HACPG2A; the presence of active brain metastasis; if they were a poor medical risk; HIV, Hep B or C positive; or pregnant or lactating.

Patients were required to have been offered standard chemotherapy or radiotherapy, and had either relapsed or showed no response. All patients who received I-123 radiolabelled MFECP1 also received thyroid blocking with potassium iodide 50-60mg three times a day for five days commencing two days prior to the administration of the radiolabelled product. ZD2767P must be administered into a large bore vein, and so most patients had a Hickman line inserted.

4.2.2 Materials

MFECP1 was produced in the Copley May Production Unit in the Department of Oncology, Royal Free Hospital, under the supervision of Dr Kerry Chester. MFECP1 was produced in *Pichia pastoris* by a process of fermentation, followed by IMAC purification. It was expressed as a glycosylated product, and secreted as a functional dimer. It was aliquoted into vials and stored in sterile pyrogen-free PBS at -80°C. Reconstitution involved thawing MFECP1 gently at room temperature to form a solution and then made up to 500mL with 0.9% sodium chloride for administration. Administration was intravenously over 90-120 minutes, with a test dose being given prior to the infusion commencing.

Radiolabelling of MFECP1 was performed with I-123 using the chloramine T method. TLC was performed to assess iodine incorporation and antigen binding was assessed using a CEA column. I-123 radiolabelled MFECP1 was initially administered at the end of the MFECP1 infusion, however after patient #8 it was administered during the MFECP1 infusion. Administration was intravenously over 2 minutes.

ZD2767P was manufactured and supplied by CRUK Formulation Unit, Strathclyde. It was supplied as a non-sterile product containing 610 mg of crystalline ZD2767P Hydroiodide per vial (which was equivalent to 500 mg of ZD2767P free base). 10 ml of sodium bicarbonate solution was added to this to form a solution containing 50 mg/ml of free base, which is the form used for dosing. ZD2767P was administered as three doses an hour apart, via a fast running iv infusion of Dextrose 5%, through a central (preferably Hickman) line.

4.2.3 Treatment Schedule

5000U per m^2 of MFECP1 in 500mL of 0.9% sodium chloride was given over 90-120 hours on day 1. 1mL of MFECP1 was radiolabelled with up to 500MBq of I-123 and administered as an intravenous bolus over 2 minutes either during or at the end of the infusion. Serum CPG2 measurements were performed until the serum CPG2 enzyme levels fell below a pre-determined value. This level was initially 0.05U/mL (patients #1-4), however because of early toxicity it was lowered to 0.005U/mL (patients #4-13). At this time ZD2767P prodrug was administered as 3 bolus injections, 1 hour apart, each over 5 minutes into a fast running 5% dextrose drip. Patients were then followed up for a period of at least 8 weeks from the time of MFECP1 administration.

The trial also has a second phase of repeated therapy with ADEPT, at a dose of ZD2767P below MTD, once MTD has been established. Immunosuppressive therapy may be required in this second phase to prevent the development of HAMA or HACPG2A.

4.3 Methods and Results

This clinical trial is ongoing. The first thirteen patients treated with ADEPT with MFECP1 in combination with ZD2767P will be discussed in detail below.

4.3.1 Patient Demographics

Table 28 shows the demographics of the thirteen patients treated with ADEPT. There have been six males and seven females treated, with a median age of 58 years. All patients had CEA expressing tumours, with the majority having colorectal cancer (nine patients). The median number of prior chemotherapy regimens is three.

Table 28: Patient Demographics

Pt No.	ZD2767P dose level (mg/m2)	Gender	Age (yrs)	WHO PS	CEA (µg/L)	Primary Tumour	Disease sites	Prior chemoRx regimens
#1	12.42	Female	53	1	549.5	Colon	Lung and liver	5
#2	12.42	Male	41	0	177.5	Gastro-oesophageal	Liver	4
#3	12.42	Female	45	0	471.8	Unknown primary adenoca	Lung and liver	2
#4	16.15	Male	61	1	369.9	Colon	Lung. Regional and metastatic nodes	5
#5	12.42	Male	75	1	213	Colon	Liver	2 (both same regimen)
#6	12.42	Female	62	1	501.3	Colorectal	Liver	3
#7	12.42	Male	64	0	499.9	Colon	Lung and liver	3
#8	16.15	Male	69	1	18.9	Colon	Lung, liver and pelvic metastases	3
#9	16.15	Female	54	1	598	Breast	Liver and bone	4
#10	21.0	Female	35	1	123.3	Breast	Lung, bone and brain	5
#11	21.0	Female	65	0	55.8	Gastric and Colon‡	Lung and liver	3
#12	33.6	Male	58	0	36.3	Colon	Liver	1
#13	33.6	Female	41	0	201.8	Colon	Lung, liver and pelvic metastases	2

Abbreviations: WHO PS - World Health Organisation Performance Status; chemoRx – chemotherapy; adenoca - adenocarcinoma

‡ Patient #11 had two primary tumours. Both tumours were expressing CEA and the patient was allowed into the study.

4.3.2 Toxicity/MTD/DLT

Method

The toxicity of MFECP1 and ZD2767P was assessed and recorded using the NCI-CTC Version 2.0.

Results

The tolerability of ADEPT was assessed with regard to both MFECP1 and ZD2767P prodrug. MFECP1 had not previously been administered to humans, so to minimise risk, the infusion was started very slowly and completed over 2 hours. The only toxicity directly attributable to MFECP1 fusion protein was Grade I rigors/chills, Grade I allergy/immunology-other and Grade I fever seen in a total of two of thirteen patients. No other significant toxicity attributable to MFECP1 has been recorded at the fixed dose of 5000U/m^2 used.

The dose of ZD2767P has been escalated in this study and has been examined at four dose levels: 12.42 mg/m^2, 16.15 mg/m^2, 21.0 mg/m^2 and 33.6 mg/m^2. All drug-related adverse events (AEs) of ADEPT with MFECP1 in combination with ZD2767P are listed in **Table 29**. There have been very few drug-related toxicities seen and even fewer Grade 3 or 4 drug-related AEs reported.

A DLT (Grade 3 thrombocytopenia) was seen in Patient #3, at the first dose level of 12.42 mg/m^2. The Grade 3 thrombocytopenia was first experienced at Day 14, and this patient required platelet support. Additionally this patient experienced Grade 3 leucopaenia and Grade 3 neutropaenia, also thought to possibly be drug-related. The serum CPG2 enzyme level in this patient prior to ZD2767P prodrug administration was the highest of all patients' treated to date (0.0167 U/ml). Unfortunately this patient also had rapidly progressive malignant disease, with the new development of brain metastasis whilst on follow-up for ADEPT. This patient's Day 29 CT scan confirmed progression of systemic disease, and she was too unwell for her Day 57 CT assessment. The possibility remains that this patient's bone-marrow failure may at least, in part, have been as a result of the

involvement of bone marrow by tumour for which there was evidence on MRI and bone scan.

In view of the DLT experience at a ZD2767P dose of 12.42 mg/m^2, this dose level was expanded to six patients. A protocol amendment was also instituted so that ZD2767P prodrug would be given at CPG2 enzyme levels of <0.005 U/ml rather than <0.05 U/ml (which was in place at the first dose level). This amendment was initiated as a result of the toxicity experience by Patient #3, and the possibility that this toxicity may have been as a result of activation of ZD2767P prodrug in the peripheral circulation by circulating CPG2 enzyme. Since this change has been instituted there have been no reported drug-related haematological toxicities. In view of the perceived added safety of this 10-fold reduction in CPG2 enzyme activity, an amendment was approved to allow the dose escalation schedule to return to the original planned scheme, and dose-doubling was recommenced.

There have been no drug-related serious adverse events.

Table 29: Summary of adverse events related to ADEPT (worse grade per patient)

Adverse Event (CTC Version 2.0)	Dose level (mg/m^2)	Maximum Grade				Number of Patients		
		1	2	3	4	Total	%	% with Grade 3/4
ALLERGY / IMMUNOLOGY								
Allergy/Immunology-other	12.42	1	0	0	0	1	7.7%	0%
	16.15	0	0	0	0	0	0%	0%
	21.0	0	0	0	0	0	0%	0%
	33.6	0	0	0	0	0	0%	0%
	All dose levels	**1**	**0**	**0**	**0**	**1**	**7.7%**	**0%**
HAEMATOLOGICAL								
Leucopaenia	12.42	0	0	1	0	1	7.7%	7.7%
	16.15	0	0	0	0	0	0%	0%
	21.0	0	0	0	0	0	0%	0%
	33.6	0	0	0	0	0	0%	0%
	All dose levels	**0**	**0**	**1**	**0**	**1**	**7.7%**	**7.7%**
Neutropaenia	12.42	0	0	1	0	1	7.7%	7.7%
	16.15	0	0	0	0	0	0%	0%
	21.0	0	0	0	0	0	0%	0%
	33.6	0	0	0	0	0	0%	0%
	All dose levels	**0**	**0**	**1**	**0**	**1**	**7.7%**	**7.7%**
Thrombocytopaenia	12.42	1	1	1	0	3	23.1%	7.7%
	16.15	1	0	0	0	1	7.7%	0%
	21.0	0	0	0	0	0	0%	0%
	33.6	0	0	0	0	0	0%	0%
	All dose levels	**2**	**1**	**1**	**0**	**4**	**30.8%**	**7.7%**
CONSTITUTIONAL								
Fatigue	12.42	2	2	0	0	4	30.8%	0%
	16.15	0	1	0	0	1	7.7%	0%
	21.0	0	0	0	0	0	0%	0%
	33.6	0	0	0	0	0	0%	0%
	All dose levels	**2**	**3**	**0**	**0**	**5**	**38.5%**	**0%**
Rigors, chills	12.42	1	0	0	NA	1	7.7%	0%
	16.15	0	0	0	NA	0	0%	0%
	21.0	0	0	0	NA	0	0%	0%
	33.6	0	0	0	NA	0	0%	0%
	All dose levels	**1**	**0**	**0**	**NA**	**1**	**7.7%**	**0%**
Fever	12.42	0	0	0	0	0	0%	0%
	16.15	0	0	0	0	0	0%	0%
	21.0	0	0	0	0	0	0%	0%
	33.6	1	0	0	0	1	7.7%	0%
	All dose levels	**1**	**0**	**0**	**0**	**1**	**7.7%**	**0%**
GASTROINTESTINAL								
Nausea	12.42	2	0	0	NA	2	15.4%	0%
	16.15	1	0	0	NA	1	7.7%	0%
	21.0	0	0	0	NA	0	0%	0%
	33.6	1	0	0	NA	1	7.7%	0%
	All dose levels	**4**	**0**	**0**	**NA**	**4**	**30.8%**	**0%**
Vomiting	12.42	2	0	0	0	2	15.4%	0%
	16.15	1	0	0	0	1	7.7%	0%
	21.0	0	0	0	0	0	0%	0%
	33.6	0	0	0	0	0	0%	0%
	All dose levels	**3**	**0**	**0**	**0**	**3**	**23.1%**	**0%**

NA = not applicable

4.3.3 Mechanistic studies

A5CP Pharmacokinetics – serum CPG2 enzyme levels and clearance of I-123 radiolabelled A5CP

Method

A 2.5 ml blood sample was taken into a plain tube for CPG2 levels and 1 ml of blood was taken into an EDTA tube for I-123 levels at 5 min, 1h, 2h, 3h, 4h, 5h and 6h after the MFECP1 fusion protein. If the patient's serum CPG2 enzyme level was above 0.05 U/ml (later amended to 0.005 U/ml) further blood samples were taken on Day 2. In addition, a blood sample for CPG2 activity was taken immediately before the first ZP2767P administration and at the time of tumour or bone marrow biopsy (if this was performed).

The catalytic activity of CPG2 was measured by HPLC using methotrexate as a substrate. A 5 min incubation assay was used for Patients #1 to #10 (pre-prodrug samples for Patients #6 to #10 were incubated for 30 min) and a 30 min incubation assay was adopted for Patients #11 to #13. The limit of quantitation for the 5 min incubation assay was 0.005 U/ml and for 30 min incubation assay was 0.002 U/ml.

Blood samples were measured for I-123 radioactivity by a Packard Cobra 11^{th} Series Auto gamma counter, and were decay corrected to time of injection. They were expressed as %injected dose/kg blood.

HPLC and gamma counter analysis was performed by SK Sharma.

Results

Figure 34 displays the pooled serum CPG2 enzyme levels from HPLC analysis for all data points for which there was an absolute value recorded for Patients #1 to #13. Values of below the sensitivity of the assay (recorded as '<0.005U/mL' or '<0.002U/mL') could not be plotted. The data was modelled based on biexponential clearance, and an α and a β half-life has been calculated (model applied by AJ Green). The α half-life was 0.35 h and the β half-life was 6.0 h.

Figure 34: CPG2 enzyme levels by HPLC with biexponential clearance model

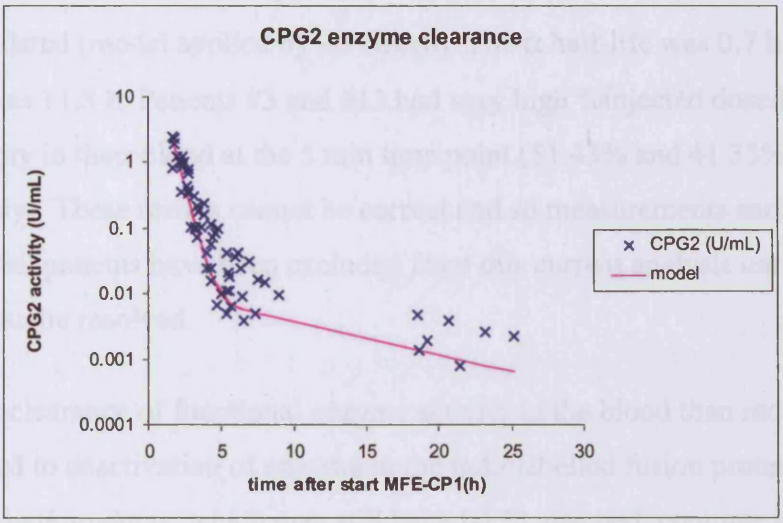

Table 30 displays the serum CPG2 enzyme level prior to ZD2767P prodrug administration (and the time at which the blood sample was taken) for Patients #1 to #13.

Table 30: CPG2 enzyme levels at the time of ZD2767P administration

Pt No.	Time of first ZD2767P (hrs after start of MFE-CP1)	Time of Serum Sample (hrs after start of MFE-CP1)	CPG2 activity (U/ml)
#1	7.57	7.32	0.00516
#2	7.13	5.38	0.0111
#3	7.52	7.48	0.0167
#4	6.85	6.53	<0.005
#5	8.42	6.37	<0.005
#6	23.47	22.90	<0.002
#7	21.28	18.57	<0.002
#8	20.70	20.58	<0.002
#9	25.82	25.10	0.00232
#10	21.75	21.57	<0.002
#11	20.45	17.50	<0.002
#12	21.85	18.48	<0.002
#13	21.45	21.20	<0.002

Figure 35 displays the pooled blood radioactivity data for patients who had radiolabelled MFECP1 administered (Patients #1 to #6 and #8 to #13). A biexponential model has been applied to the data and an α and β half-life has been calculated (model applied by AJ Green). The α half-life was 0.7 h and the β half-life was 11.8 h. Patients #3 and #11 had very high %injected dose/kg radioactivity in their blood at the 5 min time point (51.43% and 41.35% respectively). These results cannot be correct and so measurements earlier than 30 min in all patients have been excluded from this current analysis until this problem can be resolved.

The faster clearance of functional enzyme activity in the blood than radioactivity is attributed to deactivation of enzyme in the radiolabelled fusion protein, whilst its breakdown products, which may still have I-123 attached, continue to circulate. This is consistent with findings in animal models (see **chapter 3**).

Figure 35: Blood clearance of I-123 radiolabelled MFECP1

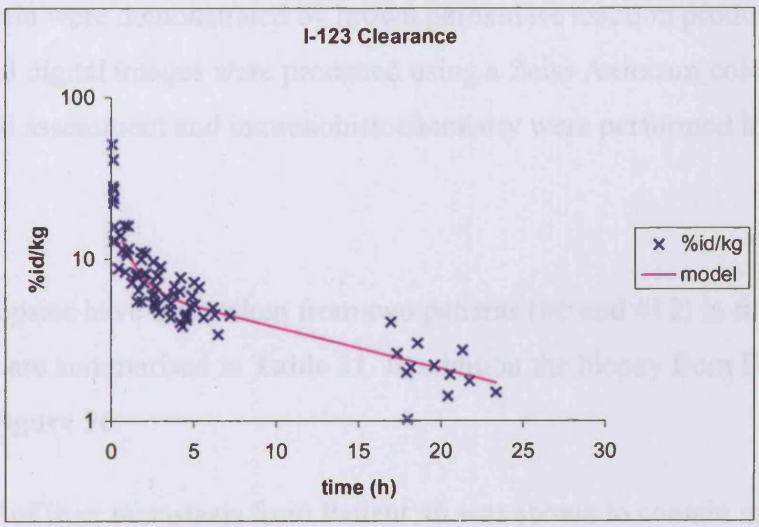

CPG2 enzyme levels in tumour and normal tissues

Method

Tumour biopsies were obtained from patients who consented to this additional procedure. Biopsies were performed under radiological guidance on the day of administration of ZD2767P and, where possible, within 30-120 min post final ZD2767P administration. The tissue was then divided and distributed where appropriate for histological assessment and immunohistochemistry.

Biopsy tissue was snap frozen in iso-pentane (cooled in liquid nitrogen) and 5μm cryostat sections cut. Sections were acetone-fixed and stained by haematoxylin and eosin (H+E) to reveal morphology. CEA and MFECP1 distribution was demonstrated by immunohistochemistry using monoclonal anti-CEA antibody (A5B7) and anti-CPG2 antibodies (SB43 mouse monoclonal and CAMR polyclonal), respectively. Appropriate controls were included to confirm specificity of immunohistochemistry. Distribution of target antigen and antibody fusion protein were demonstrated by brown peroxidase reaction product in the sections and digital images were produced using a Zeiss Axiocam colour camera. Histological assessment and immunohistochemistry were performed by G Boxer.

Results

Tumour biopsies have been taken from two patients (#6 and #12) in this study. The results are summarised in **Table 31**. In addition the biopsy from Patient #6 is shown in **Figure 36**.

The biopsy of liver metastasis from Patient #6 was shown to contain metastatic adenocarcinoma surrounded by fibromyxoid stroma. Immunohistochemistry with anti-CEA antibody confirmed that these tumour areas expressed CEA. Further immunohistochemistry with anti-CPG2 antibody confirmed the presence of CPG2 in the CEA expressing tumour areas, consistent with tumour localisation of MFECP1 in this patient (**Figure 36**). The sensitivity of immunohistochemistry with anti-CPG2 and anti-CEA antibodies is not known and although positive data

demonstrate the principal of localisation the significance of a negative result is uncertain.

The CPG2 enzyme levels could not be measured because the biopsies were too small (approximately 1 mg). There was not sufficient tumour tissue for comet assay.

Table 31: Tumour biopsy results

Pt no.	Biopsy site	Time of biopsy (hrs after start MFECP1)	Histopathology	Immunohistochemistry	
				CEA	CPG2
#6	liver	6.13	1) necrotic tumour	not interpretable	not interpretable
			2) adenocarcinoma	positive	positive
#12	liver	*25.33	1) adenocarcinoma	positive	negative
			2) normal liver	negative	negative
			3) normal liver	negative	negative

**exact time not recorded – this is an estimate*

Figure 36: Digital image of a liver biopsy from ADEPT pt #6

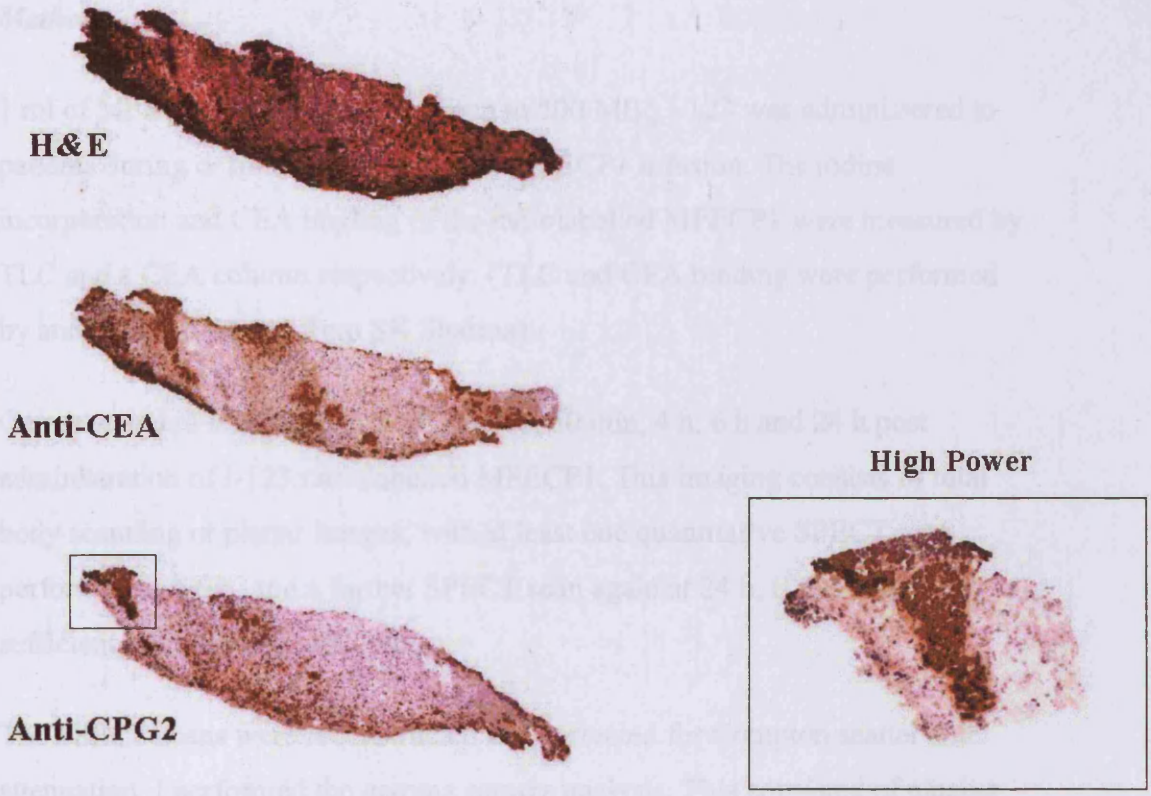

Consecutive histopathological slices from a tumour biopsy of liver metastasis from a patient with colorectal cancer. The H+E stain shows tumour heterogeneity with small clumps of tumour areas. Immunohistochemistry has been performed with the positive areas showing as brown. Immunohistochemistry with an anti-CEA antibody shows a positive reaction in areas consistent with tumour clumps. The anti-CPG2 antibody shows a positive reaction in the same areas. The high power view of the anti-CPG2 antibody reaction shows a tumour area in more detail.

These results indicate the presence of both CEA and CPG2 enzyme in these tumour areas. This provides evidence, in this one patient, of localisation of enzyme to CEA positive tumour areas.

Gamma camera imaging

Method

1 ml of MFECP1 radiolabelled with up to 500 MBq I-123 was administered to patients during or immediately after the MFECP1 infusion. The iodine incorporation and CEA binding of the radiolabelled MFECP1 were measured by TLC and a CEA column respectively. (TLC and CEA binding were performed by and results obtained from SK Sharma).

Gamma camera imaging was performed at 30 min, 4 h, 6 h and 24 h post administration of I-123 radiolabelled MFECP1. This imaging consists of total body scanning or planar images, with at least one quantitative SPECT scan performed at 4-6 h, and a further SPECT scan again at 24 h, if there was sufficient radioactivity remaining.

The SPECT scans were reconstructed and corrected for Compton scatter and attenuation. I performed the gamma camera analysis. This consisted of placing regions of interest (ROI) on tumour areas and normal tissues, including liver, lung, heart and kidney, as outlined in **chapter 2**. Where available, [F-18] FDG PET scans were used to visually correlate tumour areas. The % injected dose/kg of radioactivity was calculated for each tumour site and normal tissues, using a calibration factor derived from a phantom with a known amount of radioactivity scanned under clinical conditions. The amount of enzyme units could only be estimated in tumour, due to the known problems with rapid breakdown of MFECP1 leading to misrepresentation of radioactivity for active enzyme in non-tumour tissues. The enzyme activity in tumour was calculated by multiplying the % injected dose/kg of radioactivity in tumour by total injected enzyme units and dividing by 1000 to convert to units per gram (Green *et al*, 1990; Francis *et al*, 2002).

Results

Table 32 displays the CEA binding and the TLC results for the I-123 radiolabelled MFECP1. This was performed on the radiolabelled sample prior to administration to the patient. The median CEA binding was 56.19% (range 48.1-65.2%) and the median % iodine incorporation by TLC was 97.86% (range 92.75-99.152%).

Table 32: I-123 radiolabelling of MFECP1

Pt no.	CEA binding (%)	TLC (% incorporation)
#1	51.6	96.9
#2	48.1	97.68
#3	55.57	95.198
#4	57.99	95.6
#5	62.84	95.0
#6	58	92.75
#7	not radiolabelled	not radiolabelled
#8	50.6	98.75
#9	56.3	98.5
#10	65.2	99.11
#11	58.4	99.152
#12	56.07	99.03
#13	54.02	98.03

Abbreviation: TLC – thin layer chromatography

Total body scans visually confirmed the rapid hepatic clearance of MFECP1, with 30 min scans showing high levels of radioactivity in the liver (see **Figure 37**). The 4-6 h time point shows less hepatic uptake, with more evidence of free I-123 as a result of metabolism of the MFECP1 by the liver. This was seen as I-123 uptake in the stomach and excretion in the urinary system. There were no unexpected areas of uptake.

Figure 37: Total body gamma camera scans showing uptake of I-123 radiolabelled MFECP1

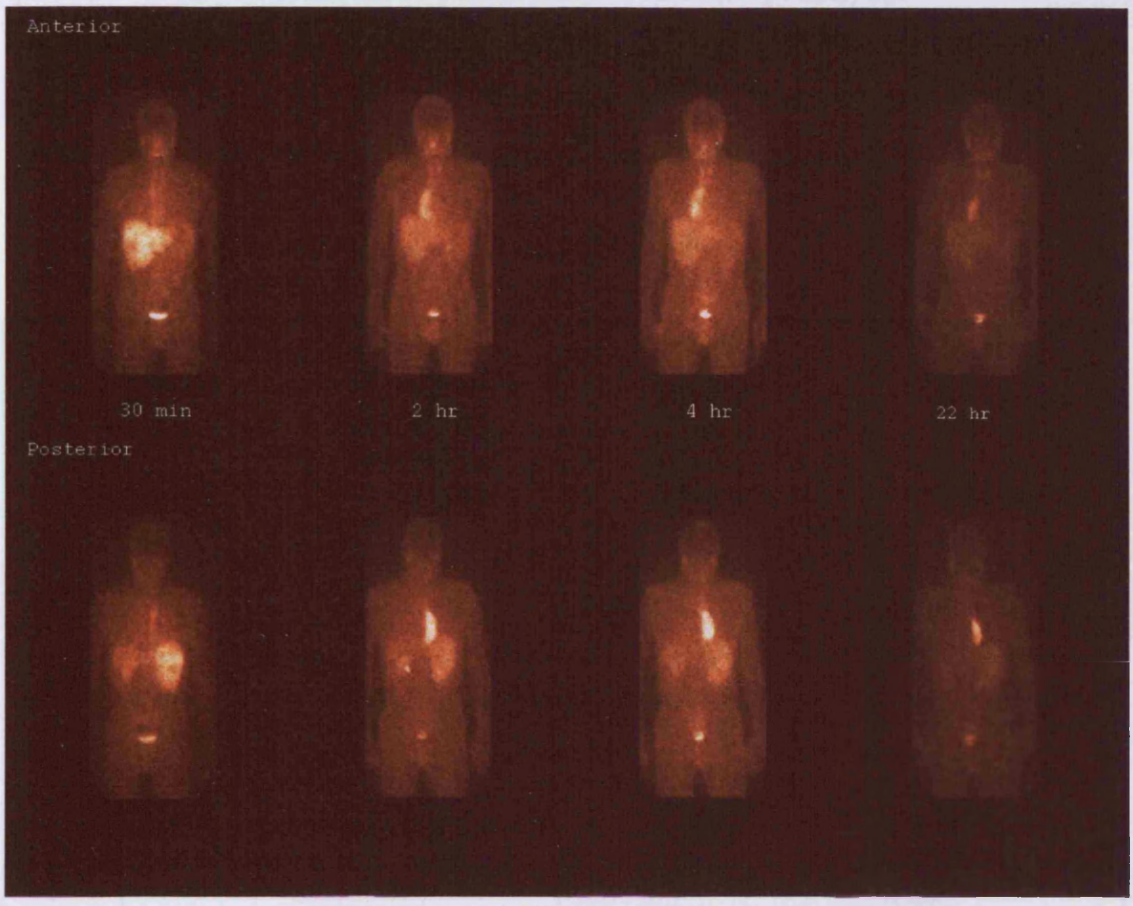

Total body gamma camera images, anterior and posterior at 30 min, 2, 4 and 22 h after injection of I-123 radiolabelled MFE-CP1 in Patient #2. The 30 min time-point shows high hepatic uptake of radioactivity, which has reduced at the later time-points. At 2, 4 and 22 h free I-123 can be seen in the stomach (seen in the thorax of this patient who had a partial oesophagectomy with gastric-pullup performed), renal pelvis and bladder. This patient had hepatic metastasis from gastro-oesophageal cancer.

The patients who had quantitative SPECT scans performed are displayed in **Table 33**. Due to camera faults four patients had SPECT scans for which quantitative analysis could not be performed (one had corrupt data, one transmission scan failed, two had camera failure and so the patients were scanned in the Department of Nuclear Medicine on a non-calibrated camera). One patient received insufficient radioactivity for SPECT scans to be performed (Patient #1).

Table 33: SPECT scans in ADEPT patients

Pt No.	Activity I-123 (MBq)	Time of SPECT scan (hrs after radiolabel)	Comments
#1	7	not done	7 MBq injected dose - no SPECT performed
#2	100	4.77	Exact injected activity uncertain due to residual activity in syringe post injection not being measured
		5.22	
#3	137.4	4.45	
#4	138.2	4.58	
		5.12	
#5	213.7	4.73	SPECT data corrupt
#6	134.8	3.67	
#7	not done	not done	no radiolabel administered
#8	264.6	4.22	bilateral ureteric obstruction
		20.35	
#9	231.7	2.92	ADAC camera fault – patient scanned in Nuclear Medicine (non-quantitative data)
#10	300.7	3.97	transmission scan failed so no attenuation correction applied (non-quantitative data)
#11	171.2	3.87	
#12	275.7	2.13	ADAC camera fault – patient scanned in Nuclear Medicine (non-quantitative data)
		18.17	
#13	227.2	4.35	
		21.18	

Figure 38 shows the %injected dose/kg of radioactivity in each organ and tumour area for all patients for whom quantitative SPECT analysis was possible.

Figure 38: SPECT analysis at 4-6 hours in individual patients

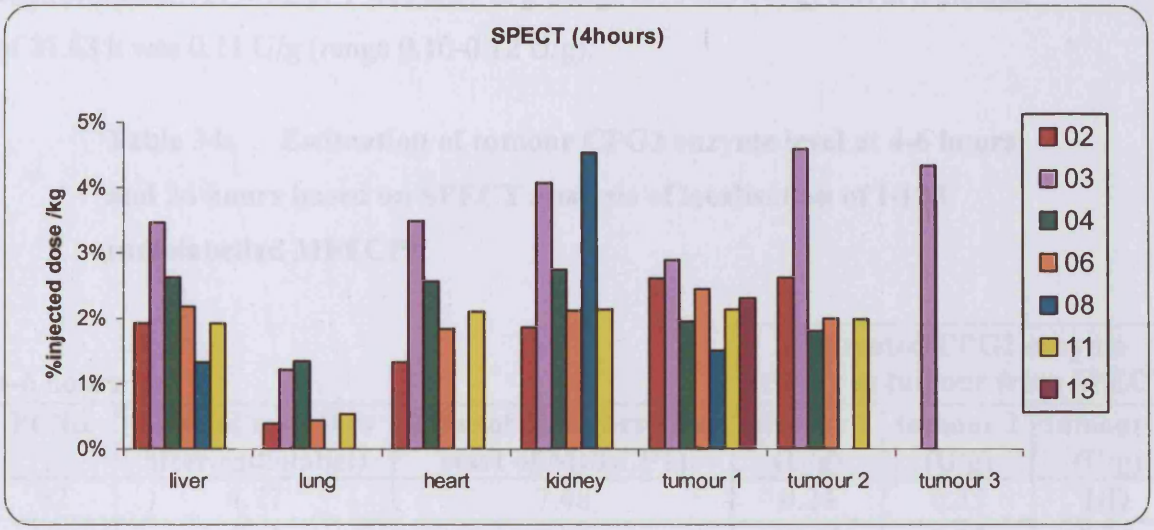

Figure 39 displays the median %injected dose/kg of radioactivity for each organ at both 4-6 h and 24 h.

Figure 39: Median %injected dose/kg of I-123 radiolabelled MFECP1 at 4-6 hours and 24 hours

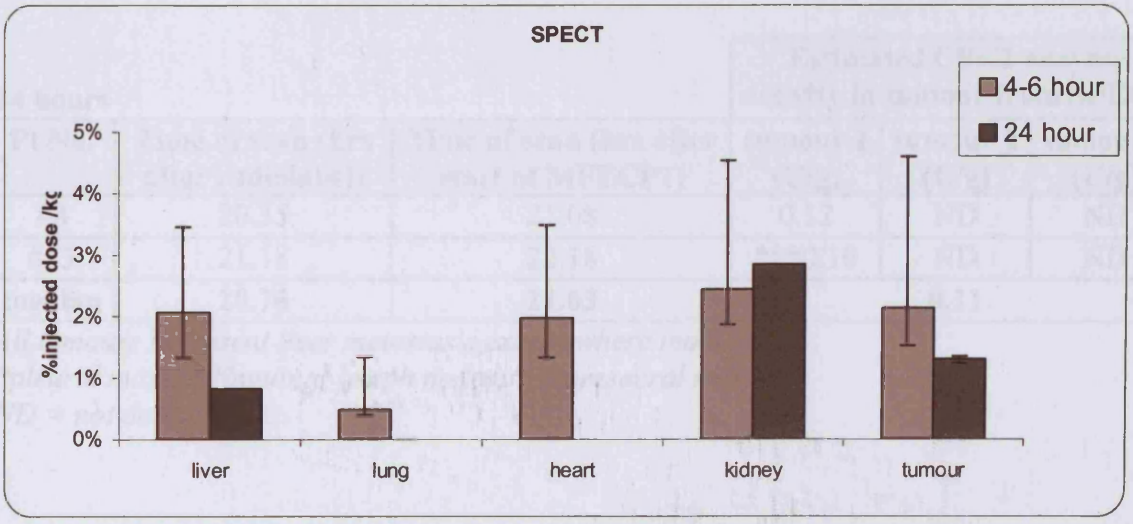

(The error bars represent the entire range of the data set)

As already discussed, radioactivity in the liver, heart and kidneys were unlikely to reflect intact MFECP1. Consequently only tumour CPG2 activity was estimated (**Table 34**), and not normal tissue enzyme levels. The estimated median CPG2 enzyme activity in tumour sites at a median of 5.47 h after the commencement of MFECP1 was 0.20 U/g (range 0.13-0.37 U/g) and at a median of 21.63 h was 0.11 U/g (range 0.10-0.12 U/g).

Table 34: Estimation of tumour CPG2 enzyme level at 4-6 hours and 24 hours based on SPECT analysis of localisation of I-123 radiolabelled MFECP1

4-6 hours			**Estimated CPG2 enzyme activity in tumour from SPECT**		
Pt No.	**Time of scan (hrs after radiolabel)**	**Time of scan (hrs after start of MFECP1)**	**tumour 1 (U/g)**	**tumour 2 (U/g)**	**tumour 3 (U/g)**
#2	4.77	7.48	0.24	0.25	ND
#3	4.45	7.72	*0.23	0.37	0.35
#4	5.12	7.20	**0.20	**0.18	ND
#6	3.67	5.47	0.21	0.17	ND
#8	4.22	4.95	0.13	ND	ND
#11	3.87	4.42	0.17	0.16	ND
#13	4.35	5.35	***0.19	ND	ND
median	**4.35**	**5.47**	**0.20**		

24 hours			**Estimated CPG2 enzyme activity in tumour from SPECT**		
Pt No.	**Time of scan (hrs after radiolabel)**	**Time of scan (hrs after start of MFECP1)**	**tumour 1 (U/g)**	**tumour 2 (U/g)**	**tumour 3 (U/g)**
#8	20.35	21.08	0.12	ND	ND
#13	21.18	22.18	***0.10	ND	ND
median	**20.76**	**21.63**	**0.11**		

All tumours represent liver metastasis except where marked:
**pleural mass; **inguinal lymph nodes; ***presacral mass*
ND = not done

Figure 40 and **figure 41** are examples of transverse slices of SPECT scans, with the equivalent [F-18] FDG PET scans, showing tumour areas. It can be seen that, despite reasonably high levels of background radioactivity, that areas of increased radioactive tracer occurred in regions that would be in keeping with the tumour areas, based on the [F-18] FDG PET functional images.

Figure 40: [F-18] FDG PET and SPECT images on patient #2

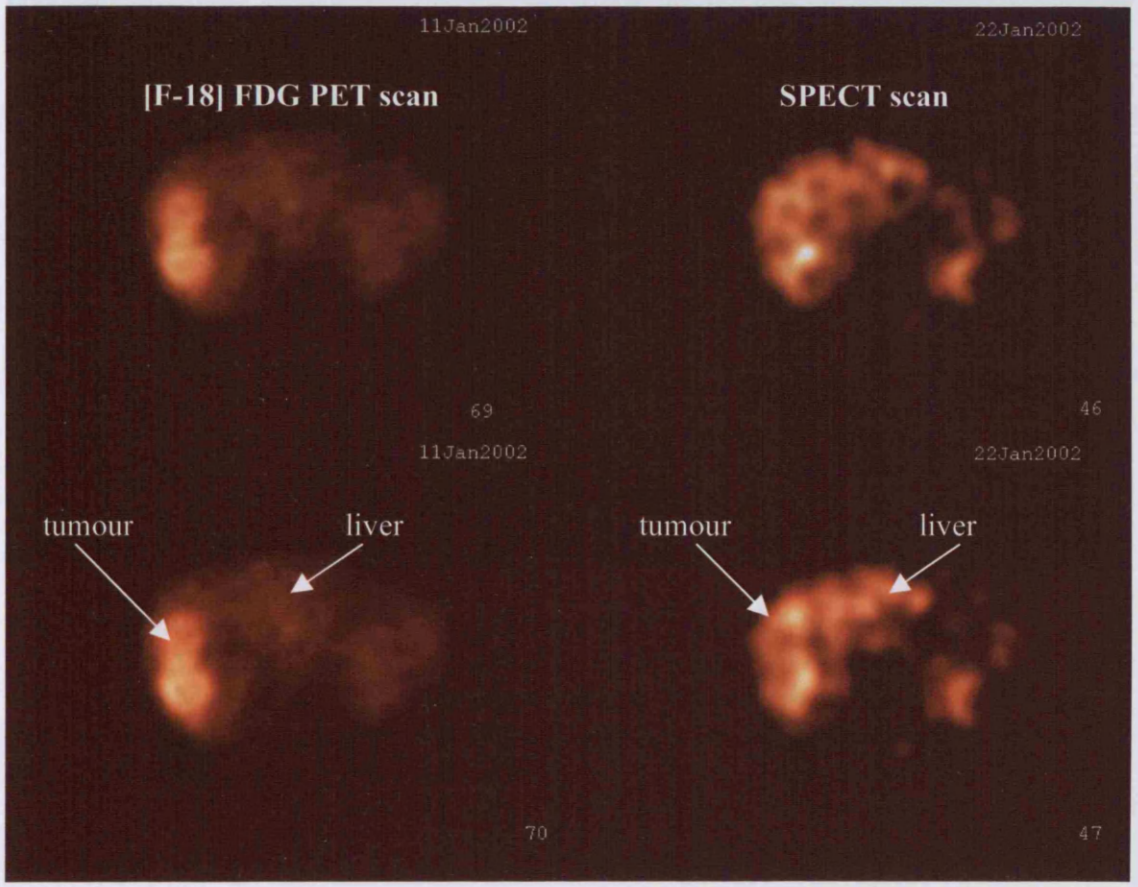

Visually equivalent transverse slices (2 consecutive slices) of the pre-treatment [F-18] FDG PET scan and the 6 hour SPECT scan on patient #2. The liver is shown, with metastatic tumour regions clearly visible on the [F-18] FDG PET scan. The SPECT scan shows increased radiolabel uptake in the area of the liver that corresponds to the tumour lesions on [F-18] FDG PET. There is a high background level of radioactivity in the liver on the SPECT scan.

Figure 41: [F-18] FDG PET and SPECT images on patient #4

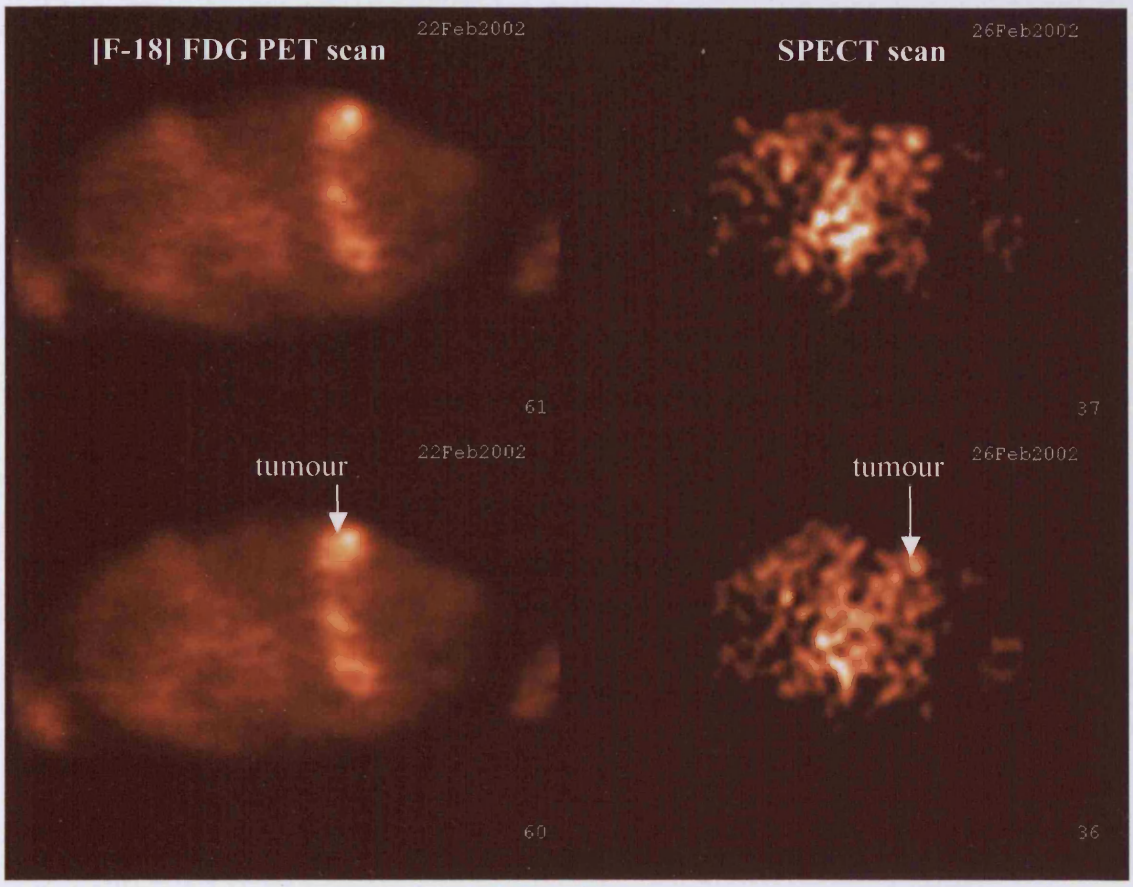

Visually equivalent transverse slices (2 consecutive slices) of the pre-treatment [F-18] FDG PET scan and the 6 hour SPECT scan on patient #4. This patient has inguinal lymph node metastasis from colorectal cancer, shown on the [F-18] FDG PET scan as a 'hot spot'. The SPECT scan also shows increased uptake in this region, indicating tumour localisation.

Immunogenicity

Method

A 10 ml blood sample was taken into a plain blood tube for HAMA/HACPG2A levels at the following times: pre-study and at weekly intervals while on study, for example on Days 8, 15, 22, 29, 36, 43, 50 and 57.

Immunogenicity was assessed by ELISA against A5B7 (HAMA assay) and CPG2 (HACPG2A assay). Results are presented as Positive or Negative for HAMA and HACPG2A at each time point tested. Levels below an optical density (OD) of 0.2 (see **Figure 42**) are defined as negative (>3 standard deviations above the mean for pre-treatment values for 20 patients before treatment with ADEPT). Analysis was performed by and data obtained from SK Sharma.

Results

Pre-treatment samples showed all 13 patients (100%) were negative for HAMA and HACPG2A.

The post treatment samples showed all 13 patients (100%) were negative for HAMA and 10 patients (76.9%) were negative for HACPG2A at all time-points. The three patients who were positive for HACPG2A were Patients #2, #3 and #12. Patient #2 was positive from 21 days after treatment but was negative at Day 56. Patient #3 was positive at 43 days after treatment and Patient #12 was positive from Day 18 after treatment (see **Figure 42**).

Figure 42: Human anti-CPG2A (HACPG2A) response in patients who have received MFECP1

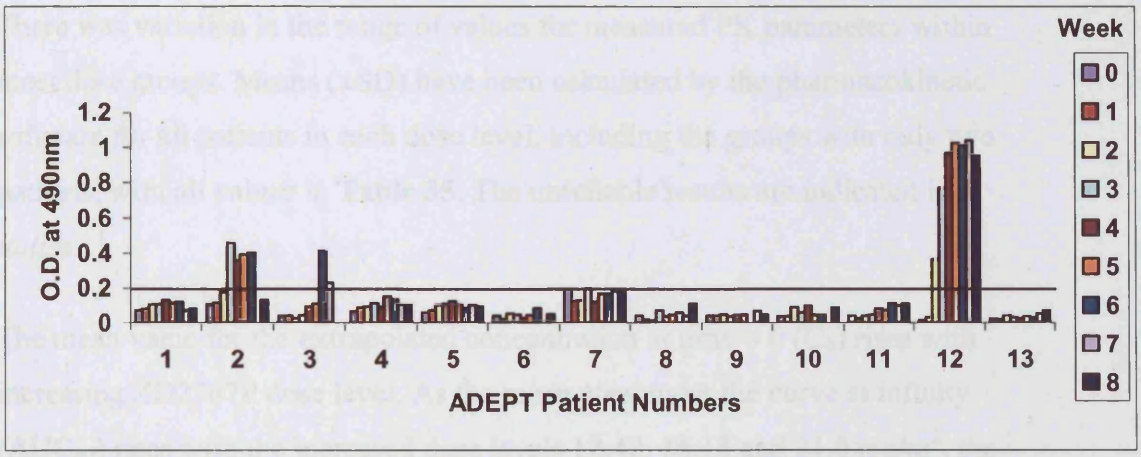

ELISA results of weekly patient serum collected to assess for the presence of HACPG2A. The line represents 3 standard deviations above mean pre-treatment values (O.D. of 0.2)
Abbreviations: O.D. – optical density

ZD2767P (prodrug) pharmacokinetics

Method

A 2.5 ml blood sample was taken into a heparinised tube containing rat serum albumin (RSA) at 2 min following each of the first two doses of ZD2767P prodrug given at hourly intervals. Similar samples were taken after 2, 5, 10, 15, 30 and 60 min following the third dose of ZD2767P, given at a further 1 h interval. Each sample was analysed by HPLC and a full pharmacokinetic profile was generated for each patient with WinNonLin software. Means (+/- standard deviation [SD]) were calculated from input of all patient data in each group, regardless of reliability (including groups with two patients). Analysis was performed by and data obtained from C Springer and J Martin.

Results

Figure 43 represents the ZD2767P prodrug plasma elimination profiles in all 13 patients. There appears to be no build-up of ZD2767P prodrug in the plasma

during the course of the three doses, and prodrug is essentially eliminated from the plasma within 1 hour of the third dose for all the dose levels.

There was variation in the range of values for measured PK parameters within most dose groups. Means (±SD) have been calculated by the pharmacokinetic software for all patients in each dose level, including the groups with only two patients, with all values in **Table 35**. The unreliable results are indicated in *italics*.

The mean value for the extrapolated concentration at time = 0 (C_0) rises with increasing ZD2767P dose level. As the mean area under the curve at infinity (AUC_{inf}) rises with the increased dose levels 12.42, 16.15 and 21.0 mg/m^2, the mean clearance rate was seen to fall. The individual and the mean dose group values for volume of distribution at steady state (V_{ss}) indicate likely containment in the blood. The overall mean elimination half-life ($T_{1/2}$) of all patients with reliable results was 8.54 minutes (±SD 3.17minutes with a median of 7.9 minutes.

Figure 43: Plasma elimination profiles after third dose of ZD2767P

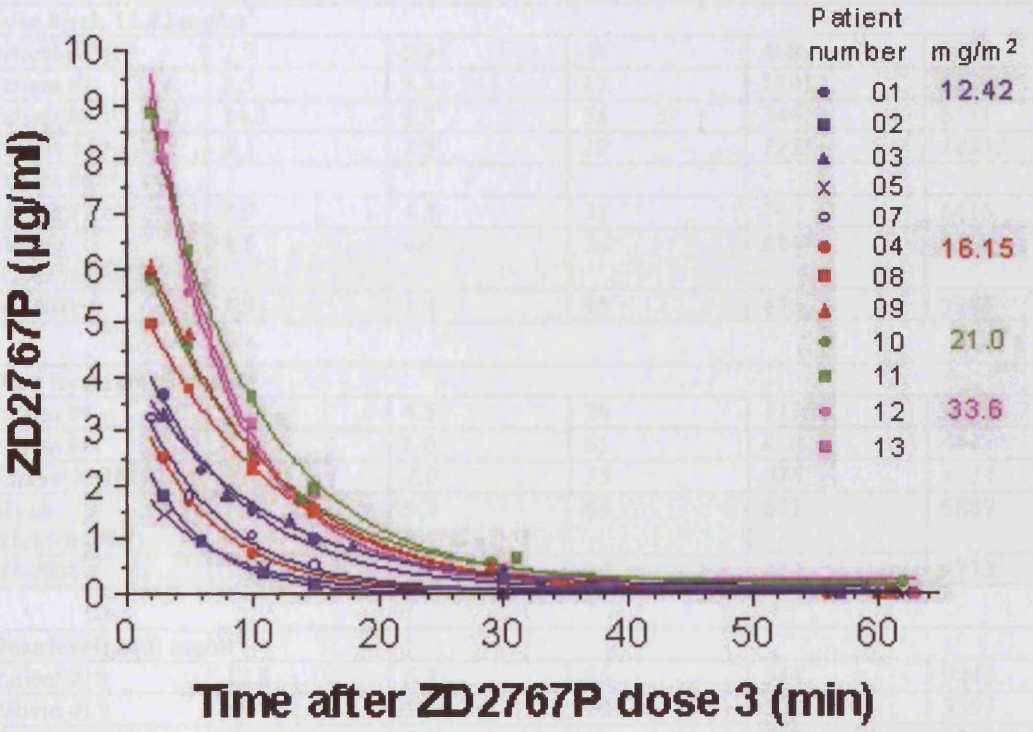

Table 35: Summary of ZD2767P phamacokinetic values

	Elimination $T_{1/2}$ (min)	C_0 (µg/ml)	AUC_{inf} (µg.ml.min)	CL (ml/min)	V_{ss} (ml)
Dose level: 12.42 mg/m²					
Patient #1	7.5	5.9	48	408	4065
Patient #2	3.5	3.4	17	1391	6879
Patient #3	14.3	4.8	58	344	6131
*Patient #5**	*9.1*	*2.3*	*19*	*1236*	*14352*
Patient #6**					
Patient #7	8.0	4.8	31	740	6416
Mean (12.42 mg/m²)	**8.5**	**4.2**	**34**	**824**	**7568**
(+/- SD)	**3.9**	**1.4**	**18**	**475**	**3943**
Dose level: 16.15 mg/m²					
Patient #4	6.4	4.5	28	1136	9085
Patient #8	6.4	6.0	61	468	4447
*Patient #9****	*8.3*	*7.0*	*75*	*378*	*4135*
Mean (16.15 mg/m²)	**7.0**	**5.8**	**55**	**671**	**5889**
(+/- SD)	**1.1**	**1.3**	**24**	**433**	**2773**
Dose level: 21.0 mg/m²					
Patient #10	12.8	6.8	86	544	9240
Patient #11	10.1	11.0	108	303	3557
Mean (21.0 mg/m²)	**11.5**	**8.9**	**97**	**424**	**6398**
(+/- SD)	**1.9**	**3.0**	**16**	**170**	**4019**
Dose level: 33.6 mg/m²					
Patient #12	7.8	14.0	96	743	6878
Patient #13	8.6	14.7	98	582	5379
Mean (33.6 mg/m²)	**8.2**	**14.3**	**97**	**663**	**6128**
(+/- SD)	**0.60**	**0.49**	**1.2**	**114**	**1060**

* *Time point 6 min omitted from input PK data as possible saline contamination.*

** *No results as single lumen Hickman line allowed prodrug contamination of plasma samples.*

*** *Time points 10, 15, 29 and 60 min unreliable as only 2/3 of LOW quality control samples acceptable due to technical difficulties with normal plasma used to construct LOW calibration range, but used for pharmacokinetic analysis.*

Abbreviations: $T_{1/2}$ - half-life; C_0- concentration at time = 0; AUC_{inf} - area under the curve at infinity; C_L – clearance; V_{ss}.- volume of distribution at steady state; SD -standard deviation

Comet assay

Method

Comet assays were performed to indirectly assess activation of ZD2767P into an active cytotoxic alkylating agent, ZD2767D. ZD2767D has too short a half-life for direct measurement of drug levels, and therefore the presence of DNA interstrand crosslinks, as assessed on a comet assay, may provide indirect evidence of ZD2767D formation and effect. Comet assays were performed on 10 ml blood samples (taken into heparinised tubes), at 60-120 min after the last ZD2767P was administered, and where applicable, on tumour or bone marrow biopsy specimens. If a tumour or bone marrow biopsy was performed the blood sample was taken within 10 min of the biopsy.

The result was recorded as a percentage reduction in tail moment (%RTM) and was calculated as the change in comet tail compared to control. A negative value for %RTM indicates crosslinking. Analysis was performed by and data obtained from J Hartley.

Results

No tumour or bone marrow biopsy specimens had comet assay performed (one tumour biopsy was performed prior to prodrug administration – patient #6, and so the comet assay was not performed, the other had insufficient tissue for comet to be performed – patient #12). The comet assay was therefore only performed on peripheral blood lymphocytes. The results are shown in **Table 36**. No patients have had substantial crosslinking seen in their circulating lymphocytes. These results are consistent with the low levels of haematological toxicity experienced in this ADEPT study to date. Patient #11 has the most crosslinking (23.75% reduction in tail moment) however this patient did not experience haematological toxicity.

Table 36: Comet assay (lymphocytes)

Pt No.	%RTM
#1	-6.4
#2	-8.9
#3	1.9
#4	9.4
#5	2.48
#6	13.2
#7	3.2
#8	0
#9	8.2
#10	10.8
#11	-23.75
#12	-4.0
#13	4.5

Abbreviations: %RTM – percentage reduction in tail moment

4.3.4 Efficacy

Radiological Assessment

Method

A minimum of one course of ADEPT (defined as MFECP1 followed by ZD2676P) was required for a patient to be considered evaluable for response. The response criteria used in this study were RECIST (Therasse *et al*, 2000). Tumour assessments were performed pre-study and then every 28 days or more frequently, if clinically indicated. All patients had CT scans for response assessment.

Results

Thirteen patients (100%) were evaluable for tumour response to at least Day 29 (see **Table 37**). Six patients (46.2%) had stable disease at Day 29, which was reduced to four patients (30.8%) at Day 57 (Patient # 6 withdrew from the study; Patient #13 progressive disease at Day 57). Seven patients (53.8%) had progressive disease at Day 29 and Day 57. There were two patients (15.4%) who did not have a Day 57 disease assessment performed as they came off study

before Day 57 (Patient #3 was too unwell for Day 57 assessment and Patient #6 voluntarily withdrew from the study).

Table 37: Radiological response to ADEPT

Assessment Day	Response	Number of patients (%) n = 13	Pt No.
Day 29	Stable Disease	6 (46.2%)	#1, #6, #7, #10, #11, #13
	Progressive Disease	7 (53.8%)	#2, #3, #4, #5, #8, #9, #12
	Not Evaluable	0 (0%)	-
Day 57	Stable Disease	4 (30.8%)	#1, #7, #10, #11
	Progressive Disease	7 (53.8%)	#2, #4, #5, #8, #9, #12, #13
	Not Evaluable	2 (15.4%)	#3, #6

Serum tumour markers

Method

Serum tumour markers (CEA, CA19-9 and where, appropriate, CA15-3) were taken pre treatment and at day 29 and 57 after ADEPT.

Results

The serum tumour marker results on all patients are shown in **Table 38**. As MFECP1 is an anti-CEA antibody this may make interpretation of serum CEA levels difficult. The serum CA19-9 or CA15-3 tumour marker levels on all patients increased after ADEPT except patient #10, who had a small fall in serum CA15-3 tumour marker from a level of 344.4 U/mL pre-treatment to 289 U/mL at 46 days after treatment with ADEPT. This patient also had a small fall in serum CEA from 123.3 μg/L to 115.9 μg/L at 46 days after ADEPT. This fall in tumour markers was accompanied by stable disease on CT scan at day 29 and 57 after ADEPT.

Patient #1 had a fall in serum CEA tumour marker levels (from 549.5 μg/L pre ADEPT to 468.6 μg/L at day 56), however this was not reflected in this patient's CA19-9 tumour marker levels, which rose from 348 U/mL pre ADEPT to 766

U/mL at day 56. Patient #1 also attained stable disease on CT scan at day 29 and 57.

Table 38: Serum tumour marker levels in patients who received ADEPT

Pt No.	CEA(µg/L)			CA19-9 (U/mL)			CA15-3 (U/mL)		
	pre	Day29	Day57	pre	Day29	Day57	pre	Day29	Day57
#1	549.5	439.8	468.6	348	642	766	ND	ND	ND
#2	177.5	466.8	799.2	11	11	15	ND	ND	ND
#3	471.8	802.8	860.7	ND	ND	ND	ND	ND	ND
#4	396.9	397.4	404.7	956	1046	880	ND	ND	ND
#5	214.8	516.6	773	295	463	678	ND	ND	ND
#6	501.3	973.4	950.7	ND	ND	ND	ND	ND	ND
#7	499.9	562	773	508	878	1539	ND	ND	ND
#8	18.9	38.9	67.1	43	50	76	ND	ND	ND
#9	587	977	1551	ND	ND	ND	>300	1549	2145
#10	123.3	116	115.9	ND	ND	ND	344.4	349	289
#11	57.8	84.9	129.4	NR	NR	NR	ND	ND	ND
#12	23.9	48.7	133.1	28	61	116	ND	ND	ND
#13	190	202.6	415.6	42	42	55	ND	ND	ND

ND – not done
NR- not raised- tumour marker levels were taken, but did not fall outside the normal range.

F-18 FDG PET scans

Method

[F-18] FDG-PET scans were performed on consenting patients to assess changes in tumour glucose metabolism with therapy. Scans were performed pre study and at approximately 2-4 weeks and then 8 weeks post ADEPT therapy. Patients fasted for 5 hours prior to injection of 130 MBq of F-18 FDG. Scans were performed at 90 min on an ADAC Vertex Plus Co-Incidence camera. Acquired data was reconstructed using standard iterative protocols, with attenuation correction (attenuation maps were acquired using Caesium–137 sources).

Analysis of [F-18] FDG PET scans were performed after correction for injected dose and time to scanning. I performed the analysis using the volume of interest quantitative technique (VOI) as discussed in **chapter 5**. The total counts obtained

from tumour volumes were used to quantify change as a percentage of the pre-study tumour total counts. Mathematically derived volumes of interest were also defined on normal background tissues (usually liver, lung and chestwall) in order to validate changes in tumour FDG uptake.

Results

Nine of thirteen patients participated in the [F-18] FDG PET component of the ADEPT study. Quantitative analysis was performed in seven of these patients' scans (the baseline [F-18] FDG PET scan for Patient #6 was corrupt and no analysis could be performed, and problems with the injection of FDG for the second scan for Patient #2 meant that the exact injected dose was uncertain). All patients show an increase in tumour FDG uptake after ADEPT (**table 39**). In two patients (#8 and #11) quantitative tumour volumes could not be defined on the baseline [F-18] FDG PET scan, however they could be defined on the post treatment scan. This is consistent with disease progression. Quantitative analysis of Patient #9 revealed an abnormal degree of change in FDG uptake in background normal tissues (lung and chestwall) between the pre-study and 6 week scan, which would suggest that the quantitation of tumour FDG uptake may not be reliable.

Table 39: [F-18] FDG PET analysis

			Quantitative –VOI	
Pt No.	**CT Response (4weeks)**	**CT Response (8 weeks)**	**Early PET Response (2-4 weeks)**	**Late PET Response (8 weeks)**
#3	PD	**ND**	240%	**ND**
#4	PD	PD	129%	**ND**
#5	PD	PD	144%	379%
#7	SD	SD	109%	126%
#8	PD	PD	PD	PD
#9	PD	PD	**ND**	*601%
#11	SD	SD	PD	**ND**

% in table represent a % change compared to baseline – no change from baseline would be recorded as 100%, a reduction from baseline has a value <100% and an increase from baseline has a value >100%

** background 'normal'/ tissues in this patient varied greatly between scans, indicating that data may not be accurate.*

*Reasons for **ND** (not done): Patient #3 too unwell for 8 weeks scan; Patients #4 and #11 ADAC camera fault for 8 weeks scan; Patient #9 scan performed at 6 weeks due to fault in ADAC camera prior to this.*

Abbreviations: PD = progressive disease; SD = stable disease; VOI – volume of interest

4.4 Discussion

The results from the first 13 patients treated with ADEPT will be discussed in terms of the hypotheses proposed at the commencement of this trial (**section 4.1.3**).

MFECP1 safety

There has been little precedent for the administration of a protein such as MFECP1 in humans. The combination of a murine antibody for tumour targeting, a bacterial enzyme for prodrug activation, a hexahistidine tag for simplified purification and short-branched mannose glycosylations added by the production process in *Pichia pastoris* is, to our knowledge, unique to this molecule. Despite the potential risks of administration of such a molecule to humans, MFECP1 was found to be safe and well tolerated. It was associated with Grade I 'possible' drug-related toxicities of low grade fever and chills, in two of the thirteen patients. Fever and chills would not be unexpected after the administration of a foreign protein; and for it to have occurred only in two patients was reassuring for the safety of this molecule.

Tumour targeting of MFECP1

The tumour targeting of MFECP1 will be discussed in terms of systemic clearance, tumour localisation, and the possible impact of administered dose.

Systemic clearance of antibody-enzyme

Systemic clearance of antibody-enzyme was studied by measuring serum CPG2 enzyme levels and distribution of radiolabelled MFECP1. The two give different information; the serum CPG2 enzyme levels being a reflection of intact circulating MFECP1 and the radiolabel tracking the distribution of the protein and its breakdown products.

Measurement of serum CPG2 enzyme levels showed that functioning CPG2 enzyme was rapidly cleared from the blood. The β half-life for enzyme activity in serum was 6.0 hours. Radiolabelled MFECP1 was also shown to clear rapidly

from the blood, however not as rapidly as the active enzyme. The β half-life was 11.8 hours for clearance of radioactivity from the blood. The reason for the slower elimination of radioactivity was apparent from the gamma camera imaging. This showed radioactivity rapidly accumulating in the liver as early as 30 minutes after administration of radiolabelled MFECP1, indicating uptake of MFECP1. This was followed at 2 hours by diminishing radioactivity in the liver, but increasing uptake in the kidneys and in the stomach wall (**figure 37**). The liver contains receptors for the glycosylations of MFECP1, which appear to mediate the rapid uptake of MFECP1. This is followed by catabolism of the protein, leading to loss of enzyme activity. Radiolabelled peptide fragments and free iodine are then released back into the circulation and cleared through the kidneys, or excreted by the stomach and other parts of the gastrointestinal tract. This process accounts for the slower clearance of radioactivity than of enzyme activity in normal tissues.

Anecdotally it was noted that patients with extensive hepatic involvement of tumour tended to clear MFECP1 from the blood much slower than those with no, or minimal hepatic involvement by tumour. Patients who were noted to have particularly extensive infiltration of their liver with tumour were patients #3, #6 and #9. Patients #6 and #9 had the slowest clearance of CPG2 enzyme from their blood, and patient #3 had dose limiting toxicity. This supports the concept that the rapid clearance of CPG2 from the systemic circulation is likely to be from hepatic metabolism.

In the previous ADEPT trial clearance of CPG2 enzyme from the systemic circulation was slow, with a β half-life for A5CP of over 15 hours (Campaign 4) (**chapter 2**). The more rapid clearance of MFECP1 was a design feature in order to allow administration of prodrug at a much earlier time-point than was possible with A5CP. It was hypothesised that this would increase the likelihood of their being sufficient CPG2 in tumours at this time, and that the CPG2 enzyme that was present would be likely to be located in viable tumour areas, rather than in the necrotic centre of the tumour where its effectiveness would be limited.

The rapid systemic clearance of MFECP1 resulted in serum CPG2 enzyme levels considered safe for administration of prodrug at 24 hours after MFECP1

administration, compared to a median of 3 days for A5CP. This was despite an increase in administered dose of CPG2 enzyme from 3000U/m^2 in the A5CP ADEPT trial to 5000U/m^2 for this trial.

Tumour Localisation of MFECP1

The total amount of CPG2 that is delivered to tumour is likely to influence the effectiveness of activation of prodrug, and subsequently the potential efficacy of ADEPT. It was therefore desirable to ascertain the amount of functional enzyme in tumour at the time of prodrug administration. The information was attained by the measurement of functional enzyme in tumour on tumour biopsy specimens and by estimation of tumour antibody-enzyme localisation by gamma camera imaging of radiolabelled MFECP1.

Two tumour biopsies have been obtained in the 13 patients reported here. It was impractical to perform tumour biopsies on the earlier patients in the study, as the timing of the biopsies were such that they would have been performed in the evening, outside routine working hours. As liver biopsies may be associated with potential morbidity and complications, this was avoided.

One tumour biopsy of liver metastasis from colorectal cancer taken at approximately 6 hrs after the commencement of MFECP1 showed immunohistochemical evidence of CPG2 enzyme localisation in tumour at sites containing CEA (**Figure 36**). Enzyme appeared to have localised in all the tumour areas of this biopsy and in none of the non-tumour areas. However, another tumour biopsy of liver metastasis from colorectal cancer taken at approximately 24 hrs after commencement of MFECP1 failed to demonstrate the presence of CPG2. Immunohistochemistry is non-quantitative and the levels of detection are not known – it is possible that the assay was too insensitive to detect the presence of CPG2, or that there was indeed no significant amount of CPG2 present in the tumour of this patient at 24 hours.

The tumour biopsy specimens were too small for an accurate measurement of the amount of active CPG2 to be made by methotrexate reduction assay on HPLC.

Quantitative gamma camera imaging of I-123 labelled MFECP1 was also used to ascertain whether adequate localisation of MFECP1 was occurring. It was estimated that the median tumour enzyme level at approximately 6 hours after commencement of MFECP1 was 0.2 U/g, and at approximately 22 hours, 0.11 U/g. These levels of CPG2 activity are expected to be sufficient to activate prodrug (ZD2767P). Although gamma camera imaging is an indirect method of determining enzyme levels, it has correlated well with direct enzyme levels measured in tumour biopsies in two previous clinical trials (Napier *et al,* 2000; Francis *et al*, 2002).

As discussed above, radioactivity was also found to be distributed in non-tumour areas (liver, kidneys, stomach, blood). Preclinical models have supported the concept explained above, that radioactivity in blood and normal tissues is not representative of functioning enzyme, and is instead a reflection of fragments of radiolabelled protein, or free iodine. However in tumour areas measurements of radioactivity do seem to provide a reasonable estimation of actual enzyme activity. Importantly, radioactivity was not found to be distributed in any sites other than those expected from preclinical experience. In particular there was no evidence of specific bone marrow uptake of radioactivity.

Unfortunately only 2 of the 13 patients had SPECT scans at 24 hours that were suitable for quantitative analysis. Although it was hoped that patients would receive 500MBq of I-131 radiolabelled MFECP1, problems with the radiolabelling lead to only a median of 192MBq was administered (range 7-300 MBq). This meant that with the short half-life of I-123 of 13 hours, and the rapid metabolism and dehalogenation of I-123 radiolabelled MFECP1, very little radioactivity was present at 24 hours. Even with prolonged SPECT scan times image quality was poor, and count rates very low. Recalibration of the camera had to be performed at these very low count rates in order to validate the scans quantitatively. This problem may be overcome by using I-131 instead of I-123. I-131 has a half-life of 8 days, and radioactive decay over 24 hours will therefore be less problematic. I-131 also appears to have a better labelling efficiency than I-123, which should lead to a more satisfactory amount of radiolabel applied to MFECP1.

In summary, there is preliminary evidence to suggest that MFECP1 localises to tumour, with one tumour biopsy at approximately 6 hours showing immunohistochemical evidence of the presence of CPG2, and gamma camera imaging estimating tumour CPG2 enzyme levels to be 0.20U/g at approximately 6 hours and 0.11U/g at approximately 22 hours after commencement of MFECP1. These enzyme levels are likely to be capable of activating prodrug. Additionally there is a tumour to blood ratio of at least 50:1 at the time of prodrug administration, which should provide tumour selectivity.

Administered dose of MFECP1

In the current clinical study, ZD2767P is administered at approximately 24 hours after MFECP1. This time-point ensures that active CPG2 enzyme has cleared from systemic tissues, and this is reflected in serum CPG2 levels, which have been <0.002U/mL in the majority of patients. However, in some patients this enzyme level is attained in serum even as early as 6-8 hours after the commencement of MFECP1. Although quantitative SPECT analysis indicates that sufficient CPG2 enzyme for activation of prodrug should be present in tumour areas even at 24 hours, this has not yet been confirmed by tumour biopsy.

In preclinical models ZD2767P was administered at 6, 7 and 8 hours post MFECP1, whereas currently in the clinical trial ZD2767P is administered at 22-24 hours after MFECP1. It may be that at 24 hours there is not sufficient CPG2 enzyme in the tumour to activate prodrug. Administering ZD2767P at a time-point between 6 and 24 hours post administration of MFECP1 is challenging in the clinical setting, due to the constraints of medical and nursing staff availability, the instability of ZD2767P, which must be administered within 20 minutes of reconstitution, radiolabelling and gamma camera requirements, and the feasibility of tumour biopsies which should be performed within normal working hours. The reduction in time between 24 to 6 hours will also have to be performed in a careful step-wise fashion, as severe and potentially life-threatening myelotoxicity has resulted with much lower ZD2767P doses than are currently being used, when activation has occurred through residual enzyme in normal tissues.

An alternative strategy would be to reduce the administered dose of MFECP1, which should result in serum CPG2 levels of <0.002 U/mL at earlier time-points. A dose scheduling study has been performed in preclinical models, in which the most favourable tumour to normal tissue ratios achieved at 6 hours post administration of MFECP1 were for human dose equivalents of MFECP1 of 2400-3600U/m^2 (**Table 40**) (Data obtained with permission from SK Sharma).

Table 40: Dose scheduling of MFECP1 in preclinical model

	MFECP1 dose			
MFECP1 dose in mice	15U	20U	30U	60U
'Human equivalent' MFECP1 dose	1800U/m^2	2400U/m^2	3600U/m^2	7200U/m^2
Plasma CPG2 enzyme level at 6 hours by HPLC (U/mL)	<0.002	<0.002	<0.002	0.032
Tumour CPG2 enzyme level at 6 hours by HPLC (U/g)	0.31	0.95	1.6	2.54
Tumour to plasma CPG2 ratio	>155:1	>475:1	>800:1	79:1

MFECP1 was administered to nude mice bearing LS174T human colorectal cancer xenografts. Plasma and tumour CPG2 enzyme levels were measured by methotrexate reduction assay on HPLC at 6 hours after administration, and tumour to plasma ratios were calculated. (Data obtained with permission from SK Sharma)

Reducing the administered dose of MFECP1 may allow the administration of ZD2767P 6-8 hours after commencement of MFECP1. However, the reduction in total administered dose of MFECP1 may be associated with an overall reduction in the amount of CPG2 enzyme that is delivered to tumour. Increasing the administered MFECP1 dose to 10000U/m^2 or even 20000U/m^2 should deliver more antibody-enzyme to tumour, however it may take longer for serum CPG2 enzyme levels to fall below 0.002U/mL, and administration of prodrug will probably be at 24 hours. This may also be a reasonable strategy, providing there is evidence that active CPG2 remains in viable tumour areas at this time-point. This would require biopsy confirmation of active CPG2 enzyme in tumour areas at 24 hours, with the addition of immunohistochemistry to confirm its location.

More tumour biopsies in this clinical trial are therefore required to provide invaluable information regarding the amount of functional CPG2 enzyme at 24 hours in the tumour, and will help guide the decision on whether the amount of MFECP1 being administered is appropriate for the time of prodrug administration.

Dose escalation of ZD2767P

In the previous ADEPT study, the MTD of ZD2767P was attained at 15.5mg/m^2, which was much lower than predicted based on preclinical models, and likely to be too low for efficacy. It was theorised that the slow systemic clearance of A5CP lead to circulating CPG2 being present at the time of prodrug administrations, and consequently peripheral activation of ZD2767P occurred, with resultant toxicity in the form of myelosuppression. The more rapid systemic clearance of MFECP1 should obviate this problem, and allow greater dose escalation of ZD2767P to occur. Two factors therefore appear to influence the amount of active drug generated from ZD2767P; CPG2 enzyme levels and the administered dose of ZD2767P.

CPG2 enzyme level

The protocol was designed to have a fixed dose of MFECP1 administered, and the dose of ZD2767P prodrug escalated to establish MTD. One incidence of DLT (Grade 3 myelosuppression) was experienced at the first dose level of ZD2767P (12.42 mg/m^2). The serum CPG2 enzyme level prior to ZD2767P administration in this patient was 0.0167 U/ml. It is possible that ZD2767P was activated in blood at this enzyme concentration, which may have caused this patient's myelosuppression. This patient also had very aggressive malignant disease, with bone marrow involvement, which may have contributed to the development of myelosuppression.

In the initial phase of this study prodrug was given when the serum enzyme concentration was below 0.05 U/ml and subsequently, because of this episode of dose limiting myelosuppression, the serum enzyme level at which prodrug could be administered was reduced to 0.005 U/ml. This modification was made

possible by the improvements attained in the HPLC methotrexate reduction assay for functional CPG2 activity. The previous ADEPT trial used the Cobas analyser for a rapid (within 1 hour) measurement of serum CPG2 enzyme levels however it was only sensitive to a CPG2 level of >0.05U/mL. HPLC was required to define CPG2 enzyme levels below this however, in the last ADEPT study, the HPLC assay took 2-3 hours to attain a result. This would not have been practical for this trial as MFECP1 cleared rapidly, and the CPG2 enzyme level had to be known within an hour, in order that the decision to proceed with prodrug administration could be instigated. Improvements in the efficiency of this assay, and extensive validation testing, meant that a 5 minute incubation assay was developed, validated to a minimum CPG2 enzyme level of 0.005 U/mL and a 30 minute incubation assay valid to 0.002 U/mL.

Dose escalation of prodrug was resumed and for Patients #5 to #13 no further myelosuppression attributable to ADEPT was observed. To attain this level of CPG2 enzyme in the blood, prodrug administration was delayed until the following day. There has been no evidence of myelosuppression in these patients, and the comet assays performed on peripheral blood lymphocytes confirm no convincing evidence of cross-links in the peripheral blood samples, which is in keeping with the low levels of myelotoxicity seen.

It appears therefore that at a serum CPG2 enzyme level of < 0.002U/mL no significant activation of ZD2767P in the peripheral circulation occurs. This is in keeping with *in vitro* data looking at the level of CPG2 enzyme activity required in the serum/plasma of a variety of species to activate an otherwise non-toxic dose of ZD2767P to kill 50% of LoVo tumour cells (**Table 41**).

Table 41: CPG2 concentration required to activate a non-toxic ZD2767P concentration and inhibit cell growth by 50%

Media	CPG2 concentration (U/ml)
No serum	0.0129 ±0.0037
Foetal calf serum (10%)	0.0129 ± 0.0037
Human plasma (10%)	0.0193 ± 0.0093
Mouse plasma (10%)	0.023 ± 0.0087
Monkey plasma (10%)	0.034 ± 0.0127

The CPG2 concentration required to activate a non-toxic dose of ZD2767P sufficiently to inhibit cell growth of 50% of LoVo cells. Each result is the median of 3 experiments. The CPG2 concentration required differs with each different species' plasma/serum. The lower the value, the less CPG2 is required for activation. (Data obtained, with permission, from D. Blakey and H. Newell).

In 10% human plasma a CPG2 level of 0.0193 U/mL in combination with ZD2767P will cause 50% inhibition of growth of LoVo cells. In mouse and monkey plasma the CPG2 enzyme levels required are higher than this. It has been recognised that ZD2767P in combination with CPG2 is more unstable human plasma than with some other species. To counteract continued conversion from prodrug to active drug occurring for the pharmacokinetic analysis of ZD2767P, rat serum albumin is added to heparinised blood tubes, as ZD2767P in combination with CPG2 is more stable in rat serum than in human plasma. As ZD2767P activation occurred in 10% human plasma at 0.0193U/ml, it is likely that the critical level for significant activation of prodrug in the systemic circulation for the purposes of this trial, will occur somewhere between 0.02 and 0.002U/ml. This is consistent with the clinical data acquired in this trial so far.

The enzyme level in the systemic circulation or in normal tissues is therefore an important determinant of toxicity from ADEPT, however, the enzyme level in the tumour is a determinant of efficacy. Selective tumour targeting of antibody-enzyme is designed to create a differential between functional enzyme levels in tumour and normal tissues. This forms a therapeutic window when CPG2 enzyme levels in the systemic circulation or other normal tissues are below the threshold required to activate ZD2767P, whilst sufficient CPG2 enzyme is present in tumour to result in prodrug activation. It is likely that the current

administration schedule of administering ZD2767P, 24 hours after MFECP1 when serum CPG2 enzyme levels are <0.005 U/ml will avoid systemic prodrug activation, however it is not yet clear that sufficient CPG2 enzyme is in tumour at this time for activation of prodrug. Based on the data collected in the trial to date, a tumour CPG2 enzyme level of 0.11 U/g at 24 hours (SPECT data) should be adequate for activation of prodrug, however, as discussed already, tumour biopsy data would be desirable to confirm this levels of CPG2 enzyme activity. A > 50:1 tumour to normal tissue gradient of CPG2 enzyme activity, as appears to be the current situation from the data acquired to date, should create a sufficient therapeutic window for selective tumour targeting, and allow safe dose escalation of ZD2767P prodrug, and potentially efficacy once an adequate ZD2767P dose is reached.

ZD2767P dose

The dose levels of ZD2767P prodrug attained in the clinical trial results presented here were 12.42 mg/m^2 to 33.6 mg/m^2. Dose escalation is continuing in the clinical trial with doubling of the dose after every two patients. The dose of ZD2767P prodrug used in preclinical mouse models was 70mg/kg (210 mg/m^2) and the aim of the dose escalation scheme is to reach this level in this study. Two further patients have been safely treated at 66.2 mg/m^2, and one patient at 132.4mg/m^2 without evidence of myelosuppression, at the time of writing of this thesis. Dose limiting toxicity for ZD2767P prodrug has not been reached when prodrug is administered at the current protocol serum enzyme level (< 0.005 U/ml). There is therefore a prospect of reaching a prodrug level equivalent to that which was necessary for effective therapy of human colon cancer in an animal model system.

The ZD2767P pharmacokinetic data can be used to assist in understanding whether doses of ZD2767P are being achieved that are equivalent to those which resulted in efficacy in the preclinical studies. As discussed previously the active drug formed from ZD2767P has too short a half-life to be measured as part of a clinical trial. The concentration of ZD2767P (in combination with CPG2) required to be cytotoxic to 50% of LoVo cells in vitro was 0.32μM (Blakey *et al*, 1996) (**table 7, chapter 2**). The concentration extrapolated to the time of

administration (C_0) of ZD2767P in plasma from the clinical samples taken at a ZD2767P dose of 33.6mg/m^2 was 14.3 μg/mL (mean value). Using the molecular weight of ZD2767P (as a free base) of 590, this gives a molar concentration of 0.024μM, which is significantly less than would be expected to result in cytotoxicity. A more recent publication by Monks *et al* has tested the *in vitro* sensitivity of a range of colorectal cancer cell lines and non small cell lung cancer cell lines to the combination of ZD2767P + CPG2 (Monks *et al*, 2002). It was found that there was a differential sensitivity between the cell lines ranging from a ZD2767P dose (in combination with CPG2) required to inhibit 50% of the cells (IC_{50}) of 0.04μM to 2.2 μM (Monks *et al*, 2002). The most sensitive cell line was LS174T. They also looked at the proportion of cells developing DNA cross-linking by comet assay, and found that significant levels of cross-linking were usually only attained at ZD2767P concentrations (+CPG2) 10-100 times higher than the IC_{50} concentrations (Monks *et al*, 2002).

This *in vitro* data would indicate that the concentration of ZD2767P required to result in potential tumour efficacy is at least 10-20 times higher than is currently being attained with the present administered dose of ZD2767P. It may be expected therefore that another 3-4 dose-doublings of ZD2767P may be required to reach potentially therapeutic ZD2767P concentrations.

ZD2767P alone has cytotoxicity, although the dose required to attain this is approximately 100 fold higher than its active drug (Blakey *et al*, 1996; Monks *et al*, 2002). If dose escalation continues with only minimal conversion to active drug, due to very low CPG2 enzyme levels both systemically and in tumour areas, then theoretically a dose may eventually be reached in which the prodrug itself has cytotoxicity. This could be tested by administering prodrug alone to patients who have toxicity with full ADEPT, as was done in the previous ADEPT trial.

In view of the pharmacokinetic data, it is clearly too early in this study to make a meaningful assessment of efficacy because an optimal prodrug dose has not yet been achieved, and there has been no attempt at repeated therapy. Stable disease has been observed in four of 13 assessable patients, and in one patient, with breast cancer known to be responsive to alkylating agents, this was accompanied

by stabilisation of tumour markers. [F-18] FDG PET analysis indicated that the patients with radiological stable disease, appeared to have metabolic tumour progression, further supporting the need to further escalate ZD2767P dose to attain therapeutic levels. No tumour biopsies have had sufficient tissue for comet analysis, and so evidence of the development of DNA cross-linking indicating prodrug activation, has not been attained yet for this trial. The opportunity for assessing this should arise as the trial continues, and more tumour biopsies are obtained.

In summary, the conditions appear now to have been established to support the continued dose doubling of ZD2767P, with the aim of attaining a dose likely to result in tumour cytotoxicity.

Repeated therapy

Three of 13 patients made measurable levels of HACPG2A during the period of the study (56 days). This contrasts with 26 of 27 patients developing antibody to CPG2 at a median of 15 days in the previous study using A5CP (Francis *et al*, 2002). The presence of the hexahistidine tag on the C terminus of CPG2 is a possible reason for this reduced immunogenicity because this may interfere with the immunogenicity of the major B cell epitope of CPG2, CM79, which involves the C terminus ([2]Sharma *et al*, 2001; Spencer *et al*, 2002).

There is also no evidence that HAMA has formed with the administration of MFECP1. The ELISA used to assess for the presence of HAMA is against A5B7 as there is no positive control for MFE-23, as no human antibodies have yet been produced against MFE-23 in the two clinical trials in which it was used (Begent *et al*, 1996; Mayer *et al*, 2001). A5B7 is also a murine antibody, and it is possible that antibodies to MFE-23 if formed would be cross reactive with A5B7. This is not entirely satisfactory, as antibodies directed specifically against epitopes unique to MFE-23 may be missed. In order to try and minimise this problem ELISAs were also performed against MFE-23, using the pre treatment serum and post –treatment serum of the same patient, in the same ELISA plate. No clear evidence of increasing optical density after treatment with MFECP1 was found in any of the 13 patients, thereby providing some reassurance that immune

complex formation between MFE-23 and antibodies in human serum was unlikely to have occurred (SK Sharma, personal communication).

The low immunogenicity of MFE23 may be due to its small molecular size, resulting in a minimal amount of murine protein exposure. The protein folding of MFECP1 may also protect MFE-23 from immune exposure. In addition the presence of glycosylations may be assisting in its escape from immune activation by initiating rapid hepatic clearance and catabolism of MFECP1 or by shielding potentially immunogenic sites.

MFECP1 therefore presents a potentially unique opportunity to be able to administer repeated therapy with ADEPT without the need for immunosuppressive treatment. This is very encouraging as preclinical studies confirm that repeated therapy with ADEPT results in improved efficacy, with no significant additional toxicity, as assessed by weight loss. The average tumour growth delays in LS174T xenograft model with single cycle of ADEPT was 9 days and with repeated cycle ADEPT, in which 3 cycles were administered 5-7 days apart, average tumour growth delays of 21days were achieved. The important advantage of the MFECP1 ADEPT system pre-clinically is its greatly reduced toxicity compared to A5CP. ADEPT with A5CP causes significant weight loss, which prevents administration of repeated therapy for a 14-day period. However, ADEPT with MFECP1 does not cause this weight loss, and allows 3 cycles of therapy to be administered within 14 days without toxicity.

The scheduling of MFECP1 would need to be considered if repeated therapy was to be undertaken. Myelosuppression with ADEPT has, in the clinical trials performed to date, occurred with a nadir at 4-6 weeks, which is later than with conventional chemotherapy. It may be therefore argued that ADEPT cycles should be 4-6 weeks apart, to ensure additive toxicity does not result. However this may limit the number of cycles that could be administered before immunogenicity results. The alternative would be to administer a dose that does not cause myelosuppression (ie: a dose below MTD) and administer ADEPT cycles more frequently, such as two or three times a week. This may allow the administration of six or more cycles before immunogenicity develops. This disadvantage of this approach may be that less prodrug is administered on each

occasion, so efficacy may be compromised, and bone marrow toxicity may accumulate and potentially be more severe. As the trial progresses and more data is collected on the tolerability of ADEPT at higher ZD2767P doses, it may become more apparent as to which strategy should be undertaken. The preclinical evidence suggests, however, that repeated therapy may be required for significant therapeutic efficacy to result from ADEPT.

Mechanistic studies

The mechanistic studies incorporated into this trial protocol have provided data necessary to make informed decisions during the trial, and will help the interpretation of the clinical data in order to rationally modify ADEPT for the future.

In particular the decisions regarded optimal timing of administration of prodrug could not have been made without the serum CPG2 enzyme measurements, or the gamma camera data. The serum CPG2 enzyme measurements were required to define a limit for when ZD2767P could be administered to avoid activation in the systemic circulation, and the gamma camera imaging was used to quantify tumour enzyme levels, and to confirm that there were no unexpected areas of uptake of MFECP1. The ZD2767P pharmacokinetic data provided guidance on how close the dose levels reached in the trial were to attaining similar pharmacokinetic profile to those associated with efficacy in preclinical models. The comet assay, as an indirect indicator of prodrug activation, has confirmed no significant DNA cross-linking in circulation lymphocytes, in agreement with the low levels of toxicity attained so far, and will be used to assess whether any evidence of prodrug activation can be seen in tumours from biopsy specimens. Immunogenicity data is a requirement for assessing the feasibility of administering ADEPT repeatedly. [F-18] FDG PET data confirms that there is not yet any evidence of metabolic response to ADEPT, further supporting the need for further dose escalation of ZD2767P.

Without the mechanistic data, dose escalation of ZD2767P would have been slowed to 30% at the first dose level. However, by being able to measure the serum CPG2 enzyme levels, and make decisions on the timing of administration

of ZD2767P based on these, dose escalation has been able to safely continue at a dose – doubling rate. This is an important concept, as without this mechanistic data, the clinical trial may have been halted due to the development of early toxicity. The ZD2767P dose level required for efficacy appears to be significantly higher than 12.42 mg/m^2, and stopping the trial at a dose around 12.42 mg/m^2 would have been premature.

A two year interval between completion of the previous ADEPT clinical trial and commencement of this one is rapid given the requirement of having to develop a new targeting system. This is an advantage of mechanistic trial design, as by allowing the identification of factors which are likely to improve the efficiency and efficacy of a system, these factors can be focussed on and modified, rather than blindly having to alter the system. This should ultimately speed up drug development times.

The mechanistic data collected in this trial has therefore provided the means to allow examination and interpretation of the hypotheses proposed at the inception of this clinical trial. The mechanistic studies have defined the conditions required to allow safe escalation of ZD2767P to dose levels beyond those attained in the previous ADEPT trial. By defining these conditions, dose escalation has been re-initiated at a dose-doubling rate, which should accelerate the speed at which potentially efficacious dose levels of ZD2767P are reached. The mechanistic studies will also be used to obtain data for directing modifications to ADEPT for the future.

4.5 Conclusion

Data is presented on thirteen patients treated with ADEPT with MFECP1 in combination with ZD2767P prodrug. MFECP1 has fulfilled its design potential of low toxicity, rapid blood clearance and low immunogenicity. There is some preliminary evidence to suggest that adequate tumour localisation is occurring, however further tumour biopsies and gamma camera data are required to define this further. Administration of ZD2767P prodrug is possible at higher doses than were achieved previously, provided that serum enzyme levels are below 0.005 U/ml. Dose escalation of ZD2767P prodrug is currently continuing with the

potential, in three more dose levels, to reach the levels of prodrug that were effective in human colon carcinoma xenografts in mice. The low immunogenicity of MFECP1 allows the possibility of repeated therapy, without the requirement for immunosuppressive therapy. These data provide the basis for continuing dose escalation of ZD2767P to define MTD, and for then proceeding as proposed to a repeated therapy component of this clinical trial, in which efficacy may be more meaningfully assessed.

4.6 Acknowledgements

As with the ADEPT study of A5CP and ZD2767P, this clinical trial involved the integration of many people, with specialist knowledge and expertise. The clinicians and scientists, who made direct contributions to the trial, are listed both in the text of this chapter and in the table below (**table 42**). As all of the data from the trial is so integral to the understanding of ADEPT it has been included in the main body of the text.

I was a co-investigator in this trial and was a major contributor to the development of the trial protocol, the formulation of hypothesis of the trial and the interpretation of the data. My responsibilities during the trial were for the recruitment, treatment, follow-up and clinical care for the patients who participated in the study. I performed the SPECT and [F-18] FDG PET analysis for all of the patients in the trial. I was also responsible for the collection and integration of the data from this trial. I was a major contributor to writing of the interim report for this trial, which was submitted to AstraZeneca.

Table 42: Contributors to ADEPT clinical trial

Contributor	Contribution
[1]Prof Richard Begent	Principal Investigator
[1] Dr Surinder Sharma	CPG2 enzyme measurements (HPLC) Immunogenicity
[2]Prof Caroline Springer [2]Jan Martin	ZD2767P pharmacokinetics
[1]Prof Janet Hartley	Comet assay
[1]Dr Alan Green	Gamma camera and [F-18] FDG PET scanning of patients and reconstruction of data
[1]Dr Kerry Chester	Manufacture and validation of MFECP1
[3]Dr Isobel Frisken	Measurement of CT scans (RECIST)
[4]Gilly Hepplewhite	Radiolabelling of MFECP1
[5]Dr David Blakey	Interpretation of data/ pharmacokinetic advice
[1]Laura Hope-Stone [1]Valerie Knell	Clinical care and management of patients Case report form data entry
[6]Clare Cruickshank [6]Adele Robbins [6]Lindsey Gumbrell	Data monitoring and data entry at CRUK Drug Development Office. Assistance in of writing of interim report.

[1] Cancer Research UK Targeting and Imaging Group, Department Oncology, Royal Free and University College Medical School, University College London, London NW3 2PF
[2] Cancer Research UK Centre for Cancer Therapeutics, Institute of Cancer Research, Sutton, Surrey, SM2 5NG
[3] Radiology Department, Royal Free Hospital NHS Trust, London NW3
4 Radiopharmacist, Royal Free Hospital NHS Trust, London NW3
[5]AstraZeneca, Alderley Park, Macclesfield, Cheshire, SK10 4TG, UK
[6]CRUK Drug Development Office

This trial was supported by Cancer Research UK, AstraZeneca, Ronald Raven Trust and The Wolfson Trust.

5 [F-18] FDG PET for response assessment

5.1 Background

The assessment of efficacy is an essential component in the development of new cancer therapeutics. The current accepted method of response assessment is by dimensional change in tumour size on conventional radiological imaging. This is discussed in detail in **Chapter 1**. This method of assessing efficacy has several limitations including not being able to define viable tumour from necrotic tissue or fibrosis, difficulty with measuring lesions that are poorly delineated, problems with representing three dimensional tumour volumes in two dimensions, insensitivity to the biological anti-tumour effect of treatments and measurement inconsistencies.

[F-18] FDG PET scans in contrast, by representing glucose metabolism, provide both a metabolic and a morphological assessment of tumours (see **Chapter 1**). Tumours are extremely heterogeneous, and this heterogeneity is well represented on [F-18] FDG PET scans, as they reflect the viable tumour mass. Necrotic centres can be seen as 'cold' areas surrounded by a 'hot' viable ring (**Figure 44**). Even within the viable tumour mass there are variations in the degree of metabolic activity.

Figure 44: [F-18] FDG PET image

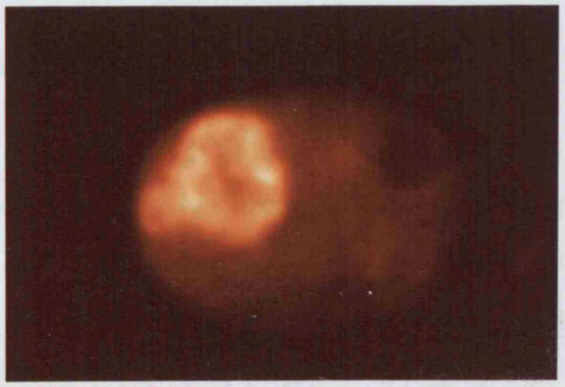

Gamma camera [F-18] FDG PET image showing a transverse slice through the liver of a patient with a large liver metastasis from colorectal cancer. The heterogeneity of [F-18] FDG uptake throughout the metastasis is apparent. There is an outer rim of increased [F-18] FDG activity and a 'cold' necrotic core.

[F-18] FDG PET scans are quantitative 3 dimensional images and therefore tumours may be assessed in terms of shape, volume and intensity. This is of particular value in the assessment of change with therapy in a heterogeneous tumour mass. In addition, as [F-18] FDG uptake represents viable tumour, a reduction in uptake may be an earlier and more sensitive method of assessing the efficacy of a treatment than radiological imaging.

5.1.1 Methods of assessing response using [F-18] FDG PET

One of the current limitations to the more widespread use of [F-18] FDG PET for response assessment is the lack of consensus on how change in tumour [F-18] FDG uptake after therapy should be measured. The current methods of assessment of response to chemotherapy with [F-18] FDG PET are visual analysis, semi-quantitative techniques and kinetic modelling.

Visual analysis

Visual analysis is a process of visually comparing the tumours seen on an [F-18] FDG PET performed pre-treatment with one performed post treatment in the same patient. Visual analysis depends on the change in tumour compared to background tissue (Hoekstra *et al*, 2000). It is a subjective method, and therefore may have problems with reproducibility, reliability, and operator experience and fatigue. It is difficult to quantify visual changes, and therefore visual analysis may be of limited use in clinical trials of efficacy.

Semi-quantitative techniques

The standardised uptake value (SUV) (also called dose uptake ratio – DUR) is a semi-quantitative technique that has been widely adopted for quantitation of intensity of [F-18] FDG uptake in tumours. It is a value derived from the mean tumour radiotracer concentration (MBq/L), which is then corrected for injected activity (MBq) and body weight (kg) (**Figure 45**).

Figure 45: SUV equation

$$SUV_{BW} = \frac{Q \times W}{Q_{inj}}$$

Abbreviations:
SUV_{BW} – standardised uptake value corrected for body weight
Q- radiotracer concentration in tissue (MBq/L)
W – body weight of patient (kg)
Q_{inj} – injected activity of [F-18] FDG (MBq)

SUV measurements are performed on scans obtained from dedicated PET scanners, and are only suitable for images that have had measured attenuation correction applied. A region of interest (ROI) is placed within an area of tumour and an SUV obtained pre and post treatment. A reduction in SUV indicates a response to treatment and an increase in SUV indicates tumour progression. SUV analysis is performed on static PET images, which are acquired after [F-18] FDG uptake into cells is complete ('plateau phase'). This is usually assumed to be at 60 minutes after injection.

SUV is a simple method that is suitable for widespread use, however, it has several limitations. A correction is applied for body weight or body surface area; however this is not particularly relevant when serial scans are performed in the same patient, as there body weight does not usually change greatly between scans (Kim *et al*, 1994; Kim and Gupta 1996). There is no correction for blood glucose level, or time to scanning, both of which may significantly affect SUV measurements (Langen *et al*, 1993; Keyes, 1995). There is no agreement on the size or placement of ROI, or whether mean or maximum counts/voxel should be recorded. Also there is no correction for partial volume effects, which occur particularly in lesions less than twice the resolution of the PET scanner (Young *et al*, 1999). In addition, SUV values account for tumour intensity alone, and do not represent any change that may occur in tumour volume or mass with therapy. Despite these limitations SUV is currently the most frequently used method of reporting response on [F-18] FDG PET scans.

Tumour to background ratios are based on a similar technique to SUV, however ROI are placed on tumour areas and on background 'normal' tissues. These are then compared between pre and post treatment scans. Attenuation correction is

not necessarily required for this type of analysis (Imran *et al*, 1998). This technique is limited by the arbitrary placement of ROI (as with SUV) and the possibility that normal tissues may change with chemotherapy, thereby influencing the tumour to background measurement (Hoekstra *et al*, 2000).

Kinetic analysis

Kinetic analysis is performed on dynamically acquired [F-18] FDG PET scans. This involves measuring the metabolic rate of glucose within tumours over time. It has been most widely used for cerebral PET, but has also been used for whole body PET ([1]Wahl *et al*, 1993; Römer *et al*, 1998; Smith *et al*, 2000; Choi *et al*, 2002; Spence *et al*, 2002). Kinetic analysis is complex and time-consuming, and is unlikely in its current form to be suitable for routine use. It also has several areas of potential inaccuracies, including not accounting for tumour heterogeneity, the assumption that intracellular dephosphorylation of [F-18] FDG is negligible and the assumption that the cellular transport and phosphorylation of [F-18] FDG is equivalent to glucose (lumped constant = 1) (Hoekstra *et al*, 2000). Also it requires arterial blood sampling, which is laborious and not practical out of the research environment.

5.1.2 Gamma camera [F-18] FDG PET

Most studies of response assessment to chemotherapy have been performed with dedicated PET systems. Gamma camera PET is a versatile and affordable alternative to dedicated PET, particularly for centres without an on-site cyclotron. Its reduced sensitivity may limit its clinical applicability; in terms of staging or lesion detection, however, it should not limit its capability to reflect change in a visible tumour mass after therapy. The potential widespread availability and multifunctionality of gamma camera PET means it could feasibly be accessible on a much greater scale than dedicated PET, and thereby applicable to both research and clinical settings.

Studies have shown that the differences in lesion detection between gamma camera PET and dedicated PET are more apparent for lesions < 1.5cm (Ak *et al*, 2001). This is particularly problematic for small lung lesions when gamma

camera PET is performed without attenuation correction. Therefore the utilisation of gamma camera [F-18] FDG PET for response assessment should be feasible, providing the lesions followed are of a size that is appropriate for the resolution of the camera.

At the time this work was undertaken there were no published studies using gamma camera [F-18] FDG PET to assess response to chemotherapy. One study has since been published using visual analysis to assess response to chemotherapy and predict prognosis in patients with aggressive non-Hodgkin's and Hodgkin's lymphoma using gamma camera [F-18] FDG PET (Kostakoglu *et al*, 2002). There remains no published quantitative method of assessing response to chemotherapy using gamma camera [F-18] FDG PET.

5.1.3 Quantitative gamma camera [F-18] FDG PET analysis to assess response to chemotherapy

It was proposed that a new method of defining tumour regions and of analysing change in these tumour regions was required to assess response to chemotherapy using gamma camera [F-18] FDG PET. It was desirable for the tumour regions obtained to represent both tumour morphology and intensity of metabolic activity, and the analysis of change to also reflect change in both of these parameters. It was hypothesised that this may represent an improvement over methods of analysis that only take into account changes in tumour [F-18] FDG intensity.

Once the methodology was developed it was proposed that it would be validated in a series of patients receiving conventional chemotherapy, and compared with other measurements of assessment of response including CT scans, tumour markers and patient outcome measures such as survival. It was also proposed to ascertain if response to chemotherapy could be predicted using this methodology after 2-4 weeks of treatment, and to ascertain if gamma camera [F-18] FDG PET scans were of value in the interpretation radiological stable disease.

5.2 Development of a novel method of assessing change in tumour [F-18] FDG uptake with therapy

5.2.1 Method

The two components required to assess response to therapy using [F-18] FDG PET were:

a) a method of delineating tumour regions which was reproducible, objective and representative of both tumour morphology and metabolic activity
b) a means of quantitating change in tumour regions between scans that takes into account changes in tumour size and changes in intensity of [F-18] FDG uptake

Automated programs were developed for both these components by Dr Alan Green, using a programming interface installed on the ADAC workstations called ProVision, which provides an interface between the nuclear medicine imaging system and the C++ programming language. The development process for the region defining program was conjoint work between myself and Dr Alan Green, in consultation with Professor Richard Begent. The concept of a histogram method of analysis was initially derived from Dr Peter Amlot, and then implemented by Dr Alan Green.

5.2.2 Results

Delineation of tumour volumes

An automated iterative adaptive threshold based region program was developed to delineate tumour volumes in an objective and reproducible way. This is a mathematically derived methodology which requires an operator to identify the tumour and then place a seed-point anywhere within the tumour area. The operator then defines a threshold value (a percentage). The tumour region will grow contiguously from the seed-point to including any voxels with counts/voxel above the current threshold. The mean is recalculated after each iteration and the

threshold percentage value reapplied. This process continues until no further voxels can be drawn. To ensure reproducibility, once the final volume is defined, the region is re-grown from the maximum count/voxel, outwards. This ensures that wherever the seed-point is placed within the tumour the same region will always be grown.

The principles of the automated region growing program are represented diagrammatically in **Figure 46**. **Figure 47** displays a tumour volume drawn by the program. The tumour regions drawn by this method are termed volumes of interest (VOI).

Figure 46: Automated region growing program

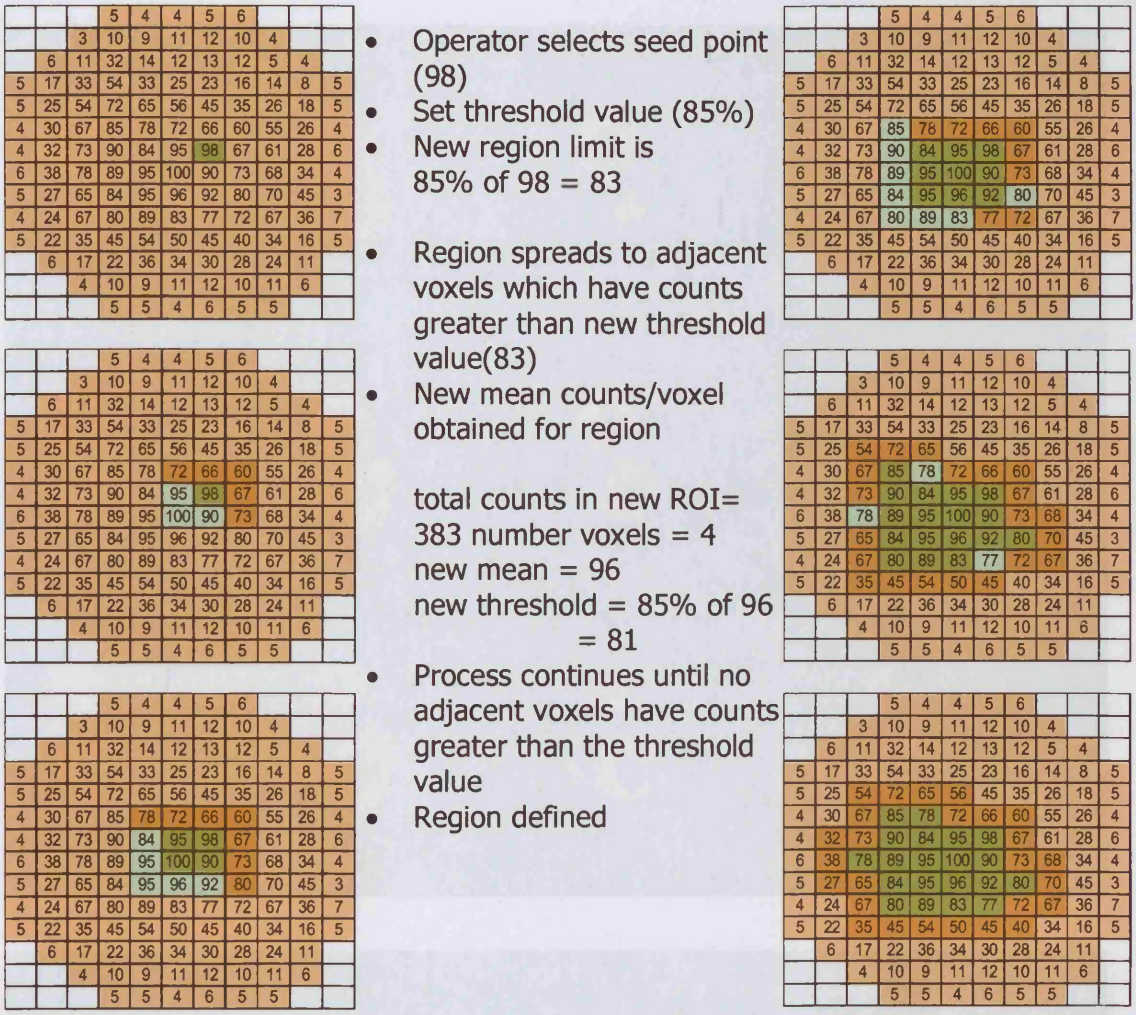

Diagrammatic representation of the automated region-growing program. Each square represents a voxel with the counts in that voxel represented numerically. The seed point is chosen within a tumour area, which is seen as a 'hotspot' on the scan. The program then generates regions by assessing contiguous voxels to ascertain if their value is above the current nominated threshold. This threshold is adaptive – it changes with each new region formed, to remain constantly 85% of the current mean of the region.
Green squares are those which are included in the tumour VOI, blue squares represent the contiguous voxels with counts above the current threshold (will be included in VOI), orange squares represent contiguous voxels with counts below the current threshold (will not be included in tumour VOI). The tan squares represent the remainder of the voxels.

Figure 47: VOI region generation

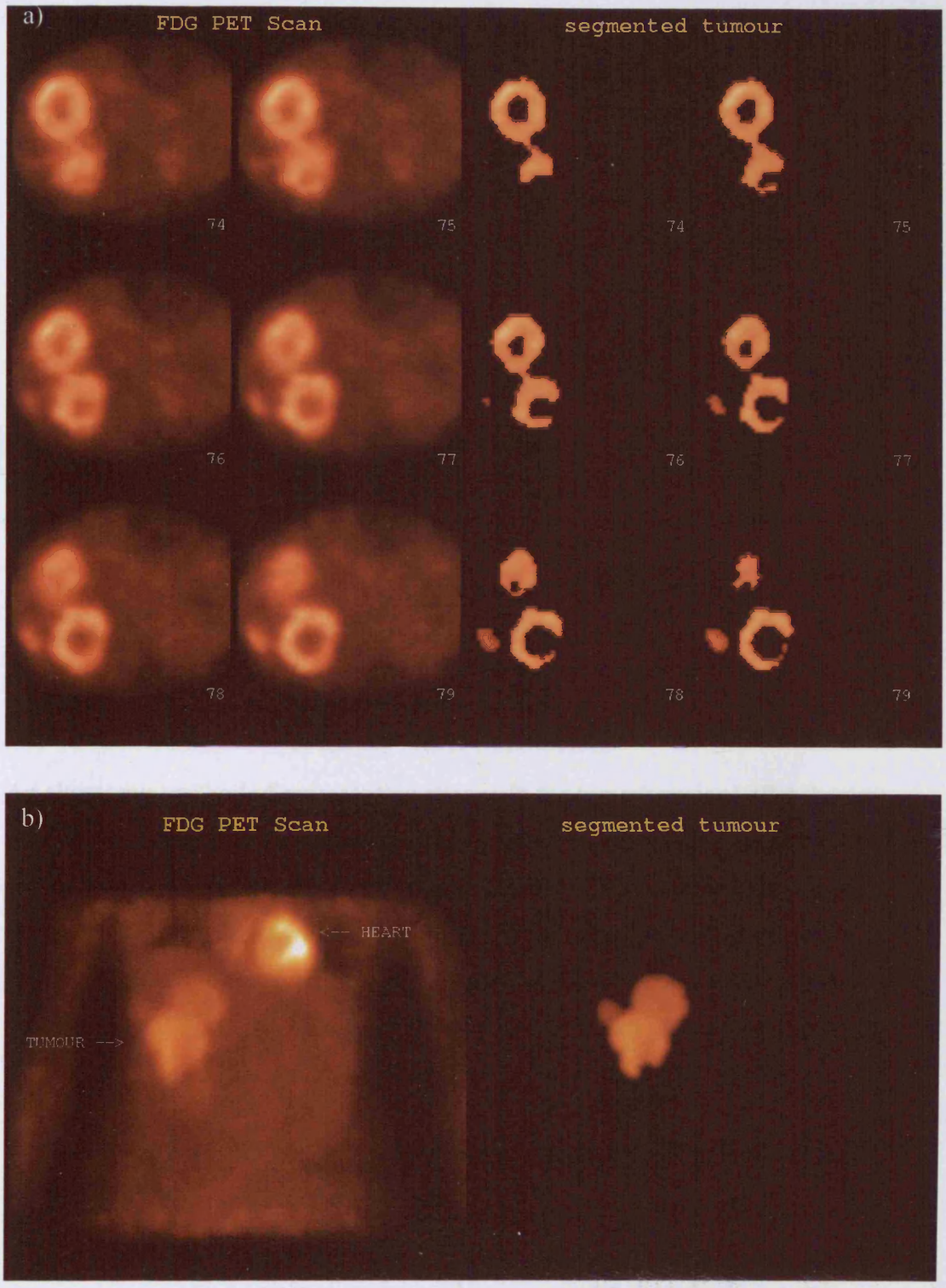

Figure 47 a) displays consecutive cross-sections of a patient with liver metastases from colorectal cancer with the VOI generated from the automated region growing program. Figure 47 b) displays a projected view from the 3-dimensional data set of the PET scan in the same patient, with the tumour VOI created from the automated region growing program.

Quantitating change in tumour uptake of [F-18] FDG

Once the tumour areas have been delineated a method is required to assess if change has occurred between scans. This should take into account changes that may occur in tumour intensity and size.

Lesion statistics can be generated from the tumour volumes derived from the automated region-growing program. The statistics generated and how they represent the tumour is shown in **table 43**.

Table 43: Lesion statistics

Lesion statistic	**Represents in tumour**
Number of voxels	Size (volume) of tumour
Mean counts/voxel	Intensity of metabolic activity
Maximum counts/voxel	Maximal intensity of metabolic activity
Total counts	Total tumour [F-18] FDG uptake

An alternative method of representing change in the tumour regions after therapy is to plot histograms of the tumours, with the x axis representing counts/voxel and the y axis the number of voxels (**figure 48**). This gives a representation of the distribution of counts within the tumour and how the counts change with therapy. Changes in the 'count density histogram' are more difficult to quantity than simple lesion statistics, but they do provide an overall view of the change in count distribution in a tumour with therapy.

Both the lesion statistics and the count density histograms will be used in the [F-18] FDG PET response assessment study.

Figure 48: Count density histogram

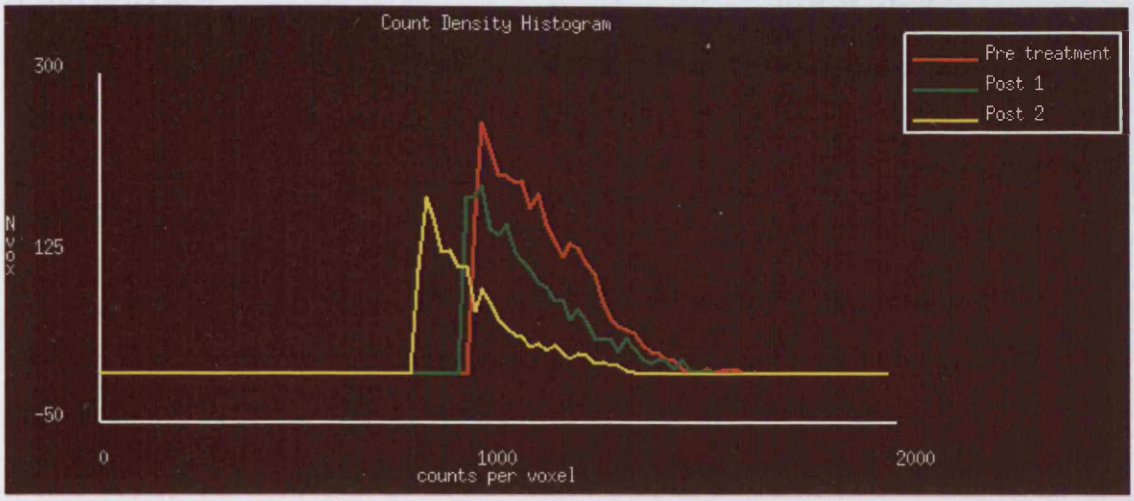

Count density histograms displaying the change in [F-18] FDG uptake in a tumour after chemotherapy. The x axis is the number of counts per voxel, and the y axis is the number of voxels with that number of counts per voxel. The red line represents the tumour histogram prior to receiving chemotherapy, the green histogram is after 3 weeks of chemotherapy, and the yellow histogram is after 12 weeks of chemotherapy. The area under the curve (AUC) represents tumour volume.
There has been a shift of the peak to the left over the 12 weeks, indicating a reduction in intensity of the tumour. There us also a reduction in the AUC of the histograms, representing a reduction in volume of the tumour after therapy. These histograms would therefore be indicative of a tumour response to chemotherapy.

5.3 [F-18] FDG PET response assessment study

5.3.1 Trial outline

Trial aims

The trial was designed to assess the measurement of response to chemotherapy using gamma camera PET, in a broad range of tumour types and over a variety of expected tumour responses, in order to validate the automated region growing program, the VOI lesion statistics and histogram methods of analysis. In addition the trial aimed to determine whether changes in tumour [F-18] FDG uptake predict response to chemotherapy after only 2-4 weeks of treatment, and to ascertain whether gamma camera [F-18] FDG PET can assist in the interpretation

of radiological 'stable disease'. The assessment of response to chemotherapy on [F-18] FDG PET was compared to conventional response criteria including radiological imaging, WHO performance status, tumour markers and patient outcome.

Patient selection

Thirty-one patients with advanced or metastatic solid tumours, who were to receive chemotherapy with standard first or second line regimens, were recruited into the study. The study had Administration of Radioactive Substances Advisory Committee (ARSAC) approval and Local Research Ethics Committee (LREC) approval. The eligibility criteria included age > 18 years, WHO performance status 0, 1 or 2, life expectancy of >9-12 weeks and serum creatinine <150 mmol/L. Patients were also required to have measurable disease by conventional radiological imaging according to the RECIST criteria. Patients were excluded if they were pregnant, had uncontrolled diabetes or any other significant co-morbidity which may prevent them from completing the study. Patients were required to sign a consent form for the study, and were made aware that the [F-18] FDG PET scan results could not be used to influence their clinician's management decisions regarding efficacy of therapy.

Treatment schedule

Patients had conventional imaging and serum tumour marker measurements performed within 2 weeks prior to commencing chemotherapy and again after 9-12 weeks of treatment (after 6 cycles of chemotherapy for 2 weekly regimens, and 3 cycles of chemotherapy for 3 or 4 weekly regimens). [F-18] FDG PET scans were performed within 2 weeks prior to commencing chemotherapy, at 2-4 weeks after the commencement of treatment (after 2 cycles of chemotherapy for 2 weekly regimens, and after 1 cycle of chemotherapy for 3 or 4 weekly regimens) and again at 9-12 weeks (after 6 cycles of chemotherapy for 2 weekly regimens, and 3 cycles of chemotherapy for 3 or 4 weekly regimens). Patients were followed until the completion of their chemotherapy. Additional radiological imaging and tumour marker measurements were recorded every 9-12 weeks for patients who proceeded with chemotherapy, until chemotherapy

was completed. The trial protocol stipulated that the [F-18] FDG PET scan results would not be used to influence management decisions.

[F-18] FDG PET scans

Patient preparation

Patients were asked to fast for 5 hours prior to injection of [F-18] FDG. [F-18] FDG was acquired from a commercial offsite cyclotron. 130MBq of [F-18] FDG was administered, and scans were commenced at 90 minutes post injection. Patients were rested after injection. Patients with pelvic tumours had 20mg intravenous frusemide administered at the time of [F-18] FDG injection. Blood sugar levels were recorded by dextrostix and by a laboratory blood sugar measurement taken from the time of [F-18] FDG injection. Patients had their height and weight measured on each visit.

Once chemotherapy had commenced, [F-18] FDG PET scans were scheduled to be performed at least 1 week after the administration of chemotherapy in order to try and prevent false positive results due to a 'tumour flare' reaction to chemotherapy.

[F-18] FDG PET Scan protocol

[F-18] FDG PET scans were performed on an ADAC Vertex Plus dual headed gamma camera 90 minutes after injection of [F-18] FDG. Transmission and emission scans were acquired. The full width half maximum (FWHM) for the camera was 4.8mm (manufacturer's specifications). Emission scans had a 50.8cm field of view and were acquired according to the manufacturers recommendations. Correction for decay was applied on the fly. Transmission scans were performed with Caesium-137 point sources. Most patients had 2 rotations performed; however some patients required 3 rotations. The set-up position of the patient was recorded and each subsequent scan utilised the same set-up procedure. Scan protocols were kept consistent in the same individual patient on subsequent scans.

Reconstruction was performed using standard ADAC iterative reconstruction protocols, with correction for attenuation and scatter. A rescaling factor was applied to the images prior to analysis. The rescaling was for injected dose of [F-18] FDG, time to scanning and frame time of the scans. The frame time was always kept constant, and so the only variables were injected dose of [F-18] FDG and time to scanning. The correction for time to scanning was for radioactive decay that occurs due to the short half life of [F-18] radioisotope. The formula for the correction factor is shown in **figure 49**.

Figure 49: Correction factor applied to [F-18] FDG PET scans prior to analysis

$$\mathbf{cf = A*B*C}$$

where

$$A = \text{activity[MBq]}\mathbf{T_0} \,/\, \text{activity[MBq]}\mathbf{T_x}$$

$$B = EXP\{(\Delta t\ (\text{mins})\mathbf{T_0} - \Delta t\ (\text{mins})\ \mathbf{T_x})*(LN(0.5))/t^1/_2 FDG\}$$

$$C = \text{frame (secs)}\mathbf{T_0} \,/\, \text{frame (secs)}\mathbf{T_x}$$

Abbreviations: cf – correction factor; activity – injected activity; T_0 – baseline scan; T_x - subsequent scan; EXP – exponential; Δt – time between injection and commencement of scan; mins – minutes; LN – log; t½[F-18] FDG – half-life of FDG (factor used was 109.2 minutes); frame – time per frame during scan; secs - seconds

A formal correction for blood glucose levels was not made, however data with blood glucose levels outside the range 4-7mmol/L were deemed unreliable. Patient weights were recorded for each scan; however no formal correction for weight was applied.

Previous validation studies of the camera demonstrated a non-linear relationship between activity (MBq) and measured counts/voxel at high singles count rates due to dead-time effect due to detector flooding (Green *et al*, 1999). All patients were therefore scanned within the quantitative range, aiming for a singles count rate of approximately 700kcps.

Scanning at 90 minutes post injection was adopted to try and ensure scanning at a time when glucose uptake in to tumours was complete (plateau phase). Scanning

at later time points than this was impractical, as [F-18] FDG was obtained from an off-site supplier, and was not received until the afternoon.

Patient's [F-18] FDG PET scan conditions including the injected activity, time to scanning, patient set-up position, scan protocols and image reconstruction methods were all kept as consistent as possible in serial scans, in order that these factors would not influence tumour [F-18] FDG uptake results.

5.3.2 Methods

Radiological assessment

Radiological response assessment was performed according to the RECIST criteria (Therasse *et al*, 2000). A Radiologist, who was unaware of the patient's clinical course, performed the analysis.

Tumour markers

Relevant tumour markers (CEA, CA19-9, CA15-3 or AFP) were measured prior to the commencement of chemotherapy, and repeated every 9-12 weeks whilst chemotherapy continued.

[F-18] FDG PET analysis

Automated region generation / VOI generation

Tumour volumes were defined on the corrected images, using the automated region-growing program discussed above. The threshold used was 85% at all times. Each individual tumour site had a seed point placed in it, to draw each individual tumour volume. The tumour volumes (at all sites) were then all added together to obtain final VOI.

A modification of this method, termed 'VOI subtraction', was also used. This involved defining the initial VOI as described above, and then subtracting this tumour volume from the scan, followed by reapplying the automated region growing program to the new image. Subtraction was applied until all tumour areas were defined. The final region obtained was termed 'VOI subtraction'.

Normal tissue volumes were also defined, by placing a seed point in normal liver, lung or chest wall, and the automated region growing program generating regions based on +/- 20% threshold of the current mean.

Lesion statistics

Lesion statistics were calculated from the final VOI for each time-point. The lesion statistics used were tumour volume (total number of voxels), mean counts/voxel, maximum counts/voxel and total counts. The change in each lesion statistic was then displayed as a percentage change compared to baseline. If a tumour's [F-18] FDG uptake reduced the value was <100% and if it increased it was >100%.

Histogram analysis

Tumour volumes of interest were defined as above and then displayed as count density histograms, with the counts per voxel on the x-axis, and total number of voxels on the y-axis. The histograms were displayed before and after chemotherapy to assess change.

Normal tissue volumes of interest were also plotted on the count density histogram to assess the degree of variation in background tissues between scans.

Overall Survival

The overall survival of patients was recorded, and the survival time in days calculated from the first day of commencing chemotherapy. Kaplan Meier analysis and log rank analysis were performed on this data using Prism software.

5.3.3 Results

Patient demographics

Thirty-one patients were recruited into the study over a two-year period commencing in July 2000. The demographics of the patients are listed in **Table 44**.

Table 44: Patient demographics

Pt No.	Age (yrs)	Gender (M/F)	Primary tumour	Site of metastasis	1st or 2nd line chemo	Chemo type	Schedule (weekly)
#1	60	M	Oesophageal	Local recurrence Subcut nodules	1st	Taxol	3 wkly
#2	57	M	Colorectal	Liver	1st	Irino/ 5FU	2 wkly
#3	55	M	Colorectal	Liver	1st	Irino/ 5FU	2 wkly
#4	56	F	Colorectal	Liver	1st	Irino/ 5FU	2 wkly
#5	52	M	Pancreatic	Local recurrence	1st	Gem	4 wkly
#6*	69	M	Pancreatic	Local recurrence	1st	Gem	4 wkly
#7	70	M	Colorectal	Liver, presacral	1st	5FU/ oxali	2 wkly
#8	63	M	Colorectal	Liver	1st	Irino/ 5FU	2 wkly
#9	62	M	HCC	Lung, liver	1st	Cis/ 5FU	2 wkly
#10	53	F	Colorectal	Liver	1st	Irino/ 5FU	2 wkly
#11	49	M	Oesophageal	Lung, bone, adrenal	2nd	ELF	4 wkly
#12	56	M	Colorectal	Lung, liver	1st	5FU/ oxali	2 wkly
#13	60	M	Oesophageal	Local recurrence	1st	ECF	3 wkly
#14	63	M	Colorectal	Lung, liver	1st	5FU (MdG)	2 wkly
#15	73	M	Colorectal	Liver	1st	5FU (MdG)	2 wkly
#16	58	F	Colorectal	Liver	1st	5FU/ oxali	2 wkly
#17	37	F	Breast	Liver	2nd	Taxotere	3 wkly
#18	45	M	HCC	Lung	1st	5FU/ cis	2 wkly
#19	46	F	HCC	Liver	1st	5FU/ cis	2 wkly
#20	68	M	Colorectal	Lung	1st	5FU (MdG)	2 wkly
#21	60	M	Colorectal	Lung, liver	2nd	Irino/ 5FU	2 wkly
#22	58	F	Colorectal	Liver	1st	5FU (MdG)	2 wkly
#23	67	F	Breast	Liver, bone	1st	ECF	3 wkly
#24	45	F	Unknown	Lung, liver, bone, paraortic LN	2nd	Irino/ 5FU	2 wkly
#25*	34	F	Breast	Lung, bone, brain	2nd	CMF	3 wkly
#26	43	F	Lung	Lung, mediastinal LN	1st	Gem/carbo	3 wkly
#27	77	F	Colorectal	Liver	1st	capecitabine	3 wkly
#28	71	F	Colorectal	Liver, lung	2nd	Irino/ 5FU	2 wkly
#29*	52	M	Pancreatic	Liver	1st	Gem	4 wkly
#30	74	M	Colorectal	Liver, lung	2nd	Oxali/ 5FU	2 wkly
#31	65	F	Breast	Lung, liver, ovary, ascites, paraumbiliacal	2nd	Paclitaxel	3 wkly

Abbreviations: M-male, F-female; chemo – chemotherapy; HCC – hepatocellular carcinoma; LN – lymph node; irino – irnotecan; 5FU - 5 fluorouracil; MdG – modified de Gramont; gem – gemcitabine; oxali – oxaliplatin; CMF – cyclophosphamide, methotrexate and fluorouracil; carbo – carboplatin; cis – cisplatin; ECF – epirubicin, cisplatin and fluorouracil; ELF – epirubicin, leucovorin and fluorouracil

** diabetic*

There were eighteen males and thirteen females. The median age was 58 years (range 34-77 years). Three patients were diabetic. The patient group was derived from a range of primary solid tumour types; sixteen patients had colorectal carcinoma, three patients had oesophageal carcinoma, four patents had breast cancer, three patients had pancreatic carcinoma, three patients had hepatocellular carcinoma, one patient had non-small cell lung cancer and 1 patient had an unknown primary (suspected oesophageal).

Twenty-eight patients had metastatic disease, and three patients had advanced local disease or local recurrence, unsuitable for curative resection. Twenty-three patients were having first-line chemotherapy, and eight patients were having second-line chemotherapy. Multiple chemotherapy regimens were used, with nineteen patients having 2 weekly treatment and twelve patients having 3 or 4 weekly cycles.

Radiological assessment

The response to chemotherapy according to radiological assessment by RECIST criteria is listed in **Table 45**.

Table 45: Radiological response to chemotherapy (RECIST)

RECIST response	9-12 week assessment		18-24 week assessment	
	Total	Pt No.	Total	Pt No.
CR	0		0	
PR	7	#8, #15, #16, #17, #21, #22, #26	6	#4, #8, #16, #17, #21, #31
SD	15	#2, #3, #4, #5†, #6, #9, #10, #12, #14, #19, #20, #23, #25, #27, #31	4	#6, #14, #25, #27
PD	5	#11, #24, #28, #29*, #30*	0	
NA	4	#1, #7, #13, #18	21	#1-3, #5, #7, #9-13, #15, #18-20, #22-24, #26, #28-30

Abbreviations: CR – complete response; PR –partial response; SD- stable disease; PD- progressive disease; NA – not assessable
† measured by ultrasound
** progression due to appearance of new lesions*

Twenty-seven patients had a radiological response assessment performed at 9-12 weeks. In all patients this was performed using spiral CT, except for patient #5, who was assessed by ultrasound. There were no complete responses seen, seven patients attained a partial response, fifteen patients had stable disease, and five patients fulfilled the RECIST criteria for disease progression. Two of the patients who had disease progression by RECIST criteria developed new lesions on CT, without significant increase in dimensional size of lesions. Four patients did not have a 9-12 week response assessment performed; patients #1 and #18 died prior to having a response assessment performed, patient #13 had radiotherapy performed and was taken off study and patient #7 was found to have non-measurable disease on MRI of pelvis and no formal response assessment by radiological criteria could be performed.

Ten patients went on to have an 18-24 week radiological response assessment. Six patients attained a partial response and four patients had stable disease.

Tumour markers

Table 46 displays the tumour marker results for all patients, and compares them to the RECIST radiological assessment.

Table 46: Tumour markers

Pt ID	RECIST (9-12 wks)	RECIST (18-24 wks)	CEA (mmol/L)					CA19-9 (Units/L)				
			Pre	9-12 wks	(% of pre)	18-24 wks	(% of pre)	Pre	9-12 wks	(% of pre)	18-24 wks	(% of pre)
#1	NA	NA	No assessable tumour markers									
#2	SD	NA	242	130	(54%)	86	(36%)	1152	613	(53%)	294	(26%)
#3	SD	NA	No assessable tumour markers									
#4	SD	PR	18006	8864	(49%)	9385	(52%)	1572	937	(60%)	1194	(76%)
#5	SD	NA	No assessable tumour markers									
#6	SD	SD	No assessable tumour markers									
#7	NM	NM	NA	NA		NA		45	4	(9%)	NA	
#8	PR	PR	651	12	(2%)	16	(2%)	5624	127	(2%)	106	(2%)
#9	SD	NA	No assessable tumour markers									
#10	SD	NA	846	2223	(263%)	NA		2578	4789	(186%)	NA	
#11	PD	NA	252	834	(331%)	NA		NA	NA		NA	
#12	SD	NA	81	320	(395%)	NA		NA	NA		NA	
#13	NA	NA	No assessable tumour markers									
#14	SD	SD	745	422	(57%)	504	(68%)	379	372	(98%)	620	(164%)
#15	PR	NA	463	16.3	(4%)	NA		NA	NA		NA	
#16	PR	PR	293	28	(10%)	11	(4%)	272	123	(45%)	85	(31%)
#17	PR	PR	No assessable tumour markers									
#18	NA	NA	No assessable tumour markers									
#19	SD	NA	NA	NA		NA		729	332	(46%)	NA	
#20	SD	NA	No assessable tumour markers									
#21	PR	PR	No assessable tumour markers									
#22	PR	NA	277	128	(46%)	NA		NA	NA		NA	
#23	SD	NA	No assessable tumour markers									
#24	PD	NA	63	360.9	(573%)	NA		NA	NA		NA	
#25	SD	SD	No assessable tumour markers									
#26	PR	NA	No assessable tumour markers									
#27	SD	SD	302	167.4	(55%)	61	(20%)	NA	NA		NA	
#28	PD	NA	30.4	146.1	(481%)	NA		NA	NA		NA	
#29	PD	NA	No assessable tumour markers									
#30	PD	NA	773	974	(126%)	NA		678	933	(138%)	NA	
#31	SD	PR	No assessable tumour markers									

Abbreviations: CR – complete response; PR –partial response; SD- stable disease; PD- progressive disease; NA – not applicable

Fourteen patients had raised CEA tumour markers, which were appropriate for repeated assessment at 9-12 weeks. Of these, nine patients had a fall in CEA tumour marker (median 46% of pre-treatment value; range 2%-57%). Five patients had an increase in CEA tumour markers at 9-12 weeks (median 331% of pre treatment value; range 126%-481%).

Nine patients had raised CA19-9 tumour markers suitable for repeat assessment at 9-12 weeks. Of these, seven patients had a reduction in CA19-9 (median 46% of pre treatment value; range 2%-98%), and two patients had an increase in CA19-9 (median 162% of pre treatment value; range 138%-186%).

[F-18] FDG PET analysis

[F-18] FDG PET scans were performed on all patients, however for a variety of reasons, not all patients completed the trial protocol. **Table 47** summarises the number of scans performed on each patient.

Table 47: [F-18] FDG PET scans

Number of [F-18] FDG PET scans completed	Total number patients	Pt No.
1	6	#1, #13, #18, #20, #29, #31
2	3	#5, #6, #30
3	22	#2, #3, #4, #7, #8, #9, #10, #11, #12,#14,#15, #16, #17, #19, #21, #22, #23, #24, #25, #26, #27, #28

Twenty-two patients completed all three [F-18] FDG PET scans as per the trial protocol. Three patients completed two of three scans. In two of these patients the tumour could not be seen on [F-18] FDG PET scans, and so the third scan was not performed (#5, #6). In one patient the camera failed for the third PET scan (#30). In six patients only one [F-18] FDG PET scan was performed. Two of these patients deteriorated and died prior to completing the study (#1, #18). The camera failed for one patient (#29), the [F-18] FDG injection was injected into the subcutaneous tissues for one patient, leading to significant artefacts (#20), and one patient did not fast for the PET scan, and the scan was not reliable (#13). One patient could not tolerate the scan, and the scan was aborted (#31).

Four patients had [F-18] FDG PET scans performed, in which no tumour areas could be seen. These were patients #3, #5, #6 and #9. Patient #3 had a body weight of 130-138kg, and due to his body habitus the scan quality was extremely poor. Tumour areas could not be clearly defined. Patients #5 and #6 had pancreatic cancer, with locally advanced disease. Patient #9 had hepatocellular carcinoma with very small volume liver metastasis. It is likely that the gamma camera PET was of insufficient sensitivity to detect the lesions in these three patients.

Table 48 summarises the patient group according to tumour type, completion of a pre-treatment PET scan and at least one follow-up scans and subsequent tumour detection on [F-18] FDG PET.

Table 48: [F-18] FDG PET scans according to tumour type

Tumour type	**Number of patients**	**Number of patients with pre and post PET scans performed**	**Number of patients with tumour visible on PET scan**
Colorectal	16	15	14
Oesophageal	3	1	1
Pancreatic	3	2	0
HCC	3	2	1
Lung	1	1	1
Breast	4	3	3
Unknown primary	1	1	1
Total	**31**	**25**	**21**

Abbreviations: HCC – hepatocellular carcinoma

In total, therefore, twenty-one of the thirty-one patients had [F-18] FDG PET scans that were suitable for analysis to compare different forms of response assessment. Patient #7 however, was found not to have measurable disease by conventional response criteria, and therefore could not be included in the comparative analysis. Analysis is therefore reported on twenty patients who had [F-18] FDG PET scans at 2-4 weeks, nineteen of whom had [F-18] FDG PET scans also at 9-12 weeks.

Automated region growing program/ VOI generation

It was possible to generate tumour volumes for analysis from eighteen of the twenty patients (90%) with a baseline and at least one follow-up [F-18] FDG PET scan. For two patients (#15 and #25) the differentiation between tumour and surrounding normal tissue was not large enough to allow the mathematical generation of a tumour area using the automated region growing program. Therefore these patients could not be analysed by this method.

There were two patients in whom the VOI subtraction program generated tumour volumes which were visually much more representative of actual tumour load than without subtraction. These were patients #4 and #23. In particular it was apparent that without the subtraction technique large volumes of tumour had been missed on either the baseline or follow-up scan (**figure 50**).

Figure 50: Example of the VOI subtraction method compared to VOI

a)

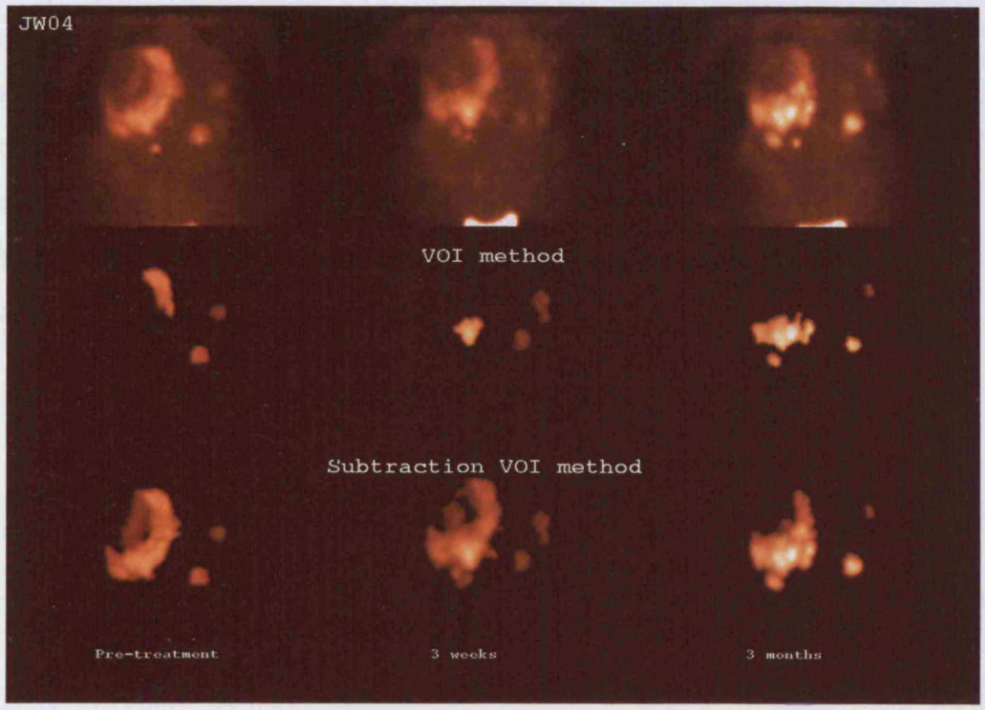

b)

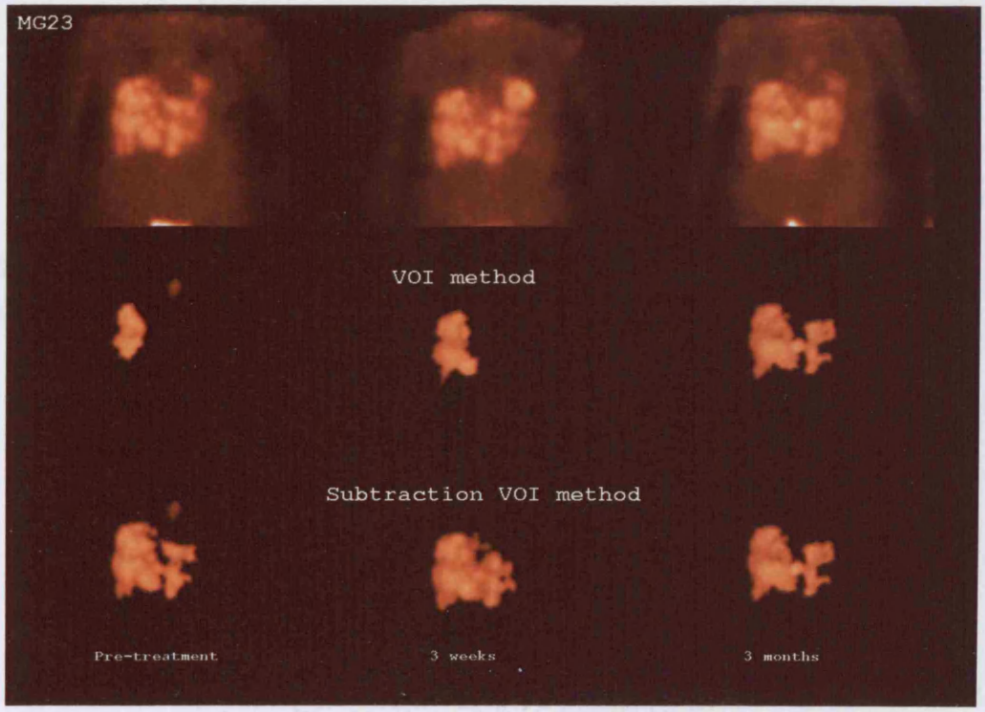

*Figure 50 displays the three PET scans on **a)** patient #4 and **b)** patient #23 with the tumour regions generated by both the VOI program and the VOI subtraction program. For both patients the VOI subtraction program provides a better representation of actual tumour mass than with the VOI program.*

Lesion statistics

Table 49 and 50 outlines the results of the analysis of [F-18] FDG PET scans pre-treatment and at 2-4 weeks and 9-12 weeks post chemotherapy, using the lesion statistics from the tumour VOI. The results have been expressed as a percentage change compared to baseline. The changes in [F-18] FDG uptake have been compared to current standard response assessment of radiological imaging, RECIST criteria, and relevant tumour markers, both taken at 9-12 weeks after commencement of chemotherapy.

Table 49: [F-18] FDG PET analysis (2-4 weeks)

a)

	9-12 weeks			[F-18] FDG PET (2-4 weeks)							
Pt No.	RECIST	(%)	Tumour markers	VOI				VOI subtraction			
				Total cts	Mean	Vol	Max	Total cts	Mean	Vol	Max
#8	PR	29%	2%	11%	97%	11%	84%	19%	74%	26%	84%
#15	PR	58%	4%	X	X	X	X	X	X	X	X
#16	PR	47%	10%	36%	58%	62%	51%	25%	63%	40%	51%
#17	PR	60%	NA	76%	73%	104%	68%	50%	95%	53%	68%
#21	PR	49%	NA	0%	0%	0%	0%	0%	0%	0%	0%
#22	PR	65%	46%	83%	81%	102%	76%	78%	82%	96%	76%
#26	PR	7%	NA	14%	46%	30%	35%	14%	46%	30%	35%
median		**49%**	**7%**	**25%**	**66%**	**46%**	**60%**	**22%**	**69%**	**35%**	**60%**

b)

	9-12 weeks			[F-18] FDG PET (2-4 weeks)							
Pt No.	RECIST	(%)	Tumour markers	VOI				VOI subtraction			
				Total cts	Mean	Vol	Max	Total cts	Mean	Vol	Max
#11	PD	214%	331%	229%	96%	240%	123%	167%	105%	160%	123%
#24	PD	123%	573%	114%	73%	155%	92%	74%	76%	104%	92%
#28	PD	141%	481%	144%	73%	196%	60%	80%	80%	99%	60%
#30	PD	106%	126%	79%	78%	101%	80%	81%	79%	103%	80%
median		**132%**	**406%**	**129%**	**76%**	**176%**	**86%**	**81%**	**80%**	**104%**	**86%**

c)

	9-12 weeks			[F-18] FDG PET (2-4 weeks)							
Pt No.	RECIST	(%)	Tumour markers	VOI				VOI subtraction			
				Total cts	Mean	Vol	Max	Total cts	Mean	Vol	Max
#2	SD	76%	54%	67%	97%	69%	96%	30%	119%	25%	96%
#4	SD	76%	49%	48%	81%	60%	101%	81%	79%	102%	101%
#10	SD	103%	263%	104%	102%	102%	71%	110%	94%	117%	71%
#12	SD	116%	395%	97%	77%	127%	82%	93%	79%	119%	82%
#14	SD	100%	57%	97%	108%	90%	110%	57%	122%	46%	110%
#19	SD	88%	46%	0%	0%	0%	0%	0%	0%	0%	0%
#23	SD	90%	NA	169%	89%	190%	92%	114%	90%	126%	92%
#25	SD	96%	NA	X	X	X	X	X	X	X	X
#27	SD	94%	55%	69%	64%	107%	68%	54%	74%	72%	68%
median		**94%**	**55%**	**83%**	**85%**	**96%**	**87%**	**69%**	**85%**	**87%**	**87%**

[F-18] FDG PET scans at 2-4 weeks after commencement of chemotherapy analysed by VOI analysis and compared to standard radiological imaging (RECIST) and tumour markers. All values are expressed a % compared to baseline – so a reduction in size/ volume or ratio is expressed as a value < 100% and in increase as > 100%.

Abbreviations: PR – partial response; PD – progressive disease; SD – stable disease; Pt No – patient number; VOI – volume of interest; Total cts – total counts; Vol – volume; NA – not applicable; X – not able to be analysed by this technique

Table 50: [F-18] FDG PET analysis (9-12 weeks)

a)

Pt No.	9-12 weeks RECIST	(%)	Tumour markers	[F-18] FDG PET (9-12 weeks) VOI Total cts	Mean	Vol	Max	VOI subtraction Total cts	Mean	Vol	Max
#8	PR	29%	2%	2%	47%	4%	42%	1%	57%	1%	42%
#15	PR	58%	4%	X	X	X	X	X	X	X	X
#16	PR	47%	10%	0%	0%	0%	0%	0%	0%	0%	0%
#17	PR	60%	NA	8%	75%	11%	56%	9%	74%	12%	56%
#21	PR	49%	NA	0%	0%	0%	0%	0%	0%	0%	0%
#22	PR	65%	46%	38%	60%	64%	58%	23%	69%	33%	58%
#26	PR	7%	NA	17%	42%	41%	32%	17%	42%	41%	32%
median		**49%**	**7%**	**5%**	**45%**	**8%**	**37%**	**5%**	**50%**	**7%**	**37%**

b)

Pt No.	9-12 weeks RECIST	(%)	Tumour markers	[F-18] FDG PET (9-12 weeks) VOI Total cts	Mean	Vol	Max	VOI subtraction Total cts	Mean	Vol	Max
#11	PD	214%	331%	360%	120%	301%	147%	321%	139%	230%	147%
#24	PD	123%	573%	407%	107%	380%	117%	1189%	80%	1478%	117%
#28	PD	141%	481%	330%	168%	197%	151%	283%	162%	174%	151%
#30	PD	106%	126%	ND	ND	ND	ND	ND	ND	ND	ND
median		**132%**	**406%**	**360%**	**120%**	**301%**	**147%**	**321%**	**139%**	**230%**	**147%**

c)

Pt No.	9-12 weeks RECIST	(%)	Tumour markers	[F-18] FDG PET (9-12 weeks) VOI Total cts	Mean	Vol	Max	VOI subtraction Total cts	Mean	Vol	Max
#2	SD	76%	54%	43%	85%	50%	81%	19%	105%	18%	81%
#4	SD	76%	49%	150%	136%	110%	128%	90%	110%	82%	128%
#10	SD	103%	263%	83%	89%	94%	56%	167%	69%	243%	56%
#12	SD	116%	395%	124%	84%	147%	94%	138%	83%	166%	94%
#14	SD	100%	57%	64%	99%	64%	98%	65%	97%	67%	98%
#19	SD	88%	46%	0%	0%	0%	0%	0%	0%	0%	0%
#23	SD	90%	NA	258%	79%	326%	76%	73%	97%	75%	76%
#25	SD	96%	NA	X	X	X	X	X	X	X	X
#27	SD	94%	55%	0%	0%	0%	0%	0%	0%	0%	0%
median		**94%**	**55%**	**74%**	**85%**	**79%**	**79%**	**69%**	**90%**	**71%**	**69%**

[F-18] FDG PET scans at 9-12 weeks after commencement of chemotherapy analysed by semi-quantitative methods and compared to standard radiological imaging (RECIST) and tumour markers. All values are expressed a % compared to baseline – so a reduction in size/ volume or ratio is expressed as a value < 100% and in increase as > 100%.

Abbreviations: PR – partial response; PD – progressive disease; SD – stable disease; Pt No – patient number; VOI – volume of interest; Total cts – total counts; Vol – volume; NA – not applicable; ND – not done; X – not able to be analysed by this technique

Comparison of lesion statistics

Table 51 displays the Pearson correlation coefficients comparing % change in VOI statistics, and VOI subtraction statistics to the % change in tumour lesion size on CT scans according to RECIST criteria.

Table 51: Correlation of semi-quantitative analysis methods with CT scan dimensional measurements

	Pearson correlation coefficient	
	2-4 week PET scan	**9-12 week PET scan**
VOI total counts	0.83	0.75
VOI mean	0.32	0.57
VOI volume	0.80	0.67
VOI max	0.49	0.67
VOIsub total counts	0.78	0.47
VOIsub mean	0.37	0.59
VOIsub volume	0.72	0.36
VOIsub max	0.49	0.67

Abbreviations VOI- volume of interest; VOIsub – VOI subtraction

At both the 2-4 week and the 3 month [F-18] FDG PET scan the semi-quantitative method with the best correlation with CT scans was the total counts statistic of the VOI method.

'Total counts' is a value that takes into account the total metabolic activity of the tumour region generated by the automated region growing program. At 2-4 weeks the six patients who had a partial response to chemotherapy by conventional assessment all had at least a 15% reduction in total counts of their tumour VOI. The median value was 25% of baseline and the smallest reduction was to 83% of baseline (range 0-83%). At the 9-12 weeks the reduction in total counts was to a median of 5% compared to baseline (range 0-38%).

There were four patients who had progressive disease on their 9-12 week CT scan. Three of these patients had a corresponding increase in tumour [F-18] FDG uptake at 2-4 weeks, as assessed by total counts (pt #30 did not have an increase in [F-18] FDG uptake, however this patient was deemed to have progressive disease on CT scans by the appearance of new lesions). The median increase was to 129% of baseline (range 79-229%). At the 9-12 week PET scan the total

counts increased in the 3 patients who had disease progression on CT scan (pt #30 did not have a 9-12 week [F-18] FDG PET scan). The median value at 9-12 weeks was 360% (range 330-407%).

In contrast, at 2-4 weeks in the six patients who obtained a partial response on CT scan, all had a fall in mean counts/voxel and maximum counts/voxel, however the tumour volume fell in four patients and increased slightly in two patients (102% and 104%). By the 9-12 week [F-18] FDG PET scan all lesion statistics had reduced in the six responding patients. In the four patients with progressive disease on CT scan, the lesion statistics on the 2-4 weeks [F-18] FDG PET showed that the tumour volumes increased in all 4 patients (although in pt #30 this was only to 101%) but the mean counts/ voxel fell in all 4 patients and the maximum counts per pixel fell in 3 patients. This would be converse to that which would be expected for a progression of disease, and indicates that disease progression may not necessarily be associated with an increase in intensity of tumour [F-18] FDG uptake. By 9-12 weeks again all of the lesion statistics reflected disease progression in the three assessable patients.

VOI or VOI subtraction

The % change in total counts for VOI subtraction compared to VOI were in most cases similar, however at 2-4 weeks in the four patients who had progressive disease on CT scans, the value was only raised in one patient (pt # 11 167%), and was reduced in the other 3 patients (pt # 24 74%, pt #28 80% and pt #30 81%).

Of the two patients in whom the VOI subtraction method produced more representative tumour volumes than VOI alone, the values obtained for change in total counts between baseline and the 2-4 week and 3 month [F-18] FDG PET scan were altered by using the VOI subtraction method. For patient #4 at 2-4 weeks the % change in total counts compared to baseline was 48% using VOI and 81% using VOI subtraction. At 9-12 weeks it was 150% using VOI and 90% using VOI subtraction. Patient #23 had a % change in total counts compared to baseline of 168% at 2-4 weeks with VOI and 114% with VOIsub. At 9-12 weeks this was 258% with VOI and 73% with VOIsub. As both patients had radiological stable disease at 9-12 weeks it is appears that the VOI sub values

were more representative than the VOI values, when compared to the CT findings.

Histogram analysis

Histogram analysis was applied to all the tumour volumes and representative normal regions including chest wall, liver and lung, derived by the VOI and VOI subtraction methods. No satisfactory method of exporting the histograms into a program that could analyse and interpret quantitatively the change in histograms with chemotherapy was developed. Consequently the histograms were just used as a visual representation of change in tumour with therapy, and as a method of confirming that the background tissues had not changed significantly after chemotherapy. **Figure 51** shows the count density histogram of the tumour of a patient who appeared to have a response to chemotherapy on [F-18] FDG PET. **Figure 52** shows the count density histogram of a patient who appeared to progress on chemotherapy. Also displayed are the corresponding histograms of normal tissues on both patients.

The normal tissues were found to overlap on histogram analysis between corrected scans on all patients used in the VOI analysis indicating that, within the relatively crude limits of this method, normal tissues remain stable in individual patients after chemotherapy. This is important as if the normal tissues were found not to be consistent the changes detected in tumour may be unreliable.

Figure 51: Histogram analysis – responding patient

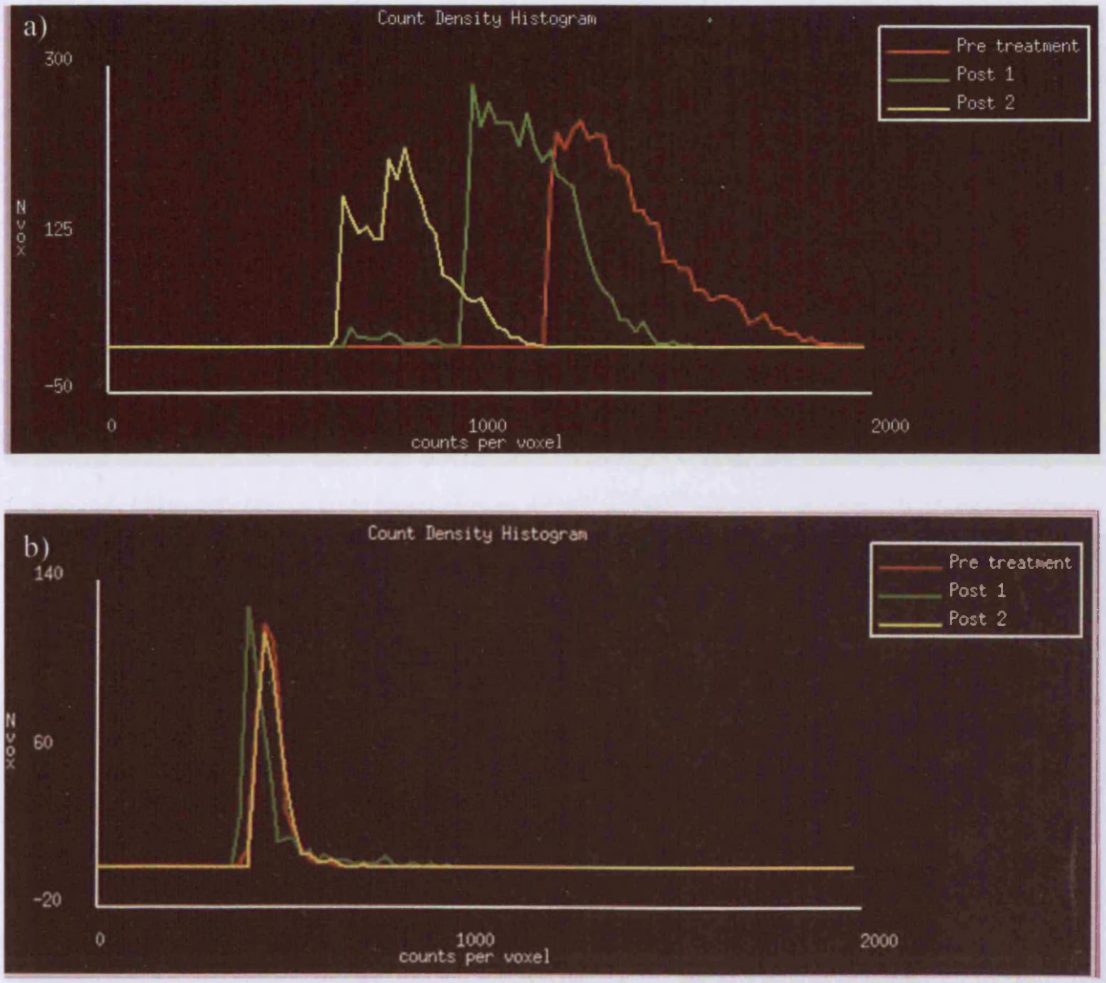

Figure 51 a) is the count density histogram of the tumour from patient #22, who attained a partial response on CT scan at 9-12 weeks. The tumour VOI represented was generated by the automated region growing program. The red line represents the histogram of the tumour pre treatment, the green line is at 2-4 weeks, and the yellow line is at 9-12 weeks. There has been a shift of the curves to the left, indicating a shift to lower intensity, and there has been a reduction in area of the curves, indicating a reduction in size of the tumour. These finding would be consistent with a response to therapy.
Figure 51 b) is the count density histogram of areas of normal liver in the same patient. The histograms overlap, indicating that the normal tissues have remained largely unchanged with treatment.

Figure 52: Histogram analysis – progressing patient

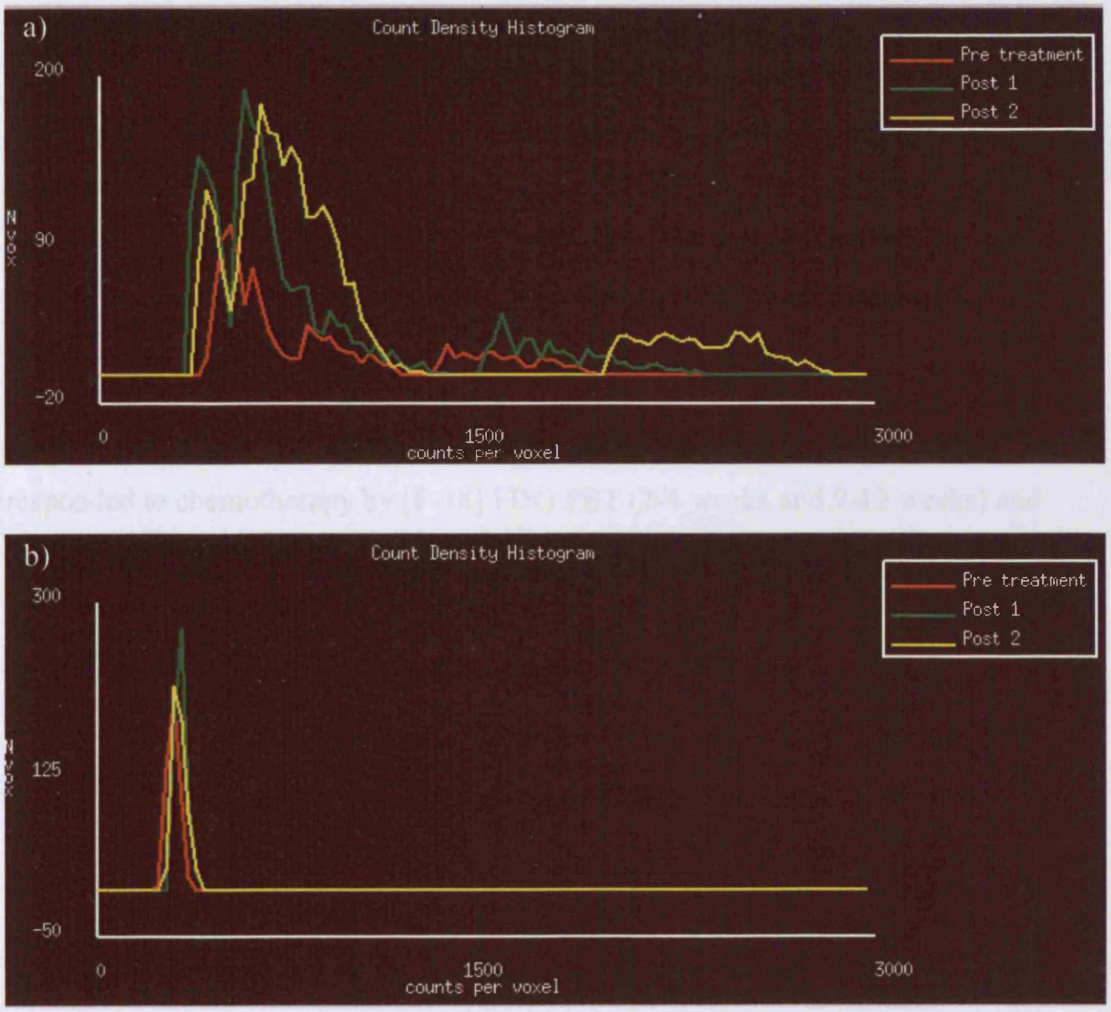

Figure 52 a) is the count density histogram of the tumour from patient #11, who developed progressive disease on CT scan at 9-12 weeks. The tumour VOI represented was generated by the automated region growing program. The red line represents the histogram of the tumour pre treatment, the green line is at 2-4 weeks, and the yellow line is at 9-12 weeks. There has been an increase in area of the curves and a small shift of the curves to the right. These finding would support the finding of progressive disease after therapy.
Figure 52 b) is the count density histogram of areas of normal liver in the same patient. The histograms overlap, indicating that the normal tissues have remained largely unchanged with treatment

Overall survival

The overall survival of patients was plotted according to their response on [F-18] FDG PET scan or CT scan. This was performed using Kaplan Meier survival curves and log rank analysis. The results are shown in **Figure 53.** A partial response on [F-18] FDG PET was defined as <85% of baseline using the total counts statistic of the VOI method, 85-110% was stable disease and >110% was progressive disease. The significance of any observed difference between the curves is expressed on the graphs.

There was a statistically significant improvement in survival for patients who responded to chemotherapy by [F-18] FDG PET (2-4 weeks and 9-12 weeks) and by CT scan (9-12 weeks).

Figure 53: Survival of patients in [F-18] FDG PET study

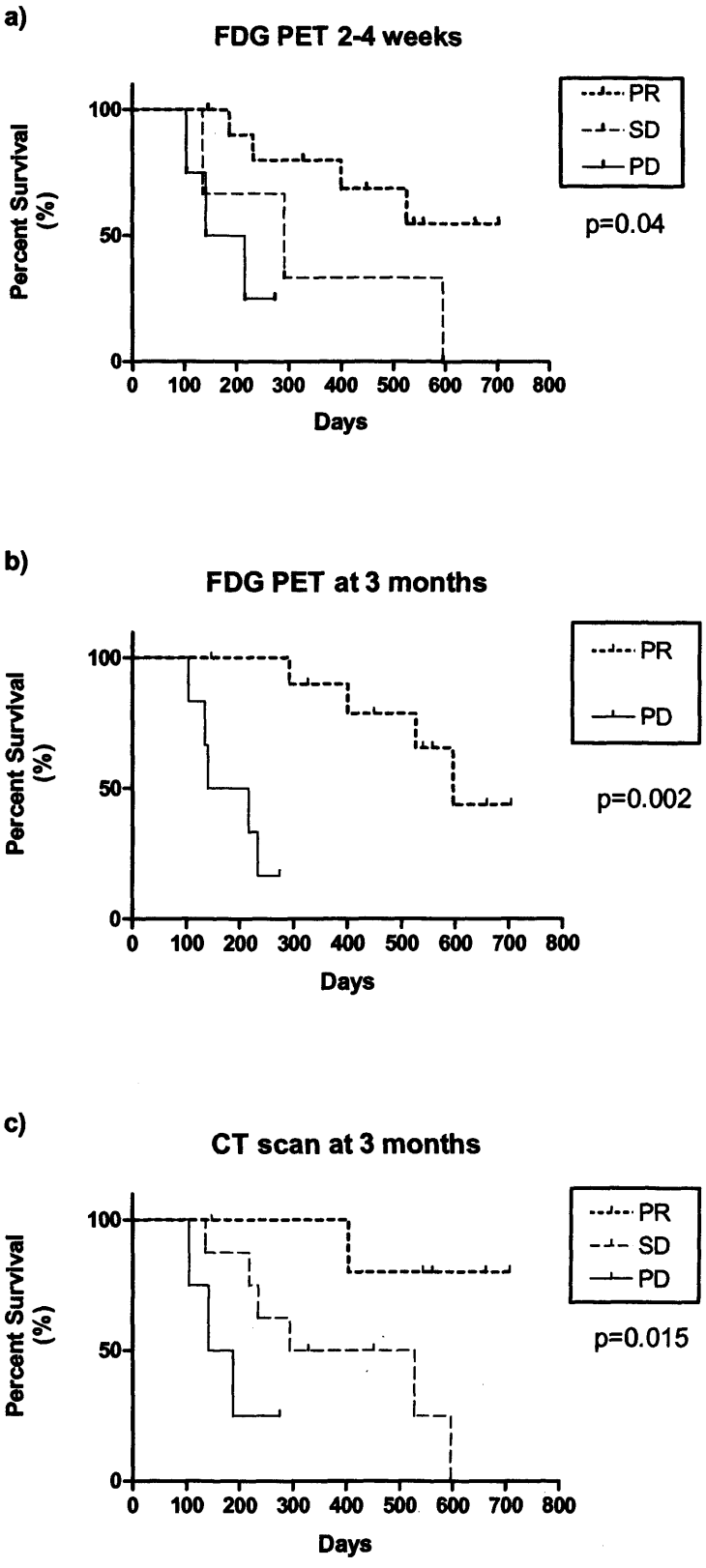

5.4 Discussion

The hypothesis tested in this chapter was that a method of analysis of tumour [F-18] FDG uptake which took into account changes in both tumour size and metabolic activity could be developed, and when applied in the clinical setting may represent an improvement over methods of analysis that take into account tumour [F-18] FDG intensity alone.

An automated region growing program was developed, and a method of analysis proposed. A clinical trial was undertaken to validate the both the automated region growing program and the method of analysis in a series of patients receiving conventional chemotherapy. The analysis compared measurements of tumour [F-18] FDG intensity with those of intensity and volume combined. The clinical trial was also designed to determine whether the response to chemotherapy could be predicted using gamma camera [F-18] FDG PET after only 2-4 weeks of treatment and to assess whether gamma camera [F-18] FDG PET could assist in the interpretation of radiological stable disease.

These objectives will be discussed individually below along with a general discussion of the use of gamma camera PET to assess response to chemotherapy.

5.4.1 Automated region growing program, lesion statistics and count density histogram – application and validation.

Delineation of tumour volumes

The VOI automated region growing program was designed because the current methods of defining regions of interest on tumour areas on [F-18] FDG PET scans were thought to be unsatisfactory, particularly for use with gamma camera PET. Methods such as SUV, which depend upon drawing 'by hand' representative regions of interest, are subjective and arbitrary in the size, shape, number and placement of the regions. In addition they are limited to only measuring the intensity of tumour [F-18] FDG uptake, and do not take into account any change in size or shape of the tumour. **Figure 54** displays an example of regions of interest drawn on three sequential [F-18] FDG PET scans.

Figure 54: ROI placement on serial scans

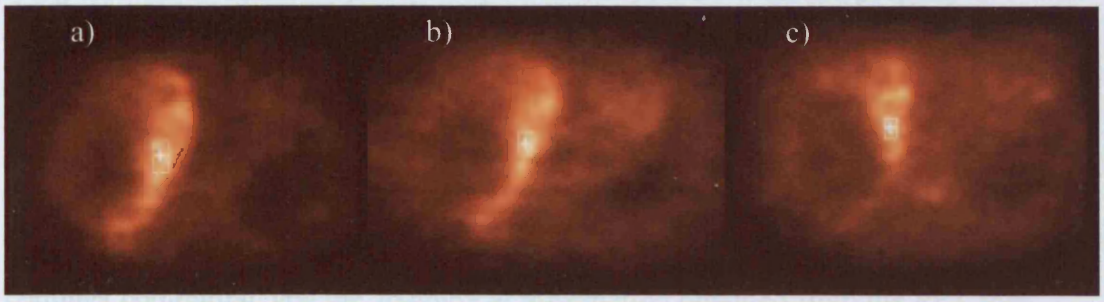

Gamma camera [F-18] FDG PET scans displaying cross-sectional slices through the liver of a patient with liver metastasis from colorectal cancer. The scans have been taken on three separate occasions, prior to (a) and after chemotherapy (b and c). A region of interest has been drawn in a representative tumour area on all three scans in the visually hottest part of the tumour.

Phantom studies using equivalent spheres filled with [F-18] FDG have shown that the differentiation between tumour and background is less for gamma camera PET than dedicated PET (Zimny *et al*, 2001). It is therefore more difficult to define by hand the outer border of tumours, and changes with therapy may be smaller in magnitude than with full ring scanners.

Co-registration of [F-18] FDG PET images with CT or MRI scans have been used with the anatomical information obtained from the CT or MRI scans used to draw tumour areas on the [F-18] FDG PET scans. This method works well for brain PET and MRI, however, there are inherent difficulties with co-registering whole-body scans. [F-18] FDG PET scans are acquired over an hour, and patients are therefore breathing regularly. CT scans are taken over only a few minutes and usually are performed with patients in maximum inspiration. There can be significant alterations in position of the lungs, diaphragm and abdominal organs between normal respiration and maximum inspiration, which creates inaccuracies with co-registration. In addition, the setup position differs between CT and PET. CT requires the arms to be raised, above the head, in order to avoid artefacts, and the [F-18] FDG PET scan (with attenuation correction) does not require this. Patients could raise their arms above their heads for the [F-18] FDG PET scan, however, as the scan is for an hour this can become uncomfortable,

and may result in movement artefacts. Also, if patients are slightly rotated when lying for their scan, the CT and [F-18] FDG PET scans will not be properly aligned.

Many co-registration software algorithms are now available, and these will align CT or MRI scans and [F-18] FDG PET scans based on internal reference points or mutual information algorithms (Studholme *et al*, 1997). This often requires complex computing, and the anatomical information obtained from the PET scan may not be sufficient for good registration. The registration of CT scans with the transmission component of the PET scan, and then reorientating the scans accordingly, may improve the registration process. Another option is to use external fiducial markers, however it was found that changes in skin surface anatomy did not always reflect changes in deep anatomy ([2]Wahl *et al*, 1993). The advent of PET/CT, in which the PET scanner and the CT scanner are mounted on the same gantry, has greatly improved the ability to accurately co-register images, as the patient is in the same position for both scans. The registration process is then much more straightforward, as the co-ordinates of both scans are used for the registration process (Israel *et al*, 2001). This has not overcome the problem of respiration artefacts, but it has greatly simplified the co-registration process, and increased its utility especially for the accurate anatomical localisation of lesions.

Once the PET image is co-registered with the CT image, tumour regions are obtained by drawing by hand around the CT defined tumour areas. This could be extremely laborious as, from the experience from our study, the volume of disease in some patients was very large. Also, there were patients in whom, particularly for liver metastasis, the CT showed a diffuse, poorly defined change, and the [F-18] FDG PET image showed clearly abnormal hypermetabolic regions. In addition, if a patient required a CT scan to accompany every PET scan for assessment of response to therapy, the radiation dose to the patient must become a factor to consider.

Another alternative would be to register the [F-18] FDG PET scans to each other, and regions drawn on the first scan may be reapplied to subsequent scans. Reproducible setup positions would need to be used, and there will be

unavoidable differences in internal organ position. Again, difficulties were envisaged with this technique. Large changes in a tumour mass with time will alter the anatomy of the underlyingorgan. Particularly this is a problem for the liver, as a responding tumour decreases in bulk and the overall liver size may reduce, and conversely, a growing liver metastasis may increase the mass of the liver. When temporally related scans are registered, the tumour areas may no longer correspond anatomically. In addition, if a tumour responds in time, the region drawn on the baseline scan would encompass the tumour, and on subsequent scans, the tumour and some normal tissue. If a tumour progresses the baseline region encompasses the tumour, but the subsequent larger tumour will fall outside the baseline region of interest. The region of interest may even fall into necrotic areas, resulting in a misleading impression of reduced [F-18] FDG uptake.

It is for all these reasons that co-registration techniques were not pursued beyond initial investigation. The initial co-registrations that were performed were very laborious and the abovementioned drawbacks became readily obvious. A method that allowed tumours to be defined based on their morphology and intensity at each timepoint was thought to be more useful than defining the baseline tumour and comparing the [F-18] FDG uptake in the same area on subsequent scans. These concepts lead to the development of the automated region growing program.

The advantages of the automated region growing program include that it is mathematically defined, and therefore is an objective, rather than subjective process. As the process is automated it is considerably less time-consuming than drawing individual regions on each slice by hand. The regions are reproducible, different operators will all define the same regions, therefore it is much more consistent than other methods of region growing. The program draws tumour volumes that are representative of both tumour morphology and metabolic activity. In the clinical trial, 90% of patients in whom tumour regions could be seen on the [F-18] FDG PET scan had their tumour volumes defined by the automated region growing program. In sixteen out of eighteen (89%) of these patients the automated region growing program defined tumour volumes that

visually appeared representative of the tumour regions (two patients required the subtraction method outlined below). The disadvantage is that it was not applicable to all patients – 10% of patients in this group could not be analysed by this method because the differentiation between tumour and normal tissue was not sufficient to allow region generation.

The VOI region growing program is also applicable to dedicated PET images, where it actually should be more effective as the higher count rate and detector efficiency allows better discrimination between tumour and normal tissue areas. It could also be applied to gamma camera PET performed without attenuation correction, although the image quality and differentiation between tumour and normal tissues may not be as sharp, and this may reduce its utility.

The VOI subtraction (VOIsub) method was adopted when volumes drawn from the automated region growing program (VOI) were not representative of the entire tumour area. In particular, if two tumours were adjacent to one another only the more metabolically active tumour was drawn. If the seed point was placed on the less metabolically active lesion the region spread to the more active lesion and did not draw the adjacent lesion. This limitation was overcome by subtracting out of the total image the VOI of the more metabolically active tumour, and then reapplying the automated region growing program. The adjacent lesion can then be drawn; however there is usually also a 'rim' which is drawn around the initial lesion (**figure 55**). This process may be repeated as many times as necessary in order to obtain representative tumour volumes.

Figure 55: VOI subtraction

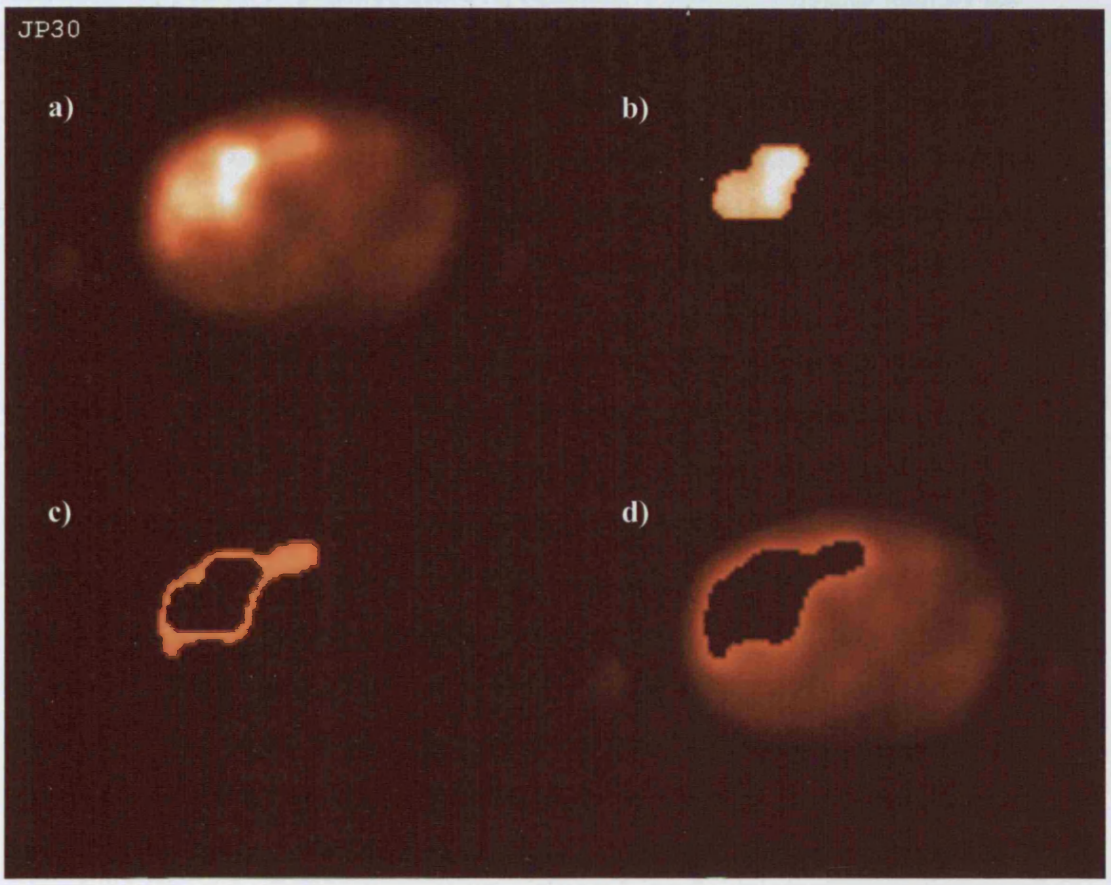

Figure 55 ***a)*** *displays a transverse section through the liver of a patient with liver metastasis from colorectal cancer. Figure 55* ***b)*** *is the region drawn on the same slice using the automated region drawing program. Figure 55* ***c)*** *is the additional region drawn using the VOI subtraction technique – it can be seen that the small tumour region adjacent to the very hot central tumour area has now been included. The rim around the original tumour is also shown Figure 55* ***d)*** *shows this final region subtracted from the original image, in order to demonstrate that the entire tumour has now been drawn.*

The VOI subtraction method has its own limitations. It is very laborious, although this could be improved with updated programming. It is much more subjective than the simple VOI method, as the user must decide how many rounds of lesion subtraction and reapplication of the program to do. Also it always leads to a reduction in mean counts/ voxel of the final tumour volume compared to the one-step VOI method, as lesions are included with lower counts/ voxel than would have been included in the VOI program with no subtraction.

In this study there were two patients (patients #4 and #23) in whom this technique appeared to produce more representative tumour volumes than by the VOI method alone. This also affected their lesion statistics. There may, therefore, be a small number of scans in which the VOI subtraction method may be more representative of tumour mass than the VOI method. It would not seem practical to employ the subtraction technique in all situations as it is time-consuming, and adds a level of subjectivity in defining when lesion subtraction should stop.

The VOI region growing program was also used to define regions of normal tissues (lung, liver, chest wall). These were used to assess variation in background tissues between scans, and thereby to validate that changes that occurred in tumour [F-18] FDG uptake were independent of the background tissues. The program was defined to grow if the adjacent voxels were +/-20% of the current mean. It became apparent, however, that a tighter range was required, as there was some spread from one normal tissue to the next. For example, seeding the lung region in the periphery of the lungs would allow 'spread' to the chest wall, and if the seed-point was too medial in the lungs the region spread to the heart. The program could be improved by restricting this count variation to +/- 10% of the current mean. In addition the normal tissue volumes were large (approximately 500 voxels), and this was problematic particularly in the liver of patients with large volume liver metastasis in whom it was difficult to find suitably large areas of normal liver to place a seed-point. This could be corrected by reducing the number of iterations performed before the program stops.

The VOI region growing program was developed on ADAC ProVision software, with minimal software support from the company. It therefore became very difficult to instigate even minor program changes. It would be desirable to transfer the program to a more widely used and flexible software system so it could be applied to different PET systems, and tested on these. This would also allow modifications to be made more easily.

The method used of an automated iterative adaptive threshold technique was one of many possible means of objectively defining the difference between tumour and non-tumour areas. It is relatively simple and has served to illustrate the principle that the differences between tumour and non-tumour areas can be

mathematically defined. There have been several published alternative methods of defining tumour volumes for quantitative analysis with [F-18] FDG PET on dedicated systems. One of these is termed spherical 3D blob analysis (Salman *et al*, 2000). This is also based on a threshold technique, and allows the automated extraction of tumour blobs in a similar manner to the VOI analysis used here. The threshold value is, however, fixed. The VOI generated is then used to calculate SUV values, and to compare to CT tumour volumes. When used in eight patients this method appeared encouraging for the assessment of response to chemotherapy. Another method used is a CT guided adaptive thresholding method, whereby the volume of a tumour is calculated from the CT scan, and based on the lesion to background ratio of the lesion on the PET scan, a threshold value is calculated and applied (Erdi *et al*, 1997). This work showed that a fixed threshold of 40% may be used to define tumour regions, provided the lesion is larger than 4mL and has a lesion to background ratio > 5:1. Unfortunately, the low count rate capability of the gamma camera PET system means that most tumours actually have a lower tumour to background ratio than this, thereby limiting the applicability of any fixed threshold system. This is in concurrence with our own experience which found that if a fixed threshold was used the resultant volume of interest was not representative of the visible tumour area.

Other techniques could include a method based on a % difference between tumour and non-tumour areas, or a 'contour mapping' technique, which takes into account the gradients of change in [F-18] FDG uptake. Both of these techniques, however, depend on background normal tissues, and if the [F-18] FDG uptake in normal tissues changed with chemotherapy this may result in misleading representation of tumour areas.

In conclusion, the VOI region growing program was found to be a very promising method for delineating tumour regions for further analysis. Its advantages were that it was rapid, reproducible, automated and in most cases provided a good representation of tumour regions. Its main limitations were that it was not able to define tumour volumes on all patients and that the program had difficulty defining two adjacent lesions separately.

Quantitating change in tumour uptake of [F-18] FDG

Once the tumour volume was defined, a method of quantifiying change in [F-18] FDG uptake was required. The methods used to assess change in tumour [F-18] FDG uptake in the tumour regions defined by the VOI region growing program were lesion statistics or histogram analysis.

Lesion statistics

The lesion statistics calculated from the tumour VOI can be divided into those that measure tumour size (volume), and those that reflect uptake intensity (mean counts/voxel, maximum counts per voxel). The total counts statistic combines both and measures total tumour [F-18] FDG uptake.

The clinical trial demonstrated that the total counts statistic appeared the most useful for assessing change in tumour [F-18] FDG uptake with chemotherapy when compared to the result of a 3 month CT scan. This may be because it reflects both tumour size and metabolic activity. The Pearson correlation coefficient obtained from a direct comparison between percentage change in dimensional measurements on CT and change in total counts from VOI was 0.83 at the 2-4 weeks PET scan and 0.75 at the 3 month PET scan.

The main situation in which VOI total counts appeared more representative of true response than VOI mean counts was in the prediction of progressive disease. Patients who had progressive disease on CT scan at 9-12 weeks did not consistently have an increase in VOI mean counts on [F-18] FDG PET at 2-4 weeks. The VOI volume did however increase. By the 3 month [F-18] FDG PET scan the VOI mean counts had increased compared to baseline. As the VOI mean counts represent the intensity of metabolic activity within a tumour, it appears, from this very limited sample, that early progression on [F-18] FDG PET may be associated with an increase in lesion size prior to an increase in metabolic intensity. More patients are required to define this relationship clearly, however this finding, if substantiated, may hold significant implications for the sensitivity of methods of analysis of [F-18] FDG PET that only take into account measurements of tumour intensity and not tumour size.

Count density histogram

The histogram method of analysis appeared very promising, as it was a means to represent changes in the distribution of [F-18] FDG activity within the tumour VOI. Unfortunately no satisfactory method of transferring the data from the workstation or analysing this data was identified and therefore it was not possible to take this method to its full potential. The shape of the histograms changed with chemotherapy, however, interpreting and reporting the significance of this change was difficult without a method of quantifying it. There were several situations in which the tumour histograms were more difficult to assess. Examples of these are displayed in **figure 56**.

The histogram method was useful for identifying whether the background tissues varied between baseline and subsequent scans, although, again without a method of quantifying or delineating this variation it was difficult to measure or record change in [F-18] FDG uptake in normal tissues after chemotherapy.

Figure 56: Tumour histograms

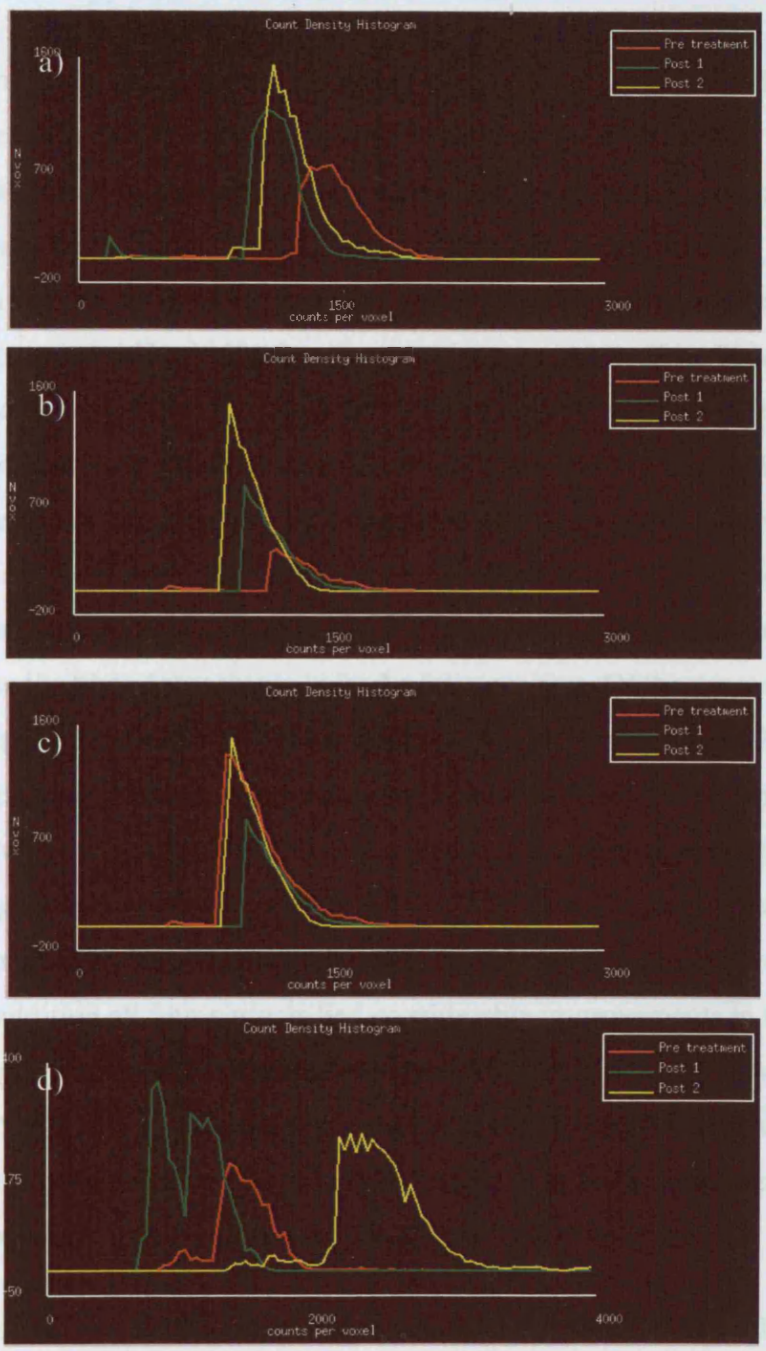

Figure 56 a) is a tumour histogram from patient #12 who had radiological stable disease at 9-12 weeks. The histogram appears to increase in size but reduce in intensity after treatment. Figure 56 b) is the tumour histograms produced using the VOI method and c) is the tumour histograms using VOI subtraction from patient #23. For this patient the VOI subtraction technique produced much more representative tumour volumes than the VOI technique. This patient also had radiological stable disease on CT scan at 9-12 weeks. Again the tumours appear to reduce in intensity but increase in size. Figure 56 d) is the tumour histogram from patient #28 who had progressive disease on CT scan at 9-12 weeks. There is clear progression from the baseline scan to the 9-12 week scan (red to yellow lines respectively), however, the 2-4 week result appears to be less intense.

5.4.2 Can gamma camera [F-18] FDG PET be used to predict response to chemotherapy after 2-4 weeks of treatment?

The data from this trial supports the emerging evidence that [F-18] FDG PET can be used to predict response to chemotherapy as early as 2-4 weeks after treatment. If a 'partial response' on [F-18] FDG PET was arbitrarily defined as a 15% or greater reduction in the total counts on tumour VOI compared to baseline, then the sensitivity at the 2-4 week [F-18] FDG PET scan for detecting a partial response would be 100%, but the specificity would be 58%. This low specificity is due to the 'false positives' of 1 patient with progressive disease (#30) and 4 patients with stable disease (#2, #4, #19, #27) on CT scan at 9-12 weeks. As previously mentioned pt #30 was deemed a 'progressive disease' on conventional imaging, due to the development of a new lesion on CT. The tumour markers of this patient increased at 9-12 weeks to 126% of baseline, confirming the likelihood that this is indeed a false positive. Of the 4 patients with stable disease who had a > 15% reduction in [F-18] FDG uptake at 2-4 weeks, three patients continued chemotherapy beyond 9-12 weeks, with pt #2 going on to liver resection, pt #4 achieving a partial response at 6 months, and pt #27 remaining with stable disease at 6 months on CT scan. The fourth patient (pt #19) was recommended to continue chemotherapy, however declined due to toxicities. In addition all four patients had considerable improvements in their serum tumour markers at 9-12 weeks (54%, 49%, 46% and 55% respectively for pts #2, #4, #19, #25). It may therefore be that the [F-18] FDG PET scan and tumour markers detected a biological response in the tumours of these four patients that was not detected by conventional radiological imaging.

If 'progression' on [F-18] FDG PET was defined as a >10% increase in [F-18] FDG uptake, then the sensitivity at 2-4 weeks using total counts on tumour VOI analysis would be 75% and the specificity 93%. Pt #30 would not have been detected as progressive disease, and pt #23 would have been deemed disease progression, whereas the radiological measurements indicated stable disease. Chemotherapy was stopped on pt #23 at 9-12 weeks due to cardiac toxicity, and this patient did not have any tumour markers for evaluation.

Table 52 demonstrates the relationship between VOI total counts at 2-4 weeks and the outcomes of patients with respect to whether they continued with the same chemotherapy regimen beyond 9-12 weeks or stopped chemotherapy at 9-12 weeks.

Table 52: VOI total counts at 2-4 weeks and patient outcome

Chemotherapy continued at 9-12 weeks			**Chemotherapy stopped at 9-12 weeks**		
Pt No.	**RECIST Response**	**2-4 week VOI total counts (%)**	**Pt no.**	**RECIST Response**	**2-4 week VOI total counts (%)**
#8	PR	11%	#11	PD	229%
#16	PR	36%	#24	PD	114%
#17	PR	76%	#28	PD	144%
#21	PR	0%	#30	PD	79%
#22	PR	83%	#10	SD	104%
#26	PR	14%	#12	SD	97%
#2	SD	67%	#19	SD	0%*
#4	SD	48%	#23	SD	168%*
#14	SD	97%			
#27	SD	69%			
	median	**58%**		**median**	**109%**

This table divides the patients into those who continued with the same chemotherapy regimen after their 3 month CT scan and those who stopped. The [F-18] FDG PET values are those from the VOI total count statistic on the 2-4 week [F-18] FDG PET scan, and are expressed as a % of baseline value.
** indicates patients who stopped chemotherapy due to toxicity*
Abbreviations: PR – partial response; SD – stable disease; PD – progressive disease

If a decision had been taken at the time of the 2-4 week [F-18] FDG PET scan to stop chemotherapy for patients who had an increase in [F-18] FDG uptake (>110% by total counts of VOI), chemotherapy would have been stopped on four patients. None of these patients actually continued chemotherapy beyond 9-12 weeks. Three had progressive disease on CT scan at 9-12 weeks, and one had stable disease with cardiotoxicity at 9-12 weeks. Importantly, no responding patients would have been missed by this method.

If a decision had been made to only continue chemotherapy on patients who had a reduction in [F-18] FDG uptake to <85% of baseline, chemotherapy would have been continued on 11 patients. 9 of these 11 patients (82%) attained a partial response or stable disease on the 9-12 weeks CT scan, and went on to continue chemotherapy beyond 9-12 weeks. 2 of the 11 patients stopped chemotherapy at 9-12 weeks (1 due to progressive disease on CT and 1 due to toxicities). Of the seven patients who did not have a fall in tumour [F-18] FDG uptake to <85% of baseline at 2-4 weeks, six (86%) actually stopped chemotherapy at 9-12 weeks, and one (14%) continued. This patient (pt#14) had stable disease on the 3 month CT scan and went on to complete 6 months of chemotherapy, and again attained stable disease on the 6 month CT scan. If this rule had been applied this patient may have had their chemotherapy stopped early, and although this patient never attained a partial response on CT scan, they did complete 6 months of chemotherapy with radiological stable disease. Again no responding patients would have been missed by applying this rule; however, one patient with stable disease would have been missed.

The ability to predict patients who respond to chemotherapy at an earlier time-point than is currently possible with radiological imaging is important for several reasons. Chemotherapy carries with it a physical and psychological burden, and the ability to inform a patient after only one treatment that they are responding would relieve considerable anxiety, and would improve patient tolerability of side-effects. If a patient is not responding they may be able to stop treatment early, and limit unnecessary toxicities. In addition, it appears that from the survival data collected in this study, patients who respond to chemotherapy with a reduction in [F-18] FDG tumour uptake at 2-4 weeks, have a statistically significantly improved survival than those who do not. This is very encouraging for responding patients, and may help identify the subset of non-responders who could benefit from earlier intervention to try and obtain a better outcome for this group of patients. Finally, there are cost-benefit implications. New chemotherapies are expensive to develop, and once licensed the cost may limit their availability as Health Authorities are unable to afford them within their budgets. This cost may be significantly reduced by the ability to detect responding patients after only one cycle of treatment, therefore reducing the

number of cycles of chemotherapy required to be given to non-responders, and any associated costs in terms of morbidity and hospitalisation to manage side-effects.

If the aim is to identify non-responders earlier, it appears from the limited number of patients available in this study, that if the VOI total counts at 2-4 weeks is >110% of the baseline value, patients are very unlikely to have a response to chemotherapy (0% subsequently responded at 9-12 weeks). In addition, these patients have a significantly worse prognosis in terms of overall survival as shown in **figure 53** (p=0.04). This is the group of patients in whom stopping chemotherapy early may be advantageous in terms of toxicities, cost and in trying to improve their prognosis by intervening earlier to try a different treatment regimen.

Conversely if a patient has a VOI total counts of <85% at 2-4 weeks they may be reassured from this study that they have >90% chance of having some benefit from chemotherapy, as only 1 of the 11 patients in this study with VOI total counts <85% at 2-4 weeks went onto have progressive disease at 9-12 weeks. This may be advantageous to patients who are struggling with the psychological or physical burden of chemotherapy. Also, reassuringly, they appear to have a survival advantage over those who did not obtain a reduction in tumour [F-18] FDG uptake after one cycle of chemotherapy.

5.4.3 Does gamma camera [F-18] FDG PET aid the interpretation of radiological stable disease?

The management of patients who obtain radiological stable disease after chemotherapy remains an undefined area. 'Stable disease' is poorly understood – it may represent a minor response to chemotherapy or no response to chemotherapy. Consequently the decision of whether to continue with the same chemotherapy regimen or whether to stop is also very difficult. It is often taken after patient – physician discussion and with the degree of toxicities experienced factored in. With the emergence of novel biological therapies for cancer with low toxicity, stable disease if sustained, may become a more acceptable outcome.

One reason for patients attaining stable disease may be that the detection of response to therapy by radiological imaging only measures dimensional changes in tumours. [F-18] FDG PET imaging, by reflecting a metabolic process, should improve the ability to ascertain the biological effect of therapies, and could help guide decision making in clinical practice.

In this study of 31 patients, overall 15 patients (48%) had stable disease by RECIST criteria on their 9-12 week assessment. This is a large proportion of patients in which it is uncertain whether they have had any benefit from their chemotherapy. Eight of these patients had [F-18] FDG PET scans that were suitable for analysis with the VOI total counts technique. **Table 53** summarises the VOI total counts values on the 2-4 week and 9-12 week [F-18] FDG PET scans, in combination with the tumour marker response and clinical outcome. The 18-24 week CT response is indicated in patients who continued chemotherapy beyond 9-12 weeks, and had a subsequent assessment performed

Table 53: Patients with CT defined stable disease

Pt No.	CT scan (9-12 wks)	Tumour Markers	VOI (2-4 wks)	VOI (9-12 wks)	Clinical outcome at 9-12 wks	CT scan (18-24 wks)
#2	SD	54%	67%	43%	Continued chemotherapy (liver resection)	ND
#4	SD	49%	*48% (81%)	*150% (90%)	Continued chemotherapy	PR
#14	SD	57%	97%	64%	Continued chemotherapy	SD
#27	SD	55%	69%	0%	Continued chemotherapy	SD
#10	SD	263%	104%	83%	Stopped chemotherapy	NA
#12	SD	395%	97%	124%	Stopped chemotherapy	NA
#19	SD	46%	0%	0%	Stopped chemotherapy due to toxicities	NA
#23	SD	ND	*168% (114%)	*258% (73%)	Stopped chemotherapy due to toxicities	NA

The outcome and clinical decision whether to continue chemotherapy on eight patients who attained stable disease on CT scan after 9-12 weeks of chemotherapy compared to the change in tumour markers at 9-12 weeks, and the change in VOI total counts at 2-4 weeks and 9-12 weeks.
** VOI total counts used, however VOIsub tumour regions were more representative in these patients The VOIsub total counts value is given in brackets.*
Abbreviations: VOI –volume of interest; SD – stable disease, PR – partial response, ND – not done, NA – not applicable

Four of the eight patients proceeded with chemotherapy after the 9-12 week assessment CTscan. All four patients had a fall in their serum tumour markers at 9-12 weeks (median 52% range 49-57%). Three patients had a fall in tumour [F-18] FDG uptake to <85% of baseline at the 2-4 week [F-18] FDG PET scan. One of these patients attained a partial response on CT scan at 18-24 weeks, one had a sustained stable disease and one went onto have a liver resection and was not further assessed. In these three patients there is the indication that the chemotherapy may have been producing a positive effect that was not detected on CT scan. The fourth patient had stable tumour [F-18] FDG uptake at 2-4 weeks (97%), which had reduced further at 9-12 weeks to 64% of baseline. These values indicate a response to chemotherapy, which is supported by the tumour marker values and the attainment of sustained stable disease on CT scan at 18-24 weeks.

Of the four patients who stopped chemotherapy at 9-12 weeks, two stopped due to toxicities. The two patients who stopped due to lack of evidence of response to the chemotherapy both had substantial increases in their tumour marker values at 9-12 weeks (263% and 395%). The VOI total counts at 2-4 weeks were not indicative of a response to chemotherapy (97-104%). By 9-12 weeks they had increased in one patient (124%) indicating progressive disease. In the other patient the tumour [F-18] FDG uptake fell to 83% of baseline. This was not in agreement with the tumour marker values or the clinical decision to stop chemotherapy.

The [F-18] FDG PET scan results were not used in this study to influence physician decisions as to whether to continue chemotherapy, however, the CT scan and tumour markers results were. There is a good correlation between tumour marker response to chemotherapy and subsequent decision of whether to proceed with chemotherapy for these patients with stable disease. This supports the utility of serum tumour markers in this situation, but this must be interpreted with some caution as it may have been because of the tumour marker result that the decision was made to continue or stop chemotherapy.

Overall the [F-18] FDG PET results did appear to be in agreement with the clinical outcome of patients, particularly for patients who continued

chemotherapy beyond 9-12 weeks in whom there was a reduction in tumour [F-18] FDG uptake at 2-4 weeks. These three patients did appear to be benefiting from chemotherapy, and continuing treatment resulted in a favourable outcome for all three patients. It appears therefore, from this limited evidence, that chemotherapy should be continued on patients who attain a reduction in tumour [F-18] FDG uptake at 2-4 weeks, and who are tolerating chemotherapy, as there does appear to be some evidence of therapeutic benefit in these patients.

5.4.4 Issues associated with use of [F-18] FDG PET for response assessment

There are several issues that were identified to be important in influencing the validity of serial [F-18] FDG PET scans. These include the timing and frequency of [F-18] FDG PET scans, patient preparation and protocol issues and the influence of partial volume effects on small lesions.

Timing and frequency of [F-18] FDG PET assessments

The timing of an [F-18] FDG PET assessment after therapy is important, as early information is very helpful for directing further management plans, however, it must be shown that the assessment is performed at a time when the results are reliable. There is a concern that there may be a 'metabolic flare' reaction to chemotherapy, which will result in a false-positive result on [F-18] FDG PET, if the timing of the PET scan is too close to the administration of chemotherapy. This has been shown to be problematic when scanning was performed at 24 hours after chemotherapy in two studies to date (Rozenthal *et al*, 1989; De Witte *et al*, 1994). However, in one recent study, responses were seen on [F-18] FDG PET at 24 hours after administration of the novel tyrosine kinase inhibitor, imatinib mesylate (Glivec) (Demetri *et al*, 2002).

The administration of radiotherapy has also been associated with an increased uptake post therapy in patients who were 'responders' (Haberkorn *et al*, 1991; Hautzel and Müller-Gärtner, 1997; Spence *et al*, 2002). This, again, was thought to be metabolic flare, and may be problematic for up to 6 months post radiotherapy (Haberkorn *et al*, 1991).

A review of response assessment using [F-18] FDG PET by the EORTC PET Study Group in 1999 recommended that a pre-treatment [F-18] FDG PET assessment be performed within 2 weeks of commencement of chemotherapy. The timing of follow-up [F-18] FDG PET scans should be dependent on the study protocol, however, to avoid possible 'flare' reaction, [F-18] FDG PET scans should ideally be timed 1-2 weeks after chemotherapy (Young *et al*, 1999).

The recommended frequency of PET assessments has not yet been established. [F-18] FDG PET scans on a dedicated PET system result in an effective radiation dose to the patient of 7-9.5mSv (using 370 – 500MBq [F-18] FDG) (Valentin, 1998). The amount of [F-18] FDG administered for a gamma camera [F-18] FDG PET scan is 20-25% of that required for a dedicated [F-18] FDG PET scan. This results in a radiation does of <3mSv (Valentin, 1998). A whole body CT scan has an estimated effective radiation dose of 12mSv (Brenner and Elliston, 2004). These radiation doses should be considered when planning trial protocols.

Patient preparation and PET protocols

Patient preparation is very important if [F-18] FDG PET scans are to be used to detect longitudinal change in tumour [F-18] FDG uptake with therapy. Tumour [F-18] FDG uptake may be affected by many factors including, the injected [F-18] FDG dose, time to scanning, the patient's blood glucose level, skeletal muscle uptake of tracer and the presence of urine in the bladder or renal pelvises.

The absolute amount of [F-18] FDG uptake within a tumour will be influenced by the injected activity. In addition, the PET camera used to scan the patient may have an optimal range of sensitivity, and large changes in injected activity, may be not correctable by simple rescaling factors. It is therefore important to try and keep the injected activity as constant as possible between the pre treatment and post treatment scans.

The time to scanning is also very important. Static [F-18] FDG PET scans are taken when the uptake of [F-18] FDG into tumours is presumed to be complete (plateau phase). Therefore the tumour uptake of [F-18] FDG should not change significantly over the scan period. Usually the plateau phase is assumed to be at

60 minutes post injection of [F-18] FDG, however, evidence is emerging that time-points later than this may be more appropriate as active tumour uptake of [F-18] FDG may still be occurring at 60 minutes. In one study the average time to attaining plateau for patients with lung cancer was almost 300 minutes (Hamberg *et al*, 1994). The difference in SUV found between taking a 60 minute SUV measurement compared to a SUV measurement at the actual plateau timepoint was found to be an average of 46% different (Hamberg *et al*, 1994). This can lead to quite significant errors. If the scan is performed before the plateau phase is attained, then differences in the time between injection of [F-18] FDG and the time to commencing the scan in serial scans may have a significant effect on the tumour [F-18] FDG uptake. Again, this may not be a linear effect, and therefore will not be correctable by simple rescaling factors.

Patients must be fasted prior to [F-18] FDG injection as [F-18] FDG competes with glucose, and high circulating glucose levels will lead to poor tumour resolution due to high background [F-18] FDG levels and low tumour uptake (Langen *et al*, 1993; Lindholm *et al*, 1993; Diederichs *et al*, 1998). It is recommended that patients be fasted for 6 hours prior to injection of [F-18] FDG and a patient's blood sugar level is between 4-7 mmol/L (Young *et al*, 1999). This is particularly important when two consecutive scans in the same person are to be compared, as the tumour [F-18] FDG uptake will be reduced as a result of high blood sugar levels, rather than therapeutic effect. This makes the scanning of patient's with uncontrolled diabetes difficult, as their blood sugar levels may vary considerably between scans.

It is important that patients are well hydrated prior to having a [F-18] FDG PET scan, as [F-18] FDG is excreted through the urinary system. Concentrated urine has very high radioactivity, and can lead to artefacts on the reconstructed images. The use of frusemide 20-40mg is recommended for areas of interest in the pelvis or near the kidneys, to avoid the image artefacts associated with concentrated urine (Young *et al*, 1999).

Skeletal muscle when exercised will take up glucose; therefore patients must rest prior to and after [F-18] FDG injection. Diazepam may be required for muscle relaxation, especially for patients with head and neck tumours (Young *et al*,

1999). Cardiac muscle also utilises glucose, however it is more difficult to control cardiac muscle glucose utilisation for [F-18] FDG PET scans. Caffeine intake can result in increased cardiac muscle uptake, and it may be useful to ask patients to have the same intake of caffeine in the 24 hours prior to their scan on each occasion.

The protocol of the [F-18] FDG PET scan must be duplicated for the baseline and the subsequent scan to ensure consistency. This includes set-up positions, time per frame, presence or absence of attenuation correction and reconstruction protocols. The set-up position is particularly important for gamma camera PET, as there is a count-rate drop-off effect towards the edges of the detectors. Also the scans are performed with a 50% overlap, which is accounted for in the reconstruction protocols. Overlaps at different parts of the scans may however, influence tumour [F-18] FDG activity due to reconstruction effects, rather than a real change.

The standardisation of all of these factors between [F-18] FDG PET scans in the same patient will reduce the errors that may occur simply as a result of inconsistent patient preparation. This is extremely important when [F-18] FDG PET is being used for quantitative response assessment.

Partial volume effects

All of the quantitative methods of analysis used commonly are potentially subject to the partial volume effect that occurs for small lesions. This is a particular problem if the lesion's size is less than two times the resolution of the camera. The ADAC Vertex Plus Gamma Camera has a FWHM of 4.8 mm when with measured attenuation correction was applied (manufacturer's specifications). Therefore for lesions of less than 1cm a significant partial volume effect may occur, leading to the lesion appearing much less intense, purely due to its size, and the camera's resolution. Partial volume effects may therefore lead to an exaggerated reduction in intensity when a tumour reduces in size, or an increase in intensity due to an increase in tumour size, as demonstrated in **figure 57**. This may result in an over estimate of the effect of a treatment. This will be problematic for all of the methods of analysis, but can be

avoided by only analysing lesions that do not fall into this low resolution range of the camera.

Figure 57: Partial volume effect

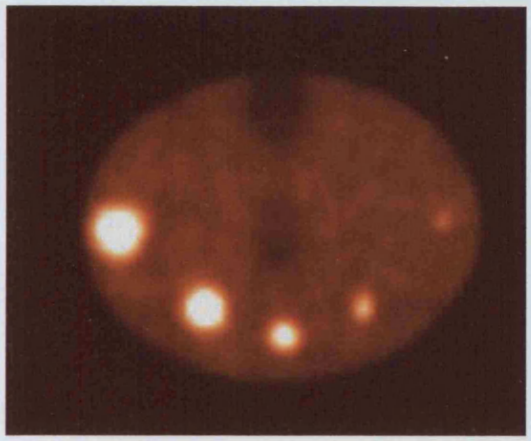

A Jasczak phantom with 5 spheres each filled with [F-18] FDG to a ratio of 10:1 to background. The spheres are sized 40mm, 30 mm, 19mm, 10mm and 6 mm from left to right. There are also two air filled spheres of 40mm and 30mm. The phantom has been scanned using the clinical protocol, and measured attenuation has been applied. The spheres appear to be less intense as they reduce in size – this is due to the partial volume effect that occurs due to a loss of resolution as lesion size approaches the FWHM of the system (data obtained with permission from KL Adamson).

In the [F-18] FDG assessment study, all of the patients with lesions for which the VOI region growing program was able to generate tumour volumes had tumours of > 2cm, and so the partial volume effects should therefore have been minimal.

Figure 58 demonstrates a patient with a 4cm lung metastasis, which reduced to 2cm on CT scan at 9-12 weeks. There is almost certainly some partial volume effect occurring in the tumour at the 2-4 week, and 9-12 week [F-18] FDG PET scan. The automated region growing program was unable to define tumour volumes at these time points, and therefore lesion statistics could not be obtained.

Figure 58: Partial volume effects in clinical setting

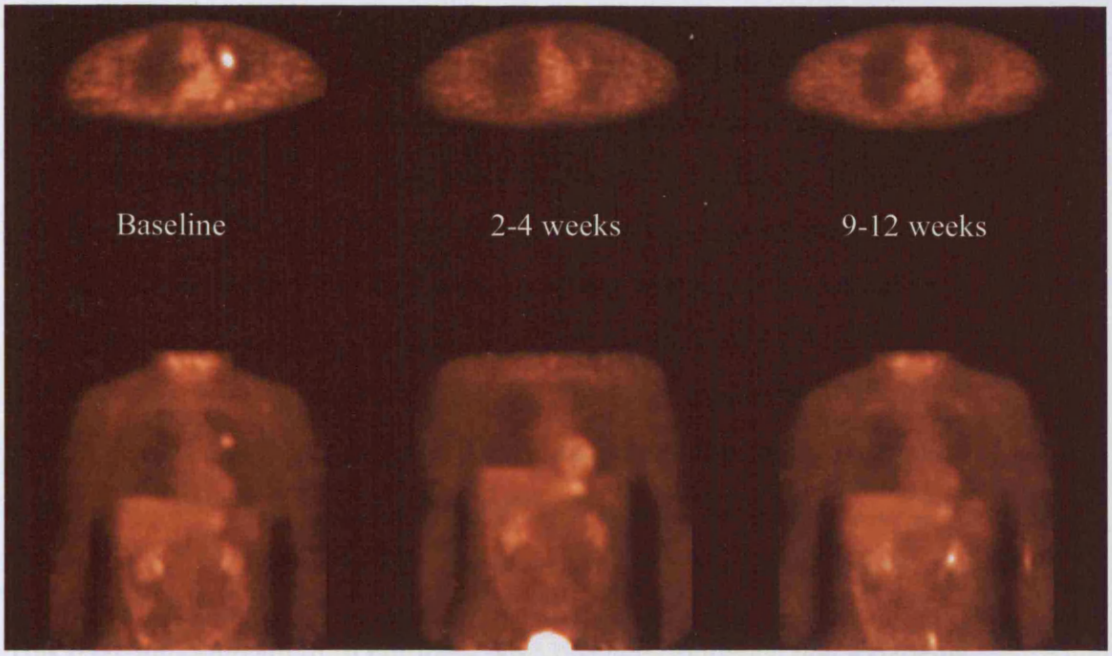

Transverse and volume views of a patient with a lung metastasis from colorectal cancer. The lesion is clearly visible on the baseline study and barely visible at 2-4 weeks and 9-12 weeks. The size of this lesion may have contributed to its reduced intensity due to partial volume effects.

5.5 Conclusion

A method of objectively, rapidly and reproducibly defining [F-18] FDG PET tumour regions has been developed and the analysis of these regions, taking into account both tumour [F-18] FDG uptake intensity and volume, applied in a clinical setting. This method of assessing response to chemotherapy using gamma camera [F-18] FDG PET was shown to correlate with conventional response assessment using RECIST criteria. Importantly the [F-18] FDG PET response was also found to be a statistically significant indicator of survival in this patient group. Therefore within the limitations of this relatively small study, it can be concluded that gamma camera [F-18] FDG PET using volume of interest analysis is a valid tool for assessing response to chemotherapy.

This trial, although small in numbers, also provides evidence that a patients' response to chemotherapy and their survival may be predicted by gamma camera [F-18] FDG PET at 2-4 weeks after the commencement of chemotherapy (1-2 cycles). This is valuable in determining those who should persevere with chemotherapy, and may identify those who are not responding at an earlier stage, in order that their treatment plan may be modified appropriately. Gamma camera [F-18] FDG PET also appeared to provide useful additional information for the interpretation of stable disease.

In conclusion gamma camera [F-18] FDG PET for assessment of response to chemotherapy warrants further investigation, and the VOI technique appears a useful method of semiquantitative assessment of response in this setting.

5.6 Acknowledgements

This clinical trial was kindly supported by The Wolfson Trust, The Ronald Raven Trust, and the Golden Charitable Trust.

6 [F-18] FDG PET and the assessment of response in phase I/II ADEPT clinical trials

6.1 Background

[F-18] FDG PET for the assessment of response to therapy has predominantly been used to assess the effect of established chemotherapy regimens. However, a potentially important role for [F-18] FDG PET exists in the assessment of the efficacy of agents being tested in the Phase I and II clinical trial setting (Price *et al*, 1995). Patients who participate in Phase I/II clinical trials are often heavily pre-treated and their tumours are likely to be less chemosensitive than patients with chemo-naive tumours. Additionally they often have a large tumour burden, and may have some alteration in functioning of critical organs or overall performance status. Agents tested in phase I/II clinical trials may not be fully optimised, with dosage, scheduling or timings being manipulated and modified as part of the clinical trial design protocol. These factors all contribute to reduce the likelihood of a radiological response to agents tested in the phase I/II setting.

[F-18] FDG PET scans, by representing a metabolic process, have been shown to be more sensitive at detecting response to chemotherapy than CT scans (Jansson *et al*, 1995; Findley *et al*, 1996; Bokemeyer *et al,* 2002). They can also assess response earlier than by CT scans, and evidence is emerging of their use for prognosis in terms of survival (Weber *et al*, 2003). The ability to detect response earlier and the improved sensitivity for detection of response over CT assessments are important attributes for early studies of cancer therapies.

6.1.1 Application of [F-18] FDG PET imaging to ADEPT clinical trials

Phase I/II clinical trials of ADEPT are subject to all of the factors listed above which reduce the likelihood of attaining a clear radiological response after treatment. In addition, the immunogenicity of the antibody-enzyme used in ADEPT may limit therapy to only one 'cycle' of treatment, which further reduces the likelihood of attaining a reduction in size of the tumour. By being a complex strategy, there are many variables that may be modified in ADEPT, and

having a more sensitive means of detecting effect of the treatment on the tumour may aid in directing these modifications.

Previous clinical trials of ADEPT have been associated with cohorts of patients who attain stable disease by radiological imaging (Bagshawe *et al*, 1995; Napier *et al*, 2000). Understanding the significance of this has been difficult. It may indicate that ADEPT has been ineffective, or it may indicate some therapeutic benefit, but not of sufficient magnitude to have resulted in a radiological response. As ADEPT is designed to be relatively free of toxicities 'stable disease' may be an acceptable endpoint if it does indeed reflect some degree of therapeutic benefit. A greater understanding of the effect of ADEPT on tumours that have radiological stable disease is therefore required.

Serum tumour markers have been used to assess response to chemotherapy (Rustin, 2003), however ADEPT utilises an anti-CEA antibody, which makes the interpretation of subsequent change in CEA levels difficult. A fall in CEA levels may occur as a result of clearance of serum CEA by the anti-CEA antibody. Additionally the formation of HAMA may interfere with the assay used for serum tumour marker estimation, which adds further uncertainty to these measurements.

The combination of a non-optimised treatment in a potentially resistant patient group, the tendency to attain radiological stable disease in past ADEPT clinical trials and the absence of an alternative means of assessing efficacy, such as tumour markers, have lead to the need for a better method of assessing the effect of ADEPT in phase I/II clinical trial setting. It was hypothesised that [F-18] FDG PET, by reflecting changes in tumour glucose metabolism, may provide a more sensitive means of detecting response in ADEPT. It was also proposed that [F-18] FDG PET could be used to aid the interpretation of radiological stable disease in the phase I/II ADEPT clinical trials.

These hypotheses were examined as part of the phase I/II ADEPT clinical trials using the methodology developed in **chapter 5** to assess change in tumour [F-18] FDG uptake with the therapy.

6.2 [F-18] FDG PET in phase I/II ADEPT trials

The method and analysis for both clinical trials are presented separately as there were differences in the timing and protocols used for [F-18] FDG PET scans, and in the method of CT response assessment.

6.2.1 ADEPT A5CP and ZD2767P

Method

[F-18] FDG PET scans were performed on patients within 2 weeks prior to commencing ADEPT, at 4 weeks and then at 8 weeks after ADEPT. Patients were fasted for 4-6 hours prior to injection and scanning was performed on an ADAC Vertex Plus dual headed gamma camera. Initially patients were injected with 185MBq of [F-18] FDG and scanned at 45-60 minutes post injection. Subsequent phantom studies revealed that this exceeded the quantitative range of count rate capability of the detectors of the camera, and consequently from patient #11 onwards all patients received a maximum of 150MBq of [F-18] FDG and were scanned at a minimum of 60 minutes.

Attenuation correction capabilities were not available for the ADAC Vertex Plus gamma camera until the end of this ADEPT trial. Therefore the majority of patients were scanned with the collection of only emission data. Emission scans had a 50.8cm field of view and were acquired according to the manufacturer's specifications. Correction for decay was applied on the fly. Most patients had 2 rotations performed; however some patients required 3 rotations. Patients were scanned with their arms above their head, out of the field of view.

Reconstruction was performed using standard ADAC iterative reconstruction protocols. A correction for attenuation was performed using Chang attenuation correction of uniform ellipses (Chang, 1978). A rescaling factor was applied to the images prior to analysis, correcting for injected activity of [F-18] FDG and time to scanning (**figure 49, Chapter 5**).

A formal correction for blood glucose levels was not made, however data with blood glucose levels outside the range 4-7mmol/L were deemed unreliable.

Analysis was performed, where data was deemed reliable, using the automated region growing program as described in **Chapter 5,** to define tumour volumes. A threshold of 85% was applied at all times. VOI subtraction was only applied if the tumour region, drawn by the region drawing program, did not appear visually representative of the total tumour burden. Lesion statistics were obtained and count density histograms drawn as described previously. The lesion statistics used were tumour volume (total number of voxels), mean counts/voxel, maximum counts/voxel and total counts. The change in each lesion statistic was then displayed as a percentage change compared to baseline. The count density histograms of tumours were displayed, but not quantified. The count density histograms of the normal tissues (liver, lung) were displayed, and used to aid interpretation of whether the background tissues of the scan had altered compared to baseline.

CT scans were performed on patients prior to the commencement of ADEPT and at 4 and 8 weeks after ADEPT as outlined in the trial protocol (**chapter 2**) Response on CT scan was assessed using WHO criteria of bidimensional measurements.

Results

Table 54 outlines the details of the [F-18] FDG PET scans performed on the patients in the ADEPT study.

Table 54: [F-18] FDG PET scans in ADEPT A5CP and ZD2767P clinical trial

Pt No.	No. scans	Chang/AC	Quantitative	Comment
#1	0	NA	NA	camera not functional
#2	3	Chang	no	
#3	3	Chang	no	
#4	3	Chang	no	high blood glucose (diabetic)
#5	3	Chang	no	
#6	3	Chang	no	
#7	3	Chang	no	
#8	1	Chang	no	pt did not receive ADEPT
#9	2	Chang	no	camera fault scan 3
#10	3	Chang	no	
#11	3	Chang	yes	
#12	1	Chang	no	pt deceased
#13	2	Chang	no	pt unwell scan 3
#14	2	Chang	yes	pt unwell scan 3
#15	3	Chang	yes	
#16	1	Chang	yes	pt unwell
#17	1	Chang	yes	pt unwell
#18	3	Chang	yes	corrupt data scan 3
#19	3	Chang	yes	
#20	3	Chang	yes	
#21	2	Chang	NA	pt unwell scan 3. data corrupt scan 1 and 2
#22	2	Chang	yes	tumour not seen
#23	2	Chang	yes	camera fault scan 3
#24	3	Chang	yes	
#25	0	NA	yes	camera fault
#26	3	Chang	yes	
#27	3	AC	no	no rescaling information

Data was regarded as non-quantitative if the singles count rate for the scan was outside the quantitative range.
Abbreviations: NA – not applicable, AC – attenuation correction.

Of the twenty seven patients who received ADEPT, fifteen patients completed three PET scans in accordance with the trial protocol. Six patients completed two of the three intended scans. Three patients were too unwell for their final PET scan, the camera had a fault for the final scan in two patients and no tumour was visible for one patient, and so the third scan was not performed. Four patients had only their baseline [F-18] FDG PET scan performed. One of these patients did not go on to receive ADEPT, due to becoming ineligible just prior to receiving treatment. The three remaining patients were too unwell for further [F-18] FDG

PET scans. Two patients had no [F-18] FDG PET scans performed. This was due to the camera not being functional for both patients.

Attenuation correction transmission scans were only performed on all three scans of patient #28. All other patients only had emission scans performed, and Chang attenuation correction of uniform ellipses applied during reconstruction.

Eleven patients (#2-10, #12, #13) received 185MBq of [F-18] FDG and were scanned at 45-60 minutes, and consequently were deemed to not have quantitative scans due to this exceeding the count rate capability of the camera. For one patient (#28) the scan set-up and rescaling information were not recorded, and consequently rescaling could not be applied to the scans.

Therefore there were nine patients in whom quantitative analysis could be performed.

Table 55 shows the results of the quantitative [F-18] FDG PET analysis performed on the patients who received ADEPT with A5CP and ZD2767.

Table 55: Quantitative analysis of [F-18] FDG PET scans in patients who received ADEPT (A5CP and ZD2767P)

Pt No.	Assessment time	CT scan response	VOI			
			total counts	mean	volume	max
#15	4 wks	SD	539%	73%	738%	77%
	8wks	SD	758%	82%	924%	88%
#19	4 wks	SD	138%	90%	154%	96%
	8wks	PD	161%	92%	175%	101%
#18	4 wks	SD	X	X	X	X
	8wks	SD	NA	NA	NA	NA
[redacted]						
#11	4 wks	PD	146%	106%	138%	109%
	8wks	PD	114%	120%	135%	128%
#14	4 wks	PD	381%	125%	305%	165%
	8wks	NA	NA	NA	NA	NA
#20	4 wks	PD	81% (111%)	94% (104%)	87% (107%)	107% (107%)
	8wks	PD	114% (162%)	108% (121%)	105% (134%)	109% (109%)
#24	4 wks	PD	59%	79%	75%	79%
	8wks	*PD	102%	102%	100%	98%
#26	4 wks	PD	184%	91%	201%	92%
	8wks	PD	182%	62%	293%	66%
#23	4 wks	PD	X	X	X	X
	8wks	PD	NA	NA	NA	NA

The quantitative [F-18] FDG PET analysis results on the nine patients in whom analysis was possible participating in the ADEPT A5CP and ZD2767P clinical trial. Values are expressed as a percentage of baseline value. Where applicable, values obtained from VOI subtraction are identified in parenthesis. It was not possible to define tumour regions on patient #18, as the tumour was adjacent to the bladder, and could not be differentiated from it, or on patient #23, as there was inadequate tumour differentiation from background for regions to be generated.

**Patient #24: one of two mediastinal lesions had progressed by on CT scan at 4 weeks, but by 8 weeks the dimensions of this lesion had decreased in size and showed no change when compared to baseline. According to the response criteria used in this study, the response assigned was progressive disease because of the initial progression recorded*

Abbreviations: PD – progressive disease; SD – stable disease; VOI – volume of interest; NA – not applicable; X – not able to be analysed by this technique.

The automated region drawing program was able to define tumour regions on seven of the nine patients (78%). In one patient (patient #18) the tumour was a presacral mass and situated immediately adjacent to the bladder. The region growing program was unable to draw the lesion, as the region drawn spread to the bladder as it was hotter than the tumour. Even with subtraction techniques the presacral mass could not be defined. The second patient's tumours were not sufficiently contrasted from the background tissues to allow region generation (patient #23). In one patient (patient #20) VOI subtraction was required to define visually acceptable tumour regions, and the VOI subtraction values were deemed more representative than the VOI values (displayed in **Figure 59**)

Figure 59: VOI and VOI subtraction in patient #20

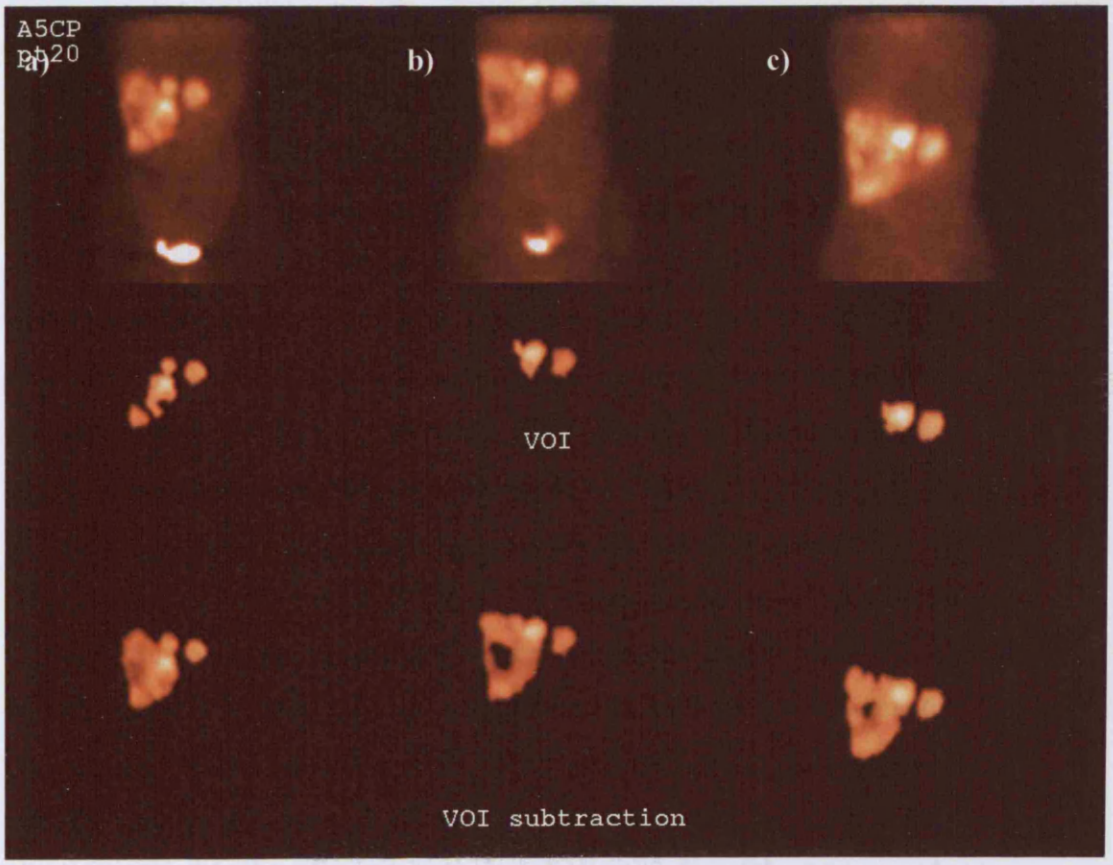

[F-18] FDG PET images from patient #20 in ADEPT A5CP and ZD2767P clinical trial. The [F-18] FDG PET scans are volume images performed a) pre ADEPT, b) 4 weeks after ADEPT and c) 8 weeks after ADEPT. The volumes of interest (VOI) obtained are displayed, along with the volume of interest obtained using subtraction (VOI subtraction). The VOI subtraction images appear more representative of the total tumour mass than the VOI images.

Three patients had stable disease on CT scan at 4 weeks, two of which continued to have stable disease on CT scan at 8 weeks post ADEPT. VOI analysis was performed on two of these patients and both showed an increase in VOI total counts at 4 and 8 weeks. Therefore the [F-18] FDG PET scans in these patients suggest progressive disease.

Of the seven patients who had progressive disease at the 4 and 8 week CT scan, five had VOI analysis performed. The median VOI total counts value at 4 weeks in these patients was 146% (range 59-381%), and at 8 weeks was 132% (range 102-182%). Using an increase of total counts on VOI analysis to 110% compared to baseline as a PET definition for progressive disease, four of the five patients had PET progressive disease at 4 and 8 weeks. The fifth patient was patient #23, in whom the CT scan at 4 weeks showed progression of one mediastinal mass, which reduced in size by 8 weeks. This patient had a CEA expressing non small cell lung cancer with mediastinal lymphadenopathy, previously treated with radiotherapy. The mediastinal masses were very difficult to assess and measure on CT scan as there was uncertainty as to whether abnormal tissue was active tumour, or scarring post radiotherapy. This patient had stable tumour markers with treatment (pre-treatment CEA 85μg/l, 4 weeks 88μg/l, 8 weeks 92μg/l) and remained well on follow-up without the requirement for further chemotherapy or radiotherapy for 10 months after completion of ADEPT. The patient then relapsed with brain metastasis. The [F-18] FDG PET scans on this patient are shown in **figure 60**. The quantitative analysis shows a VOI total count statistic of 59% of baseline at 4 weeks and 102% at 8 weeks. There was a large reduction in the background normal tissues at 4 weeks (liver mean counts/voxel was 72% of baseline), which had returned to acceptable limits by 8 weeks (liver mean counts/voxel was 102% of baseline), which will account for some of the reduction in tumour [F-18] FDG uptake at 4 weeks. However, even with allowance for this, it appears that the metabolic activity of the tumour at least remained stable with ADEPT in this patient.

Figure 60: [F-18] FDG PET scans ADEPT patient #24

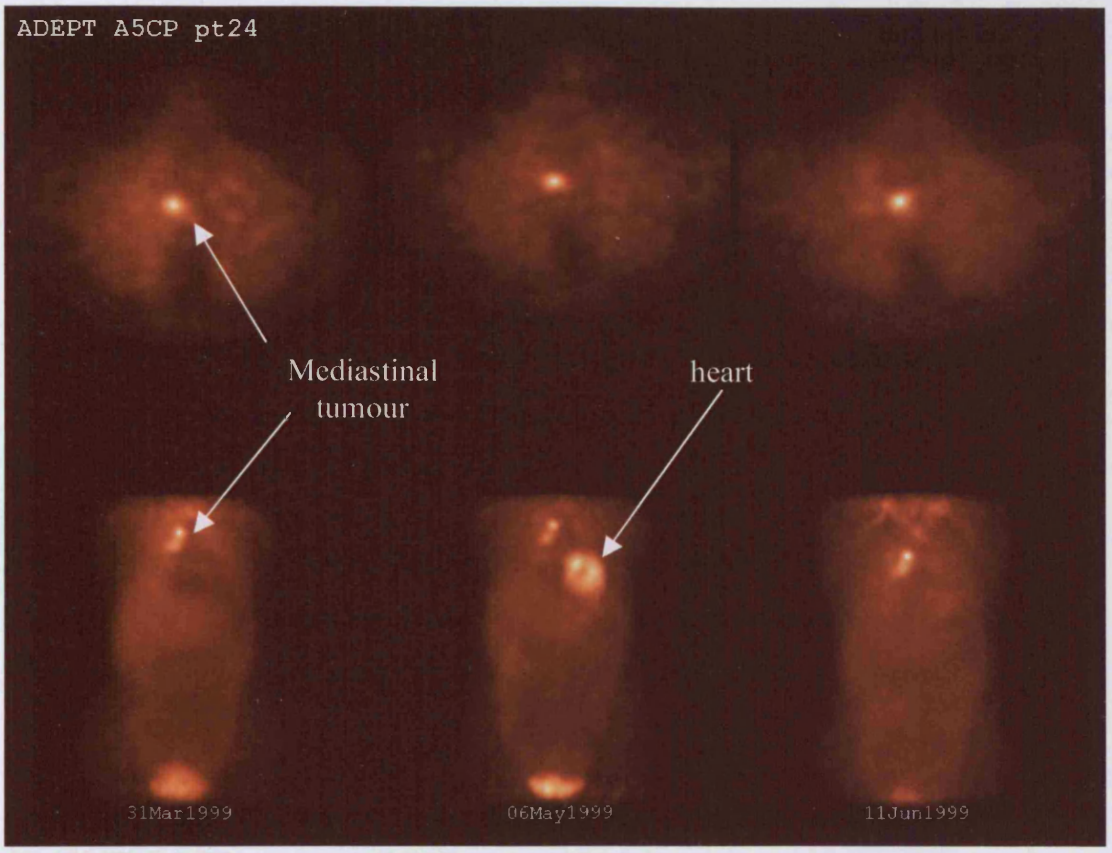

[F-18] FDG PET scans on ADEPT patient #24 taken pre treatment and at 4 and 8 weeks after commencement of treatment. Visually equivalent transverse slices through the mediastinum are displayed, along with volume images.

There were three patients in whom the statistics obtained from the normal tissue regions (liver and lung), and the histograms, suggested a large variation in background [F-18] FDG uptake. These were patients #14, #24 and #26. These results may need, therefore, to be interpreted with caution.

6.2.2 ADEPT MFECP1 and ZD2767P

Method

[F-18] FDG PET scans were a voluntary component of the ADEPT MFECP1 and ZD2767P clinical trial, and were performed pre study, at 2-4 weeks and then 8 weeks post ADEPT therapy. Patients were asked to fast for five hours prior to injection of 130 MBq of [F-18] FDG. Scans were performed at 90 min on the ADAC Vertex Plus Co-Incidence camera. Acquired data was reconstructed using standard iterative protocols, with attenuation correction (attenuation maps were acquired using Caesium–137 sources).

Emission scans had a 50.8cm field of view and were acquired according to the manufacturer's recommendations. Correction for decay was applied on the fly. Most patients had 2 rotations performed; however some patients required 3 rotations.

Reconstruction was performed using standard ADAC iterative reconstruction protocol, with attenuation correction applied based on transmission data. Analysis of [F-18] FDG PET was performed after correction for injected dose and time to scanning. A formal correction for blood glucose levels was not made, however data with blood glucose levels outside the range 4-7mmol/L were deemed unreliable.

Analysis was performed using lesion statistics derived from the regions obtained from the automated region drawing program, as described above. Count density histograms were also displayed for tumour and normal tissue (live, lung, chest wall) regions.

CT scans were performed on patients prior to the commencement of ADEPT and at 4 and 8 weeks after ADEPT as outlined in the trial protocol (**chapter 4**) Response on CT scan was assessed using unidimensional measurements as part of the RECIST criteria (Therasse *et al*, 2000).

Results

Nine of thirteen patients participated in the [F-18] FDG PET component of the ADEPT study (**table 56**).

Table 56: [F-18] FDG PET scans in ADEPT MFECP1 and ZD2767P clinical trial

Pt No.	Number of [F-18] FDG PET scans	Comment
#1	0	Camera fault
#2	2	2nd scan – problems with [F-18] FDG injection
#3	2	3rd scan - patient too unwell
#4	2	3rd scan - camera fault
#5	3	
#6	2	scan 1 - corrupt data
#7	3	
#8	3	
#9	2	2nd scan performed at 6 weeks. No 3rd scan
#10	0	Patient refused
#11	2	3rd scan - camera fault
#12	0	Camera fault
#13	0	Camera fault

Quantitative analysis was performed in seven of these patients' scans (the data acquired for patient #6 was corrupt and no analysis could be performed, and problems with the injection of [F-18] FDG for the second scan for Patient #2 meant that the exact injected dose was uncertain).

All patients show an increase in tumour [F-18] FDG uptake after ADEPT (see **Table 57**) In two patients (#8 and #11) tumour regions could not be defined on the baseline [F-18] FDG PET scan, however they could be defined on the post treatment scan. This would be consistent with disease progression (PD). Quantitative analysis of Patient #9 revealed an abnormal degree of change in [F-18] FDG uptake in background normal tissues (lung and chest wall) between the pre-study and 6 week scan, which would suggest that the quantitation of tumour [F-18] FDG uptake may not be reliable.

The patient with the smallest increases in tumour [F-18] FDG uptake by VOI total counts was patient #7, who attained stable disease on CT scan. This may indicate that the degree of tumour progression in this patient was less than for the other patients, however, the small sample size makes further interpretation difficult.

Table 57: [F-18] FDG PET analysis of patients in ADEPT trial of MFECP1 and ZD2767P

Pt No.	Assessment time	CT scan response	VOI			
			total counts	mean	volume	max
#7	4 wks	SD	109%	120%	90%	128%
	8wks	SD	126%	129%	98%	138%
#11	4 wks	SD	PD	PD	PD	PD
	8wks	SD	ND	ND	ND	ND
#3	4 wks	PD	240%	98%	244%	106%
	8wks	PD	ND	ND	ND	ND
#4	4 wks	PD	129%	138%	94%	158%
	8wks	NA	ND	ND	ND	ND
#5	4 wks	PD	173%	120%	144%	134%
	8wks	PD	469%	124%	379%	147%
#8	4 wks	PD	PD	PD	PD	PD
	8wks	PD	PD	PD	PD	PD
#9	4 wks	PD	ND	ND	ND	ND
	8wks	PD	*601%	*224%	*268%	*227%

The quantitative [F-18] FDG PET analysis results on the seven patients in whom analysis was possible participating in the ADEPT MFECP1 and ZD2767P clinical trial. Values are expressed as a percentage of baseline value.
** background 'normal'/ tissues in this patient varied greatly between scans, indicating that data may not be accurate.*
Reasons for ND (not done): Patient #3 too unwell for 8 weeks scan; Patients #4 and #11 ADAC camera fault for 8 weeks scan; Patient #9 scan performed at 6 weeks due to fault in ADAC camera prior to this.
Abbreviations: PD – progressive disease; SD – stable disease; VOI – volume of interest; NA – not applicable; ND – not done; X – not able to be analysed by this technique

Figure 61 displays the volume of interest drawn by the automated region growing program for patient #5. **Figure 62** displays the count density histogram for the tumour volumes. The count density histogram and the lesion statistics in this patient indicate tumour progression, with an increase in tumour [F-18] FDG uptake after treatment with ADEPT. **Figure 63** displays the count density histograms of the normal tissues (liver, lung, chestwall) from patient #5, showing very little variation in background [F-18] FDG uptake between scans.

Figure 61: VOI derived from automated region growing program for patient #5

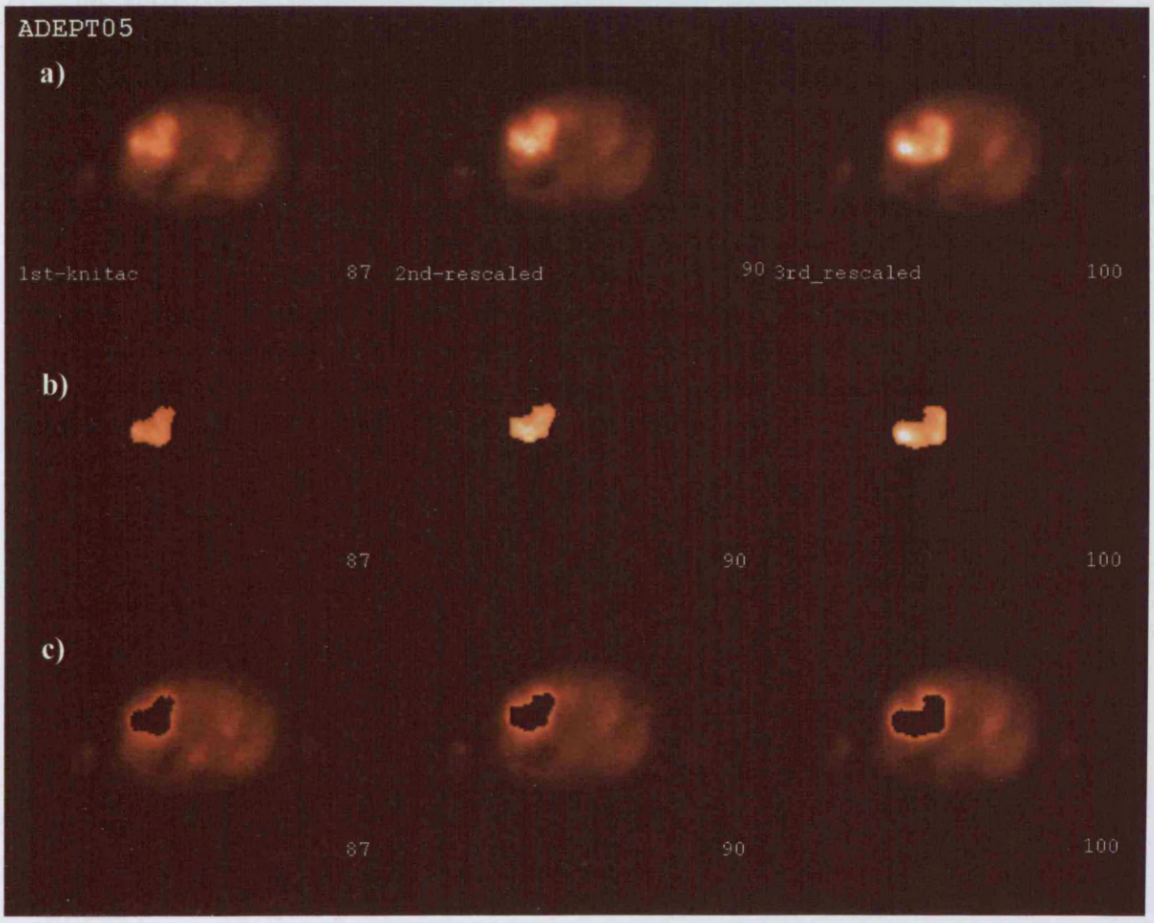

Figure 61 a) displays equivalent transverse slices of the three [F-18] FDG PET scans performed on patient #5. The images show a liver metastasis from colorectal cancer. Figure 61 b) displays the tumour region derived using the automated region drawing program at the same transverse slice. Figure 61 c) displays the tumour region subtracted out of the image.

Figure 62: Count density histogram of tumour regions from patient #5

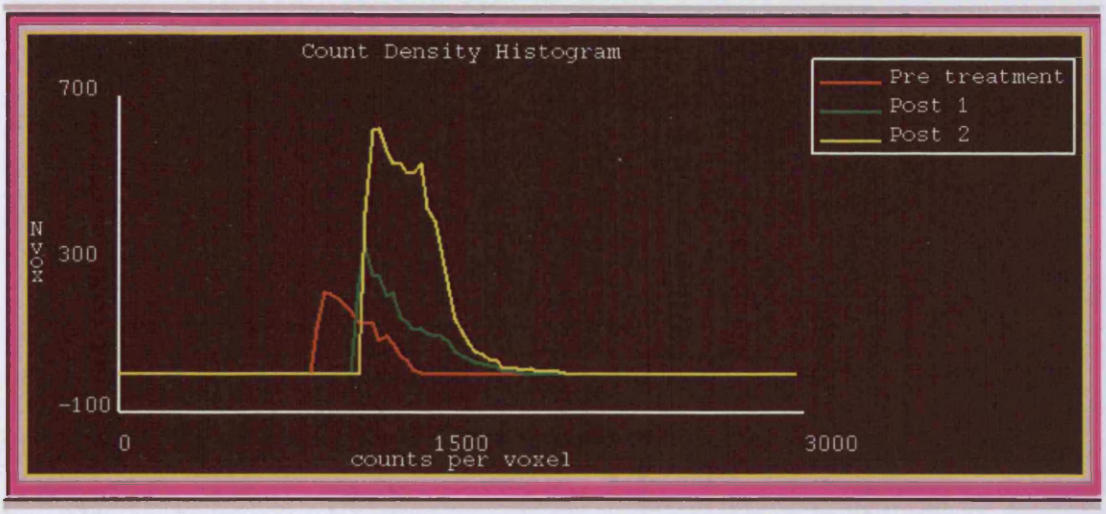

Count density histograms of the tumour regions derived from patient #5 using the automated region drawing program. The tumour region derived from the pretreatment [F-18] FDG PET scan is red, the 4 week scan is the green line and the 8 week scan is the yellow line. There has been a right shift on the x-axis after treatment, representing an increase in intensity of [F-18] FDG uptake. There is also an increase in volume of the tumour region after treatment, as represented by an increase in area under the curve. The increase in both intensity and tumour volume are consistent with tumour progression.

Figure 63: Count density histograms of normal tissue regions from patient #5

a)

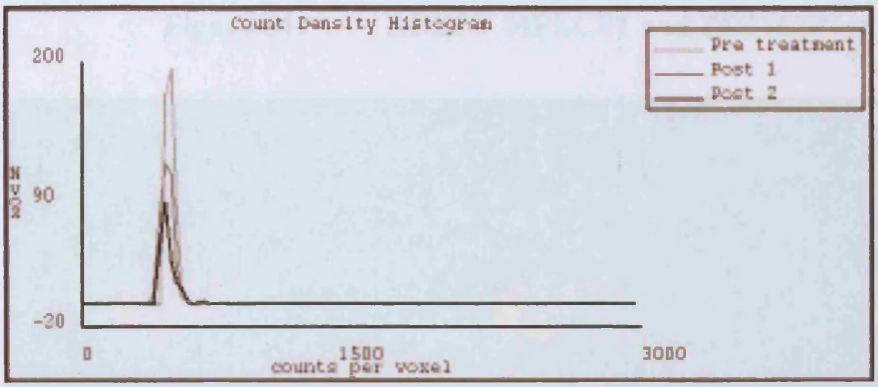

b)

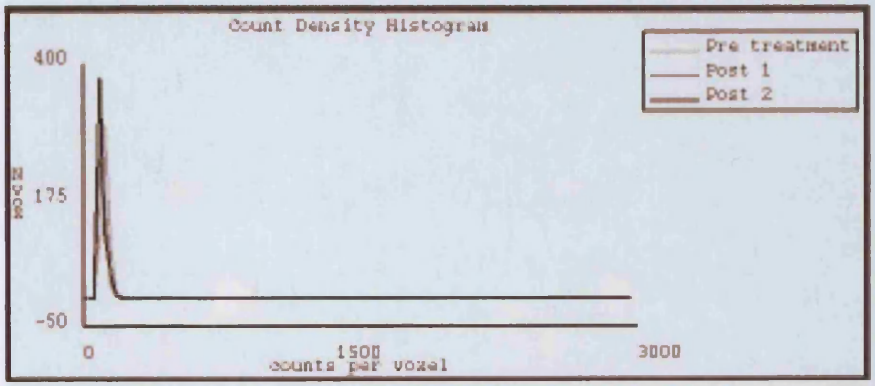

c)

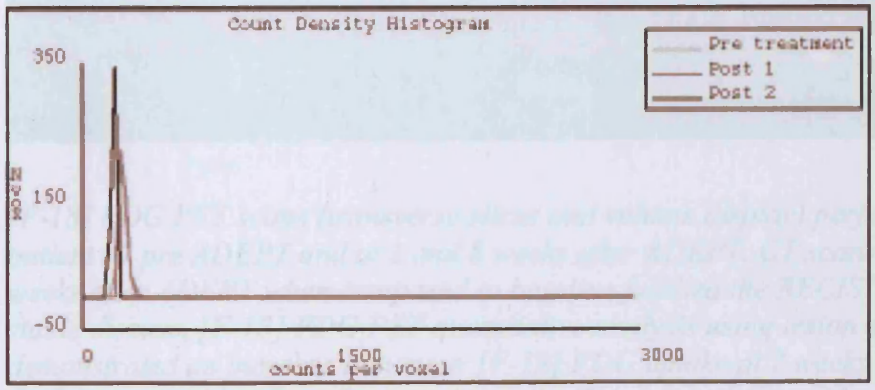

Normal tissue count density histograms from patient #5 taken pre ADEPT, then 2 and 8 weeks post ADEPT.
a) Liver
b) Lung
c) Chestwall
There is very little variation in the background tissues, suggesting the background tissues did not change significantly between scans, This supports the concept that the changes found in the tumour areas were real changes, and not as a result of variations in the overall [F-18] FDG uptake in the scans.

Figure 64 displays the [F-18] FDG PET images from patient #7 who attained stable disease on CT scan at 4 and 8 weeks.

Figure 64: ADEPT MFECP1 and ZD2767P – patient #7

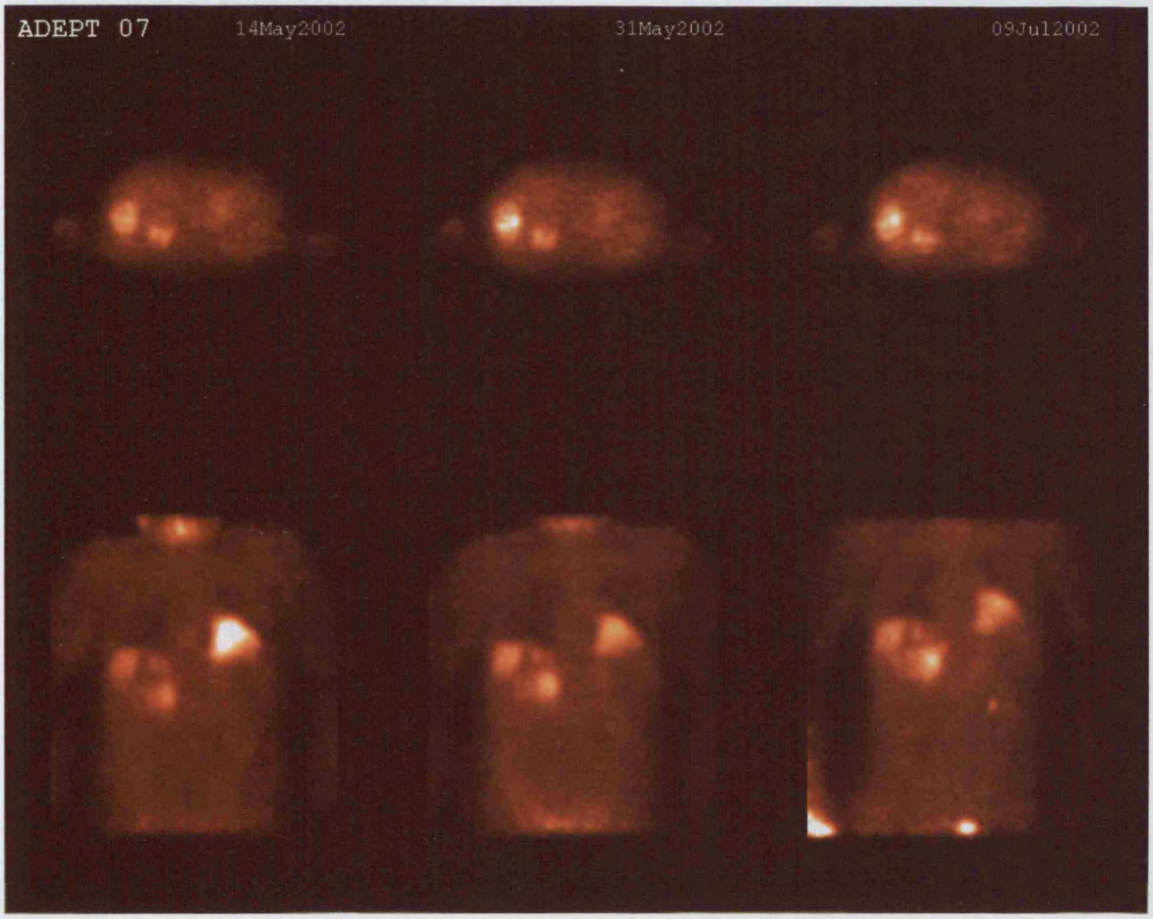

[F-18] FDG PET scans (transverse slices and volume display) performed on patient #7 pre ADEPT and at 2 and 8 weeks after ADEPT. CT scans at 4 and 8 weeks after ADEPT when compared to baseline fulfilled the RECIST criteria for stable disease. [F-18] FDG PET quantitative analysis using lesion statistics demonstrated an increase in tumour [F-18] FDG uptake at 2 weeks, which had further increased at 8 weeks post treatment. This is consistent with progressive disease by [F-18] FDG PET analysis.

6.3 Discussion

[F-18] FDG PET scans were performed as part of the ADEPT phase I/II clinical trials to enhance the assessment of response to ADEPT and to aid in the interpretation of radiological stable disease.

The concept of using [F-18] FDG PET to assess dose-responsiveness of a phase I drug was proposed in 1995 by Price *et al* (Price *et al*, 1995). This concept can be adapted for ADEPT phase I/II clinical trials as they are dose-escalation studies. It is proposed that at initial prodrug doses there may be an initial increase in tumour [F-18] FDG uptake as the prodrug dose is inadequate for therapeutic effect. As therapeutic doses are reached the tumour [F-18] FDG uptake reduces. If there is a dose-dependent effect on the tumour, tumour [F-18] FDG uptake may reduce incrementally with increasing prodrug doses. This could provide evidence for efficacy of ADEPT, even if radiological imaging did not result in 'responses'.

[F-18] FDG PET to assess response to ADEPT will be discussed below in terms of the interpretation of the [F-18] FDG PET results in both ADEPT studies and a discussion of the technical issues and feasibility of using [F-18] FDG PET for response assessment

6.3.1 Response in ADEPT phase I/II clinical trials as assessed by [F-18] FDG PET

In the ADEPT clinical trial of A5CP and ZD2767P, all patients, except patient #24, had an increase in tumour [F-18] FDG uptake after ADEPT. The two patients (#15 and #19) who had radiological stable disease and [F-18] FDG PET scans suitable for quantitative VOI analysis, both had increases in tumour [F-18] FDG uptake, indicating a lack of response to ADEPT. This would be consistent with the trial's mechanistic study findings, which indicate that there was inadequate tumour targeting of A5CP. This would lead to a very low likelihood of efficacy.

Anecdotally, patient #24, who was a chemo-naive patient with mediastinal lymph node involvement from non small cell lung cancer, had an initial reduction in

tumour [F-18] FDG uptake and then returned to baseline levels of [F-18] FDG uptake. The background normal tissues also showed a drop in [F-18] FDG uptake at the 4 week PET scan, which may account for some of the fall in tumour [F-18] FDG uptake. At 8 weeks the background [F-18] FDG uptake and tumour [F-18] FDG uptake was stable. This patient's CT scan was difficult to interpret due to previous mediastinal radiotherapy leading to some uncertainty as to the size of mediastinal lymph nodes. This is an area where CT scans have limitations, as differentiation between post radiotherapy fibrosis and tumour recurrence cannot be easily identified. The CT scan measurements indicated an increase in tumour size at 4 weeks and a reduction to baseline tumour size at 8 weeks. This patient did not, however, require any further treatment for her non small cell lung cancer for 10 months after ADEPT, and her tumour markers remained stable. This patient had many features that would increase the likelihood of her tumour responding to ADEPT. Non small lung cancer is known to be responsive to alkylating agents, she had not had any previous chemotherapy and the volume of her disease was small. It is possible therefore, that in this one patient, tumour [F-18] FDG uptake was stable after ADEPT, and metabolically the tumour may have therefore been stable with treatment.

In the ADEPT study of MFECP1 and ZD2767P, again all tumours showed an increase in tumour [F-18] FDG uptake after ADEPT. This included two patients with stable disease on CT scan. This trial remains in the dose escalation phase, with dose escalation occurring at dose-doubling rates. The preclinical data suggests that a much higher prodrug dose than is currently being used is required for efficacy. It is again, therefore, not unexpected that there has been no reduction in tumour [F-18] FDG uptake after ADEPT, as the prodrug doses used so far in the clinical trial are likely to be subtherapeutic. It is perhaps encouraging that the smallest increase in tumour [F-18] FDG uptake occurred in patient #7, who attained radiological stable disease after ADEPT. This may suggest that there has been some minor effect of ADEPT in this patient, by reducing the amount of tumour [F-18] FDG uptake relative to the other patients, or it may just be a reflection of a more indolent disease in that patient.

As none of the patients participating in either ADEPT clinical trial had a response to ADEPT on their [F-18] FDG PET scans, it appears unlikely that any patients have had a metabolic response to therapy. The reasons for this are understood – for ADEPT with A5CP and ZD2767P, there was inadequate localisation of antibody-enzyme, and for ADEPT with MFECP1 and ZD2767P dose escalation in continuing. It is difficult therefore to accept or refute the hypothesis that [F-18] FDG PET may be more sensitive in detecting a response to ADEPT than conventional imaging. [F-18] FDG PET imaging did, however, appear useful in the interpretation of radiological stable disease. In the four combined patients from both ADEPT trials who had stable disease on CT scan and quantifiable [F-18] FDG PET scans, all appeared to have progression of disease by metabolic imaging.

6.3.2 Technical issues in using [F-18] FDG PET for assessment of response in ADEPT

Attenuation correction

[F-18] FDG PET scans performed on patients in the ADEPT A5CP and ZD2767P study were performed without attenuation correction. This presents several potential problems. Firstly the patients must be scanned with their arms out of the field of view (usually held above their head), as the arms will attenuate the emissions from the body. This can be very difficult for the patient as the scan time is usually 60 minutes. Secondly a uniform correction algorithm of ellipses had to be applied to the scan for attenuation correction (Chang, 1978). This is based in the principle that the deeper within the body that the photon originated from, the more the attenuation that occurs prior to it reaching the detectors. This method does not take into account the different amounts of attenuation that occur as the photon passes through different substances. Air, water and solid organs all attenuate the photon differently. Transmission scans identify these different states in order to apply an appropriate correction for the attenuation that occurs in the photon as it passes through. However, without this information the correct attenuation factor cannot be applied. Consequently, the ability to detect small lesions, particularly in the lung, is reduced without measured attenuation correction (Ak *et al*, 2001). In addition, the differentiation between tumour and

normal tissues may not be as well defined as with attenuation corrected images. This may hinder the ability of the automated region drawing program to depict tumour regions.

Despite these limitations, it was possible to define tumour regions using the automated region growing program, in seven of nine patients. In two patients the automated region growing program could not define the tumour – in patient #18 the tumour was a presacral mass and was adjacent to the bladder. Even when subtraction techniques were employed, the tumour could not be generated as the tracer within the bladder could not be separated from the tumour. In patient #23, there was inadequate differentiation between tumour and surrounding liver to allow a region to be generated. This patient's scans are displayed below (**Figure 65**). There was one patient (patient #20) in whom the initial tumour region did not appear representative of the entire tumour, therefore VOI subtraction was employed.

Figure 65: [F-18] FDG PET scans from Patient #23 ADEPT A5CP and ZD2767P

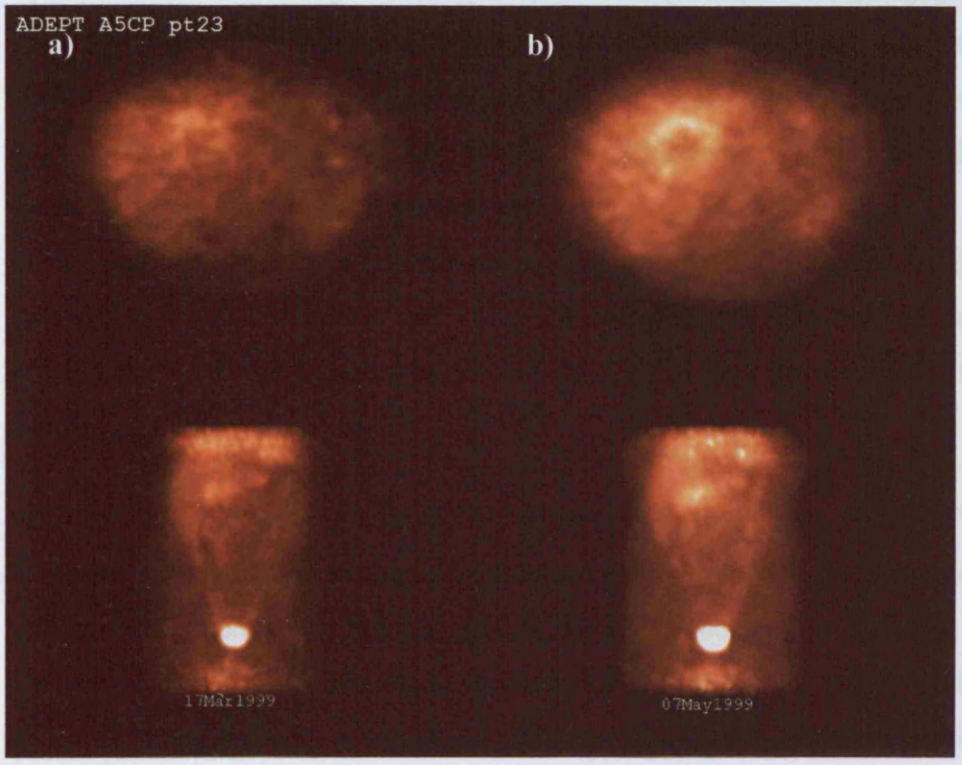

Chang attenuated [F-18] FDG PET scans (transverse slice and volume display) on patient #23 performed a) pre and b) post treatment with ADEPT A5CP and ZD2767P. The differentiation between tumour (liver metastasis from colorectal cancer) and normal liver was not adequate for region generation.

Singles count rates and detector flooding

In the ADEPT A5CP and ZD2767P study the data on eleven patients could not be used as it was found that the injected dose of [F-18] FDG and the time to scanning were such that the acquired singles count rate exceeded the quantitative range of count rate capability of the camera. This resulted in 'flooding' of the detectors. Consequently the relationship between count rate and radioactivity at these high levels was non-linear, and therefore was not quantitative.

Scan setup and patient preparation

In the ADEPT A5CP and ZD2767P trial [F-18] FDG PET scans were performed at 60 minutes post administration of [F-18] FDG. As previously discussed evidence is emerging that the uptake of [F-18] FDG into tumour cells may not

have reached a plateau at this time point, and waiting longer between time of injection and time of scanning would therefore be more desirable for reproducible results. The protocol developed in the [F-18] FDG PET assessment study (**chapter 5**) was followed for the ADEPT MFECP1 and ZD2767P study, with the injected dose of [F-18] FDG reduced to 130MBq and the time of scanning to 90 minutes. In addition [F-18] FDG PET scans were performed at 2 weeks rather than 4 weeks after treatment. This, along with the additional advantage of having measured attenuation correction available for the ADEPT MFECP1 trials means that the data collected from this study is more comparable with the results obtained from the [F-18] FDG PET assessment study than the ADEPT A5CP trial.

As discussed in **chapter 5**, it is of critical importance that if serial [F-18] FDG PET scans are to be used to assess response to therapy, the patient preparation parameters and scan setup parameters must be kept as constant as possible between scans. This includes injected [F-18] FDG dose, time to scanning, fasting time, number of rotations scanned, patient's position on the camera, camera start and stop points. This allows the possible confounding effects of all of these features to be minimised as much as possible. The count density histograms of the normal tissues (liver, lung , chest wall) are used as an indication of how much the 'background' of the scan has varied at serial time points. The majority of patients, especially in the ADEPT MFECP1 study, had normal tissue regions that remained very consistent in their [F-18] FDG uptake between scans. This improves the likelihood that a change in tumour [F-18] FDG uptake is a true tumour specific effect related to the therapy given, rather than a global 'whole body' change in [F-18] FDG uptake.

6.3.3 Feasibility of using [F-18] FDG PET in the assessment of response in phase I/II ADEPT clinical trials

The addition of [F-18] FDG PET scans to the trial protocol appeared feasible, with the main reason that some patient did not complete the [F-18] FDG PET scans being camera faults. The availability of off-site [F-18] FDG was adequate in both the clinical trials and did not prove to be a limiting factor.

The main limitation to the addition of the [F-18] FDG PET scans to the ADEPT trial protocols is that it requires patients to have three additional scans. Patients who participate in phase I/II clinical trials may undergo a large number of invasive or non-invasive tests as a result of being in a clinical trial. The addition of three [F-18] FDG PET scans may be too much of a burden for some patients. It was for this reason that the [F-18] FDG PET component of ADEPT was made optional in the ADEPT MFECP1 study.

The region growing program for the delineation of tumour regions and the subsequent interpretation of these regions using lesion statistics and histogram analysis was successfully applied in the majority of patients. Two of nine patients (22%) could not have regions defined in the ADEPT A5CP group. The absence of true attenuation correction for these scans may have contributed to the difficultly in defining tumour regions in these patients. Two of the seven patients in the ADEPT MFECP1 group could not have tumour defined on the baseline scan, but they were defined on subsequent scans, indicating a progression of disease. Unfortunately however, because the initial tumour regions could not be defined, the degree of progression could not be quantified.

6.4 Conclusion

Both ADEPT clinical trials reported in this thesis included [F-18] FDG PET for the assessment of response to therapy. This was undertaken in order to ascertain if [F-18] FDG PET was more sensitive than conventional radiological imaging in the detection of response in a phase I/II clinical trial setting, and to assist in the interpretation of radiological stable disease. None of the patients in either ADEPT clinical trial, including those who attained stable disease on CT scans, demonstrated a metabolic response to ADEPT using [F-18] FDG PET. The reasons for a lack of response to ADEPT are understood, and the [F-18] FDG PET analysis results therefore supported the findings of the mechanistic studies performed in both clinical trials.

The inclusion of [F-18] FDG imaging protocols in future ADEPT clinical trials appears feasible, and the VOI analysis technique developed and validated in **chapter 5** were applicable in the phase I/II clinical trial setting. The collection of

more data as the ADEPT MFECP1 clinical trial progresses will be valuable to the understanding of the role metabolic tumour imaging may have in the assessment of response to therapy in phase I/II clinical trials.

7 ADEPT Conceptual Model and Ontology

7.1 Background

Mechanistic trials generate large quantities of data, which can be overwhelming. Interpreting this data into knowledge is challenging, especially as increasing information is attained. The clinical trials reported in this thesis are the third and fourth ADEPT clinical trials using this particular ADEPT system, and integrating clinical trial data from all four trials would greatly add to knowledge, but logistically is difficult. In addition the world-wide knowledge base about tumours, targets, genomics, proteomics and novel therapeutics is constantly growing and changing rapidly. A system of organising and integrating all of this data is therefore required. It is proposed that this process will facilitate clinical trial design and further direct the rational development of ADEPT.

7.2 Aim

Informatics aims to organise data in a meaningful way for the purpose of aiding interpretation and knowledge of complex data. Bioinformatics is 'the application of tools of computation and analysis to the capture and interpretation of biological data' (Bayat, 2002). Bioinformatics has been adopted as the term used to describe the organisation of molecular and pathway data, whereas informatics refers to the organisation of non-molecular data. Both informatics and bioinformatics are rapidly expanding fields. The Human Genome Project and the advent of array technology have been some of the driving forces behind it. The amount of data that has been generated on genomics and proteomics has been astronomical. Organising these data into a form that can be accessed by others, and used in a meaningful way has been challenging.

One method of organising data is by using a relational ontology. An ontology has been defined as specification of a conceptualisation, or a description of all the concepts and relationships of a specified agent (Gruber, 1993). An ontology is designed to enhance 'knowledge sharing' or re-use of knowledge. A relational ontology aims to list concepts and relationships in a hierarchical way. Ontologies

are now publicly available via the internet for gene and protein structure and function. They have been developed with the aim of organising this information and making it more accessible.

It is hypothesised therefore that the development of a hierarchical ontology of ADEPT may aid in the organisation of the data acquired from ADEPT. The ontology is used to define the key terms of ADEPT. A conceptual model may be additionally used in order to visually represent the overlap and relationship between components. From this identification of terms and relationships a database may be developed in which the mechanistic data acquired from ADEPT may be stored in an organised manner, which would be accessible for queries. The organisation of data may also be useful to direct clinical trial design by identifying where more data needs to be collected to develop an understanding of the mechanism of ADEPT in the clinical setting. It may also help identify and direct the areas of modification required to enhance ADEPT for the future.

The three aims of the ADEPT Ontology and Conceptual Model therefore were to

1) organise the data acquired from ADEPT
2) aid in clinical trial design by identifying areas where the acquisition of mechanistic data may provide useful information to improve the understanding of ADEPT in the clinical setting.
3) identify areas of ADEPT which may require improvement

7.3 ADEPT Ontology

7.3.1 Method

The ADEPT ontology was created using Protégé-2000, an ontology tool, from Stanford University School of Medicine (Protégé, 2000). Protégé-2000 is an open-source java tool for creating the architecture for a hierarchical ontology. It consists of 'classes', which are the components of the agent being described, and 'slots' which make up the features and attributes of the classes. 'Instances' consist of data entered into the slots, and can form, in conjunction with the Ontology and its classes, a knowledge base.

In practical terms, classes of the Ontology are defined, and then ordered into a subclass-superclass hierarchy. Slots are then developed, which are 'data entry points'. Limitations can be made on the type of data entry required. For example it is possible to stipulate if a description is required or a yes/no data point. In addition, data may be compulsory or optional. The data that is entered is into the slots are the 'instances'.

It was beyond the scope of this current work to fully define all slots and instances for the ADEPT Ontology. Instead, the class structure was the main focus, and examples of slots and instances have been used throughout.

7.3.2 Results

The ADEPT Clinical Trials Ontology has five 'superclasses': Patient, Tumour, Target, Therapeutic and Therapy (**figure 66**). Each will be described individually below.

Figure 66: ADEPT Ontology – superclasses

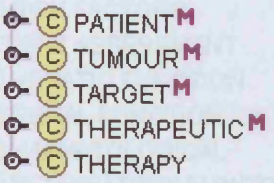

Patient

The patient forms the environment in which any therapy is ultimately tested. Being able to access data that describes and defines the patient is therefore required. This allows a record to be kept of the features of the patient group in which a therapy has been tested. Clinical trial protocols will outline inclusion and exclusion criteria, aimed to define a relatively homogenous physiological environment within a patient group. In particular body systems such as renal function, liver function and bone marrow function may influence biodistribution, metabolism, excretion and toxicity from a therapy. These will usually have limits placed on them and values recorded for them in a clinical trial. Additional information that may be important to store include patient demographics (age, gender, body surface area), a record of current medications and any co-morbidities.

In addition the patient has a disease state which, for this ontology, is cancer. This also needs describing in terms of tumour type and classification (link to TUMOUR superclass), previous treatments, and an assessment of disease burden – which may require re-assessment at a variety of time points. These assessments may consist of a record of disease sites, radiological assessment (eg: CT scan), functional imaging assessment (eg: [F-18] FDG PET), tumour markers and temporal measures such as survival (**figure 67**).

Figure 67: Patient subclasses in Ontology

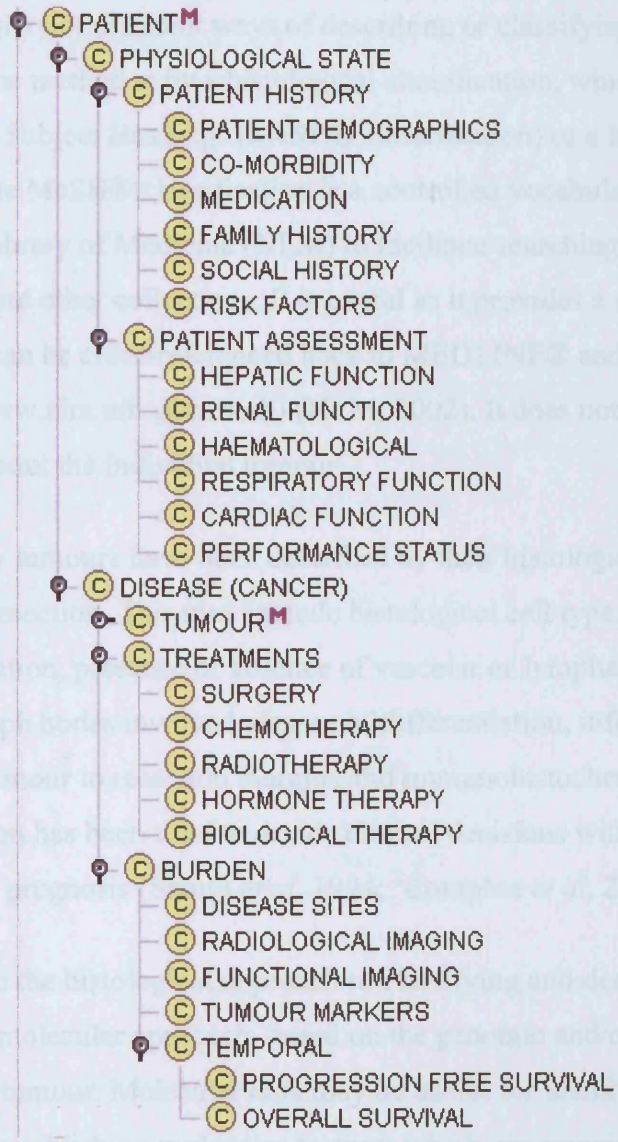

Tumour

There are a variety of different ways of describing or classifying a tumour (**figure 68**). One method is by a histological classification, which may include either Medical Subject Headings (MeSH® classification) or a histological description. The MeSH® classification is a controlled vocabulary developed by the National Library of Medicine (NLM) to facilitate searching for articles in MEDLINE® and other collections. It is useful as it provides a standardised language that can be cross-referenced back to MEDLINE® and other search tools (http://www.nlm.nih.gov/mesh) (NLM, 2002). It does not however provide specific data about the individual tumour.

Conventionally tumours have been described by their histological appearance after surgical resection. This may include histological cell type, grade, stage, TNM classification, presence or absence of vascular or lymphatic invasion, number of lymph nodes involved, degree of differentiation, information on proximity of tumour to resection margins and immunohistochemistry findings. This information has been used to decide clinical decisions with regard to treatments and prognosis (Stangl *et al*, 1994; [2]Compton *et al*, 2000).

An alterative to the histological approach to classifying and describing tumours, there is now a molecular approach, based on the genomic and/or proteomic features of the tumour. Molecular data may be useful for identifying targets for therapy, or by establishing molecular features which are associated with increased or decreased likelihood of responding to a particular treatment (Adlard *et al*, 2002).

A gene ontology termed GO (Gene Ontology) has been developed by the Gene Ontology Consortium (The Gene Ontology Consortium, 2001). It may be accessed by amiGO, which is an HTML browser for the Gene Ontology, and allows navigation through the Ontology via the internet (www.godatabase.org). The Gene Ontology is actually three ontologies used to describe attributes of gene products. These three ontologies are biological process, cellular component and molecular function.

Ensembl is a genome database that collects and stores all available genomic data (www.ensembl.org). DNA sequences or known genomic constructs can be located and viewed via the database.

An example of a database of proteins is InterPro (www.ebi.ac.uk/interpro) (Apweiler *et al*, 2000). It consists of protein families, domains and functional sites in which identifiable features found in known proteins can be applied to unknown protein sequences.

These gene and protein ontologies and databases could be linked to by the ADEPT clinical trial ontology or database, in order to access molecular information relevant to the tumours being studied.

Figure 68: Tumour subclasses

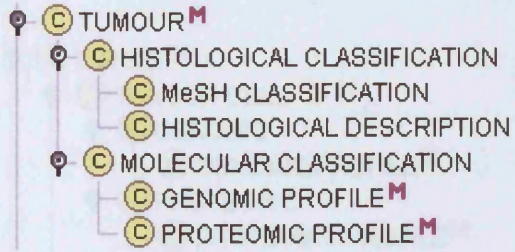

Target

Potential targets for tumour-directed treatments may be part of the tumour cell or may occur in the surrounding tumour vasculature or stroma (**figure 69**). Genomics and proteomics are having an increasing role in defining specific molecular features of tumours, which may represent abnormalities of 'normal' biological processes (Saijo *et al*, 2003; Workman, 2003). These may form suitable targets for novel treatments. As part of the Ontology, links could be created between the superclass TARGET and known genomic and proteomic databases and Ontologies to facilitate target identification and characterisation.

For the purpose of this Ontology, the Proteomic subclass of Tumour Cell has been further subdivided into Cell Process, Differentiation Antigen, Immunoglobulin Idiotype or Tumour Antigens. The cell processes in tumour cells which may be targeted include signal transduction pathways (eg: growth

factor receptors, tyrosine kinases, RAS signal transduction proteins), cell cycle regulators (eg: cyclin-dependent kinases) or apoptotic pathways (eg: p53). Differentiation antigens (eg: CD20, CD25, CD33) and immunoglobulin idiotypes (B cell lymphomas) are of particular relevance to haematological malignancies. Melanomas may however also express differentiation antigens (eg: MelanA/MART-1, gp100/Pmel 17, gp75/TRP-1) (Roitt *et al*, 2001) Tumour antigens are a heterogenous group of molecules that have been found to be associated with tumours, but their molecular role in carcinogenesis is not always well understood. These may include the oncofetal proteins (carcinoembryonic antigen, alphafetoprotein, human chorionic gonadotrophin), cancer testis antigens (eg: MAGE, GAGE, BAGE), or other glycoproteins (eg: CA17-1A, CA19-9, CA15-3).

Figure 69: Target subclasses

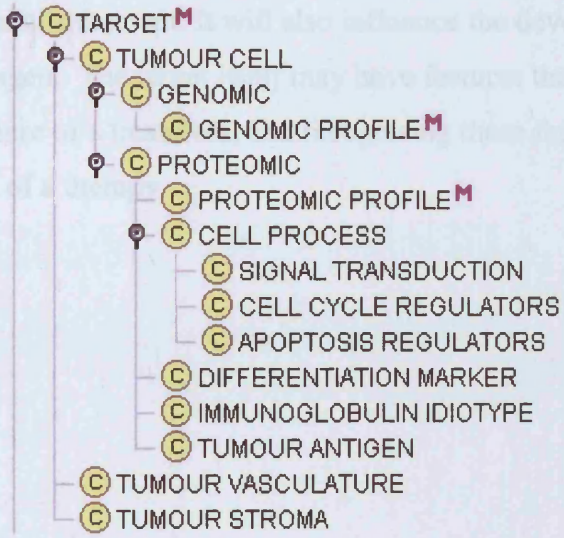

The Tumour Antigen subclass has had slots defined for it in the Ontology, as this is of particular relevance for the ADEPT system discussed in this thesis. These slots aim to define the characteristics of the tumour antigen. They include name, classification, molecular size, structure, chromosome, function, site (intracellular or cell surface), normal tissue expression, distribution in tumour, mechanism of expression, secreted form (yes or no), cancer types which express it, possible cross-reactivity, prevalence, method of measurement of serum levels and tumour levels of expression, and values for serum quantity or tumour quantity of expression. These slots have been chosen as they both describe the antigen, and

are of relevance to its usefulness as a target. There are also slots linking the instance to known Ontologies and Databases available on the internet. These include GO gene consortium (www.godatabase.org), the Ensembl gene database (www.ensembl.org), InterPRO (www.ebi.ac.uk/interpro) and Swiss-Prot (www.ebi.ac.uk/swissprot).

CEA, as the target for ADEPT in this thesis, has been entered in as an Instance (**figure 70**). The characteristics of CEA have been listed and links to the gene and protein databases recorded. These existing databases allow access to detailed information such as chromosome location, DNA sequence, amino acid sequence and function. An example of some of the information that can be accessed is displayed in **figure 71**.

CEA is just one of many possibilities as a target for a treatment such as ADEPT. Listing the attributes of a target may aid in deciding the most appropriate target to use for a particular treatment. It will also influence the development process for a therapeutic agent. The target itself may have features that will contribute to the success or failure of a treatment, and recognising these features should be a part of the design of a therapy.

Figure 70: Tumour Antigen Slots with CEA entered as an Instance

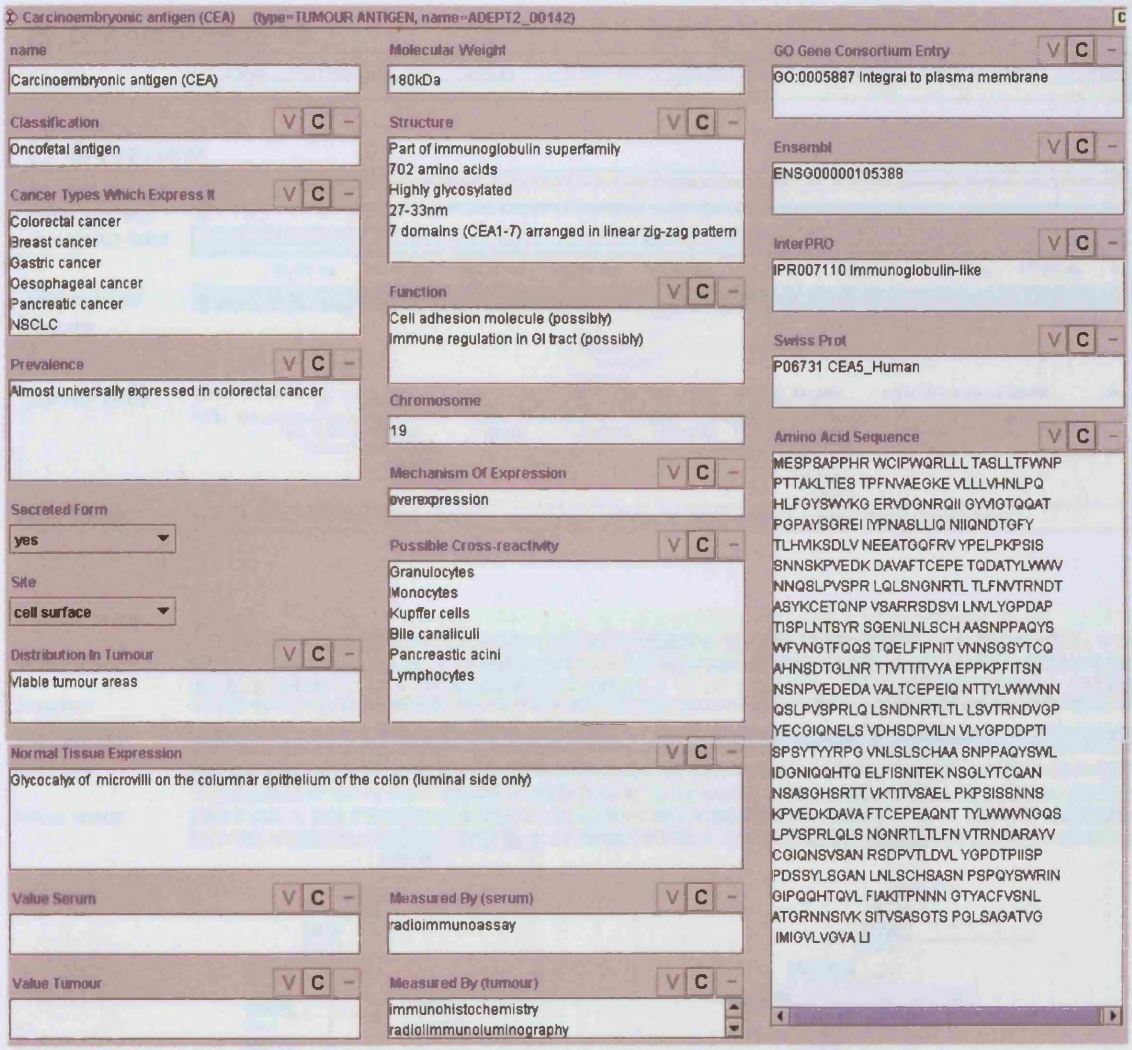

Figure 71: CEA chromosome location and sequence information

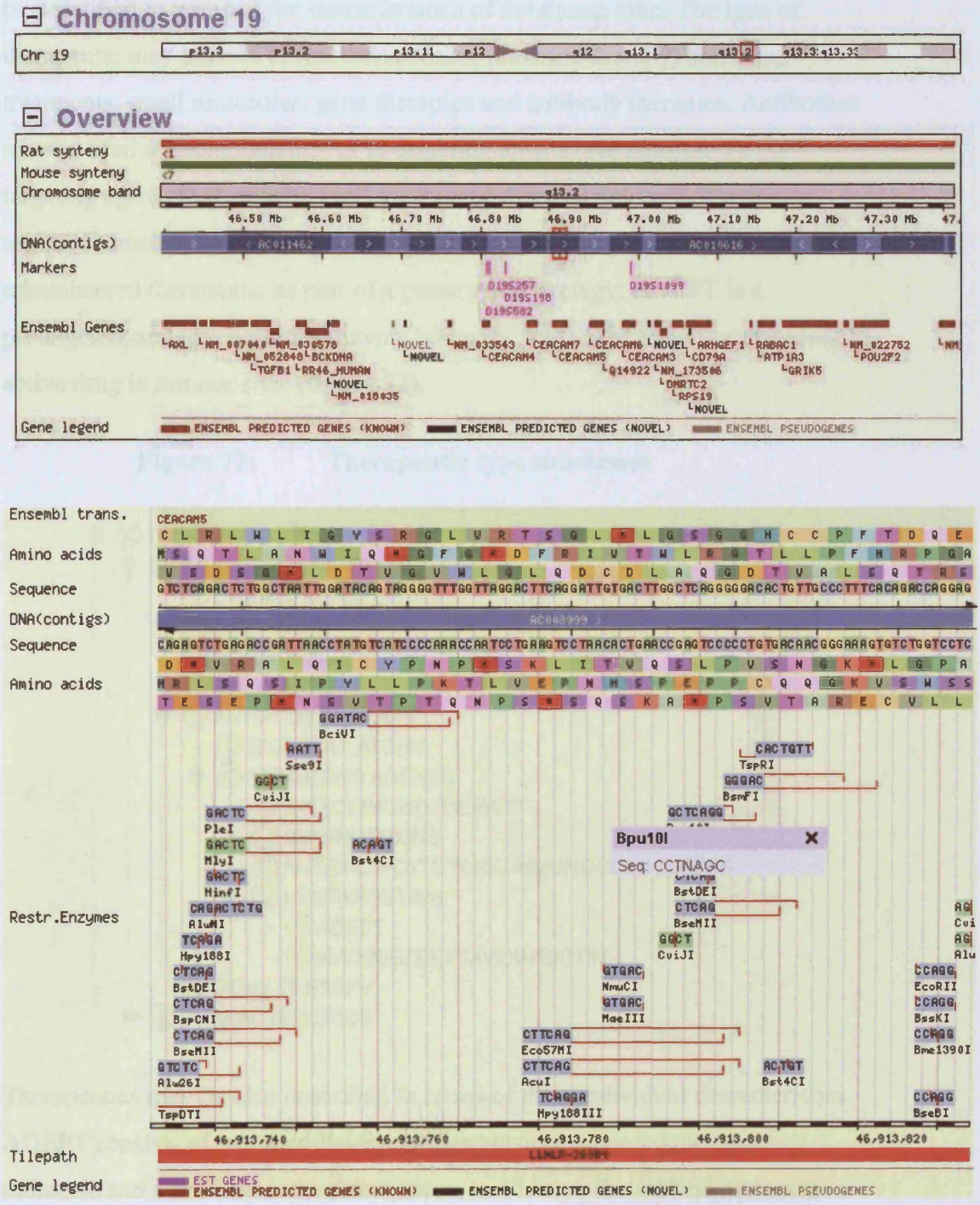

(image from www.ensembl.org)

Therapeutic

The THERAPEUTIC superclass may be divided into the therapeutic type or may be described in terms of the characteristics of the therapeutic. The type of therapeutic may include chemotherapeutics, radiation therapy, hormonal treatments, small molecules, gene therapies and antibody therapies. Antibodies may be used as biomodulators or as targeting agents (**see chapter 1**). As targeting agents they may be used for tumour directed delivery of radiation, toxins, chemotherapeutics, or a 'tag' which will be recognised by a second administered therapeutic as part of a pretargeted strategy. ADEPT is a pretargeted strategy, with the enzyme being the 'tag' used to activate prodrug to active drug in tumour sites **(figure 72).**

Figure 72: Therapeutic type subclasses

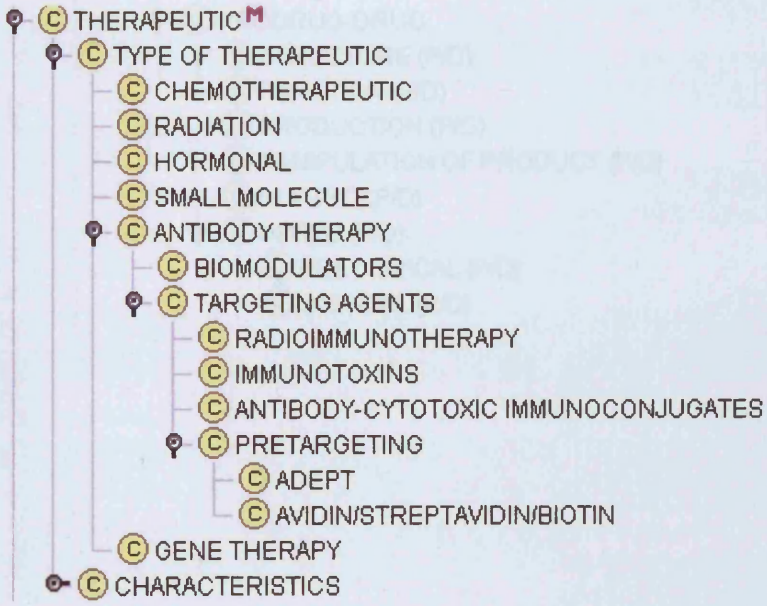

Therapeutics may be also described in terms of their individual characteristics. ADEPT consists of two therapeutic entities, an antibody-enzyme targeting molecule and a prodrug activation system. In addition the antibody-enzyme moiety may either be described as a whole or in terms of its individual components – antibody and enzyme.

Each therapeutic component may be described in terms of structure, function, method of production, manipulation of product, *in vitro* and *in vivo*

characteristics (**figure 73**). The antibody-enzyme moiety, and the prodrug/drug system will be discussed in more detail.

Figure 73: Therapeutic characteristics subclasses

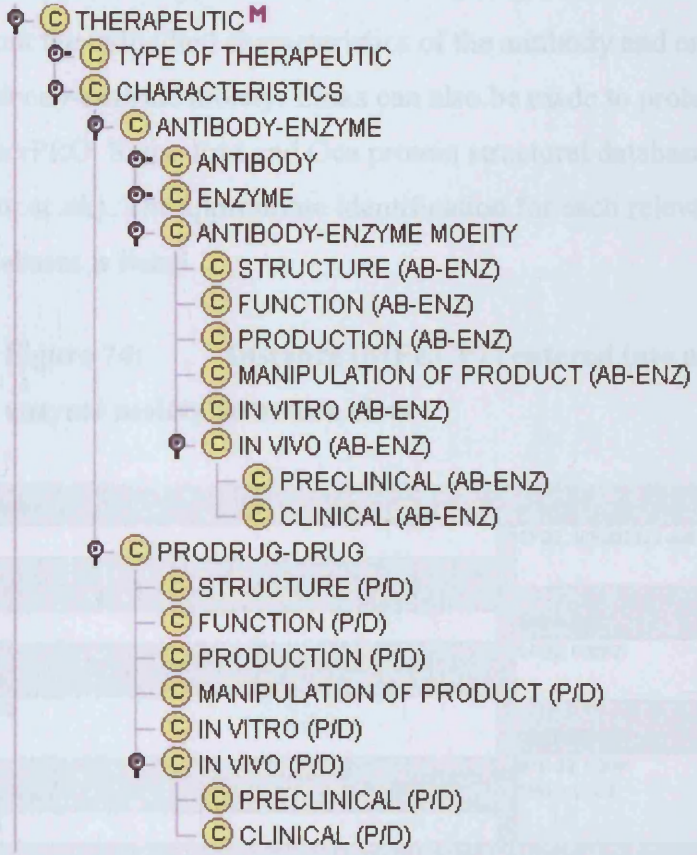

Antibody-enzyme Moiety

Figure 74 displays the 'instance' of MFECP1 entered into the **structure** slots. Antibody_name and enzyme_name can link to the appropriate instance within the antibody class and enzyme class, and more detailed information may be recorded about the individual characteristics of the antibody and enzyme used to form the antibody-enzyme moiety. Links can also be made to protein databases including InterPRO, Swiss Prot and Oca protein structural database (http://oca.ebi.ac.uk). The appropriate identification for each relevant molecule for these databases is listed.

Figure 74: Instance (MFECP1) entered into antibody-enzyme moiety structure slots

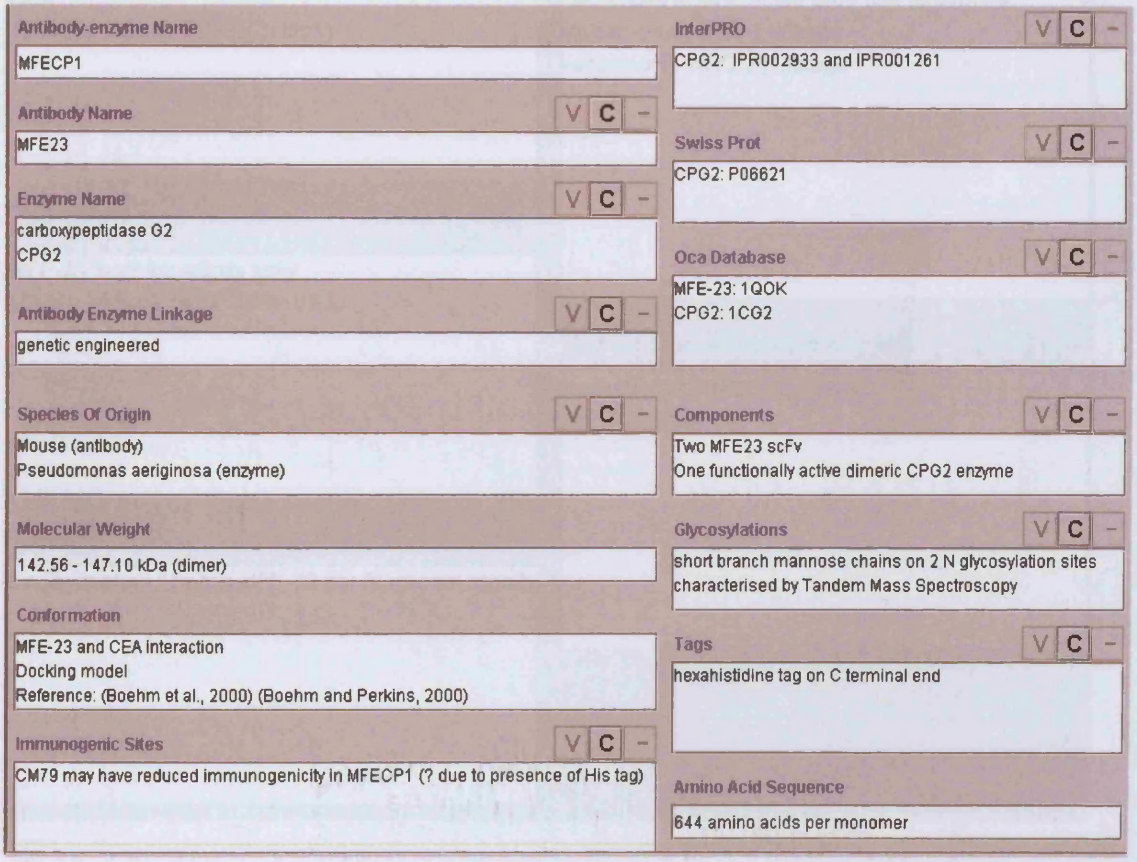

The antibody-enzyme moiety may also be described in terms of **function**. This is displayed for MFECP1 in **figure 75**. The function of the antibody is to bind to antigen, and the function of the enzyme is to catalyse a chemical reaction, which in the setting of ADEPT, is used to convert prodrug to active drug.

Figure 75: Instance (MFECP1) entered into antibody-enzyme moiety function slots

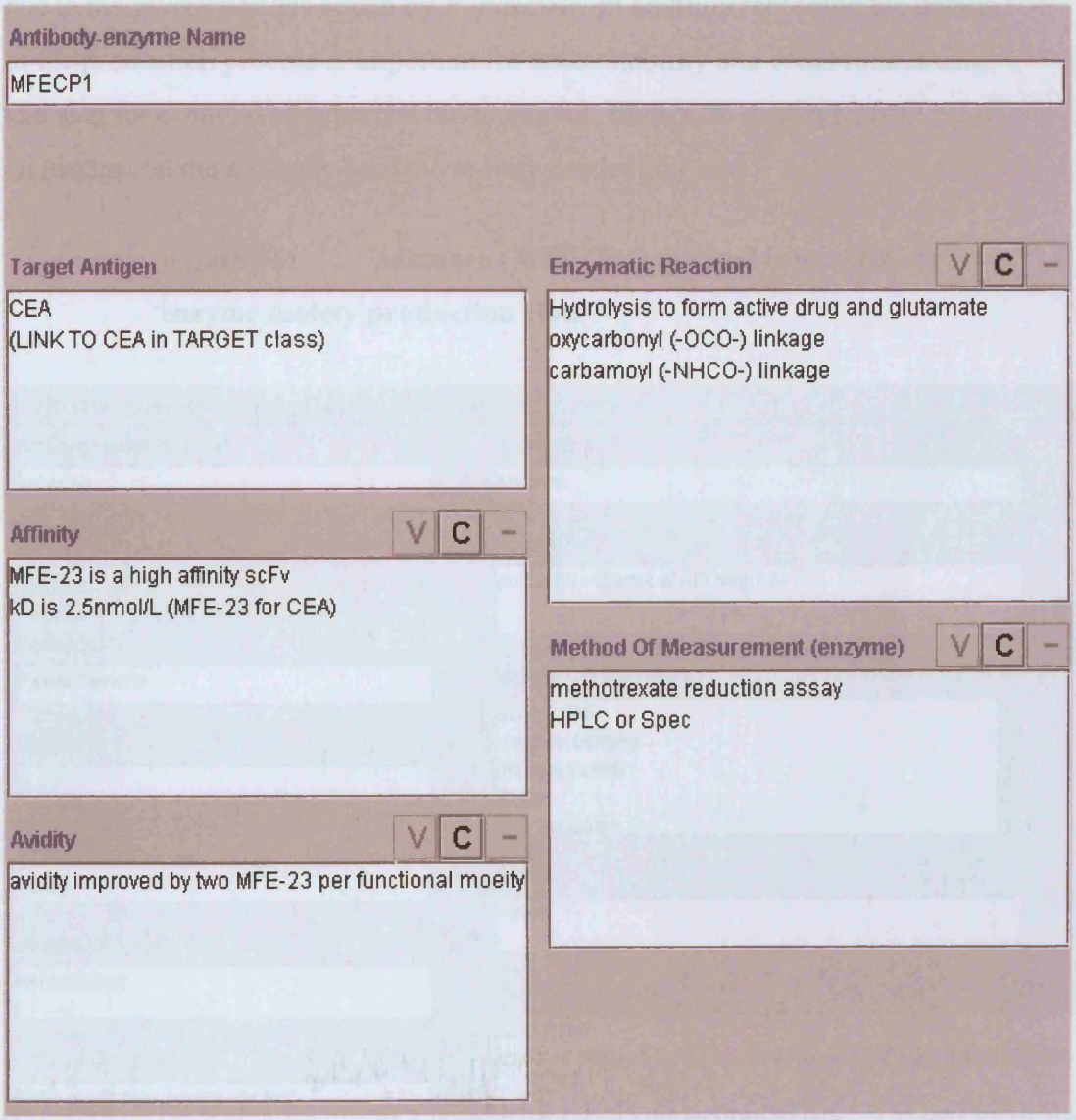

The **production** of the antibody-enzyme moiety may be described in terms of the production method, purification process, assessment process (stability, solubility), and the final formulation and storage conditions. This information is important as the production process may influence characteristics of the antibody-enzyme. For example when MFECP1 was produced in an *E. Coli* expression system it had a slower biodistribution in preclinical models than when it was produced in a *P. pastoris* expression system (see **Chapter 4**). This was due to the glycosylations added by *P. pastoris*. In addition recording the details of the production process is important for accountability and cross-referencing and also for eventual commercial development. **Figure 76** displays MFECP1 as an instance in the antibody-enzyme moiety production slots.

Figure 76: Instance (MFECP1) entered into antibody-enzyme moiety production slots

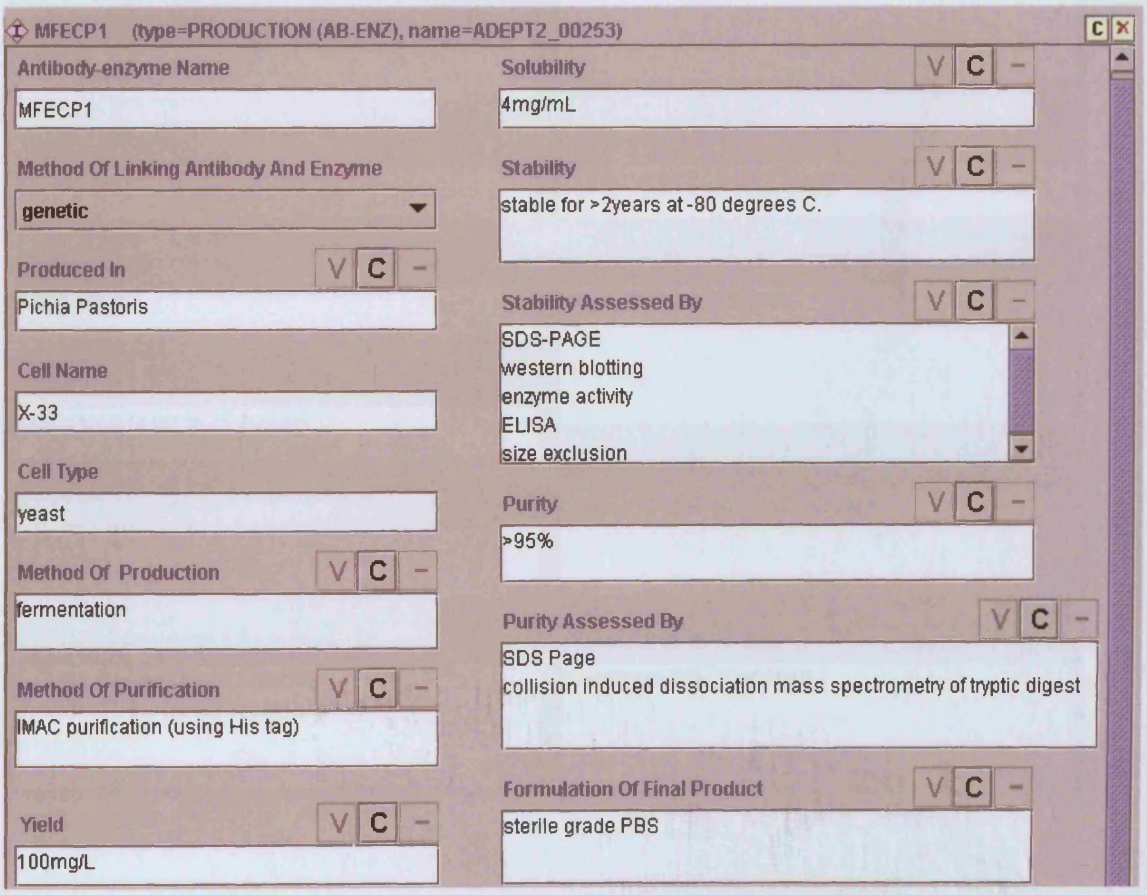

The **manipulation of product** slot may include the radiolabelling of antibody-enzyme. This could be described by defining the radiolabel used, the method of radiolabelling and any purification process required, the amount of radioactivity used, the labelling efficiency, a measurement of the antigen binding of the radiolabelled protein, and the stability of the radiolabelled protein. In addition the method of measuring radiolabelled protein in vivo can be described (**figure 77**).

Figure 77: Instance (MFECP1) entered into antibody-enzyme moiety manipulation of product slots

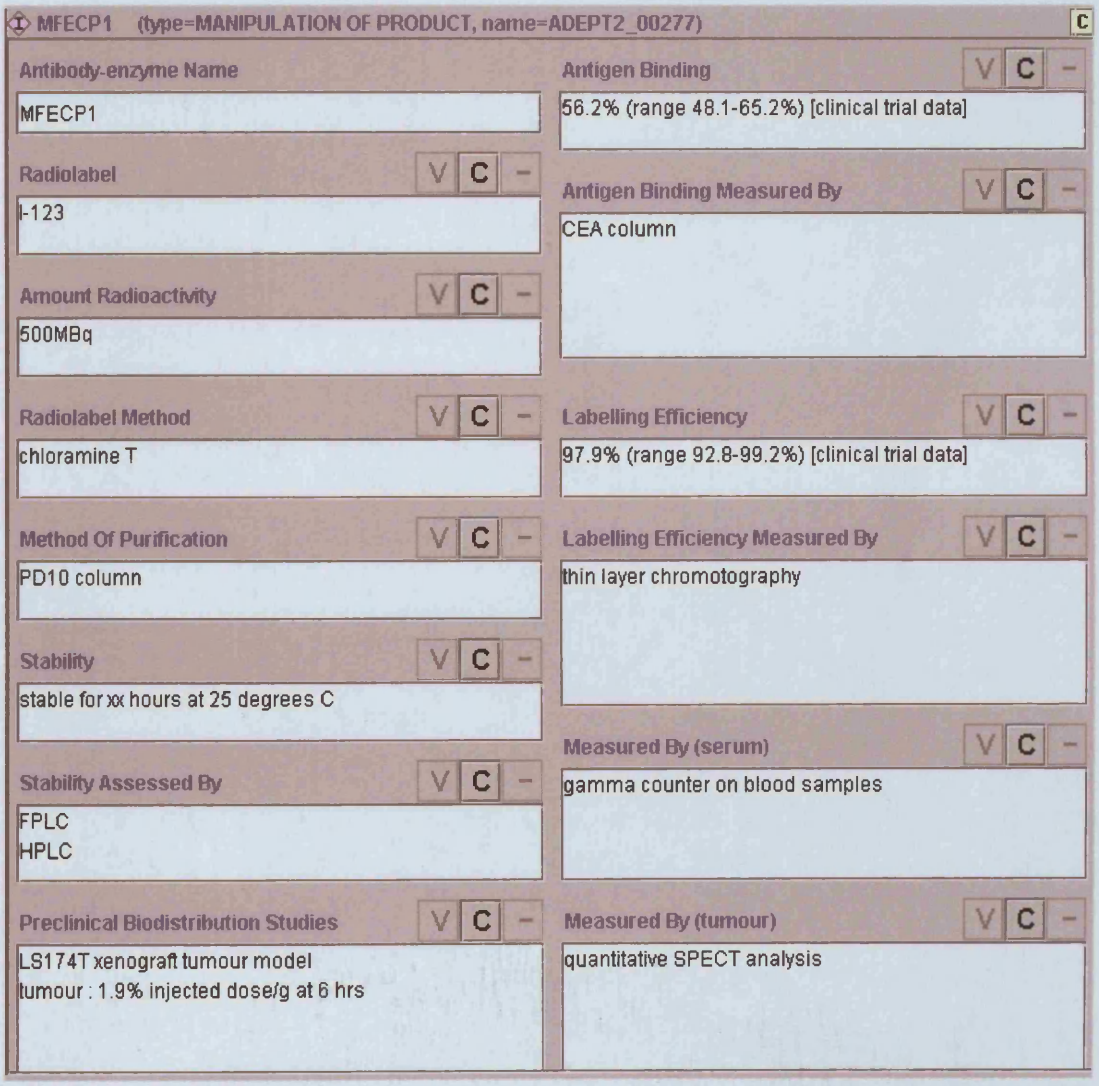

The ***in vitro*** slot of a therapeutic moiety may be used to record toxicity or efficacy. The information recorded may include the cell line name, the protocol used and the effect. As the antibody-enzyme in ADEPT is used as a targeting vehicle it would not be expected to have either significant efficacy or toxicity to cell lines in the in vitro setting, and cell-line experiments have not been performed with antibody-enzyme alone.

The ***in vivo*** slots of the antibody-enzyme moiety may include preclinical animal model data or clinical trial data. The *in vivo* data may include scheduling data, biodistribution data and toxicity data. This could be linked to the subclasses and slots used in the THERAPY superclass which is discussed in more detail below.

Prodrug-Drug

The prodrug/ drug therapeutic may also be described under the headings of **structure**, **function**, **production**, **manipulation of product**, ***in vitro*** and ***in vivo*** characteristics (**figure 78**). The prodrug activation system used in the ADEPT trials in this thesis is ZD2767P, which, when activated by CPG2, is converted to ZD2767D. The ZD2767P system will be discussed as the instance for the slots described for each subclass below.

Figure 78: Prodrug-drug therapeutic subclasses

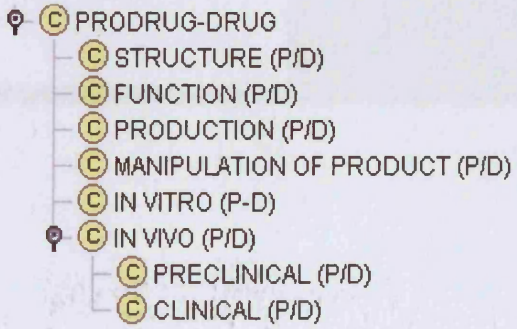

The **structure (P/D)** subclass with its slots for the prodrug/ drug therapeutic is shown in **figure 79**.

Figure 79: Instance (ZD2767P) entered into prodrug/ drug structure slots

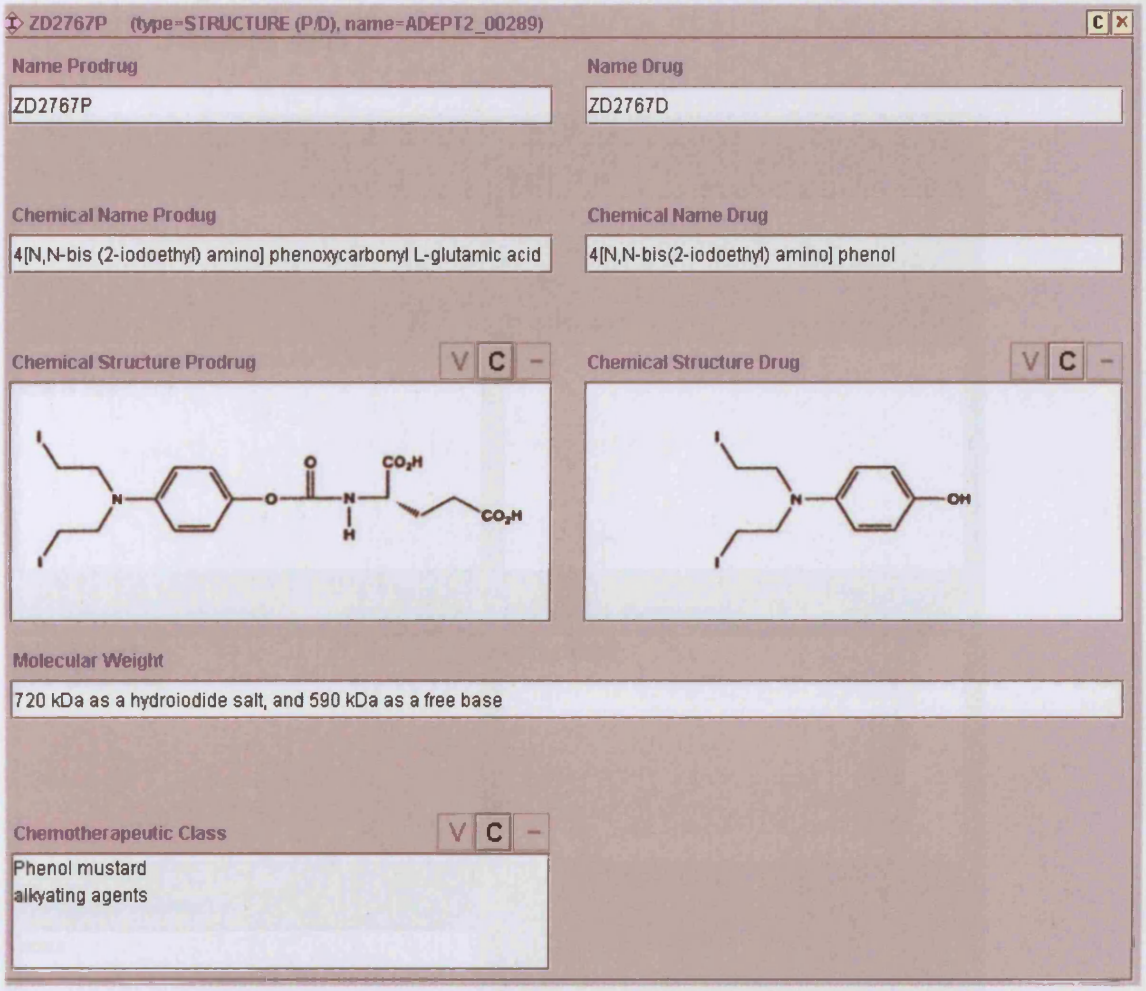

The prodrug/ drug therapeutic may also be described in terms of **function** (**figure 80**). In the ADEPT system the function of the prodrug is to be activated by a specified enzyme to form an active drug. The function of the active drug is to cause cytotoxicity. The mechanism of cytotoxicity may be described.

Figure 80: Instance (ZD2767P) entered into prodrug/ drug function slots

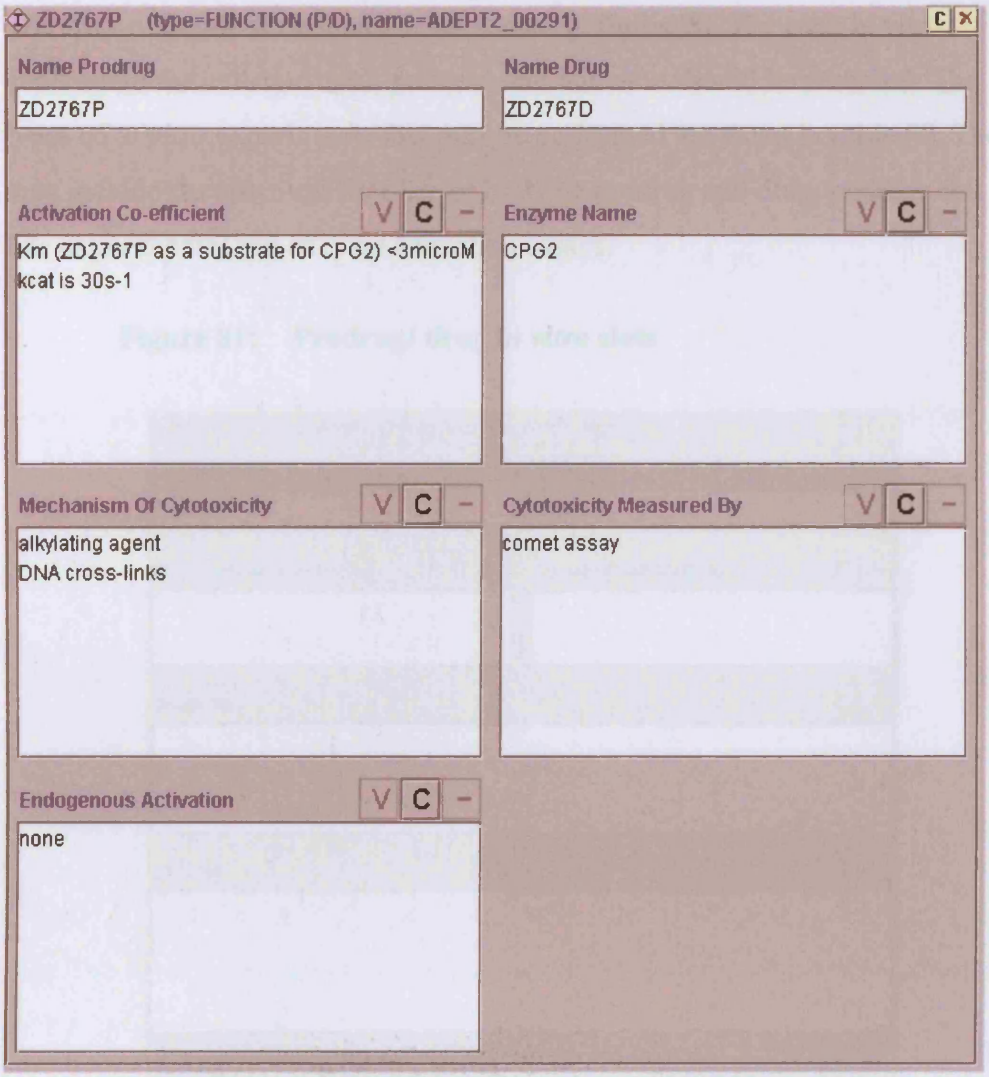

The **production** process may also be described. These slots may include method of production, stability, purity, solubility, formulation and reconstitution of the final product.

It may be useful to **manipulate** the prodrug/ drug after production by radiolabelling or 'tagging' in order to follow its biodistribution. This has not yet been done for this ADEPT system.

The slots of the ***in vitro*** subclass are shown in **figure 81**. For each in vitro experiment the cell-line used, protocol and outcome should be recorded. The types of *in vitro* experiments that may be performed are listed in **table 58.** These may include the chemical half-life of both the prodrug and drug, potency cell – line experiments, and enzyme activation assays.

Figure 81: Prodrug/ drug *in vitro* slots

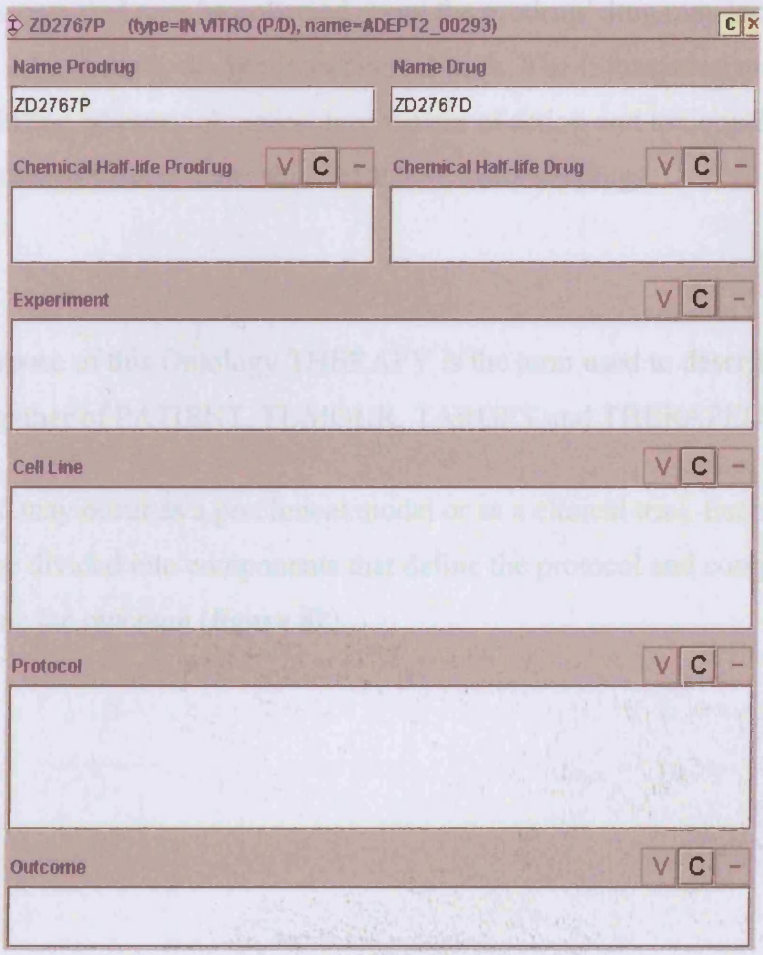

Table 58: List of *in vitro* experiments for Prodrug/ Drug

SLOTS FOR PRODRUG/ DRUG IN VITRO SUBCLASS	
Chemical half-life Prodrug	
Chemical half-life Drug	
Potency Prodrug	Cell line
	Protocol
	Outcome (IC50)
Potency Drug	Cell line
	Protocol
	Outcome (IC50)
Enzyme activation assay	Cell line
	Protocol
	Outcome (CPG2 concentration)
Mechanism of action	Cell line
	Protocol
	Outcome (comet assay)

The ***in vivo*** data that may be collected about the prodrug/ drug may include preclinical experiments, or data from clinical trials. The information may include dose scheduling, pharmacokinetics, mechanism of action and toxicity data. This will be discussed further under the THERAPY class headings.

Therapy

For the purpose of this Ontology THERAPY is the term used to describe the coming together of PATIENT, TUMOUR, TARGET and THERAPEUTIC.

THERAPY may occur as a preclinical model or as a clinical trial. Each of these may then be divided into components that define the protocol and components which define the outcome (**figure 82**).

Figure 82: THERAPY subclasses

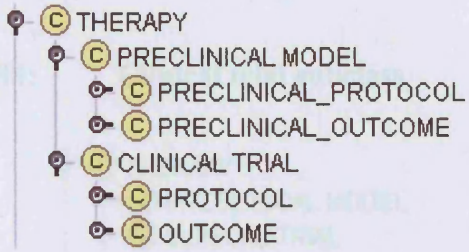

The subclass **preclinical model** may be divided into further subclasses as shown in **figure 83**.

Figure 83: Preclinical model subclass of THERAPY

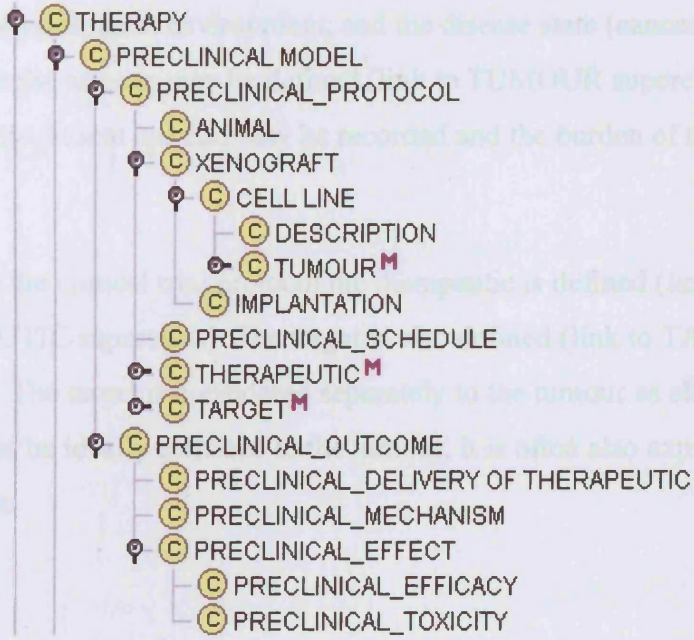

The preclinical protocol should define the animal system in which the therapy will be tested, the xenograft used, the schedule of administration, the therapeutic used (link to THERAPEUTIC) and the target (link to TARGET). The xenograft can be further divided into the cell-line used, and the protocol for implantation. The cell line may be described, and it may be linked to the TUMOUR superclass.

The preclinical outcome may be subdivided into delivery of therapeutic, mechanism and effect. Effect may be divided into efficacy and toxicity.

The Clinical Trial subclass of THERAPY may be also subdivided into **protocol** and **outcome** (**figure 84**).

Figure 84: Clinical trial subclass

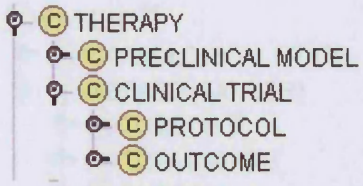

Each clinical trial has a trial **protocol**, in which the patient group in which the therapy is to be performed is defined (link to PATIENT superclass) (**figure 85**). As discussed earlier, the patient can be subdivided into the parameters which define the physiological environment, and the disease state (cancer). Within the disease state the tumour may be defined (link to TUMOUR superclass), the treatments the patient has had may be recorded and the burden of the cancer defined.

Also within the clinical trial protocol the therapeutic is defined (link to THERAPEUTIC superclass). The target is also defined (link to TARGET superclass). The target is considered separately to the tumour as although the target should be ideally confined to the tumour, it is often also expressed in non-tumour sites.

Figure 85: Clinical Trial Protocol subclasses

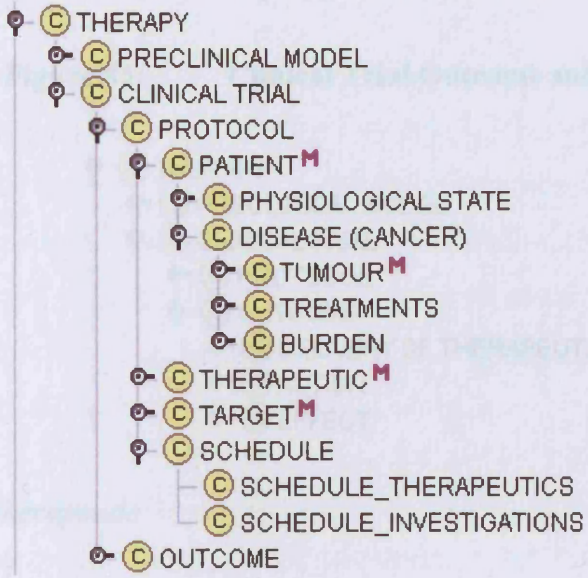

The schedule of administration of therapeutics is defined within a trial protocol. This may include the following slots (**table 59**).

Table 59: Slots defined for the Schedule_therapeutics subclass of clinical trial protocol

Slots	
Dose	Antibody-enzyme
	Radiolabelled antibody-enzyme
	Prodrug
Schedule of administration	Antibody-enzyme
	Radiolabelled antibody-enzyme
	Prodrug
Time of administration	Antibody-enzyme
	Radiolabelled antibody-enzyme
	Prodrug
Protocol defined enzyme level at the time of prodrug administration	

Also as part of schedule, is the schedule of investigations performed within a clinical trial. These are for the purposes of measuring the outcomes discussed below. They will include clinical assessments, blood tests, radiological imaging, gamma camera scans or PET scans.

Figure 86 displays the **outcome** measures of a clinical trial, which are subdivided into delivery of therapeutic, action and effect.

Figure 86: Clinical Trial Outcome subclasses

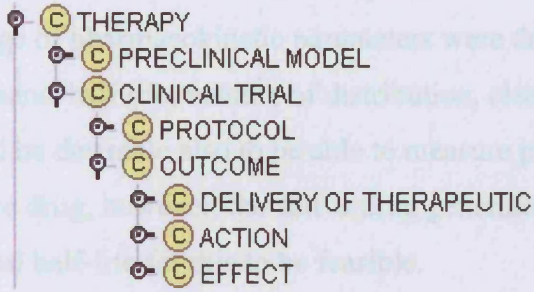

Delivery of therapeutic

The delivery of therapeutic may be divided into pharmacokinetic data, biodistribution data and immunogenicity data (**figure 87).**

Figure 87: Delivery of therapeutic subclasses

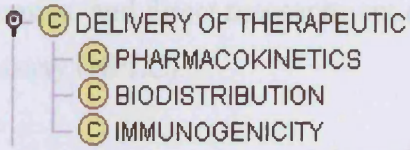

Pharmacokinetic data may be collected for antibody-enzyme or for prodrug and/or drug. In the ADEPT clinical trials presented in this thesis, pharmacokinetic measurements of antibody-enzyme were made by two methods. One involved the measurement of CPG2 enzyme activity in the serum of patients at a variety of timepoints, and the other involved the measurement of radioactivity in the blood of patients who had radiolabelled antibody-enzyme administered. The α and β half-lives were calculated for the patient group as a whole using both sets of results. Different results were obtained by each method, which is expected as both methods are measuring different aspects of the antibody-enzyme. The measurement of enzyme activity is an assessment of function of the antibody-enzyme, and is likely to represent the intact molecule. The measurement of radioactivity however, may measures the radioisotope

which may be either attached to intact antibody-enzyme, antibody-enzyme fragments or as free radioactivity in the blood.

Pharmacokinetic data was also obtained in the clinical trials for the prodrug. This was measured by HPLC, used to detect prodrug in plasma samples at a variety of time points. A range of pharmacokinetic parameters were derived, including plasma concentrations, half life, volume of distribution, clearance and area under the curve. It would be desirable also to be able to measure pharmacokinetic profile of the active drug, however, the active drug generated from ZD2767P had too short a chemical half-life for this to be feasible.

Biodistribution data is used to assess the distribution of the therapeutic in the normal tissues, and in the tumour of the patient. In the ADEPT trials the biodistribution of antibody-enzyme was assessed by radiolabelling, and using quantitative gamma camera imaging to measure tumour and normal tissue distribution of radioactivity. Tumour estimates of antibody-enzyme concentrations obtained by this method were validated in a small number of patients with tumour biopsies, and direct measurement of CPG2 enzyme level by methotrexate reduction assay (HPLC).

It was not possible to measure tumour or normal tissue biodistribution of active drug in these ADEPT clinical trials due to the very short chemical half-life of ZD2767D.

Immunogenicity has also been included in the subclass of delivery of therapeutic, because the presence of human antibodies against epitopes on the antibody-enzyme moiety may influence the delivery of antibody-enzyme. Immunogenicity was measured in both ADEPT trials, by ELISA assay. MFECP1 appeared less immunogenic than A5CP and may have the potential for repeated administration prior to the development of human antimurine or human anti-CPG2 antibodies.

Action

Figure 88 shows the subclasses of action.

Figure 88: Action subclasses

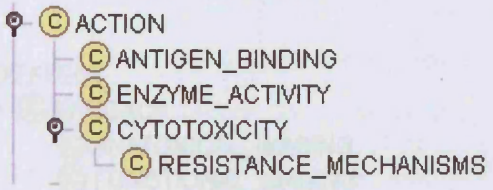

The action subclass contains data on the measurements of action of the therapeutic in the therapy setting. For example in ADEPT, the antibody-enzyme has two actions; to bind antigen, and to act as an enzyme. Currently the binding of antigen is measured indirectly on tumour biopsies by using immunohistochemistry to ascertain the presence and distribution of CEA and antibody-enzyme. This is performed by using an anti-CEA antibody and an anti-CPG2 antibody. The immunohistochemistry cannot be performed on the same histological slide so consecutive slides are used. The enzyme activity of CPG2 is assessed in tumour sites directly in tumour biopsies with measurement of CPG2 activity by methotrexate reduction assay.

The prodrug/drug therapeutics' action is to cause cytotoxicity. ZD2767D is an alkylating agent, and its mechanism of cytotoxicity is by forming DNA cross-links. This can be measured on single cells from tumour biopsies, bone marrow aspirates or peripheral blood lymphocytes, by a comet assay (described in **chapters 2 and 4**).

Tumours are also known to have resistance mechanisms, which may counteract the cytotoxicity of the therapeutic agent being tested. DNA repair mechanism may counteract the DNA cross-links formed from the alkylating agents used in ADEPT. The presence of resistance mechanisms will affect the potential efficacy of a therapeutic system.

Effect

Effect may be divided into effect on tumour, termed efficacy, or effect on non-tumour tissues, termed toxicity (**figure 89**).

Figure 89: Effect subclasses

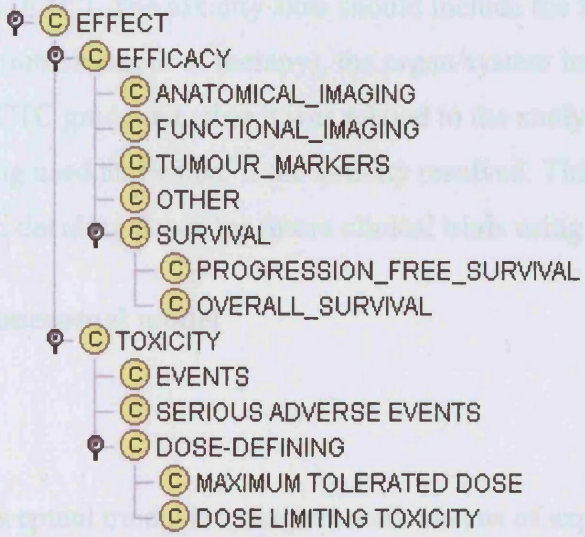

Efficacy can be assessed by anatomical imaging, such as CT scans or MRI. Anatomical imaging provides a measure of change in dimensions of a tumour with therapy. Alternatively functional imaging may be used, such as [F-18] FDG PET, as discussed in **chapter 5 and 6**. This may provide an assessment of metabolic activity of the tumour with therapy. Tumour markers may also be used to assess response to therapy, although in most tumour types they will be used in conjunction with other assessments of response as their role has not yet been fully validated. Other measures of response may include changes in 'overall well-being' of patients such as WHO Performance Status, Quality of Life measures or measures of exercise capacity. Temporal measures may also provide data on the effectiveness of a treatment. This includes survival measures such as overall survival or progression free survival.

For each of these subclasses the slots used could include assessment time (time of assessment related to commencement of therapy), the method used (such as RECIST criteria for anatomical imaging), and the result.

Toxicity may be sub-classified into a record of toxicity events in a clinical trial, serious adverse events or the dose- defining toxicities. The dose-defining toxicity subclass may be divided into maximum tolerated dose and dose limiting toxicities.

The standard method for measuring toxicity in clinical trials is by the Common Toxicity Criteria (CTC). The toxicity slots should include the time of the event (in relation to commencement of therapy), the organ/system involved, the CTC description, the CTC grade, whether it was related to the study drug or drugs, the dose of study drug used and when/ if the toxicity resolved. This information is very useful when deciding doses for future clinical trials using the same agents.

7.4 ADEPT conceptual model

7.4.1 Method

The ADEPT conceptual model is a diagrammatic means of expressing the relationship between the 5 core superclasses identified in the ADEPT Ontology (PATIENT, TUMOUR, TARGET, THERAPEUTIC and THERAPY). It serves as an adjunct to the Ontology and aims to define some of the interactions between the superclasses. Overlap particularly occurs in the THERAPY superclass, because it represents a 'coming together' of all of the superclasses. A Venn diagram system has been used to show the relationships between the five superclasses in the conceptual model.

7.4.2 Results

The diagrammatic representation of the basis of the conceptual model is shown in **figure 90**. Four of the superclasses defined in the ADEPT Ontology are 'objects' (PATIENT, TUMOUR, TARGET and THERAPEUTIC), whilst THERAPY is the 'action' of adding the THERAPEUTIC to PATIENT/ TUMOUR/ TARGET.

Figure 90: ADEPT conceptual model

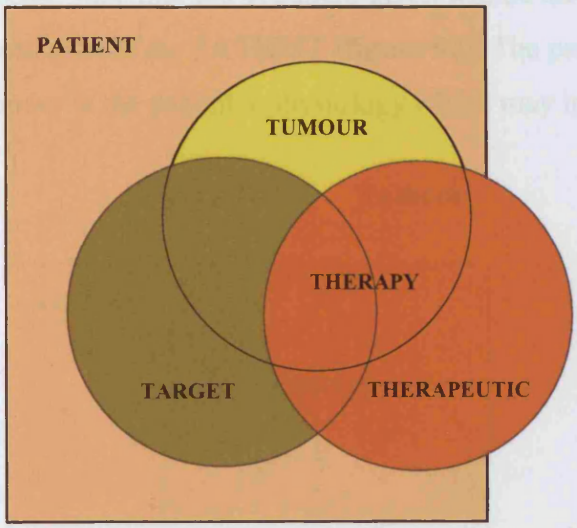

The model may be considered in layers.

The first layer is the PATIENT, as the patient forms the environment for the therapy to occur **(figure 91)**. The features of a PATIENT are described in the ADEPT Ontology.

Figure 91: Patient

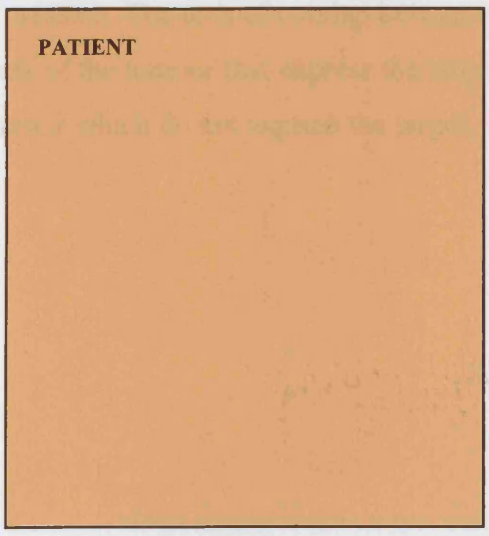

The next layer is the TUMOUR. This is found within the PATIENT, and is the disease state that the treatment given will be directed against. It conceptually forms part of the PATIENT **(figure 92)**. The part of the PATIENT which is not tumour is the patient's physiology which may influence the treatment given.

Figure 92: Tumour

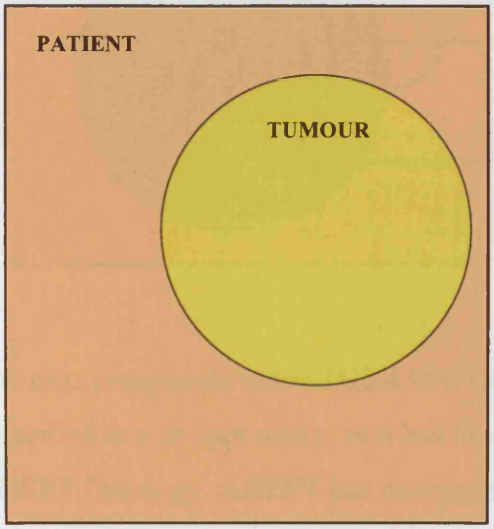

The next layer is the TARGET **(figure 93)**. This should be predominantly expressed in the tumour, but may also have a component of non-tumour expression. The area of overlap between TARGET and TUMOUR represents the parts of the tumour that express the target. There are however also parts of the tumour which do not express the target.

Figure 93: Target

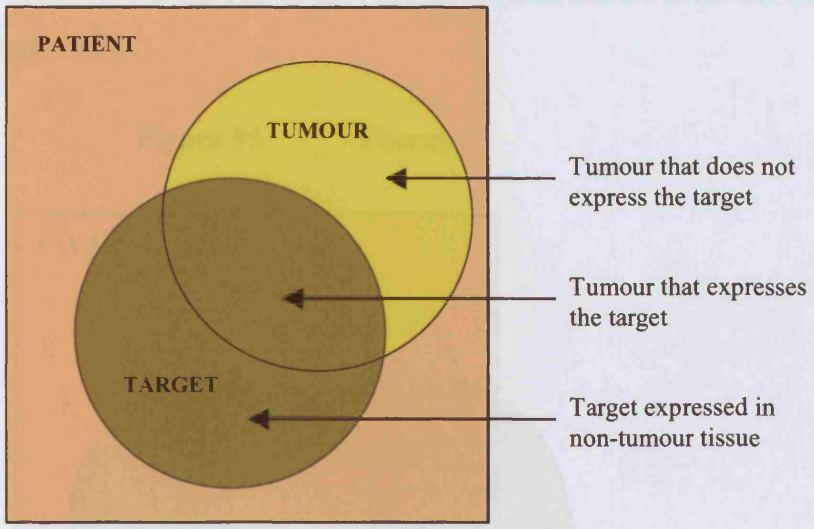

The next component is the THERAPETIC **(figure 94)**. The therapeutic can be described as a unique entity, as it has its own characteristics as outlined in the ADEPT Ontology. ADEPT has two molecules which constitute the 'THERAPEUTIC'. These are the antibody-enzyme, and the prodrug/drug. Both can be described in terms of structure, function, production, manipulation of product, *in vitro* characteristics and *in vivo* characteristics.

Figure 94: Therapeutic

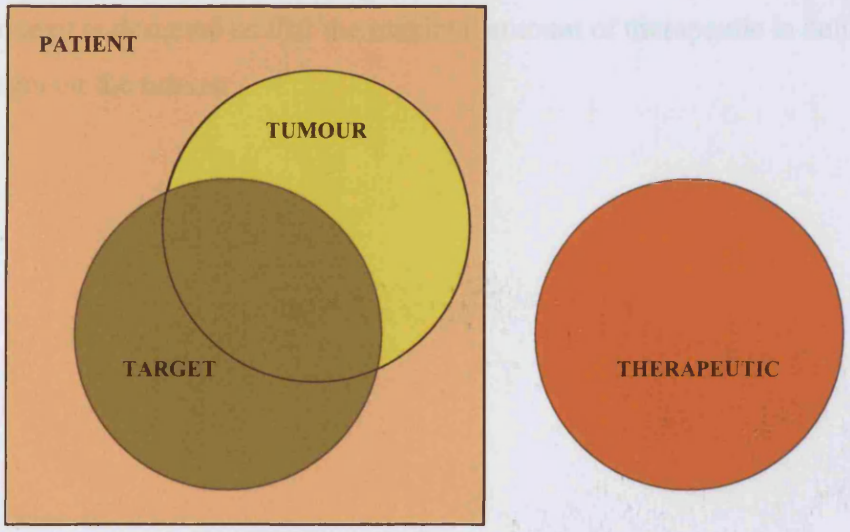

THERAPY is the term used in the model and the Ontology for the administration of the THERAPEUTIC to the PATIENT (who has a TUMOUR and TARGET) (**figure 95**).

Figure 95: Therapy

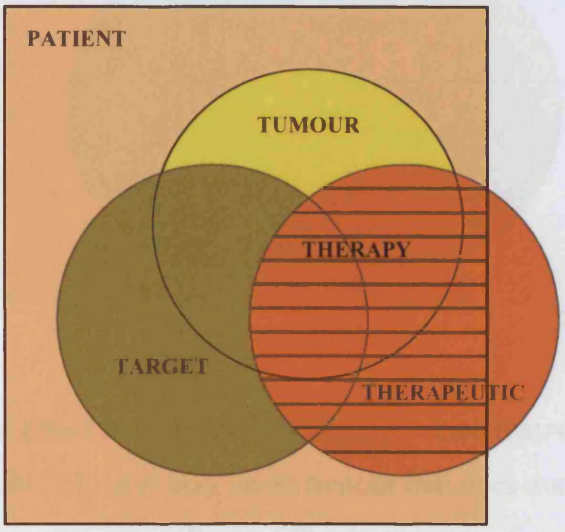

The outcome components of THERAPY that can be represented in the model are **delivery of therapeutic** and **effect**.

Delivery of therapeutic involves the interaction of the therapeutic with the PATIENT, and with the TARGET and the TUMOUR (**figure 96**). A targeted strategy is designed so that the maximal amount of therapeutic is delivered to the target on the tumour.

Figure 96: Delivery of therapeutic

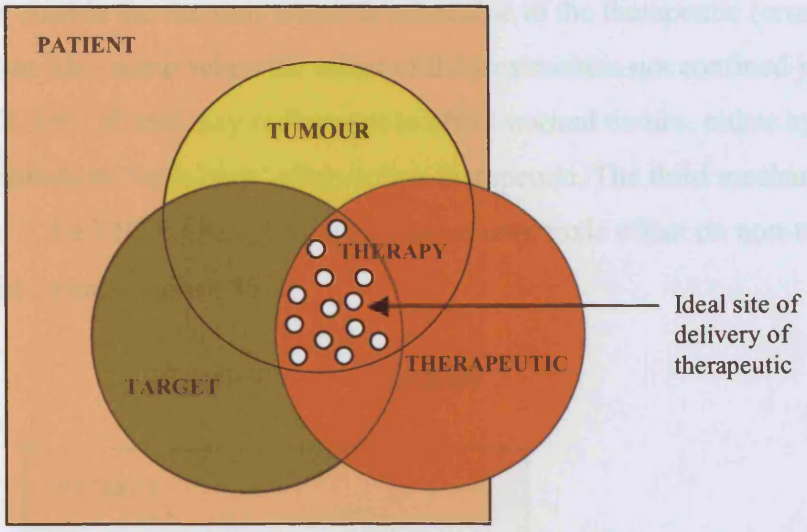

The **effect** may be one of efficacy, which may occur in TUMOUR that has the TARGET, or it may be on tumour that does not have the TARGET, by a bystander effect **(figure 97)**.

Figure 97: Efficacy

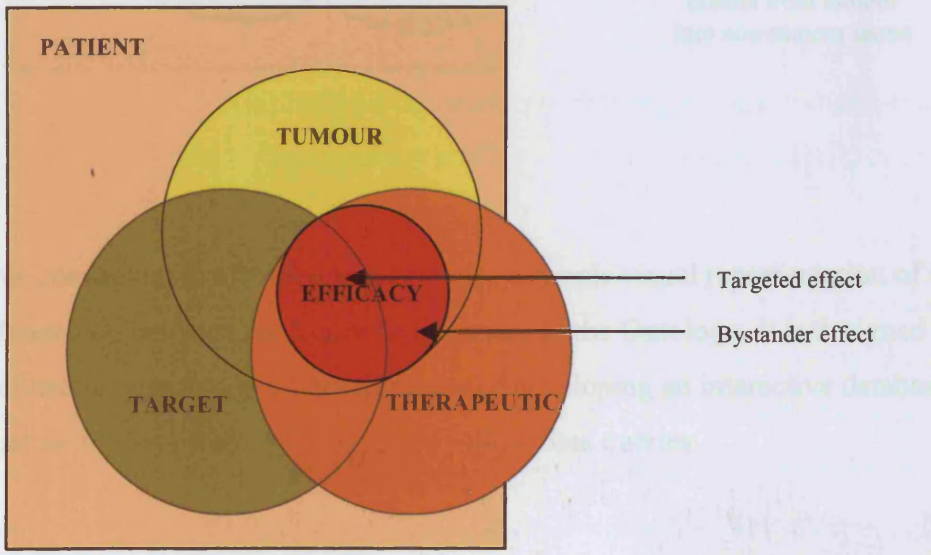

The effect may also be toxicity, which may occur when there is a TARGET that is outside the tumour, which is accessible to the therapeutic (cross-reactivity). It may also occur when the effect of the treatment is not confined just to the TUMOUR and may radiate out to effect normal tissues, either by direct extension, 'leak-back' of an active therapeutic. The third mechanism of toxicity is if the THERAPEUTIC agent has its own toxic effect on non-tumour tissue in the patient (**figure 98**).

Figure 98: Toxicity

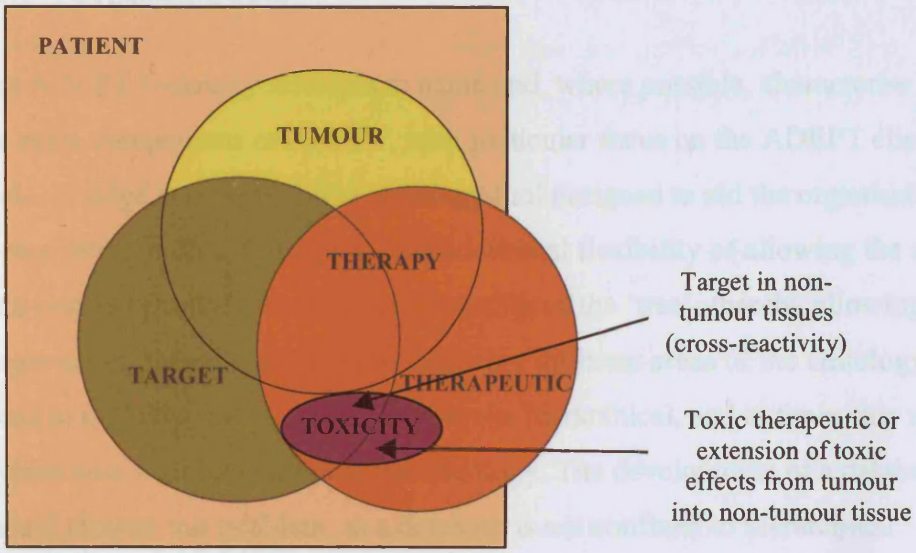

This conceptual model therefore provides a simple visual representation of the relationship between the 5 core superclasses of the Ontology. It is designed to facilitate the next stage of development of developing an interactive database to store all the data from ADEPT, and to allow data queries.

7.5 Discussion

The discussion of the ADEPT Ontology and Conceptual Model will focus on the three aims outlined at the beginning of the chapter. These included the concept that the Ontology and Conceptual Model could be used to organise data from ADEPT, that once the data was organised it may allow the identification of areas where more data could be acquired in a clinical trial setting and also to identify areas for rational improvement in ADEPT.

7.5.1 Organising data

The ADEPT Ontology attempts to name and, where possible, characterise all of the main components of ADEPT, with particular focus on the ADEPT clinical trials. Protégé is a hierarchical Ontology tool designed to aid the organisation and accessibility of data. Protégé has the additional flexibility of allowing the same data element to appear on different branches of the 'tree', thereby allowing a single query to generate the same data from different areas of the Ontology. Clinical trial data are, however, not always hierarchical, and at times this was problematic when constructing the Ontology. The development of a database should obviate this problem, as a database is not confined to hierarchical relationships. However, before a database can be designed, the components of it need to be identified. The Ontology was used to name, define and organise these components.

The ADEPT Ontology was designed to link to other Ontologies or databases where appropriate. For example the TUMOUR, TARGET and THERAPEUTIC superclasses could link via molecular profiling or structural and functional data to known genomic or proteomic databases and ontologies. It is important to create these links in order to access emerging data and information, and to maximise the opportunities for data acquisition and utilisation.

The Ontology was also designed to encompass commonly used terminology to facilitate cross-referencing and to enhance search facilities. For example, the inclusion of the MeSH classification in the TUMOUR superclass. The MeSH classification provides keyword associations, and is used for common search

tools, such as Medline. By including a number of methods of describing the TUMOUR, the accessibility to other data trails is possible. This may ultimately lead to the acquisition of relevant data, and accessibility to shared data, in order to enhance overall knowledge. Data sharing is becoming an important concept as the volume of data generated world-wide escalates.

The Conceptual Model describes, in basic terms, the relationships between the five superclasses defined in the Ontology. It was designed to show how the components of the Ontology are related, and should therefore be useful in defining the relationships of these components into an ADEPT database. The majority of the terms used in the Ontology and the Conceptual Model are applicable not only to ADEPT but also to other targeted therapeutic strategies.

The ADEPT Ontology and Conceptual Model are therefore the initial step in the design of an ADEPT database, into which all of the data acquired on ADEPT could be entered, stored, organised and queried. A database for ADEPT would be extremely valuable, as it would facilitate the development of a complex therapeutic strategy by making the data more accessible. The development of the database was beyond the scope of this Ph.D and would present a large undertaking in terms of software engineering. Importantly, however, the Ontology and Conceptual Model will provide the framework for a relational database should this be undertaken.

7.5.2 Guiding mechanistic clinical trial design

One of the motivating reasons for developing an ADEPT Ontology and Conceptual Model was that it might help guide mechanistic clinical trial design. Clinical trials provide unique opportunities to test a new therapy in its 'real-life' setting. Obtaining maximal information during a clinical trial is critical to developing an understanding of the therapy, and to guiding rationale modifications to the system. This has to be balanced with an understanding that phase I clinical trials are performed on patients who have incurable cancer, have usually exhausted conventional treatment options, and who may have already in their 'cancer journey' had a variety of scans, tests, and invasive procedures performed.

The Ontology and Model identify the five 'superclasses' as being PATIENT, TUMOUR, TARGET, THERAPEUTIC and THERAPY. Clinical trials should therefore, where possible, collect data on all of these components.

The data collected for the PATIENT superclass is listed in the Ontology, and involves collecting data on the 'physiological' state of the patient and the 'disease state' of the patient. This data is now fairly standard for clinical trials.

The data collected on the TUMOUR has conventionally been based on a histological description, such as the tumour type, stage, grade, TNM classification, lymphovascular invasion. It is becoming more apparent that tumours should be also characterised based on their genomic or proteomic profile, as this may be more relevant for treatment responsiveness and tumour prognosis (Adlard *et al*, 2002; O'Neill and Song, 2003). It may be useful in current clinical trials to collect and store data on each tumour's genomic or proteomic profile, for future reference, as it may be that certain genomic or proteomic features make a patient more or less likely to respond to a given treatment. This is the concept of 'tailoring' treatments to individuals, as opposed to giving the same treatment to everyone with the same tumour cell type. The increased accessibility to genomic and proteomic data is now making a more 'rationale' approach theoretically possible.

Limited data is acquired on the microenvironment of the TUMOUR at the time of treatment. The development of functional imaging using PET may provide increasing opportunities to collect data non-invasively on the 'functional state' of a tumour. This may be in terms of glucose metabolism ([F-18] FDG), amino acid utilisation ([C-11]-methionine), DNA synthesis ([F-18]–3′-deoxy-3′-flourothymidine) or blood flow ([O-15] water) (Tewson and Krohn, 1998). This information may again determine the likelihood of treatment success, or may influence the prognosis of the patient.

In the ADEPT clinical trials presented in this thesis the data collected on the TARGET for each individual patient has been limited. All patients have serum CEA levels checked, and are 'eligible' for ADEPT if their CEA is between 10-1000μg/L. Only in patients with serum CEA levels < 10 μg/L, is

immunohistochemistry performed on tumour specimens to ascertain the presence of tumour CEA. Immunohistochemistry is non-quantitative; however it does provide some data on the distribution of CEA in the tumour. Radioimmunoluminography (RILG) is a technique that can provide quantitative data on CEA distribution in tumour (Boxer *et al*, 1998). This can be performed on histological sections or tumour blocks. CEA levels estimated by RILG have been shown to correlate with levels of tumour localisation of an anti-CEA antibody in study of radioimmunoguided surgery (Boxer *et al*, 1998). It may be useful therefore to incorporate RILG assays for CEA in tumour on all patients in the ADEPT trials to assess if there is a correlation between antigen concentration and distribution with antibody localisation and treatment efficacy. This may aid in the more appropriate selection of patients for therapy. The limitation of this is that the tumour sections and blocks used for assessment of antigen distribution are usually obtained from the original surgical specimen, which may be taken months to years before the ADEPT treatment. It may not reflect the antigen distribution or accessibility in the tumour at the time of ADEPT treatment. At present there is no suitable non-invasive method of assessing this. Tumour biopsies can be performed and quantitative assessment of CEA obtained by RILG. However, tumour biopsies are invasive, associated with potential complications and only small samples of tissue are obtained. There is currently therefore no satisfactory way of assessing TARGET concentrations or accessibility in the tumours of patients receiving ADEPT.

The THERAPEUTIC will be discussed in the context of THERAPY, as this relates to when it is actually administered to the patient. The Ontology divides THERAPY (clinical trial) into protocol and outcomes. The measurement of outcomes is a key feature of mechanistic clinical trials. With regard to ADEPT the outcomes have been divided into three groups; delivery of therapeutic, mechanism and effect. The outcomes should be considered in terms of both antibody-enzyme and prodrug/drug.

The delivery of antibody-enzyme is assessed currently in clinical trials by the direct measurement of CPG2 enzyme activity in blood and in tumour biopsy samples, and by the assessment of biodistribution of radiolabelled antibody-

enzyme. The measurement of CPG2 enzyme in blood gives an estimation of the half-life of antibody-enzyme, and is useful in guiding the timing of administration of prodrug, so as to minimise activation if prodrug in systemic tissues. The direct measurement of CPG2 enzyme in tumour is, however, more problematic as it depends upon attaining a sample of tumour via a tumour biopsy. This is an invasive procedure, usually performed under ultrasound guidance, but even with this assistance, viable tumour areas are not always obtained. The sample is usually very small, which limits the amount of information that can be obtained from it. A small sample is also difficult to analyse, as it will often have to be diluted further in the analysis process, and consequently the amount of enzyme activity within the sample may be less than the detection range of the assay used.

Radiolabelling antibody-enzyme provides, by SPECT analysis, a non-invasive means of assessing antibody-enzyme delivery. It does, however, also have limitations. The radiolabelling process may damage the antigen binding of the molecule, therefore reducing the ability of the radiolabelled molecule to reflect non-radiolabelled antibody-enzyme. In addition radioactivity is measured by this method, and so there is no discrimination between intact antibody-enzyme and non-functional fragments with radiolabel attached, or free radiolabel. Despite these limitations it has been shown to provide a reasonable estimate of tumour A5CP antibody-enzyme localisation when compared to the actual measured CPG2 activity from tumour biopsies. The rapid metabolism of MFECP1, due to its glycosylations, adds further difficulties for SPECT analysis. MFECP1 is rapidly cleared from non-tumour sites, particularly by the liver. CPG2 enzyme measurements confirm that clearance is associated with loss of enzyme activity in non-tumour sites. However, as radiolabel may be attached to multiple sites on the MFECP1 molecule, it will be present in non-tumour areas attached to non-functioning molecules, and not provide a good estimation of intact functional molecule in these sites.

Ideally a non-invasive method of assessing CPG2 function in the body is required. As CPG2 is responsible for the activation of prodrug it is a key issue to be able to quantitatively measure its presence in both tumour and normal tissues,

in order to decide when prodrug should be administered, and also to maximise the likelihood of efficacy and minimise the likelihood of toxicity. There is no current satisfactory solution to this problem, and currently radiolabelling is continuing to be used, with the caveat for MFECP1 that tumour radioactivity may reflect actual antibody-enzyme localisation, but non-tumour radioactivity is likely to be a poor reflection of active enzyme.

Immunogenicity may affect delivery of the antibody-enzyme. ELISA has been used in both ADEPT clinical trials to measure HAMA and HACPG2A. The ELISA studies performed in the ADEPT A5CP and ZD2767P trial suggested that all patients developed antibodies to A5CP after one administration. This limits the potential for repeat therapy. For MFECP1 there was no pre-existing positive control for MFE-23 for the ELISA assay, as although MFE-23 had previously been administered to 45 patients, none appeared to develop antibodies to it (Begent *et al*, 1996; Mayer *et al*, 2000). This required A5B7 to be used in the ELISA assay as a substitute for MFE-23. As discussed in **chapter 4**, as A5B7 and MFE-23 may have different epitopes, this may not detect the presence of human anti-MFE-23 antibodies. The ability to detect antibodies against MFECP1 would be very important if repeat therapy was to be administered.

With regard to the biodistribution of prodrug/ drug, with ZD2767P, the prodrug can be measured in blood by HPLC, but the drug has too short a chemical half-life to be measured. It would be desirable to be able to quantitatively measure the generation of active drug and its distribution. It is, however, difficult to design a tag that would preferentially be expressed on active drug and not on prodrug. The prodrug is expected to be widely distributed in the body. It is only when it is activated by enzyme that it forms a highly cytotoxic agent. It is of interest to identify the sites of activation of drug, and whether, once activated, it remains confined to tumour sites or 'leaks' into surrounding normal tissue.

The action of antibody-enzyme is antigen binding and an enzymatic reaction. The ability to successfully bind antibody-enzyme to antigen is currently assessed by immunohistochemistry. Immunohistochemistry is, however, not quantitative, and whilst a positive result suggests that there has been antigen binding, a

negative result does not exclude it. A quantitative means of assessing binding would therefore be desirable.

The CPG2 enzyme needs to be functional in order to act to convert prodrug to drug. This is currently assessed by the measurement of CPG2 activity on tumour biopsies. The limitations of this method have been discussed above. A non-invasive means of assessing CPG2 function would therefore be desirable.

The measurement of drug activity is by the formation of DNA cross-links as detected on comet assay. The formation of DNA cross-links does not guarantee cytotoxicity as DNA repair mechanisms may correct the cross-links, and create 'resistance' in the cancerous cells. The activity of DNA repair mechanisms may be assessed if serial biopsies were performed to look at DNA repair rates. This, however, is rarely practical in a clinical setting as most patients would be unwilling to have serial biopsies performed.

The effect of therapy is divided into efficacy and toxicity. As discussed in **chapter 5 and 6**, the assessment of efficacy by conventional anatomical imaging, such as by CT scans is limited. Functional imaging, such as with [F-18] FDG PET may however, provide an earlier and more sensitive assessment of response to therapy, and may represent a means of improving the assessment of efficacy in phase I clinical trials. As [F-18] FDG PET assesses the glucose metabolism of the cells it provides an indirect assessment of effect. More mechanism specific functional imaging may be useful such as radiotracers which are used to assess DNA synthesis.

Table 60 lists the mechanistic studies that may be desirable for ADEPT.

Table 60: Desirable mechanistic studies for ADEPT

Superclass	Measurement required
PATIENT	
TUMOUR	genomic and proteomic profile of tumour
	assessment of tumour microenvironment by functional imaging
TARGET	quantitative distribution/ accessibility of CEA in tumour
THERAPEUTIC/THERAPY	
delivery_of_therapeutic	non-invasive quantitative measurement of CPG2 biodistribution in tumour and normal tissues
	non-invasive quantitative measurement of drug activation and distribution of active drug in tumour and normal tissues
action	measurement of DNA repair mechanism (serial biopsies)
effect	assessment of effect on tumour (functional tumour imaging)

7.5.3 Identifying areas of improvement for ADEPT

The ADEPT Ontology and Conceptual Model were also theorised to be useful for identifying areas of potential improvement for ADEPT, and thereby with the data incorporated into them, rationally direct modifications to the system.

Again the 5 superclasses may be used to discuss areas of potential modification to ADEPT. The components of ADEPT that may therefore be modified are the PATIENT group, the TUMOUR, the TARGET, the THERAPEUTIC or the THERAPY (protocol).

The selection of the PATIENT group for ADEPT is likely to influence the outcome. Either the patient's physiological characteristics or their tumour burden may be contributing to the success or failure of the system. For example, with the ADEPT MFECP1 clinical trial, the antibody-enzyme was glycosylated, and appeared to be cleared by the liver. A patient therefore with impaired liver function may clear the antibody-enzyme at a different rate than a patient with

normal liver function. The current protocol states that a patient may have serum transaminase levels up to 5 times the upper limit of normal in the presence of liver metastasis. Changing these limits to exclude patients with this degree of liver impairment, and therefore setting a more stringent physiological environment, may limit the inter-patient variability in metabolism of antibody-enzyme that occurs.

The burden of tumour that a patient has may also influence the likelihood of ADEPT being efficacious. This may be because of the tumour burden's influence on normal physiological function or because of the total number of tumour cells required to be killed to achieve a cure.

The TUMOUR chosen for ADEPT may influence the likelihood of ADEPT. Tumours with a poor blood supply are unlikely to be accessible to antibody-enzyme. Also those with intact DNA repair mechanism will be more resistant to the effects of alkylating agents.

The TARGET could also be modified. CEA is currently used, and has many favourable characteristics. It is common and usually abundant, it has a cell surface location, it does have non-tumour expression, but in a location which is usually inaccessible. Its disadvantage may be that is secreted into the circulation, which may reduce tumour localisation of antibody-enzyme. The discovery of many more targets using proteomics and genomics may lead to the identification of a target more favourable than CEA.

The THERAPEUTIC may be modified in a number of ways. The antibody-enzyme could be modified in terms of the antibody, the enzyme or the antibody-enzyme moiety. Changes such as antigen affinity, molecular size, immunogenicity, enzymatic reaction, presence of tags or glycosylations may all influence the likelihood of success of the therapy. Similarly there are many opportunities for modification of the prodrug/drug chosen. Characteristics such as half-life, size, solubility, stability, chemical structure and potency may all affect the likelihood of efficacy. For example the development of a drug which formed DNA cross-links that were not vulnerable to DNA repair mechanisms

may improve the likelihood of efficacy of ADEPT, but it may also increase the potentially seriousness of toxicity.

The protocol used for THERAPY may also influence the likelihood of treatment efficacy. The dose of therapeutic used and the administration schedule may influence tumour and normal tissue biodistribution, and the likelihood of efficacy or toxicity. The timing of administration of prodrug in ADEPT is critical – it must be at a time when there is active enzyme present in tumour and minimal or no enzyme present in normal tissues. There needs to be an adequate amount of enzyme in tumour and enough prodrug to generate sufficient quantities of drug for cytotoxicity.

The number of potential modifications to the ADEPT system is therefore very large, and deciding which modification may be beneficial is difficult. The acquisition and organisation of mechanistic data can be used as a means of directing this decision process. The formation of a relational database may help rationalise this decision. In addition the development of mathematical models based on *in vitro* or *in vivo* data has the potential to direct decisions regarding modifications to ADEPT.

7.6 Conclusion

An Ontology and Conceptual Model have been developed for the purpose of organising data relevant to ADEPT. They provide the framework for the development of a database that would have the additional advantages of allowing data queries and improved data accessibility. The principals of both the Ontology and Conceptual Model are applicable to other targeted therapies. Allowing access to data and linking to other databases is an important concept in 'data sharing' and should lead to enhancement of knowledge. The organisation of data relevant to ADEPT has introduced areas for improvement in both mechanistic clinical trial design in ADEPT, and potential areas for improvement in ADEPT therapy itself. In the future the development of mathematical models could be used to predict rational modifications to the ADEPT system by using complex data acquired, organised and accessible as a result of a relational ADEPT database.

8 Conclusion

8.1 Background

The three hypotheses that have been addressed in this thesis are:

a) *That a mechanistic trial design improves understanding and development of ADEPT.*
b) *That a quantitative method of metabolic response assessment in ADEPT may augment the assessment of response in a phase I clinical trial setting, and in particular it may aid in the interpretation of radiological stable disease.*
c) *That the organisation of the data collected in the ADEPT clinical trials into an Ontology and Conceptual Model of ADEPT can direct mechanistic clinical trial design and identify areas for improvement in ADEPT.*

These hypotheses will be discussed in detail below, with particular emphasis on my individual contribution to the work presented.

8.2 A mechanistic trial design improves understanding and development of ADEPT

This hypothesis explores the concept that designing phase I/II clinical trials in a mechanistic fashion is an improvement on convention clinical trial design. Conventional phase I/II clinical trials focus predominantly on dose escalation to attain MTD. Once the MTD is defined efficacy may be assessed in a small cohort of patients. Mechanistic clinical trial design aims to test that each component of a therapy is functioning as proposed in a clinical trial setting. The trial design is therefore often more complicated and patients may individually undergo more investigations than in conventional trial designs, however the total number of patients may be minimised by the ability to make decisions based on the data collected. Mechanistic trials may potentially be safer for patients than standard dose escalation schemes, as data attained from previous patients may guide the dose escalation, and toxicities may be predicted or avoided. The therapy may be

better understood and therefore more rationally developed based on the data acquired in a clinical trial setting. Therapies that do not produce efficacy may, instead of being discarded as 'non-efficacious' instead be modified appropriately and further developed.

There are, however, disadvantages to mechanistic clinical trial design. The clinical trial itself is often complex and expensive, requiring many specialised staff for the trial. Co-ordination between staff is required. The recruitment rate may therefore be much slower than with conventional trial design, and overall the trial may take longer to complete. The large amount of data generated requires interpretation during the trial in order that appropriate modifications may be made. An assumption is made that outcomes in individual patients may be translatable to other patients. Overall a significant amount of time is spent on developing each individual therapy; whereas it may be argued that the time may be spent developing new therapies.

The potential advantages and disadvantages of a mechanistic clinical trial design are listed in **table 61**.

Table 61: Mechanistic clinical trial design

Advantages	Disadvantages
minimises number of patients required in clinical trial	many investigations performed in each individual patient (large burden to individual patients)
allows rational modifications to be made to therapy whilst trial is progressing	time-consuming and complex trial protocol
maximises information attained during clinical trial	requires co-ordination of many specialised medical and scientific staff expensive
minimises patient toxicities	assumes that outcomes from individual patients are translatable to others
improves overall understanding of a therapy	large amount of data generated which may be difficult to interpret
accelerates development of a therapy	each clinical trial may take longer than with a conventional trial design
unlikely to falsely discard a therapy as non-efficacious	significant time spent developing each individual therapy

A mechanistic clinical trial approach was used for both ADEPT clinical trials presented in this thesis, and it has been demonstrated that this design did, in fact, improve understanding of ADEPT for both trials.

The first clinical trial (A5CP and ZD2767P) was designed to examine if the enhanced features of ZD2767P, including increased potency and a short half-life of it active drug, would provide an advantage in terms of efficacy and reduced toxicity compared to the previous prodrug, CMDA (**chapter 2**). In addition it was proposed that the increased potency of ZD2767P would obviate the requirement for a clearing antibody system, as even low levels of CPG2 in tumour regions may be sufficient to allow enough ZD2767D to be generated for cytotoxic effect.

Efficacy in this trial was not achieved. The collection of quantitative mechanistic data allowed an understanding of the reason for this. Without a clearing antibody system inadequate tumour specific targeting occurred with low tumour to normal tissue ratios and minimal tumour enzyme localisation (tumour CPG2 enzyme levels 0.01 U/g by tumour biopsy and gamma camera analysis). Toxicity occurred at doses of ZD2767P too low for therapeutic effect, and was likely to be due to activation of ZD2767P by circulating CPG2 enzyme. As a result of the mechanistic data acquired the part II phase of the study was not performed, as the likelihood of these patients attaining efficacy from ADEPT was small. Without the mechanistic clinical trial design 14 patients would have been treated at MTD to assess efficacy.

The other important mechanistic information attained from this trial was that the antibody-enzyme conjugate, A5CP, was almost universally immunogenic, thereby limiting its potential for use for repeat therapy. It was also found to be difficult to manufacture with significant variability occurring in enzyme activity and protein concentration of each batch, resulting in different pharmacokinetic and radiolabelling profiles. Based on this data, a decision was made to develop a new antibody-enzyme for use in ADEPT, with the aim of having the features identified as being important, including improved tumour targeting, reduced immunogenicity and a more consistent product after manufacture. Without the

mechanistic data acquired from the trial these decisions could not have been made.

MFECP1, a genetically engineered fusion protein, was subsequently developed and manufactured for ADEPT, and a new clinical trial protocol was designed within two years of the previous trial ending. The aims of the clinical trial of MFECP1 and ZD2767P were to assess the safety and targeting ability of MFECP1, and to attempt to escalate the ZD2767P dose to levels likely to result in efficacy. Preliminary data has been presented in **chapter 4** on the first 13 patients treated with MFECP1 and ZD2767P. Again mechanistic studies were used to facilitate an understanding of function in the clinical trial setting. The preliminary data suggests that MFECP1 clears rapidly from the systemic circulation, as was proposed by preclinical data. The data from localisation of radiolabelled MFECP1 by quantitative SPECT imaging suggest there should be adequate levels of tumour CPG2 enzyme for prodrug activation, however this has yet to be confirmed by tumour biopsy. Prodrug dose escalation in continuing and it is predicted that the levels of ZD2767P required for efficacy may be obtained in a further 3 dose-doublings. Importantly, MFECP1 also appears to be associated with reduced immunogenicity compared to A5CP, which will have implications for repeated therapy.

The collection and analysis of quantitative mechanistic data has therefore been used throughout this thesis to assess if the design features of the components of ADEPT function *in vivo* as proposed. In this way limitations to the system have been understood and modifications proposed. These modifications have been rationally developed and implemented, which was only made possible due to the ability to collect mechanistic data on patients participating in the clinical trials. Mechanistic studies for ADEPT have therefore resulted, as hypothesised, in an improved understanding and development of ADEPT.

My clinical contribution to the ADEPT A5CP and ZD2767P clinical trial was in the recruitment and consenting of patients for the trial and the day to day care of patients on the trial. I co-ordinated the investigations performed on the patients, including liaising with scientific staff, other medical departments, wards, nursing staff and the patients. I analysed the gamma camera scans and [F-18] FDG PET

scans on all patients. I co-ordinated the collection and recording of the trial data and it was my role to integrate and interpret this data. I was involved in decisions regarding dose escalation, patient recruitment, timing of treatment and protocol modifications. I supervised the data entry into the Case Report Forms, and was responsible for answering data queries. I presented updates to the local ethics committee and reported adverse events and serious adverse event as required by the trial protocol. I presented data at the AstraZeneca quarterly meeting and was an important contributor to the interim and final reports issued to AstraZeneca.

As part of the development process for MFECP1 and its preparation for use in the clinical trial, I performed radiolabelling studies using technetium carbonyl for MFECP1. The methods and results of these radiolabelling studies are presented in **chapter 3**. I performed all of the radiolabelling experiments, including stability studies, CEA binding studies and a biodistribution experiment.

For the MFECP1 and ZD2767P clinical trial I was actively involved in the clinical trial design, the writing of the protocol and submission of the protocol to the appropriate regulatory committees (CIRB, ARSAC, LREC). As with the first ADEPT trial I had a clinical responsibility for the recruitment, consenting and management of patients on the trial. I, again, co-ordinated the running of the trial, and managed the timings of investigations and the co-ordination of staff and patients. I performed all of the gamma camera and FDG PET analysis for the patients on the trial. I supervised data entry into the case report forms and was responsible for the notification of serious adverse events. I played an active role in treatment decisions including dose escalations, timing of treatments and protocol modifications. I played a significant role in the collation, integration and interpretation of the mechanistic data collected on the 13 patients reported in this thesis. I was a key contributor to the interim report issued to AstraZeneca.

The points of discussion and conclusions formed about both clinical trials are my own, and were developed in collaboration and consultation with Prof R Begent and other key senior scientific and clinical staff. The contribution of other scientists and clinical staff to both trials was essential and I gratefully acknowledge their work.

8.3 A quantitative method of metabolic response assessment in ADEPT may augment the assessment of response in a phase I clinical trial setting, and in particular it may aid in the interpretation of radiological stable disease

The second hypothesis addressed in this thesis is based on the concept that the metabolic assessment of response in tumours may provide additional information when compared to conventional dimensional response assessment, particularly in a phase I/II clinical trial setting with non-optimised treatment being administered to heavily pre-treated patients with resistant tumours. It is in this setting that a sensitive assessment for therapeutic effect is required.

In order to test this hypothesis as part of the ADEPT clinical trials I had to first develop a method of quantitative response assessment for gamma camera [F-18] FDG PET and then test the method on a group of patients having conventional chemotherapy. The development of the automated region growing program was conjoint work with Dr Alan Green, in collaboration with Prof R Begent. The automated region growing program generates tumour volumes in a mathematically defined, reproducible and rapid manner, which provides a significant advantage over previous subjective methods of region drawing. Dr Green designed and implemented the program.

I planned, wrote and submitted to LREC the protocol for the clinical trial of using gamma camera [F-18] FDG PET to assess response to chemotherapy in patients with a broad range of tumour types receiving conventional first or second line chemotherapy. I was involved in the recruitment and consent of patients, and I co-ordinated the clinical trial. I designed the case report forms, supervised the data entry into these and provided annual reports on the trial's progress to LREC. I analysed the [F-18] FDG PET scans using the methods outlined in **chapter 5**. I was responsible for the interpretation of the data and for the conclusions attained as a result of the data acquired.

The clinical trial demonstrated that the automated region growing program could be applied to gamma camera [F-18] FDG PET scans, and that a statistical

measure that accounted for both tumour size and intensity of [F-18] FDG uptake correlated best with conventional measures of response and provided an advantage over methods that account for intensity alone. The trial also showed that quantitative gamma camera [F-18] FDG PET could be used to predict response to chemotherapy after 2-4 weeks of treatment. Importantly an [F-18] FDG PET response at 2-4 weeks correlated not only with CT response at 9-12 weeks, but also with overall patient survival. The trial also demonstrated that [F-18] FDG PET was useful for the assessment of patients with radiological stable disease, in whom it is often difficult to know if a therapy is efficacious.

Based on these results, I applied the VOI analysis, using the automated region growing program, to the [F-18] FDG PET scans performed on the patients who participated in the ADEPT clinical trials. I performed the analysis and I interpreted the [F-18] FDG data for these patients. In the ADEPT A5CP clinical trial the two patients who attained stable disease with ADEPT and had [F-18] FDG PET scans that could be analysed, both had an increase in VOI total counts, indicating a metabolic progression after therapy. In the ADEPT MFECP1 clinical trial, both patients with radiological stable disease and [F-18] FDG PET scans again progressed on metabolic imaging, although one of the patients had minimal progression, especially on the early [F-18] FDG PET scan. These results indicate limited efficacy of ADEPT in these patients, despite the patients attaining radiological stable disease.

These preliminary results indicate that metabolic imaging using [F-18] FDG PET may provide additional information on the response of tumours to ADEPT. The collection of more data would be valuable to further assess this. In particular the demonstration of a dose-response relationship between ZD2767P dose and tumour [F-18] FDG uptake would provide encouraging evidence for potential efficacy of ADEPT, even in the absence of a radiological response.

I have also demonstrated in this thesis that VOI analysis using the automated region growing program is a promising technique for the analysis of [F-18] FDG PET scans performed on gamma camera PET. It has the potential for wider application, in particular for quantitative response assessment of response to

therapies using [F-18] FDG PET, and is likely to be applicable to dedicated PET systems as well as gamma camera PET.

8.4 The organisation of the data collected in the ADEPT clinical trials into an Ontology and Conceptual Model of ADEPT can direct mechanistic clinical trial design and identify areas for improvement in ADEPT

The third hypothesis for this thesis was that by organising the data collected on ADEPT, future clinical trial design could be improved and areas for enhancement of ADEPT could be identified. The ADEPT Ontology and Conceptual Model presented in **chapter 7** is designed to form the framework for organising data on ADEPT. I developed the Ontology using Protégé-2000, on open-source java based ontology tool. I designed and implemented the Ontology and the Conceptual Model. From the Ontology and Conceptual Model I was able to organise the data collected on ADEPT, in particular with reference to clinical trials. I was then able to identify several areas where improved clinical trial design may provide further information on ADEPT and to identify some preliminary areas for improvement in ADEPT.

This work should provide the foundation to developing a relational database to enter, store, organise and query the data, and to develop mathematical models of ADEPT in order that proposed modifications to ADEPT could be 'tested' prior to implementation.

8.5 Conclusion

ADEPT was developed as a therapeutic strategy when it became apparent in the 1980s that for most solid tumours systemically delivered chemotherapeutics were unlikely to achieve cure. Since then a much greater molecular understanding of the pathogenesis of cancer has developed, as has an understanding of the limitations of conventional chemotherapy. Despite these advances there remains the prospect of only palliation for the vast majority of patients who have advanced disease with most of the common solid tumour types.

The advantage of a two-step system of ADEPT is that by generating active drug specifically in tumour sites systemic toxicity is minimised and tumour cytotoxicity is maximised. Theoretically the large quantities of cytotoxic agent generated in tumour may be sufficient to overcome resistance mechanisms and attain cure.

ADEPT is a complex strategy as it encompasses two therapeutic systems, and there are a vast number of modifications that could be made to the system that may affect its likelihood of success. I have presented in this thesis two clinical trials of ADEPT, which have both been designed in a mechanistic fashion in order that a maximal amount of relevant data could be obtained on the functioning of ADEPT in a clinical trial setting. This has been for the purpose of guiding potential modifications to the ADEPT system.

A mechanistic approach has been successful in identifying the limitations of therapy in the first ADEPT clinical trial presented in this thesis using A5CP and ZD2767P. This trial had no clinical responses however the mechanistic data allowed an understanding of why this occurred. The mechanistic data also identified the areas in which ADEPT needed to be improved. The second ADEPT clinical trial utilised a new targeting system, MFECP1, with potentially enhanced tumour targeting, reduced immunogenicity and a more robust production process. Data collected on the thirteen patients treated to date, shows improved tumour to normal tissue ratios of enzyme compared with A5CP, and therefore should allow escalation of prodrug doses to levels that may be efficacious. That trial is continuing and further mechanistic data will be

generated which should be able to enhance the understanding of ADEPT, and direct further modifications for the future.

The metabolic imaging of tumours using [F-18] FDG PET is emerging as a promising method of assessing response to therapies. I was involved in the development of an automated region growing algorithm to define tumour volumes and I designed a clinical trial to test the program in a cohort of patients receiving first or second line chemotherapy. I found that the use of statistics that took into account a change in tumour volume and metabolic activity correlated with patient response using conventional imaging and survival. This method was then applied to analysis of [F-18] FDG PET scans acquired in patients receiving ADEPT, and was particularly useful for the assessment of patients with radiological stable disease.

Mechanistic trial design leads to the generation of large amounts of data, and this data needs to be converted to information and then knowledge. It is becoming increasing difficult to store, recall, and analyse the vast quantities of data that are generated by mechanistic studies without the use of informatics to aid in the organisation and accessibility of this data. My development of an ADEPT Ontology and Conceptual Model was designed to initiate this process, by identifying the components of ADEPT, and broadly defining their relationships.

The Ontology serves to organise the data associated with ADEPT and can be used to identify components of ADEPT mechanistic clinical trial design that may be modified and improved. It highlights the potential complexity of ADEPT, particularly by identifying a number of possible alterations that may be made to the system. The future development of a relational database and ultimately of detailed mathematical models for ADEPT based on the framework provided by the Ontology and Conceptual Model should further facilitate the development of ADEPT for the future.

The concepts explored throughout this thesis of mechanistic clinical trial design and data organisation have used ADEPT, a complex therapeutic strategy, as the example. Many of the principles however, are widely applicable to phase I/II

clinical trial design and rational therapeutic development, and should therefore translate to other therapeutic approaches.

In conclusion, this thesis has outlined how a mechanistic approach to ADEPT has been used to collect data on a complex therapeutic strategy in a clinical setting, and how mechanistic data can be organised to facilitate an understanding of ADEPT and to identify areas of potential improvement to the system. It is by generating and interpreting this data that rational change to the system may be made, thereby speeding up the development process and improving the likelihood of efficacy. Although ADEPT is a complex therapeutic strategy, this should not in itself be a barrier to its successful development. As our understanding of the complexity of the genome and proteome develops, our knowledge of the difficulties of curing common solid tumours also increases. It is therefore becoming increasingly likely that a complex strategy will be required to cure this common and potentially terminal disease.

9 Publications and Awards in Support of the Thesis

9.1 Awards

Cancer Research UK Clinical Research Fellow (1998-2002)
Grant no: SP2116/0302

9.2 Abstracts

Francis RJ, Green AJ, Baig S, Knell V, Bowen RL, Buscombe JR, Hilson AJW, Begent RHJ. (2002) A novel approach to assessing response to cancer therapies using Hybrid Camera FDG PET. Royal Society of Medicine –Section of Oncology (oral presentation) ***Short-listed for Sylvia Lawler Prize***

Francis RJ, Green AJ, Baig S, Knell V, Buscombe JR, Begent RHJ (2002) A novel approach to assessing response to cancer therapies using Hybrid Camera FDG PET. Medical Research Society Meeting (poster presentation)

Francis RJ, Green AJ, Baig S, Knell V, Bowen RL, Buscombe JR, Hilson AJW, Begent RHJ. (2002) A novel approach to assessing response to cancer therapies using Hybrid Camera FDG PET. Society of Nuclear Medicine Meeting (poster presentation)

Francis RJ, Mather SJ, Chester K, Bhatia J, Sharma SK, Boden R, Waibel R, Green AJ, Begent RHJ. (2002) Radiolabelling of glycolsylated MFE-23-CPG2 fusion protein with ^{99m}Tc-carbonyl to determine biodistribution of active CPG2 enzyme in ADEPT systems. European Association of Nuclear Medicine Meeting (poster presentation)

Francis R, Sharma SK, Sena L, Springer C, Green AJ, Hope-Stone LD, Martin J, Adamson KL, O'Malley D, Tsiompanou E, Shahbakhti H, Webley S, Hochhauser D, Hilson AJ, Begent RHJ (2000) A Phase I Trial of Antibody Directed Enzyme Prodrug Therapy (ADEPT) in patients with advanced colorectal carcinoma or other CEA producing tumours. British Cancer Research Meeting (oral presentation) *Br. J. Cancer* 83 (S1), 18

Francis RJ, Sharma SK, Springer C, Green AJ, Hope-Stone LD, Sena L, Martin J, Adamson KL, O'Malley D, Tsiompanou E, Shahbakhti H, Webley S, Hochhauser D, Hilson AJ, Begent RHJ (2000) A Phase I Trial of Antibody Directed Enzyme Prodrug Therapy (ADEPT) in patients with advanced colorectal carcinoma or other CEA producing tumours. Advances in the Application of Monoclonal Antibodies in Clinical Oncology (oral presentation)

Francis RJ, Green AJ, Adamson KL, Buscombe JR , Begent RHJ (2000) A Visual Comparative System to Assess Response to a Novel Anti-Cancer Agent using FDG Gamma Camera PET. British Nuclear Medicine Society Meeting (oral presentation)

Webley SD, **Francis R**, Begent RHJ, Hartley JA, Hochhauser D. (1999) Measurement of the Critical DNA Lesions Produced by Antibody Directed Enzyme Prodrug Therapy. British Cancer Research Meeting (poster presentation) *Br. J. Cancer* 80 (S2), 47

9.3 Publications

Francis RJ, Mather SJ, Chester K, Sharma SK, Bhatia J, Pedley RB, Waibel R, Green AJ, Begent RH (2004) Radiolabelling of glycosylated MFE-23::CPG2 fusion protein (MFECP1) with ^{99m}Tc for quantitation of tumour antibody-enzyme localisation in antibody-directed enzyme pro-drug therapy (ADEPT) *Eur J Nucl Med Mol Imaging* 31(8): 1090-1096

Francis RJ and Begent RHJ (2003) Monoclonal antibody targeting therapy: an overview. Targeted Therapy for Cancer Editors: Konstantinos N Syrigos and Kevin J Harrington Publisher: Oxford University Press. 29-46 (invited chapter)

Francis R, Sharma SK, Springer C, Green AJ, Hope-Stone LD, Sena L, Martin J, Adamson KL, A Robbins, L Gumbrell, O'Malley D, Tsiompanou E, Shahbakhti H, Webley S, Hochhauser D, Hilson AJ, D Blakey, Begent RHJ (2002) A Phase I Trial of Antibody Directed Enzyme Prodrug Therapy (ADEPT) in patients with advanced colorectal carcinoma or other CEA producing tumours *Br J Cancer* 87(6): 600-607

Webley SD, **Francis R**, Pedley RB, Sharma SK, Begent RHJ, Hartley JA, Hochhauser D. (2001) Measurement of the Critical DNA Lesions Produced by Antibody Directed Enzyme Prodrug Therapy (ADEPT) in vitro, in vivo and in clinical material. *Br J Cancer*; 84(12): 1671-1676

9.4 Invited lectures

Antibody Therapy for Colorectal Cancer: Past, Present and Future (2000). St Thomas Hospital Oncology Meeting

Clinical Application of Targeted Therapies – the Magic Bullet (1998) Training for the Pharmaceutical Industry (TPI) course

10 References

Adam T (1989) Radioiodination for therapy. *Ann Clin Biochem* 26: 244-245

Adams GP, Schier R, McCall AM, Simmons HH, Horak EM, Alpaugh RK, Marks J, Weiner LM (2001) High affinity restricts the localization and tumor penetration of single-chain Fv antibody molecules. *Cancer Res* 61: 4750-4755

Adlard JW, Richman SD, Seymour MT, Quirke P (2002) Prediction of the response of colorectal cancer to systemic therapy. *Lancet Oncol* 3: 75-82

Advanced Colorectal Cancer Meta-analysis Project (1992) Modulation of fluorouracil by leucovorin in patients with advanced colorectal cancer: evidence in terms of response rate. *J Clin Oncol* 10: 896-901

Ak I, Blokland JAK, Pauwels EKL, Stokkel MPM (2001) The clinical value of ^{18}F-FDG detection with a dual-head co-incidence camera. *Eur J Nucl Med* 28(6): 763-778

Alberto R, Schibli R, Egli A, Schibiger A (1998) A novel organometallic aqua complex of technetium for the labeling of biomolecules: Synthesis of $[^{99m}Tc(OH_2)_3(CO)_3]^+$ from $[^{99m}TcO_4]^-$ in aqueous solution and its reaction with a bifunctional ligand. *J.Am.Chem.Soc.* 120: 7987-7988

Alizadeh AA, Eisen MB, Davis RE, Ma C, Lossos IS, Rosenwald A, Boldrick JC, Sabet H, Tran T, Yu X, Powell JI, Yang L, Marti GE, Moore T, Hudson J Jr, Lu L, Lewis DB, Tibshirani R, Sherlock G, Chan WC, Greiner TC, Weisenburger DD, Armitage JO, Warnke R, Staudt LM (2000) Distinct types of diffuse large B-cell lymphoma identified by gene expression profiling. *Nature* 403(6769): 503-551

Amlot P, Stone M, Cunningham D, Fay J, Newman J, Collins R, May R, McCarthy M, Richardson J, Ghetie V, Ramilo O, Thorpe PE, Uhr JW, Vitetta ES (1993) A phase I study of an anti-CD22-deglycosylated ricin A chain immunotoxin in the treatment of B-cell lymphomas resistant to conventional therapy. *Blood* 82(9): 2624-2633

Amlot PL, Rawlings E, Fernando ON, Griffin PJ, Heinrich G, Schreier MH, Castaigne JP, Moore R, Sweny P (1995) Prolonged action of a chimeric interleukin-2 receptor (CD25) monoclonal antibody used in cadaveric renal transplantation. *Transplantation* 60: 748-756

Apweiler R, Attwood TK, Bairoch A, Bateman A, Birney E, Biswas M, Bucher P, Cerutti L, Corpet F, Croning MD, Durbin R, Falquet L, Fleischmann W, Gouzy J, Hermjakob H, Hulo N, Jonassen I, Kahn D, Kanapin A, Karavidopoulou Y, Lopez R, Marx B, Mulder NJ, Oinn TM, Pagni M, Servant F, Sigrist CJ, Zdobnov EM; InterPro Consortium (2000) InterPro--an integrated documentation resource for protein families, domains and functional sites. *Bioinformatics* 16(12): 1145-1150

Armand J-P, Boige V, Raymond E, Fizazi K, Faivre S, Ducreux M (2000) Oxaliplatin in colorectal cancer: an overview. *Semin Oncol* 27(5, Suppl 10): 96-104

Armstrong AC, Dermime S, Allinson CG, Bhattacharyya T, Mulryan K, Gonzalez KR, Stern PL, Hawkins RE (2002) Immunization with a recombinant adenovirus encoding a lymphoma idiotype: induction of tumor-protective immunity and identification of an idiotype-specific T cell epitope. *J Immunol* 168: 3983-3391

Bagshawe KD (1987) Antibody directed enzymes revive anti-cancer prodrugs concept. *Br J Cancer* 56: 531-532

Bagshawe KD, Springer CJ, Searle F, Antoniw P, Sharma SK, Melton RG, Sherwood RF (1988) A cytotoxic agent can be generated selectively at cancer sites. *Br J Cancer* 58: 700-703

Bagshawe KD (1989) Towards generating cytotoxic agents at cancer sites. *Br J Cancer* 60: 275-281

[1]Bagshawe KD (1994) ADEPT and related concepts. *Cell Biophysics* 24/25: 83-91

[2]Bagshawe KD (1994) Antibody-directed enzyme prodrug therapy (ADEPT) *Journal of Controlled Release* 28: 187-193

Bagshawe K, Sharma S, Springer C, Antoniw P (1995) Antibody directed enzyme prodrug therapy: a pilot scale clinical trial. *Tumour Targeting* 1: 17-30

Bagshawe KD, Sharma SK (1996) Cyclosporine delays host immune response to antibody enzyme conjugate in ADEPT. *Transplant Proc* 28(6): 3156-3158

Bayat A (2002) Bioinformatics. *BMJ* 324: 1018-1022

Begent R, Ledermann J, Bagshawe K (1990) Chimeric B72.3 antibody for repeated radioimmunotherapy of colorectal cancer. *Antibody Immunoconjugates and Radiopharmaceuticals* 3: 86

Begent RHJ and Bagshawe KD (1996) Biodistribution studies. *Advanced Drug Delivery Reviews* 22: 325-329

Begent R, Verhaar M, Chester K, Casey J, Green A, Napier M, Hope-Stone L, Cushen N, Keep P, Johnson C, Hawkins R, Hilson A, Robson L (1996) Clinical evidence of efficient tumour targeting based on single-chain Fv antibody selected from a combinatorial library. *Nature Medicine* 2: 979-984

Behr TM, Becker WS, Bair H-J, Klein MW, Stühler CM, Cidlinsky KP, Wittekind CW, Scheele JR, Wolf FG (1995) Comparison of complete versus fragmented technetium-99m-labeled anti-CEA monoclonal antibodies for immunoscintography in colorectal cancer. *J Nucl Med* 36: 430-441

Behr TM, Liersch T, Greiner-Bechert L, Griesinger F, Béré M, Markus PM, Gratz S, Angerstein C, Brittinger G, Becker H, Goldenberg DM, Becker W (2002) Radioimmunotherapy of small-volume disease of metastatic colorectal cancer. *Cancer* 94: 1373-1381

Benchimol S, Fuks A, Jothy S, Beauchemin N, Shirota K, Stanners CP (1989) Cancinoembryonic antigen, a human tumor marker, functions as an intercellular adhesion molecule. *Cell* 57: 327-334

Bernstein ID (2000) Monoclonal antibodies to the myeloid stem cells: therapeutic implications of CMA-676, a humanized anti-CD33 antibody calicheamicin conjugate. *Leukemia* 14(3): 474-475

Bhatia J, Sharma SK, Chester KA, Pedley RB, Boden RW, Read DA, Boxer GM, Michael NP, Begent RH (2000) Catalytic activity of an in vivo tumor targeted anti-CEA scFv::carboxypeptidase G2 fusion protein. *Int J Cancer* 85(4): 571-577

Bidart J-M, Thuillier F, Augereau C, Chalas J, Daver A, Jacob N, Labrousse F, Voitot H (1999) Kinetics of serum tumor marker concentrations and usefulness in clinical monitoring. *Clinical Chemistry* 45(10): 1695-1707

Bignami GS, Senter PD, Grothaus PG, Fischer JJ, Humphreys R, Wallace PM (1992) N-(4-hydrox-phenylacetyl) palytoxin: a palytoxin prodrug that can be activated by a monoclonal antibody-penicillin G amidase conjugate. *Cancer Res* 52: 5759-5764

Blair SD, Theodorou NA, Begent RHJ, Dawson PM, Salmon M, Riggs S, Kelly A, Boxer G, Southall P, Gregory P (1990) Comparison of anti-foetal colonic microvillus and anti-CEA antibodies in preoperative radioimmunolocalisation of colorectal cancer. *Br J Cancer* 61: 891-894

Blakey DC, Valcaccia BE, East SJ, Wright AF, Boyle FT, Springer CJ, Burke PJ, Melton RG, Bagshawe KD (1993) Anti-tumour effects of an antibody-carboxypeptidase G2 conjugate in combination with benzoic acid mustard prodrug. *Cell Biophys* 22: 1-8

[1]Blakey DC, Burke PJ, Davies DH, Dowell RI, Melton RG, Springer CJ, Wright AF, (1995) Antibody-directed enzyme prodrug therapy (ADEPT) for treatment of major solid tumour disease. *Biochem Soc Trans* 23: 1047-1050

[2]Blakey DC, Davies DH, Dowell RI, East SJ, Burke PJ, Sharma SK, Springer CJ, Mauger AB, Melton RG (1995) Anti-tumour effects of an antibody-carboxypeptidase G2 conjugate in combination with phenol mustard prodrugs. *Br J Cancer* 72: 1083-1088

Blakey DC, Burke PJ, Davies DH, Dowell RI, East SJ, Eckersley KP, Fitton JE, McDaid J, Melton RG, Niculescu-Duvaz IA, Pinder PE, Sharma SK, Wright AF, Springer CJ (1996) ZD2767, an improved system for antibody-directed enzyme prodrug therapy that results in tumor regressions in colorectal tumor xenografts. *Cancer Res* 56(14): 3287-3292

Boehm MK, Mayans MO, Thornton JD, Begent RH, Keep PA, Perkins SJ (1996) Extended glycoprotein structure of the seven domains in human carcinoembryonic antigen by X-ray and neutron solution scattering and an automated curve fitting procedure: implications for cellular adhesion. *J Mol Biol* 259(4): 718-736

Boehm MK and Perkins SJ (2000) Structural models for carcinoembryonic antigen and its complex with the single-chain Fv antibody molecule MFE23. *FEBS Letters* 475: 11-16

Boehm MK, Corper AL, Wan T, Sohi MK, Sutton BJ, Thornton JD, Keep PA, Chester KA, Begent RHJ, Perkins SJ (2000) Crystal structure of anti-(carcinoembryonic antigen) single chain Fv antibody MFE-23 and a model for antigen binding based on intermolecular contacts. *Biochem J* 346: 519-528

Bokemeyer C, Kollmannsberger C, Oechsle K, Dohmen BM, Pfannenberg A, Claussen CD, Bares R, Kanz L (2002) Early prediction of treatment response to high-dose salvage chemotherapy in patients with relapsed germ cell cancer using [^{18}F] FDG PET. *Br J Cancer* 86: 506-511

Boland MP, Knox RJ, Roberts JJ (1991) The differences in kinetics of rat and human DT diaphorase result in a differential sensitivity of derived cell lines to CB 1954 (5-(aziridin-1-yl)-2,4-dinitrobenzamide). *Biochem Pharmacol* 41: 867-875

Bomanjii JB, Costa DC, Ell PJ (2001) Clinical role of positron emission tomography in oncology. *Lancet Oncol* 2(3): 157-164

Boschoff C, Begent R (1996) Tumor Markers. In: Taylor I, Cook T, Guillou P, (eds). Essential General Surgical Oncology. Churchill Livingstone: 131-140

Bosslet K, Czech J, Lorenz P, Sedlacek HH, Schuermann M, Seemann G (1992) Molecular and functional characterisation of a fusion protein suited for tumour specific prodrug activation. *Br J Cancer* 65: 234-238

Bosslet K, Czech J and Hoffman D (1994). Tumor-selective prodrug activation by fusion protein mediated catalysis. *Cancer Res* 54: 2151-2159

Boulianne GL, Hozumi N, Shulman MJ (1984) Production of functional chimeric mouse/human antibody. *Nature* 312: 643-646

Boxer GM, Begent RHJ, Kelly AMB, Southall PJ, Blair SB, Theodorou NA, Dawson PM, Ledermann JA (1992) Factors influencing variability of localization of antibodies to carcinoembryonic antigen (CEA) in patients with colorectal carcinoma- implications for radioimmunotherapy *Br J Cancer* 65: 825-831

Boxer G, Abassi A, Pedley R, Begent R (1994) Localisation of monoclonal antibodies reacting with different epitopes on carcinoembryonic antigen (CEA): implications for targeted therapy. *Br J Cancer* 69: 307-314

Boxer G, Stuart-Smith S, Flynn A, Green A and Begent RHJ (1999) Radioimmunoluminography: a tool for relating tissue antigen concentration to clinical outcome. *Br J Cancer* 80: 922-926

Brenner DJ and Elliston CD (2004) Estimated Radiation Risks Potentially Associated with Full-Body CT Screening. *Radiology* 232: 735-738

Brock C, Meikle S, Price P (1997) Does fluorine-18 fluorodeoxyglucose metabolic imaging of tumours benefit oncology? *Eur J Nucl Med* 24: 691-705

Brown N and Bicknell R (1998) Thymidine phosphorylase, 2-deoxy-D-ribose and angiogenesis. *Biochem J* 334: 1-8

Brown RS, Leung JY, Kison PV, Zasadny KR, Flint A, Wahl RL (1999) Glucose transporters and FDG uptake in untreated primary human non-small cell lung cancer. *J Nucl Med* 40: 556-565

Brown SL, Miller RA, Levy R (1989) Anti-idiotype antibody therapy of B-cell lymphoma. *Semin Oncol* 16(3): 199-210

Buchegger F, Haskell CM, Schreyer M, Scazziga BR, Randin S, Carrel S, Mach J-P (1983) Radiolabelled fragments of monoclonal antibodies against carcinoembryonic antigen for localization of human colon carcinoma grafted into nude mice. *J Exp Med* 158: 413-427

Budinger TF (1998) PET instrumentation: what are the limits? *Semin Nucl Med* 28(3): 247-267

Byers V, Baldwin RW. (1988) Therapeutic strategies with monoclonal antibodies and immunoconjugates. *Immunology* 65: 329-335

Cancer Research UK (2002) Mortality-UK *CancerStats*

Carl PL, Chakravarty PK, Katzenellenbogen JA, Weber MJ (1980) Protease activated 'prodrugs' for cancer chemotherapy. *Proc Natl Acad Sci* 77: 2224-2228

Casey JL, Keep PA, Chester KA, Robson L, Hawkins RE, Begent RH (1995) Purification of bacterially expressed single chain Fv antibodies for clinical applications using metal chelate chromatography. *J Immunol Methods* 179: 105-116

Cavalli F and Sessa C (1999) Current issues in phase I trials: New study designs and informed consent procedures. *Annals Oncol* 10 (Suppl. 6): S147-S146

Cella D F, Tulsky D S, Gray G, Sarafian B, Lloyd S, Linn E, Bonomi A, Silberman M, Yellen SB, Wincour P, Brannon J, Eckberg K, Purl S, Blendowski C, Goodman M, Barnicle M, Stewart I, McHale M, Bonomi P, Kaplan E, Taylor S, Thomas C, Harris J (1993) The functional assessment of cancer therapy (FACT) scale: development and validation of the general method. *J Clin Onc* 11(3): 570-579

Chang LT (1978) A method for attenuation correction in radionuclide computerised tomography. *IEEE Trans Nucl Sci* NS-25: 638-643

Cheng TL, Wei SL, Chen BM, Chern JW, Wu MF, Liu PW, Roffler SR (1999) Bystander killing of tumour cells by antibody-targeted enzymatic activation of a glucuronide prodrug. *Br J Cancer* 79(9-10): 1378-1385

Chester KA, Begent RH, Robson L, Keep P, Pedley BR, Boden JA, Boxer G, Green A, Winter G, Cochet O, Hawkins RE (1994) Phage libraries for generation of clinically useful antibodies. *Lancet* 343: 455-456

Chester KA, Hawkins RE (1995) Clinical issues in antibody design. *Tibtech* 13: 294-300

[1]Chester KA, Bhatia J, Boxer G, Cooke SP, Flynn AA, Huhalov A, Mayer A, Pedley RB, Robson L, Sharma SK, Spencer DIR, Begent RHJ (2000) Clinical applications of phage-derived sFvs and sFv fusion proteins. *Dis Markers* 16: 53-62

[2]Chester KA, Mayer A, Bhatia J, Robson L, Spencer DIR, Cooke SP, Flynn AA, Sharma SK, Boxer G, Pedley RB, Begent RHJ (2000) Recombinant anti-carcinoembryonic antigen antibodies for targeting cancer. *Cancer Chemother Pharmacol* 46 (Suppl): S8-S12

Choi NC, Fischman AJ, Niemierko A, Ryu J-S, Lynch T, Wain J, Wright C, Fidias P, Mathisen D (2002) Dose-response relationship between probability of pathological tumour control and glucose metabolic rate measured with FDG PET after preoperative chemoradiotherapy in locally advanced non-small-cell lung cancer. *Int J Rad Oncol Biol Phys* 54(4): 1024-1035

Chung J-K, Jang J-J, Lee D-S, Lee M-C, Koh C-S (1994) Tumor concentration of carcinoembryonic antigen measured by in vitro quantitative autoradiography. *J Nucl Med* 35: 1499-1505

Cobb LM, Connors TA, Elson LA, Khan AH, Mitchley BC, Ross WC, Whisson ME (1969) 2,4-dinitro-5-ethyleneiminobenzamide (CB 1954): a potent and selective inhibitor of the growth of the Walker carcinoma 256. *Biochem Pharmacol* 18(6): 1519-1527

Colcher D, Bird R, Roselli M, Hardman KD, Johnson S, Pope S, Dodd SW, Pantoliano MW, Milenic DE, Schlom J (1990) In vivo tumor targeting of a recombinant single-chain antigen-binding protein. *J Natl Cancer Inst* 82(14): 1191-1197

Collie-Duguid ESR, Johnston SJ, Boyce L, Smith N, Cowieson A, Cassidy J, Murray GI, McLeod HL (2001) *Int J Cancer* 94: 297-301

[1]Compton C, Fenoglio-Preiser CM, Pettigrew N, Fielding LP on behalf of the Colorectal Working Group (2000) American Joint Committee on Cancer Prognostic Factors Consensus Conference. *Cancer* 88(7): 1739-1757

[2]Compton CC, Fielding LP, Burgart LJ, Conley B, Cooper HS, Hamilton SR, Hammond ME, Henson DE, Hutter RV, Nagle RB, Nielsen ML, Sargent DJ, Taylor CR, Welton M, Willett C (2000) Prognostic factors in colorectal cancer. College of American Pathologists Consensus Statement 1999. *Arch Pathol Lab Med.* 124(7): 979-994

Connors TA and Whisson ME (1966) Cure of mice with advanced plasma cell tumours with aniline mustard: the relationship between glucuronidase activity and tumour sensitivity. *Nature* 210: 866-867

Connors TA and Melzak DH (1971) Studies on the mechanisms of action of 5-aziridinyl-2-4-dinitrobenzamide (CB1954): A selective inhibitor of the growth of the Walker carcinoma. *Int J Cancer* 7: 86-92

Connors TA (1978) Anti-tumour drugs with latent activity. *Biochemia* 60: 979

Connors TA (1996) Bioreductive agents, hypoxic cells and therapy (editorial). *Eur J Cancer* 32A(11): 1833-1834

Cremerius U, Fabry U, Wildberger JE, Zimny M, Reinartz P, Nowak B, Schaefer W, Buell U, Osieka R (2002) Pre-transplant positron emission tomography (PET) using fluorine-18-fluor-deoxyglucose (FDG) predicts outcome in patients treated with high-dose chemotherapy and autologous stem cell transplantation for non-Hodgkin's lymphoma. *Bone Marrow Tranplant* 30: 103-111

Cunningham D, Pyrhönen S, James RD, Punt CJA, Hickish T, Heikkila R, Johannesen TB, Starkhammer H, Topham CA, Awad L, Jacques C, Herait P (1998) Randomised trial of irinotecan plus supportive care versus supportive care alone after fluorouracil failure for patients with metastatic colorectal cancer. *Lancet* 352: 1413-1418

Dawson PM, Blair SD, Begent RH, Kelly AM, Boxer GM, Theodorou NA (1991) The value of radioimmunoguided surgery in first and second look laparotomy for colorectal cancer. *Dis Colon Rectum* 34(3): 217-222

de Gramont A, Figer A, Seymour M, Homerin M, Hmissi A, Cassidy J, Boni C, Cortes-Funes H, Cervantes A, Freyer G, Papamichael D, Le Bail B, Louvet C, Hendler D, de Braud F, Wilson C, Morvan F and Bonetti A (2000) Leucovorin and fluorouracil with or without oxaliplatin as first-line treatment in advanced colorectal cancer. *J Clin Oncol* 18(16): 2938-2947

Demetri GD, von Mehren M, Blanke CD, van den Abbeele AD, Eisenberg B, Roberts PJ, Heinrich MC, Tuveson DA, Singer S, Janicek M, Fletcher JA, Silverman SG, Silberman SL, Capdeville R, Kiese B, Peng B, Dimitrijevic S, Druker BJ, Corless C, Fletcher CDM, Joensuu H (2002) Efficacy and safety of imatinib mesylate in advanced gastrointestinal stromal tumors. *N Engl J Med* 347: 472-480

Denny WA and Wilson WR (1993) Bioreducible mustards – a paradigm for hypoxia-selective prodrugs of diffusible cytotoxins (HPDCs). *Cancer Metast Rev* 12: 135-151

Denny WA, Wilson WR and Hay MP (1996) Recent developments in the design of bioreductive drugs. *Br J Cancer* 74(Suppl. XXVII): S32-S38

De Witte O, Hildebrand J, Luxen A, Goldman S (1994) Acute effect of carmustine on glucose metabolism in brain and glioblastoma. Cancer 74(10): 2836-2842

Diederichs CG, Staib L, Glatting G, Beger HG, Reske SN (1998) FDG PET: Elevated plasma glucose reduces both uptake and detection rate of pancreatic malignancies. *J Nucl Med* 39: 1030-1033

Douillard JY, Cunningham D, Roth AD, Navarro M, James RD, Karasek P, Jandik P, Iveson T, Carmichael J, Alakl M, Gruia G, Awad L, Rougier P (2000) Irinotecan combined with fluorouracil compared with fluorouracil alone as first-line treatment for metastatic colorectal cancer: a multicentre randomised trial. *Lancet* 355: 1041-1047

Eccles SA, Court WJ, Box GA, Dean CJ, Melton RG, Springer CJ (1994) Regression of established breast carcinoma xenografts with Antibody-Directed Enzyme Prodrug Therapy against c-*erbB2* p185. *Cancer Res* 54: 5171-5177

Eisenhauer PJ, O'Dwyer PJ, Christian M, Humphrey JS (2000) Phase I clinical trial design in cancer drug development. *J Clin Oncol* 18(3): 684-692

Emilien G, van meurs W, Maloteaux J-M (2000) The dose-response relationship in Phase I clinical trials and beyond: use, meaning and assessment. *Pharmacol Ther* 88: 33-58

Elias DJ, Hirschowitz L, Kline LE, Kroener JF, Dillman RO, Walker LE, Robb JA, Timms RM (1990) Phase I clinical comparative study of monoclonal antibody KS1/4 and KS1/4-methotrexate immunconjugate in patients with non-small cell lung carcinoma. *Cancer Res* 50(13): 4154-4159

Endo M, Shinbori N, Fukase Y Sawada N, Ishikawa H, Tanaka Y (1999) Induction of thymidine phosphorylase expression and enhancement of efficacy of capecitabine or 5′-deoxy-5-fluorouridine by cyclophosphamide in mammary tumour models. *Int J Cancer* 83: 127-134

Epenetos AA, Snook D, Durbin H, Johnson PM, Taylor-Papadimitriou A (1986) Limitations of radiolabelled monoclonal antibodies for localization of human neoplasms. *Cancer Res* 46: 3183-3191

Erdi YE, Mawlawi O, Larson SM, Imbriaco M, Young H, Finn R, Humm JL (1997) Segmentation of lung lesion volume by adaptive positron emission tomography image thresholding. *Cancer* 80: 2505-2509

Findlay M, Young H, Cunningham D, Iveson A, Cronin B, Hickish T, Pratt B, Husband J, Flower M, Ott R (1996) Noninvasive Monitoring of Tumour Metabolism using Fluorodeoxyglucose and Positron Emission Tomography in Colorectal Cancer Liver Metastasis: Correlation with Tumour Response to Fluorouracil. *J Clin Oncol* 14: 700-708

Flamen P, Van Cutsem E, Lerut A, Cambier J-P, Haustermans K, Bormans G, De Leyn P, Van Raemdonck D, De Wever W, Ectors N, Maes A, Mortelmans L (2002) Positron emission tomography for assessment of the response to induction radiochemotherapy in locally advanced oesophageal cancer. *Ann Oncol* 13: 361-368

Fletcher RH (1986) Carcinoembryonic antigen. *Annals of Internal Medicine* 104: 66-73

Flynn AA, Green AJ, Boxer GM, Casey JL, Pedley RB, Begent RHJ (1999) A novel technique, using radioluminography, for the measurement of uniformity of radiolabelled antibody distribution in a colorectal cancer xenograft model. *Int J Radiation Oncology Biol Phys* 43(1): 183-189

Flynn AA, Boxer GM, Begent RHJ, Pedley RB (2001) Relationship between tumour morphology, antigen and antibody distribution measured by fusion of digital phosphor and photographic images. *Cancer Immunol Immunother* 50: 77-81

Flynn AA, Pedley RB, Green AJ, Boxer GM, Boden R, Bhatia J, Morris R, Begent RH (2002) Antibody and radionuclide characteristics and the enhancement of the effectiveness of radioimmunotherapy by selective dose delivery to radiosensitive areas of tumour. *Int J Radiat Biol* 78(5): 407-415

Ford JM and Hait WN (1990) Pharmacology of drugs that alter multidrug resistance in cancer. *Pharm Reviews* 42(3): 155-199

Fox S, Gasparini G, Harris A (2001) Angiogenesis: pathological, prognostic, and growth-factor pathways and their link to trial design and anti-cancer drugs. *Lancet Oncol* 2: 278-289

Francis R, Sharma SK, Springer C, Green AJ, Hope-Stone LD, Sena L, Martin J, Adamson KL, A Robbins, L Gumbrell, O'Malley D, Tsiompanou E, Shahbakhti H, Webley S, Hochhauser D, Hilson AJ, D Blakey, Begent RHJ (2002) A Phase I Trial of Antibody Directed Enzyme Prodrug Therapy (ADEPT) in patients with advanced colorectal carcinoma or other CEA producing tumours *Br J Cancer* 87: 600-607

Frei E III, Teicher BA, Holden SA, Cathcart KNS and Wang Y (1988) Preclinical studies and clinical correlation of the effect of alkylating dose. *Cancer Res* 48: 6417-6423

Friedlos F, Davies L, Scanlon I, Ogilvie LM, Martin J, Stribbling SM, Spooner RA, Niculescu-Duvaz I, Marias R, Springer CJ (2002) Three new prodrugs for suicide gene therapy using carboxypeptidase G2 elicit bystander efficacy in two xenograft models. *Cancer Res* 62: 1724-1729

Fujimori K, Covell DG, Fletcher JE, Weinstein JN (1990) A modeling analysis of monoclonal antibody percolation through tumours: a binding site barrier. *J Nucl Med* 31: 1191-1198

Fuks A, Banjo C, Freedman S, Gold P (1974) Carcinoembryonic antigen (CEA): Molecular biology and clinical significance. *Biochim Biophys Acta* 417: 123-152

Gallagher BM, Fowler JS, Gutterson NI, MacGregor R, Wan C, Wolf A (1978) Metabolic trapping as a principle of radiopharmaceutical design: Some factors responsible for the biodistribution of [18F] 2-deoxy-glucose. *J Nucl Med* 19: 1154-1161

Garcia de Palazzo IE, Adams GP, Sundareshan P, Wong AL, Testa JR, Bigner DD, Weiner LM (1993) Expression of mutated epidermal growth factor receptor by non-small cell lung carcinomas. *Cancer Res* 53: 3217-3220

Giacchetti S, Perpoint B, Zidani R, le Bail N, Faggiuolo R, Focan C, Chollet P, Llory JF, Letourneau Y, Coudert B, Bertheaut-Cvitkovic F, Larregain-Fournier D, Le Rol A, Walter S, Adam R, Misset JL, Lévi F (2000) Phase III multicenter randomized trial of oxaliplatin added to chronomodulated fluorouracil-leucovorin as first-line treatment of metastatic colorectal cancer. *J Clin Oncol* 18(1): 136-147

Glennie MJ and Johnson PWM (2000) Clinical trials of antibody therapy. *Immunology Today* 21(8): 403-410

Gold P, Freedman S (1965) Demonstration of tumor-specific antigens in human colonic carcinomata by immunological tolerance and absorption techniques. *J Exp Med* 121: 439-462

Goldenberg DM (2002) Targeted therapy of cancer with radiolabelled antibodies. *J Nucl Med* 43: 693-713

Goodwin DA, Meares CF (1997) Pretargeting. General Principles. *Cancer* 80: 2675-2680

Gordon J, Abdul-Ahad AK, Hamblin TJ, Stevenson FK, Stevenson GT (1984) Mechanisms of tumour cell escape encountered in treating lymphocytic leukaemia with anti-idiotypic antibody. *Br J Cancer* 49: 547-557

Gottesman MM, Fojo T, Bates SE (2002) Multidrug resistance in cancer: role of ATP-dependent transporters. *Nat Rev Cancer* 2(1): 48-58

Grana C, Chinol M, Robertson C, Mazzetta C, Bartolomei M, De Cicco C, Fiorenza M, Gatti M, Caliceti P, Paganelli G (2002) Pretargeted adjuvant radioimmunotherapy with yttrium-90-biotin in malignant glioma patients: a pilot study. *Br J Cancer* 86: 207-212

Greco O and Dachs GU (2001) Gene directed enzyme/prodrug therapy of cancer: Historical appraisal and future prospectives. *J Cell Physiol* 187: 22-36

Green AJ, Dewhurst SH, Begent RH, Bagshawe KD, Riggs SJ (1990) Accurate quantification of I-131 distribution by gamma camera imaging. *Eur J Nucl Med* 16: 361-365

Green AJ, Adamson KL and Begent RHJ (1999) Validation of a gamma camera PET system for serial 18F-FDG imaging for the measurement of response to anti-cancer therapies (abstract). *J Nucl Med* 40(5) 1246

Griffiths L, Dachs GU, Bicknell R, Harris AL, Stratford IJ (1997) The influence of oxygen tension and pH on the expression of platelet-derived endothelial cell growth factor/ thymidine phosphorylase in human breast cancer cells grown *in vitro* and *in vivo*. *Cancer Res* 57: 570-572

Gruber TR (1993) A translation approach to portable ontologies. *Knowledge Acquisition* 5(2): 199-220

Haberkorn U, Strauss LG, Dimitrakopoulou A, Engenhart R, Oberdorfer F, Ostertag H, Romahn J, van Kaick G (1991) PET studies of fluorodeoxyglucose metabolism in patients with recurrent colorectal tumours receiving radiotherapy. *J Nucl Med* 32: 1485-1490

Hamberg LM, Hunter GJ, Alpert NM, Choi NC, Babich JW, Fischman AJ (1994) The dose uptake ratio as an index of glucose metabolism: useful parameter or oversimplification? *J Nucl Med* 35: 1308-1312

Hamblin TJ, Abdul-Ahad AK, Gordon J, Stevenson FK, Stevenson GT (1980) Preliinary experience in treating lymphocytic leukaemia with antibody to immunoglobulin idiotypes on the cell surfaces. *Br J Cancer* 42: 495-502

Hammarstrõm S (1999) The carcinoembryonic antigen (CEA) family: structures, suggested functions and expression in normal and malignant tissues. *Seminars in Cancer Biology* 9: 67-81

Hanessian S and Wang J (1993) Design and synthesis of a cephalosporin-carboplatinum prodrug activatable by a β-lactamase. *Can J Chem* 71: 896-906

Harwood PJ, Britton DW, Southall PJ, Boxer GM, Rawlins G, Rogers GT (1986) Mapping epitope characteristics on carcinoembryonic antigen. *Br J Cancer* 54: 75-82

Hautzel H and Müller-Gärtner H-W (1997) Early changes in fluorine-18-FDG uptake during radiotherapy. *J Nucl Med* 38: 1384-1386

Hawkins DS, Rajendran JG, Conrad EU, Bruckner JD, Eary JF (2002) Evaluation of chemotherapy response in pediatric bone sarcomas by [F-18]-fluorodeoxy-D-glucose positron emission tomography. *Cancer* 94: 3277-3284

Hawkins RE, Chester KA (1996) Antibody technology has been transformed. In: Yarnold J, Stratton M, McMillan T (eds). Molecular Biology for Oncologists. London: Chapman & Hall: 250-260

Herbst RS, Hess KR, Tran HT, Tseng JE, Mullani NA, Charnsangavej C, Madden T, Davis DW, McConkey DJ, O'Reilly MS, Ellis LM, Pluda J, Hong WK, Abbruzzese JL (2002) Phase I study of recombinant human endostatin in patients with advanced solid tumors. *J Clin Oncol* 20(18): 3792-3803

Hericourt J, Richet C (1895) De la serotherapie dans le traitment du cancer. *C R Acad Sci* 121: 567-569

Hockey MS, Stokes HJ, Thompson H, Woodhouse CS, Macdonald B, Fielding JWL, Ford CHJ (1984) Carcinoembryonic antigen (CEA) expression and heterogeneity in primary and autologous metastatic gastric tumours demonstrated by a monoclonal antibody. *Br J Cancer* 49: 129-133

Hoekstra CJ, Paglianiti I, Hoekstra OS, Smit EF, Postmus PE, Teule GJJ, Lammertsma AA (2000) Monitoring response to therapy in cancer using [18F]-2-fluoro-2-deoxy-D-glucose and positron emission tomography: an overview of different analytical methods. *Eur J Nucl Med* 27: 731-743

Hoff PM, Ansari R, Batist G, Cox J, Kocha W, Kuperminc M, Maroun J, Walde D, Weaver C, Harrison E, Berger HU, Osterwalder B, Wong AO, Wong R (2001) Comparison of oral capecitabine versus intravenous fluorouracil plus

leucovorin as first-line treatment in 605 patients with metastatic colorectal cancer: results of a randomized phase III study. *J Clin Oncol* 19(8): 2282-2292

Hoh CK, Schiepers C, Seltzer MA, Gambhir SS, Silverman DHS, Czernin J, Maddahi J, Phelps ME (1997) PET in Oncology: Will it replace the other modalities? *Semin Nucl Med* 27(2): 94-106

Houba PHJ, Boven E, Van der Meulen-Muileman IH, Leenders RGG, Scheeren JW, Pinedo HM, Haisma HJ (2001) Pronounced anti-tumour efficacy of doxorubicin when given as the prodrug dox-GA3 in combination with a monoclonal antibody- β-glucoronidase conjugate. *Int J Cancer* 91: 550-554

Huber BE, Richards CA, Krenitsky TA (1991) Retroviral-mediated gene therapy for the treatment of hepatocellular carcinoma: an innovative approach for cancer therapy. *Proc Natl Acad Sci USA* 88: 8039-8043

Hughes A and Calvert H (1999) Editorial-An update on thymidylate synthase inhibitors. *Annals of Oncology* 10(10): 1137-1139

Hughes P, Lowe C, Sherwood R (1982) Metal ion-promoted binding of proteins to immobilized triazine dye affinity adsorbants. *Biochem Biophys Acta* 700: 90-100

Huse WD, Sastry L, Iverson SA, Kang AS, Alting-Mees M, Burton DR, Benkovic SJ, Lerner RA (1989) Generation of a large combinatorial library of the immunoglobulin repertoire in phage lambda. *Science* 246: 1275-1281

Hustinx R, Bénard F, Alavi A (2002) Whole-body FDG-PET imaging in the management of patients with cancer. *Semin Nucl Med* 32(1): 35-46

Huston J, Levinson D, Mudgett-Hunter M, Tai M-S, Novotný J, Margolies MN, Ridge RJ, Bruccoleri RE, Haber E, Crea R, Oppermann H (1988) Protein engineering of antibody binding sites: recovery of specific activity in an anti-digoxin single chain Fv analogue produced in Eschericia coli. *Proc Natl Acad Sci, USA* 85(16): 5879-5883.

Ichiya Y, Kuwabara Y, Otsuka M, Tahara T, Yoshikai T, Fukumura T, Jingu K, Masuda K (1991) Assessment of response to cancer therapy using fluorine-18-fluorodeoxyglucose and positron emission tomography. *J Nucl Med* 32: 1655-1660

Imran MB, Kubota K, Yamuda S, Fukuda H, Yamada K, Fujiwara T, Itoh M (1998) Lesion-to-background ratio in non-attenuation corrected whole-body FDG PET images. *J Nucl Med* 39: 1219-1223

Ishikawa T, Sekiguchi F, Fukase Y, Sawada N, Ishitsuka H (1998) Positive correlation between the efficacy of capecitabine and doxifluridine and the ratio of thymidine phosphorylase to dihydropyrimidine dehydrogenase activities in tumors in human cancer xenografts. *Cancer Res* 58: 685-690

Israel O, Keider Z, Iosilevsky G, Bettman L, Sachs J, Frenkel A (2001) The fusion of anatomic and physiologic imaging in the management of patients with cancer. *Semin Nucl Med* 31(3): 191-205

Jansson T, Westlin J, Ahlstrom H, Lilja A, Langstrom B, Bergh J (1995) Positron emission tomography studies in patients with locally advanced and/or metastatic breast cancer: A method for early therapy evaluation? *J Clin Oncol* 13: 1470-1477

Jaszczak RS, Greer KL, Floyd CE, Harris CC, Coleman RE (1984) Improved SPECT quantification using compensation for scattered photons. *J Nucl Med* 25: 893-900

Johnson PWM and Glennie MJ (2001) Rituximab: mechanisms and applications. *Br J Cancer* 85: 1619-1623

Judson IR, Beale PJ, Trigo JM, Aherne W, Crompton T, Jones D, Bush E, Reigner B (1999) A human capecitabine excretion balance and pharmacokinetic study after administration of a single oral dose of ^{14}C-labelled drug. *Invest New Drugs* 17: 49-56

Juranka PF, Zastawny RL, Ling V (1989) P-glycoprotein: multidrug-resitance and a superfamily of membrane-associated transport proteins. *FASEB J* 3(14): 2583-2592

Kato H, Kuwano H, Nakajimi M, Miyazaki T, Yoshikawa M, Masuda N, Fukuchi M, Manda R, Tsukada K, Oriuchi N, Endo K (2002) Usefulness of positron emission tomography for assessing the response of neoadjuvant chemoradiotherapy in patients with esophageal cancer. *Amer J Surg* 184: 279-283

Kaye SB (1998) Multidrug resistance: clinical relevance in solid tumour and strategies for circumvention. *Curr Opin Oncol* 10(S1): S15- S19

Keyes JW Jnr (1995) SUV: standard uptake value or silly useless value. *J Nucl Med* 36: 1836-1839

Kim CK, Gupta NC, Chandramouli B, Alavi A (1994) Standardized uptake values of FDG: body surface area correction is preferable to body weight correction. *J Nucl Med* 35: 164-167

Kim CK and Gupta NC (1996) Dependency of standardized uptake values of fluorine-18 fluorodeoxyglucose on body size: Comparison of body surface area correction and lean body mass correction. *Nucl Med Commun* 17: 890-894

Kohler G, Milstein C (1975) Continuous cultures of fused cells secreting antibody of predefined specificity. *Nature* 256: 495-497

Kostakoglu L, Coleman M, Leonard JP, Kuji I, Zoe H, Goldsmith SJ (2002) PET predicts prognosis after 1 cycle of chemotherapy in aggressive lymphoma and Hodgkin's disease. *J Nucl Med* 43: 1018-1027

Kreitman RJ, Wilson WH, Bergeron K, Raggio M, Stetler-Stevenson M, Fitzgerald DJ, Pastan I (2001) Efficacy of the anti-CD22 recombinant immunotoxin BL22 in chemotherapy resistant hairy cell leukaemia. *N Engl J Med* 345(4): 241-247

Lamoyi E and Nisonoff A (1983) Preparation of $F(ab')_2$ fragments from mouse IgG of various subclasses. *J Immunol Methods* 56(2): 235-243

Landoni C, Gianolli L, Lucignani G, Magnani P, Savi A, Travaini L, Gilardi MC, Fazio F (1999) Comparison of dual head co-incidence PET versus ring PET in tumor patients. *J Nucl Med* 40: 1617-1622

Lane DM, Eagle KF, Begent RH, Hope-Stone LD, Green AJ, Casey JL, Keep PA, Kelly AM, Ledermann JA, Glaser MG, Hilson AJW (1994) Radioimmunotherapy of metastatic colorectal tumours with iodine-131-labelled antibody to carcinoembryonic antigen: phase I/II study with comparative biodistribution of intact and F(ab')2 antibodies. *Br J Cancer* 70: 521-525

Langen K-J, Braun U, Rota Kops E, Herzog H, Kuwert T, Nebeling B, Feinendegen LE (1993) The influence of plasma glucose levels on fluorine-18-flourodeoxyglucose uptake in bronchial carcinomas. *J Nucl Med* 34: 355-359

Ledermann J, Begent R, Massof C, Kelly A, Adam T, Bagshawe K (1991) A phase I study of repeated therapy with radiolabelled antibody to carcinoembryonic antigen using intermittent or continuous administration of cyclosporin A to suppress the immune response. *Int J Cancer* 47: 659-664

Leichman CG, Fleming TR, Muggia FM, Tangen CM, Ardalan B, Doroshow JH, Meyers FJ, Holcombe RF, Weiss GR, Mangalik A, Macdonald JS (1995) Phase II study of fluorouracil and its modulation in advanced colorectal cancer: A Southwest Oncology Group Study. *J Clin Oncol* 13(6): 1303-1311

Levy R, Warnke R, Dorfman RF, Haimovich J (1977) The monoclonality of human B cell lymphomas. *J Exp Med* 145: 1014-1021

Lindholm P, Minn H, Leskinen-Kaillio S, Bergman J, Ruotsalainen U, Joensuu H (1993) Influence of blood glucose concentration on FDG uptake in cancer - a PET study. *J Nucl Med* 34: 1-6

Lindmark G, Bergstrom R, Pahlman L, Glimelius B (1995) The association of preoperative serum tumour markers with Dukes' stage and survival in colorectal cancer. *Br J Cancer* 71: 1090-1094

Lokich JL, Ahlgren JD, Gullo JJ, Philips JA, Fryer JG (1989) A prospective randomized comparison of continuous infusion fluorouracil with a conventional bolus schedule in metastatic colorectal carcinoma: A Mid-Atlantic Oncology Program Study. *J Clin Oncol* 7(4): 425-432

Mach JP, Carrel S, Forni M, Ritschard J, Donath A, Alberto P (1980) Tumour localization of radiolabelled antibodies against carcinoembryonic antigen in patients with carcinoma: A critical evaluation. *N Engl J Med* 303: 5-10

Maeda K, Chung Y-S, Ogawa Y, Takatsuka S, Kang S-M, Ogawa M, Sawada T, Onoda N, Kato Y, Sowa M (1996) Thymidine phosphorylase/ platelet derived endothelial cell growth factor expression associated with hepatic metastasis in gastric carcinoma. *Br J Cancer* 73: 884-888

Mani S and Ratain MJ (1997) New phase I trial methodology. *Semin Oncol* 24(2): 253-261

Marias R, Spooner RA, Light Y, Martin J, Springer CJ (1996) Gene-directed Enzyme Prodrug therapy with a mustard prodrug/ carboxypeptidase G2 combination. *Cancer Res* 56: 4735-4742

Martin KJ, Kritzman BM, Price LM, Koh B, Kwan C-P, Zhang X, Mackay A, O'Hare MJ, Kaelin CM, Mutter GL, Pardee AB, Sager R (2000) Linking gene expression patterns to therapeutic groups in breast cancer. *Cancer Res* 60(8): 2232-2238

Martin KW and Halpern SE (1984) Carcinoembryonic antigen production, secretion and kinetics in BALBc mice and a nude mouse-human model. *Cancer Res* 44: 5475 –5481

Martin J, Stribbling SM, Poon GK, Begent RHJ, Napier M, Sharma SK, Springer CJ (1997) Antibody-directed enzyme prodrug therapy: pharmacokinetics and

plasma levels of prodrug and drug in a phase I clinical trial. *Cancer Chemother Pharmacol* 40(3): 189-201

Matsumura Y, Maeda H (1986) A new concept for macromolecular therapeutics in cancer chemotherapy: mechanism of tumoritropic accumulation of proteins and the antitumour mechanism. *Cancer Res* 46: 6387-6392

Mayer A, Chester K, Bhatia J, Pedley R, Read D, Boxer G, Begent R (1998) Exemplifying Guidelines for Preparation of Recombinant DNA Products in Phase I Trials in Cancer: Preparation of a Genetically Engineered Anti-CEA Single Chain Fv Antibody. *Eur J Cancer* 34(7): 968-976

Mayer A, O'Malley D, Boxer G, Tsiompanou E, Bhatia J, Flynn A, Chester K, Davidson B, Lewis A, Winslett M, Dhillon A, Hilson A, Begent R (2000) Radioimmunoguided surgery in colorectal cancer using a genetically engineered anti-CEA single chain Fv antibody. *Clin Cancer Res* 6: 1711-1719

McCafferty J, Griffiths AD, Winter G, Chiswell DJ (1990) Phage antibodies: filamentous phage displaying antibody variable domains. *Nature* 348: 552-554

McCulloch J, Chabner B, Bertino J (1971) Purification and properties of carboxypeptidase G1. *J Biol Chem* 246: 7207-7213

Mease RC and Lambert C (2001) Newer methods of labeling diagnostic agents with Tc-99m. *Semin Nucl Med* 16(4): 278-285

Melton RG, Boyle JM, Rogers GT, Burke P, Bagshawe KD, Sherwood RF (1993) Optimization of small-scale coupling of A5B7 monoclonal antibody to carboxypeptidase G2. *J Immunol. Methods* 158: 49-56

Meta-analysis Group in Cancer (1998) Efficacy of intravenous continuous infusion of fluorouracil compared with bolus administration in advanced colorectal cancer. *J Clin Oncol* 16(1): 301-301

Meyer DL, Jungheim LN, Law KL, Mikolajzcyk SD, Shepherd TA, Mackensen DG, Briggs SL, Starling JJ (1993) Site-specific prodrug activation by antibody-β-

lactamase conjugates: regressions and long-term growth inhibition of human colon carcinoma xenograft models. *Cancer Res* 53: 3956-3963

Michael NP, Chester KA, Melton RG, Robson L., Nicholas W, Boden JA, Pedley RB, Begent RHJ, Sherwood HJ, and Minton NP (1996) In vitro and in vivo characterisation of a recombinant carboxypeptidase G2::anti-CEA scFV fusion protein. *Immunotechnology* 2: 47-57

Milenic DE, Yokota T, Filpula DR, Finkelman MA, Dodd SW, Wood JF, Whitlow M, Snoy P, Schlom J (1991) Construction, binding properties, metabolism, and tumor targeting of a single-chain Fv derived from the pancarcinoma monoclonal antibody CC49. *Cancer Res* 51(23 Pt 1): 6363-6371

Miller AB, Hogestraeten B, Staquet M, Winkler A (1981) Reporting results of cancer treatment. *Cancer* 47: 207-214

Miller RA, Maloney DG, Warnke R, Levy R (1982) Treatment of B cell lymphoma with monoclonal anti-idiotype antibody. *N Engl J Med* 306(9): 517-522

Miller RA, Hart S, Samoszuk M, Coulter C, Brown S, Czerwinski D, Kelkenberg J, Royston I, Levy R (1989) *N Engl J Med* 321(13): 851-856

Minn H, Zasadny KR, Quint LE, Wahl RL (1995) Lung cancer: reproducibility of quantitative measurements for evaluating 2-[F-18]-fluoro-2-deoxy-D-glucose uptake at PET. *Radiology* 196: 167-173

Minton JP, Hoehn JL, Gerber GM, Horsely JS, Connolly DP, Salwan F, Fletcher WS, Cruz AB, Gatchell FG, Oviedo M, Meyer KK, Leffall LD, Berk RS, Stewart PA, Kurucz SE (1985) Results of a 400-patient carcinoembryonic antigen second-look colorectal cancer study. *Cancer* 55: 1284-1290

Mitchell EP (1998) Role of carcinoembryonic antigen in the management of advanced colorectal carcinoma. *Semin Oncol* 25(5: S11): 12-20

Miwa M, Ura M, Nishida M, Sawada N, Ishikawa T, Mori K, Shimma N, Umeda I (1998) Design of a novel oral fluoropyrimidine carbamate, capecitabine, which generates 5-Fluorouracil selectively in tumours by enzymes concentrated in human liver and cancer tissue. *Eur J Cancer* 34(8): 1274-1281

Monks NR, Blakey DC, East SJ, Dowell RI, Calvete JA, Curtin NJ, Arris CE, Newell DR (2002) DNA interstrand cross-linking and *TP53* status as determinants of tumour cell sensitivity *in vitro* to the antibody-directed enzyme prodrug therapy ZD2767. *Eur J Cancer* 38: 1543-1552

Nap M, Hammarstrõm M-L, Bõrmer O, Hammarstrõm S, Wagener C, Handt S, Schreyer M, Mach J-P, Buchegger F, von Kleist S, Grunert F, Seguin P, Fuks A, Holm R, Lamerz R (1992) Specificity and affinity of monoclonal antibodies against carcinoembryonic antigen. *Cancer Res* 52: 2329-2339

Napier M, Sharma S, Springer C, Bagshawe K, Green A, Johnson C, Martin J, Stribbling S, Cushen N, O'Malley D, Begent R (2000) Antibody-Directed Enzyme Prodrug Therapy (ADEPT): Efficacy and Mechanism of Action in Colorectal Cancer. *Clin Cancer Res* 6: 765-772

National Cancer Institute (1988) NCI Common Toxicity Criteria. *Division of Cancer Treatment*

National Library of Medicine (2002) Medical Subject Headings (MeSH®) *Factsheets* http://www.nlm.nih.gov/pubs/factsheets/mesh.html

Neuberger MS, Williams GT, Fox RO (1984) Recombinant antibodies possessing novel effector functions. *Nature* 312: 604-608

Neuberger M, Williams G, Mitchell E, Jouhall SS, Flanagan JG, Rabbitts TH (1985) A hapten-specific chimeric IgE antibody with human physiological effector function. *Nature* 314: 268-270

Newell DR, Burtles SS, Fox BW, Jodrell DI Connors TA (1999) Evaluation of rodent only toxicology for early clinical trials with novel cancer therapeutics. *Br J Cancer* 81: 760-768

Niculescu-Duvaz I and Springer CJ (1995) Antibody-directed enzyme prodrug therapy (ADEPT): A targeting strategy in cancer chemotherapy. *Current Medicinal Chemistry* 2: 687-706

O'Neill MC and Song L (2003) Neural network analysis of lymphoma microarray data: prognosis and diagnosis near-perfect. *BMC Bioinformatics* 4: 13-25

Ordoñez C, Screaton RA, Ilantzis C, Stanners CP (2000) Human carcinoembryonic antigen functions as a general inhibitor of anoikis. *Cancer Res* 60: 3419-3424

Paganelli G, Magnani P, Chinol M, Sudati F, Zito F, Mangili F, Li M, Meares CF, Siccardi AG, Fazio F (1998) Pilot therapy trial of CEA positive tumours using a three-step pretargeting approach. *Tumor Targeting* 3: 96-104

Pastan I and Gotessman M (1987) Multiple-drug resistance in human cancer. *N Engl J Med.* 316(22): 1388-1393

Patton J, Turkington T (1999) Co-incidence Imaging with a Dual-Head Scintillation Camera. *J Nucl Med* 40: 432-441

Pedley RB, Boden J, Keep PA, Harwood PJ, Green AJ, Rogers GT (1987) Relationship between tumour size and uptake of radiolabelled anti-CEA in a colon tumour xenograft. *Eur J Nucl Med* 13: 197-202

Pedley RB, Boden JA, Boden RW, Green AJ, Boxer GM, Bagshawe KD (1989) The effect of serum CEA on the distribution and clearance of anti-CEA antibody in a pancreatic tumour xenograft model. *Br J Cancer* 60: 549-554

Pedley RB, Boden JA, Boden R, Dale R, Begent RHJ (1993) Comparative radioimmunotherapy using intact or $F(ab')_2$ fragments of ^{131}I anti-CEA antibody in a colonic xenograft model. *Br J Cancer* 68: 69-73

Pedley BR. (1996) Pharmacokinetics of monoclonal antibodies. *Clin Immunother* 6(1): 54-67

Perron MJ and Page M (1996) Activation of methotrexate-phenylalanine by monoclonal antibody--carboxypeptidase A conjugate for the specific treatment of ovarian cancer in vitro. *Br J Cancer* 73: 281-287

Philpott GW, Bower RJ, Parker CW (1973) Selective iodination and cytotoxicity of tumour cells with an antibody-enzyme conjugate. *Surgery* 74(1): 51-58

Pietersz GA, Patrick MR, Chester KA (1998) Preclinical characterization and in vivo imaging studies of an engineered recombinant technetium-99m-labeled metallothionein-containing anti-carcinoembryonic antigen single chain antibody. *J Nucl Med* 39: 47-56

Press OW, Eary J, Appelbaum F, Martin PJ, Badger CC, Nelp WB, Glenn S, Butchko G, Fisher D, Porter B, Matthews DC, Fisher LD, Bernstein ID (1993) Radiolabelled antibody therapy of B-cell lymphoma with autologous bone marrow support. *N Engl J Med* 329: 1219-1224

Price P and Jones T on behalf of the EC PET Oncology Concerted Action and the EORTC PET Study Group (1995) Can positron emission tomography (PET) be used to detect subclinical response to cancer therapy? *Eur J Cancer* 31A(12): 1924-1927

Protégé (2000) The Protégé Project. http://protege.stanford.edu

Quinn M, Babb P, Brock A, Kirby L, Jones J (2001) Cancer Trends in England and Wales 1950-1999. *Studies on Medical and Population Subjects*. No. 66.

Ratain MJ, Mick R, Schilsky RL, Siegler M (1993) Statistical and ethical issues in the design and conduct of phase I and II clinical trials of new anticancer agents. *J Natl Cancer Inst* 85(20): 1637-1643

Reidhaar-Olson JF and Hammer J (2001) The impact of genomics tools on target discovery. *Current Drug Discovery* 4: 20-24

Reigner B, Blesch K, Weidekamm E (2001) Clinical pharmacokinetics of capecitabine. *Clin Pharmacokinet* 40: 85-104

Reiter Y, Brinkmann U, Lee B, Pastan I (1996) Engineering antibody Fv fragments for cancer detection and therapy: disulfide-stabilized Fv fragments. *Nat. Biotechnol.* 14(10): 1239-1245

Riechmann L, Clark M, Waldmann H and Winter G (1988) Reshaping human antibodies for therapy. *Nature* 332: 323-327

Rodrigues ML, Carter P, Wirth C, Mullins S, Lee A, Blackburn BK (1995) Synthesis and β-lactamase mediated activation of cephalosporin-taxol prodrug. *Chem Biol* 2: 223-227

Rogers GT, Burke PJ, Sharma SK, Koodie R, Boden JA (1995) Plasma clearance of an antibody-enzyme conjugate in ADEPT by monoclonal anti-enzyme: its effect on prodrug activation *in vivo*. *Br J Cancer* 73: 1357-1363

Roitt IM, Brostoff J, Male DK (eds) (2001) Chapter 18: Tumour Immunology *Immunology (Sixth edition)* Mosby Inc: 289-302

Römer W, Hanauske A-R, Ziegler S, Thödtmann R, Weber W, Fuchs C, Enne W, Herz M, Nerl C, Garbrecht M, Schwaiger M (1998) Positron emission tomography in non-Hodgkin's lymphoma: assessment of chemotherapy with fluorodeoxyglucose. *Blood* 91(12): 4464-4471

Ross D, Siegal D, Beall H, Prakash AS, Mulcahy RT, Gibson NW (1993) DT-diaphorase in activation and detoxification of quinines – bioreductive action of mitomycin C. *Cancer Metast Rev* 12: 83-101

Rougier P, Paillot B, LaPlanche A, Morvan F, Seitz JF, Rekacewicz C, Laplaige P, Jacob J, Grandjouan S, Tigaud JM, Fabri MC, Luboinski M, Ducreux (1997) 5 Fluorouracil (5-FU) continuous intravenous infusion compared with bolus administration. Final results of a randomized trial in metastatic colorectal cancer. *Eur J Cancer* 33(11): 1789-1793

Rougier P, Van Cutsem E, Bajetta E, Niederle N, Possinger K, Labianca R, Navarro M, Morant R, Bleiberg H, Wils J, Awad L, Herait P, Jacques C (1998) Randomized trial of irinotecan versus fluorouracil by continuous infusion after

fluorouracil failure in patients with metastatic colorectal cancer. *Lancet* 353: 1407-1412

Rougier P and Mitry E (2000) Colorectal cancer chemotherapy: Irinotecan. *Semin Oncol* 27(5, Suppl 10): 138-143

Rozenthal JM, Levine RL, Nicles RJ, Dobkin JA (1989) Glucose uptake by gliomas after treatment. A positron emission tomographic study. *Arch Neurol* 46: 1302-1307

Russell SJ, Llewelyn MB, Hawkins RE (1992) Principles of antibody therapy. *BMJ* 305: 1424-1428

Rustin G (2003) Use of CA-125 to Assess Response to New Agents in Ovarian Cancer Trials. *J Clin Oncol* 21(10 Suppl): 187-193

Saijo N, Tamura T, Nishio K (2003) Strategy for the development of novel anticancer drugs. *Cancer Chemother Pharmacol* 52(Suppl 1): S97-S101

Salonga D, Danenberg KD, Johnson M, Metger R, Groshen S, Tsao-Wei DD, Lenz H-J, Leichman CG, Leichman L, Diasio RB, Danenberg PV (2000) Colorectal tumors responding to 5 fluorouracil have low gene expression of dihydropyrimidine dehydrogenase, thymidylate synthase and thymidine phosphorylase. *Clin Cancer Res* 6: 1322-1327

Salman U, Martin C, Hammond L, Chintapalli K, Denis L, Kuhn J, Rowinsky E, Phillips W (2000) Use of a spherical 3-D blob analysis program as a method of determination of standardized uptake value (SUV) for following tumor response to chemotherapeutic agents (CTA) *Clin Positron Imaging* 3(4): 152

Saltz LB, Cox JV, Blanke C, Rosen L, Fehrenbacher L, Moore MJ, Maroun JA, Ackland SP, Locker PK, Pirotta N, Elfring GL, Miller LL for the Irinotecan Study Group (2000) Irinotecan plus fluorouracil and leucovorin for metastatic colorectal cancer. *N Engl J Med* 343: 904-914

Satchi R, Connors TA, Duncan R (2001) PDEPT: polymer-directed enzyme prodrug therapy. HPMA copolymer-cathepsin B and PK1 as a model combination. *Br J Cancer* 85: 1070-1076

Savage P, Rowlinson-Busza G, Verhoeyen M, Spooner RA, So A, Windust J, Davis PJ, Epenetos AA (1993) Construction, characterisation and kinetics of a single chain antibody recognising the tumour associated antigen placental alkaline phosphatase. *Br J Cancer* 68: 738-742

Sawada N, Ishikawa T, Fukase Y, Nishada M, Yoshikubo T, Ishitsuka H (1998) Induction of thymidine phosphorylase activity and enhancement of capecitabine activity by Taxol, Taxotere in human cancer xenografts. *Clin Cancer Res* 4: 1013-1019

Sawada N, Ishikawa T, Sekiguchi F, Tanaka Y, Ishitsuka H (1999) Xray irradiation induces thymidine phosphorylase and enhances the efficacy of capecitabine (Xeloda) in human cancer xenografts. *Clin Cancer Res* 5: 2948-2953

Schuller J, Cassidy J, Dumont E, Roos B, Durston S, Banken L, Utoh M, Mori K, Weidekamm E, Reigner B (2000) Preferential activation of capecitabine in tumor following oral administration to colorectal cancer patients. *Cancer Chemother Pharmacol* 45(4): 291-297

Senter PD, Saulnier MG, Schreiber GJ, Hirschberg DL, Brown JP, Hellström I and Hellström KE (1988) Anti-tumor effects of antibody-alkaline phosphatase conjugates in combination with etoposide phosphate. *Proc Natl Acad Sci USA* 85: 4842-4846

Senter PD, Schreiber GJ, Hirschberg DL, Ashe SA, Hellström KE and Hellström I (1989) Enhancement of the in vitro and in vivo antitumour activities of phosphorylated mitomycin C and etoposide derivatives by monoclonal antibody-alkaline phosphatase conjugates. *Cancer Res* 49: 5789-5792

Senter PD (1990) Activation of prodrugs by antibody-enzyme conjugates: a new approach to cancer therapy. *FASEB J* 4: 188-193

Senter PD and Springer CJ (2001) Selective activation of anticancer prodrugs by monoclonal antibody-enzyme conjugates *Adv. Drug Deliv. Rev.*53: 247-264

Sharma S, Bagshawe K, Burke P, Boden R, Rogers G (1990) Inactivation and clearance of an anti-CEA carboxypeptidase G2 conjugate in blood after localisation in a mouse xenograft model. *Br J Cancer* 61: 659-662

Sharma SK, Bagshawe KD, Springer CJ, Burke PJ, Rogers GT, Boden JA, Antoniw P, Melton RG and Sherwood RF (1991) Antibody-directed enzyme prodrug therapy (ADEPT): a three phase system. *Dis Markers* 9: 225-231

Sharma SK, Bagshawe KD, Melton RG, Sherwood RF (1992) Human immune response to monoclonal antibody-enzyme conjugates in ADEPT pilot clinical trial. *Cell Biophys* 21: 109-120

Sharma SK, Bagshawe KD, Burke PJ, Boden JA, Rogers GT, Springer CJ, Melton RG, Sherwood RF (1994) Galactosylated antibodies and antibody-enzyme conjugates in antibody-directed enzyme prodrug therapy. *Cancer* 73(3 Suppl): 1114-1120

[1]Sharma SK (1996) Accelerated clearance systems. *Advanced Drug Delivery Reviews.* 22: 315-324

[2]Sharma SK (1996) Immune response in ADEPT. *Advanced Drug Delivery Reviews.* 22: 369-376

Sharma SK, Pedley RB, Bhatia J, Minton NP, Chester KA, Begent RHJ (2000) *In vivo* characteristics of an engineered fusion protein for ADEPT. *Br J Cancer* 83(S1): 71a

[1]Sharma SK, Irwin H, Pedley RB, Bhatia J, Dearling J, Flynn A, Chester KA, Begent RHJ (2001) Biodistribution of ^{123}I-labelled MFE-CP fusion protein in LS174T xenografted nude mice. *Br J Cancer* 85(S1): 99

[2]Sharma SK, Bhatia J, Pedley RB, Spencer DIR, Minton NP, Chester KA, Begent RHJ (2001) Immunogenicity of carboxypeptidase G2 (CPG2) enzyme in ADEPT. *Br J Cancer* 85(S1): 98

Sherwood RF, Melton RG, Alwan SM and Hughes P (1985) Purification and properties of carboxypeptidase G2 from *Pseudomonas sp* strain RS-16: use of a novel triazine-dye affinity method. *Eur J Biochem* 148: 447-453

Shreve P, Steventon R, Deters E, Kison P, Gross M, Wahl R (1998) Oncological diagnosis with 2-[fluorine-18] fluoro-2-deoxy-D-glucose imaging: dual-head coincidence gamma camera versus positron emission tomographic scanner. *Radiology* 207: 431-437

Sievers EL, Appelbaum FR, Spielberger RT, Forman SJ, Flowers D, Smith FO, Shannon-Dorcy K, Berger MS, Bernstein ID (1999) Selective ablation of acute myeloid leukemia using antibody-targeted chemotherapy: a phase I study of an anti-CD33 calicheamicin immunoconjugate. *Blood* 93(11): 3678-3684

Sim BKL, Fogler WE, Zhou XH, Liang H, Madsen JW, Luu K, O'Reilly MS, Tomaszewski JE, Fortier AH (1999) Zinc ligand-disrupted recombinant human Endostatin: Potent inhibition of tumor growth, safety and pharmacokinetic profile. *Angiogenesis* 3: 41-51

Simon R, Freidlin B, Rubinstein L, Arbuck SG, Collins J, Christian MC (1997) Accelerated titration designs for phase I clinical trials in oncology. *J Natl Cancer Inst* 89(15): 1138-1147

Smith IC, Welch AE, Hutcheon AW, Miller ID, Payne S, Chilcott F, Waiker S, Whitaker T, Ah-See A, Eremin O, Heys SD, Gilber FJ, Sharp PF (2000) Positron emission tomography using [^{18}F]-fluorodeoxyglucose to predict the pathological response of breast cancer to primary chemotherapy. *J Clin Oncol* 18(8): 1676-1688

Sobrero A, Guglielmi A, Grossi F, Puglisi F, Aschele C (2000) Mechanism of action of fluoropyrimidines: relevance to the developments in colorectal cancer chemotherapy. *Semin. Oncol* 27(5): 72-77

Sokoloff L, Reivich M, Kennedy C, Des Rosiers MH, Patlak CS, Pettigrew KD, Sakurada O, Shinohara M. (1977) The [14C] deoxyglucose method for the measurement of local cerebral glucose utilization: theory, procedure, and normal values in the conscious and anesthetized albino rat. *J Neurochem.* 28(5): 897-916

Sols A, Crane RK (1954) Substrate specificity of brain hexokinase. *J Biol Chem* 210: 581-595

Spence A, Muzi M, Graham MM, O'Sullivan F, Link JM, Lewellen TK, Lewellen B, Freeman SD, Mankoff DA, Eary JF, Krohn KA (2002) 2-[^{18}F] Fluoro-2-deoxyglucose and glucose uptake in malignant gliomas before and after radiotherapy: correlation with outcome. *Clin Cancer Res* 8: 971-979

Spencer DIR, Robson L, Purdy D, Whitelegg NR, Michael NP, Bhatia J, Sharma SK, Rees AR, Minton NP, Begent RHJ, Chester KA (2000) A strategy for mapping and neutralizing conformational immunogenic sites on protein therapeutics. *Proteomics* 2: 271-279

Springer CJ, Antoniw P, Bagshawe KD, Searle F, Bisset GMF, Jarman M (1990) Novel prodrugs which are activated to cytotoxic alkylating agents by carboxypeptidase G2. *J Med Chem* 33: 677-681

[1]Springer CJ, Antoniw P, Bagshawe KD, Wilman DEV (1991) Comparison of half-lives and cytotoxicity of *N*-chloroethyl-4 amino and *N*-mesyloxyethyl-benzoyl compounds, properties of prodrugs in antibody-directed enzyme prodrug therapy (ADEPT). *Anti-Cancer Drug Design* 6: 467-479

[2]Springer CJ, Bagshawe KD, Sharma SK, Searle F, Boden JA, Antoniw P, Burke PJ, Rogers GT, Sherwood RF, Melton RG (1991) Ablation of human choriocarcinoma xenografts in nude mice by antibody-directed enzyme prodrug therapy (ADEPT) with three novel compounds. *Eur J Cancer* 27(11): 1361-1366

Springer CJ, Poon GK, Sharma SK, Bagshawe KD (1993) Identification of prodrug, active drug, and metabolites in an ADEPT clinical study. *Cell Biophys* 22: 9-26

Springer CJ, Dowell R, Burke PJ, Hadley E, Davis DH, Blakey DC, Melton RG, Niculescu-Duvaz I (1995) Optimization of alkylating agent prodrugs derived from phenol and aniline mustards: a new clinical candidate prodrug (ZD2767) for antibody-directed enzyme prodrug therapy (ADEPT). *J Med Chem* 38(26): 5051-5065

Springer CJ, Bavetsias V, Jackman AL, Boyle FT, Marshall D, Pedley RB, Bisset GM (1996) Prodrugs of thymidylate synthase inhibitors: potential for antibody directed enzyme prodrug therapy (ADEPT). *Anticancer Drug Dis.* 11(8): 625-636

Stalteri MA, Bansal S, Hider R, Mather SJ (1999) Comparison of the stability of technetium-labeled peptides to challenge with cysteine. *Bioconjugate Chem* 10: 130-136

Stangl R, Altendorf-Hofmann A, Charnley RM, Scheele J (1994) Factors influencing the natural history of colorectal liver metastases. *Lancet* 343: 1405-1410

Stoldt HS, Aftab F, Chinol M, Paganelli G, Luca F, Testori A, Geraghty JG (1997) Pretargeting strategies for radio-immunoguided tumour localization and therapy. *Eur J Cancer* 33(2): 186-192

Studholme C, Hill DL, Hawkes DJ (1997) Automated three-dimensional registration of magnetic resonance and positron emission tomography brain images by multiresolution optimization of voxel similarity measures. *Med Phys.* 24(1): 25-35

Svensson HP, Vrudhula VM, Emswiler JE, MacMaster JF, Cosand WJ, Senter PD, Wallace PM (1995) In vitro and in vivo activities of a doxorubucin prodrug in combination with monoclonal antibody β-lactamase conjugates. *Cancer Res* 55: 2357-2365

Takebayashi Y, Akiyama S, Akiba S Yamada K, Miyadera K, Sumizawa T, Yamada Y, Murata F, Aikou T (1996) Clinicopathologic and prognostic

significance of an angiogenic factor, thymidine phosphorylase, in human colorectal carcinoma. *J Natl Cancer Inst* 88: 1110-1117

Tatsumi M, Yutani K, Watanabe Y, Miyoshi S, Tomiyama N, Johkoh T, Kusuoka H, Nakamura H, Nishimura T (1999) Feasibility of fluorodeoxyglucose dual-head gamma camera coincidence imaging in the evaluation of lung cancer: comparison with FDG PET. *J Nucl Med* 40(4): 566-573

Tewson TJ and Krohn KA (1998) PET radiopharmaceuticals: State-of-the-art and future prospects. *Semin Nucl Med* 28(3): 221-234

The Gene Ontology Consortium (2001) Creating the Geno Ontology resource: Design and implementation. *Genome Research* 11: 1425-1433

Therasse P, Arbuck SG, Eisenhauer EA, Wanders J, Kaplan RS, Rubinstein L, Verweij J, Van Glabbeke M, van Oosterom AT, Christian MC, Gwyther SG (2000) New guidelines to evaluate the response to treatment in solid tumors. *J Natl Cancer Inst* 92(3): 205-216

Thomas SR, Maxan HR, Kereiaakes JC (1976) In vivo quantitation of lesion radioactivity using external counting methods. *Med Phys* 3: 253-255

Thornburg RW, Day JF, Baynes JW, Thorpes SR (1980) Carbohydrate-mediated clearance of immune complexes from circulation. A role for galactose residues in the hepatic uptake of IgG-antigen complexes. *J Biol Chem* 255(14): 6820-6825

Tjandra JJ, Pietersz GA, Teh JG, Cuthbertson AM, Sullivan JR, Penfold C, McKenzie IF, Smyth M (1989) Phase I clinical trial of drug-monoclonal antibody conjugates in patients with advanced colorectal carcinoma: a preliminary report. *Surgery* 106(3): 533-545

Tolcher AW, Sugarman S, Gelmon KA, Cohen R, Saleh M, Isaacs C, Young L, Healey D, Onetto N, Slichenyer W (1999) Randomized phase II study of BR96-doxorubicin conjugate in patients with metastatic breast cancer. *J Clin Oncol* 17(2): 478-484

Twelves C and Anthoney A (2000) Rational development of capecitabine. *Semin Oncol* 27(5): 144-148

Twelves C, on behalf of the Xeloda Colorectal Study Group (2002) Capecitabine as first-line treatment in colorectal cancer: pooled data from two large phase III trials. *Eur J Cancer* 28: S15-S20

Valentin J (1998) Radiation dose to patients from radiopharmaceuticals - (Addendum 2 to ICRP Publication 53) ICRP Publication 80 Approved by the Commission in September 1997. *Annals of the ICRP* 28(3): 1

Van Cutsem E, Findlay M, Osterwalder B, Kocha W, Dalley D, Paxdur R, Cassidy J, Dirix L, Twelves C, Allman D, Seitz J-F, Scholmerich J, Burger HU, Verweij J (2000) Capecitabine, an oral fluoropyrimidine carbamate with substantial activity in advanced colorectal cancer: results of a randomized phase II study. *J Clin Oncol* 18(6): 1337-1345

Van Cutsem E, Twelves C, Cassidy J, Allman D, Bajetta E, Boyer M, Bugat R, Findlay M, Frings S, Jahn M, McKendrick J, Osterwalder B, Perez-Manga G, Rosso R, Rougier P, Schmiegal WH, Seitz J-F, Thompson P, Vietez JM, Weitzel C, Harper P for the Xeloda Colorectal Cancer Study Group (2001) Oral capecitabine compared with intravenous fluorouracil plus leucovorin in patients with metastatic colorectal cancer: results of a large phase III study. *J Clin Oncol* 19(21): 4097-4106

Vansteenkiste JF, Stroobants SG, Leyn PR, Dupont PJ, Verbeken EK and the Leuven Lung Cancer Group (1998) Potential use of FDG PET scan after induction chemotherapy in surgically staged IIIa-N2 non-small-cell lung cancer: A prospective pilot study. *Ann Oncol* 9: 1193-1198

Venturini M (2002) Rational development of capecitabine. *Eur. J Cancer* 38: S3-S9

Verhaar MJ, Chester KA, Keep PA, Robson L, Pedley RB, Boden JA, Hawkins RE, Begent RHJ (1995) A single chain Fv derived from a filamentous phage

library has distinct tumour targeting advantages over one derived from a hybridoma. *Int J Cancer* 61: 497-501

Verhaar MJ, Keep PA, Hawkins RE, Robson L, Casey JL, Pedley RB, Boden JA, Begent RHJ, Chester KA (1996) Technetium-99m radiolabelling using a phage-derived single-chain Fv with a C-terminal cysteine. *J Nucl Med* 37(5): 868-872

Vitols KS, Haag-Zeino B, Baer T, Montejano YD, Huennekens FM (1995) Methotrexate-alpha-phenylalanine: optimization of methotrexate prodrug for activation by carboxypeptidase A-monoclonal antibody conjugate. *Cancer Res* 55(3): 478-481

Vogelstein B, Lane D, Levine AJ (2000) Surfing the p53 network. *Nature* 408(6810): 307-310

Von Hoff DD and Turner J (1991) Response rates, duration of response and dose response effects in phase I trials of antineoplastics. *Invest New Drugs* 9: 115-122

[1]Vrudhula VM, Svensson H, Kennedy KA, Senter PD, Wallace PM (1993) Antitumour activities of a cephalosporin prodrug in combination with monoclonal antibody – β-lactamase conjugates. *Bioconj Chem* 4: 334-340

[2]Vrudhula VM, Senter PD, Fischer KJ, Wallace PM (1993) Prodrugs of doxorubicin and melphalan and their activation by a monoclonal antibody – penicillin-G amidase conjugate. *J Med Chem.* 36: 919-923

Vrudhula VM, Svensson H, Senter PD (1997) Immunologically specific cephalosporin derivative of mitomycin C by monoclonal antibody – β-lactamase conjugates. *J Med Chem* 40: 2788-2792

Wagner HN (1998) A brief history of positron emission tomography. *Semin Nucl Med* 28(3): 213-220

Wagner HN, Wiseman GA, Marcus CS, Nabi HA, Nagle CE, Fink-Bennett DM, Lamonica DM, Conti PS (2002) Administration guidelines for

radioimmunotherapy of Non-Hodgkin's lymphoma with ^{90}Y-labeled anti-CD20 monoclonal antibody. *J Nucl Med* 43: 267-272

[1]Wahl RL, Zasadny K, Helvie M, Hutchins GD, Weber B, Cody R (1993) metabolic monitoring of breast cancer using positron emission tomography: initial evaluation. *J Clin Oncol* 11(11): 2101-2111

[2]Wahl RL, Quint LE, Cieslak RD, Aisen AM, Koeppe RA, Meyer CR (1993) 'Anatometabolic' tumor imaging: Fusion of FDG PET with CT or MRI to localize foci of increased activity. *J Nucl Med* 34: 1190-1197

[1]Waibel R, Alberto R, Willuda J, Finnern R, Schibli R, Stichelberger A, Egli A, Abram U, Mach J, Pluckthun A, Shubiger P (1999) Stable one-step technetium-99m labeling of His-tagged recombinant proteins with a novel Tc(I)-carbonyl complex. *Nature Biotechnology* 17: 897-901

[2]Waibel R, Stichelberger A, Alberto R, Schibli R, Novak I, and Schubiger PA (1999). Site-directed labelling of single chain antibodies with Tc-99m and Re-188. *Proceedings of 16th International Conference on Advances in the Applications of Monoclonal Antibodies in Clinical Oncology.*

Wallace PM and Senter PD (1991) In vitro and in vivo activities of monoclonal antibody – alkaline phosphatase conjugates in combination with phenol mustard phosphate. *Bioconj Chem* 2: 349-352

Wallace PM, MacMaster JM, Smith VF, Kerr DE, Senter PD, Cosand WL (1994) Intratumoral generation of 5-fluorouracil mediated by an antibody-cytosine deaminase conjugate in combination with 5-fluorocytosine. *Cancer Res* 54: 2719-2723

Warburg, O (1956) On the origin of cancer cells. Science 123(3191): 309-314

Ward U, Primrose JN, Finan PJ, Perren TJ, Selby P, Purves DA, Cooper EH (1993) The use of tumor markers CEA, CA-195 and CA-242 in evaluating the response to chemotherapy in patients with advanced colorectal cancer. *Br J Cancer* 67: 1132-1135

Weber G (1977) Enzymology of cancer cells. *N Engl J Med* 296: 541-551

Weber WA, Ziegler SI, Thödtmann R, Hanauske A-R, Schwaiger M (1999) Reproducibility of metabolic measurements in malignant tumors using FDG PET. *J Nucl Med* 40: 1771-1777

Weber WA, Ott K, Becker K, Dittler H-J, Helmberger H, Avril NE, Meitsetschläger G, Busch R, Siewart J-R, Schwaiger M, Fink U (2001) Prediction of response to preoperative chemotherapy in adenocarcinoma of the esophagogastric junction by metabolic imaging. *J Clin Oncol* 19(12): 3058-3065

Weber WA, Peterson V, Schmidt B, Tyndal-Hines L, Link T, Peschel C, Schwaiger M (2003) Positron Emission Tomography in non-small cell lung cancer: prediction of response to chemotherapy by quantitative assessment of glucose use. *J Nucl Med* 21(14): 2651-2657

Webley SD, Francis RJ, Pedley RB, Sharma SK, Begent RH, Hartley JA, Hochhauser D (2001) Measurement of the critical DNA lesions produced by antibody-directed enzyme prodrug therapy (ADEPT) in vitro, in vivo and in clinical material. *Br J Cancer* 84: 1671-1676

Weiner LM (1999) Monoclonal antibody therapy of cancer. *Semin Oncol* 26(5; Suppl 14): 43-51

Weinstein JN and van Osdol W (1992) Early intervention in cancer using monoclonal antibodies and other biological ligands: micropharmacology and the 'binding site barrier'. *Cancer Res* 52: 2747s-2751s

Whisson ME and Connors TA (1965) Cure of mice bearing advanced plasma cell tumours with aniline mustard. *Nature* 206: 689-691

WHO handbook for reporting results of cancer treatment (1979) Geneva (Switzerland): *World Health Offset Publication* No48

Wiseman GA, Kornmehl E, Leigh B, Erwin WD, Podoloff DA, Spies S, Sparks RB, Stabin MG, Witzig T, White CA (2003) Radiation dosimetry results and

safety correlations from 90Y-ibritumomab tiuxetan radioimmunotherapy for relapsed or refractory non-Hodgkin's lymphoma: combined data from 4 clinical trials. *J Nucl Med* 44(3): 465-474

[1]Witzig TE, Gordon LI, Cabanillas F, Szuczman MS, Emmanouilides C, Joyce R, Pohlman BL, Bartlett NL, Wiseman GA, Padre N, Grillo-López AJ, Multani P, White CA (2002) Randomized controlled trial of yttrium-90-labeled ibritumomab tiuxetan radioimmunotherapy versus rituximab immunotherapy for patients with relapsed or refractory low-grade, follicular or transformed B-cell Non-Hodgkin's lymphoma. *J Clin Oncol* 20: 2453-2463

[2]Witzig TE, Flinn IW, Gordon LI, Emmanouilides C, Czuczman MS, Saleh MN, Cripe L, Wiseman G, Olejnik T, Multani PS, White CA (2002) Treatment with Ibritumomab tiuxetan radioimmunotherapy in patients with Rituximab-refractory follicular non-Hodgkin's lymphoma. *J Clin Oncol* 20: 3262-3629

Workman P (2003) The opportunities and challenges of personalized genome-based molecular therapies for cancer: targets, technologies, and molecular chaperones. *Cancer Chemother Pharmacol* 52(Suppl 1): S45-S56

Xu G and McLeod HL (2001) Strategies for enzyme/prodrug cancer therapy. *Clin Cancer Res* 7: 3314-3324

Yokota T, Milenic DE, Whitlow M, Schlom J (1992) Rapid tumor penetration of a single-chain Fv and comparison with other immunoglobulin forms. *Cancer Res* 52: 3401-3408

Young H, Baum R, Cremerius U, Herholz K, Hoekstra O, Lammertsma AA, Pruim J, Price P on behalf of the European Organization for Research and Treatment of Cancer (EORTC) PET Study Group (1999) Measurement of clinical and subcliical tumour response using [^{18}F]-fluorodeoxyglucose and positron emission tomography: Review and 1999 EORTC recommendations. *Eur J Cancer* 35(13): 1773-1782

Zhu H, Jain RK, Baxter LT (1998) Tumor pretargeting for radioimmunodetection and radioimmunotherapy. *J Nucl Med* 39: 65-76

Zimny M, Kaiser H-J, Wildberger J, Nowak B, Cremerius U, Sabri O, Buell U (2001) Analysis of FDG uptake with hybrid PET using standardized uptake values. *Eur J Nucl Med* 28: 586-592

APPENDIX 1 – SPECT analysis

Examples of the SPECT data entry and analysis spreadsheets are presented below with accompanying descriptions of the process of analysis.

Table 62: Data entry spreadsheet for SPECT analysis:

	Thorax 4			**Thorax24**		
	slice	**counts**	**no. pixels**	**slice**	**counts**	**no. pixels**
lung	T45	8812	84	T45	1829	81
	T47	7929	104	T60	1759	176
	T50	4616	60	T61	1277	170
	mean	**86.1 counts/pixel**		**mean**	**11.4 counts/ pixel**	
liver	T27	5732	36	T27	1683	40
	T33	3880	25	T28	935	28
	T35	5144	30	T29	1659	42
	mean	**162.2 counts/pixel**		**mean**	**38.9 counts/ pixel**	
heart	T43	15818	72	T36	2222	56
	T44	14041	63	T37	2101	48
	T45	15316	64	T38	3475	72
	mean	**227.0 counts/ pixel**		**mean**	**44.3 counts/ pixel**	
tumour 1	T32	2764	24	T31	369	21
	T33	2350	18	T32	739	32
	T34	2339	21	T33	655	35
	mean	**118.3 counts/ pixel**		**mean**	**20.0 counts/ pixel**	
tumour 2	T24	3747	30	T17	1630	48
	T26	4199	30	T20	1032	42
	T27	5459	36	T21	712	35
	mean	**139.6 counts/ pixel**		**mean**	**27.0 counts per pixel**	

Abbreviations: T – thorax

Table 62 is an example of the data entry form used for the SPECT analysis. Regions of interest (ROI) are placed in triplicate on areas of lung, liver, heart and tumour for each scan. For each ROI the slice (and whether on the T –thorax scan or A – abdominal scan) are recorded. Also recorded is the number of pixels drawn and the total counts in the ROI. The mean counts per pixel are then calculated for each organ (total counts in the 3 ROI divided by total number of pixels).

Table 63: Analysis spreadsheet example

Patient ID	15	**half-life I-131**	192.48 hrs
Injected dose (MBq)	232 MBq	**Total dose A5CP**	5373 U
Date and time of injection	09/07/98 13:32	**correction factor**	0.002448 cps per pixel
time after injection **Thorax 4 (Tx 4)scan** **Thorax 24 (Tx 24) scan**	 4.5 hrs 25.8 hrs	**acquisition time per frame** **Tx 4 scan** **Tx 24 scan**	 25 seconds 30 seconds

	scan ID	**mean cts/pixel**	**acquisition time (s)**	**cts /sec/ pixel**	**activity (MBq/ml)**	**time after inj (h)**	**decay correction factor (T_0)**	**Activity at T_0 (MBq/ml)**	**% inj dose/ kg**	**estimated CPG2 activity (U/g)**
lung	Tx4	86.1	25	3.4	0.008	4.5	1.016	0.0086	3.7%	0.20 U/g
	Tx24	11.4	30	0.4	0.001	25.8	1.097	0.0010	0.4%	0.02 U/g
liver	Tx4	162.2	25	6.5	0.016	4.5	1.016	0.0161	7.0%	0.38 U/g
	Tx24	38.9	30	1.3	0.003	25.8	1.097	0.0035	1.5%	0.08 U/g
heart	Tx4	227.0	25	9.1	0.022	4.5	1.016	0.0236	9.7%	0.52 U/g
	Tx24	44.3	30	1.5	0.004	25.8	1.097	0.0034	1.7%	0.09 U/g
tumour1	Tx4	118.3	25	4.7	0.011	4.5	1.016	0.0118	5.1%	0.27 U/g
	Tx24	20.0	30	0.7	0.002	25.8	1.097	0.0018	0.8%	0.04 U/g
tumour2	Tx4	139.6	25	5.6	0.014	4.5	1.016	0.0139	6.0%	0.32 U/g
	Tx24	27.0	30	0.9	0.002	25.8	1.097	0.0024	1.0%	0.05 U/g

Abbreviations: Tx – thorax, U- units; h – hour; s – seconds; cts – counts; inj – injected; T_0- time zero

This spreadsheet displayed in **table 63** is representative of the data analysis used to quantitatively calculate the biodistribution of radiolabelled antibody-enzyme as part of the ADEPT clinical trials. The steps involved in the analysis are outlined below.

The **mean counts per pixel** are derived from the values obtained in the ROI data entry spreadsheet.
The **acquisition time** represents the time per frame used as part of the SPECT protocol.
The **mean counts per pixel per second** can be calculated by dividing the mean counts per pixel by the acquisition time (s).
The **activity** is the calculated by converting counts per pixel per second to MBq per ml based on a correction factor derived from phantom studies scanned with clinical SPECT parameters. The phantom contains a known amount of radioactivity, and thus the resultant conversion factor from counts per pixel per second to radioactivity per unit mass can be made. The conversion factor for I-131 on this camera is 0.002448 counts per second per pixel per ml.
A correction then needs to be made for the radioactive decay that occurs between scans due to the half-life of the radioisotope. The half-life of I-131 is 192.48 hours. The formula for decay correction is 1/(EXP(LN(0.5)*time after injection[h]/half-life)), where EXP is exponential, and LN is log.
The **decay correction factor** can be used to correct the radioactivity per ml to the time of injection (T_0).
The **percentage injected dose per kg** of tissue is then calculated by dividing the radioactivity per ml in each tissue, by the injected I-131 dose (232 MBq), converting to a percentage and then dividing by 1000 (to change from ml to kg).
The **enzyme units** in the organs may then be estimated by multiplying the %injected dose per kg, by the injected A5CP dose (5373 U) and multiplying by 1000 to convert from kg to grams.

ACKNOWLEDGEMENTS

I gratefully acknowledge the support of CRUK who funded my research position at the CRUK Targeting and Imaging Group, Royal Free Campus of Royal Free and UCL Medical School

The ADEPT clinical trials were supported by AstraZeneca, Cancer Research UK, Ronald Raven Trust and The Wolfson Trust

The FDG PET clinical trial was supported by The Wolfson Trust, The Ronald Raven Trust, and the Golden Charitable Trust.

My PhD supervisors were Prof Richard Begent, Dr Daniel Hochhauser and Dr Alan Green. I was extremely grateful for their guidance.